IL

NUOVO CIMENTO

ORGANO DELLA SOCIETÀ ITALIANA DI FISICA

SOTTO GLI AUSPICI DEL CONSIGLIO NAZIONALE DELLE RICERCHE

VOL. XIX, N. 1 | *Serie decima* | 1° Gennaio 1961

ERWIN SCHRÖDINGER

È MORTO

IL GIORNO 5 GENNAIO 1961

E. Schrödinger

Questo quartino va preposto alla pag. 1.

IL NUOVO CIMENTO Vol. XIX, N. 1 1° Gennaio 1961

Mechanical Momentum of Solutions of Liquids in a Rotating Electric Field.

E. Grossetti

Istituto di Fisica dell'Università - Napoli

(ricevuto il 27 Aprile 1960)

Summary. — In the present paper the rotational mechanical momenta have been determined for certain solutions of polar liquids in non-polar ones, and solutions of two polar liquids, with relation to the variation of the concentration, in electric fields rotating at very high frequency (100 MHz). For some solutions the behaviour of the mechanical momenta is that of a constant decrease at the variation of the concentration, while for others a maximum is noted in the behaviour of the momenta at a concentration which corresponds, nearly always, to about 70% of the polar liquid.

In a previous work A. Carrelli and M. Marinaro (1) studied the behaviour of certain solutions of polar liquids in non-polar ones, placed in rotating electric fields at low frequencies (50, 150, 840 Hz) and they found that in some cases and for certain concentrations the mechanical momentum, thus generated, is about 10^3 times greater than that foreseen by Lampa's theory, which ascribes such rotation to a conductivity effect. The authors found that for several solutions studied, all of the mechanical momenta measured in relation to the concentrations, show a maximum for low concentrations of the polar liquid

(1) A. Carrelli and M. Marinaro: *Nuovo Cimento*, **11**, 262 (1959).

in a non-polar one, and that such maxima shift, at the increase of the frequency of the rotating electric field, towards higher concentrations. In this paper, the same solutions of polar liquids in non-polar ones are studied at much higher frequencies (100 MHz). Consequently, the conductivity effect being zero, the determination of the electrical dipolar momenta was given, using Born's formula ([2]), by

$$L = \tfrac{4}{3}\pi a^3 \eta \omega (ME/kT)^2$$

through which, having determined the values of L, mechanical momenta for such solutions, one can obtain the electrical dipolar momentum M. The solutions studied are the following: ethyl alcohol-benzene; amyl alcohol-benzene; isopropyl alcohol-benzene; methyl alcohol-benzene; acetic acid-benzene; nitrobenzene-benzene; ethyl alcohol dioxane and the solutions amylic alcohol-ethylic-alcohol and amylic alcohol-methylic alcohol, both formed by polar liquids.

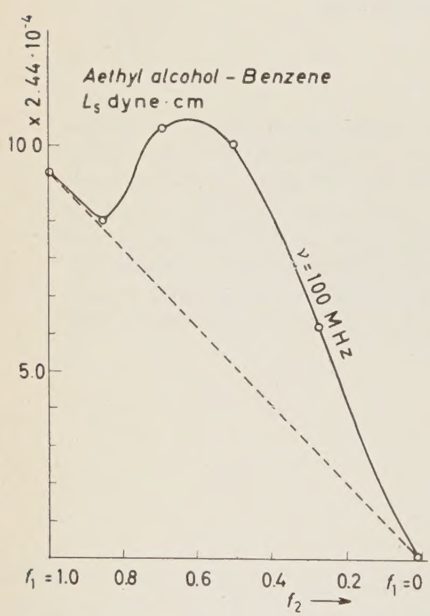

Fig. 1.

In Fig. 1-9 are plotted the curves which give the behaviour of the mechanical momenta found for the several solutions at the variation of the concentration.

While the values of the mechanical momenta obtained for the single polar component of each mixture are in good agreement with those obtained from Born's formula when M is substituted by the momenta derived from the polarization processes, the same cannot be said of the solutions when the percentage of the polar liquid, in relation to the non-polar one, is changed.

For certain solutions, such as amylic alcohol-benzene; nitrobenzene-benzene, isopropylic alcohol-benzene, the behaviour of the mechanical momenta is that of a constant decrease at the decrease of the concentration. This can be explained by the fact that the polar components of such solutions also show a constant decrease of the molecular polarization at the decrease of the concentration.

([2]) A. Lampa: *Wien. Ber.*, **115** (2), 1659 (1906).

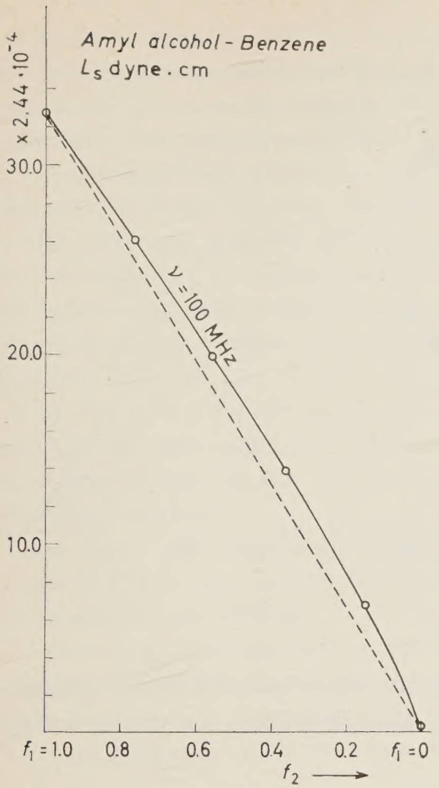

Fig. 2.

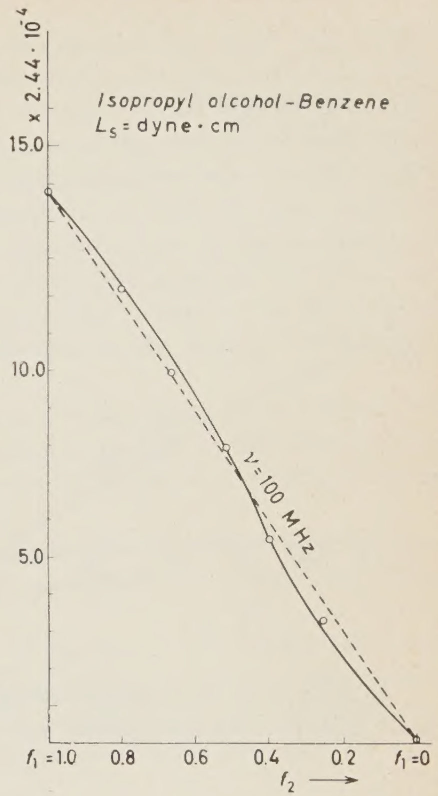

Fig. 3.

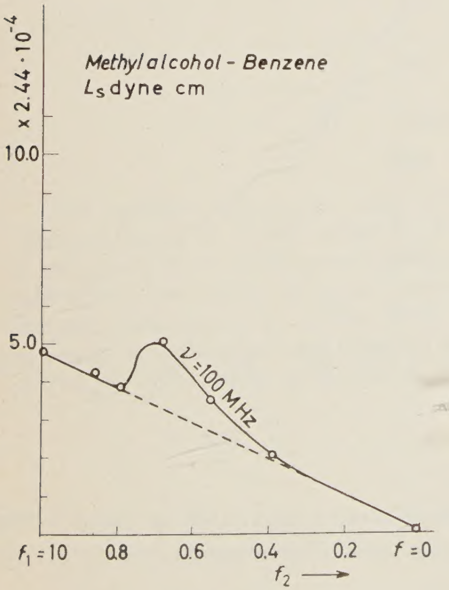

Fig. 4.

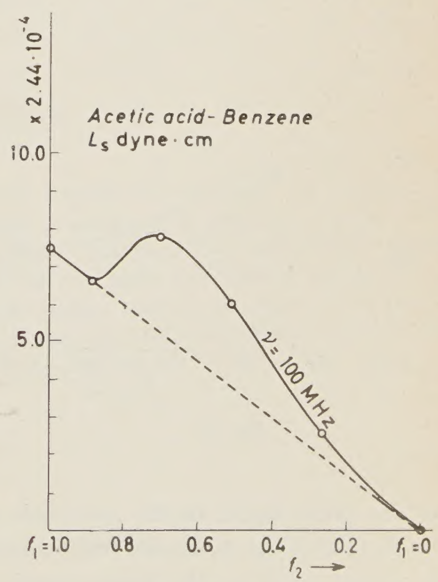

Fig. 5.

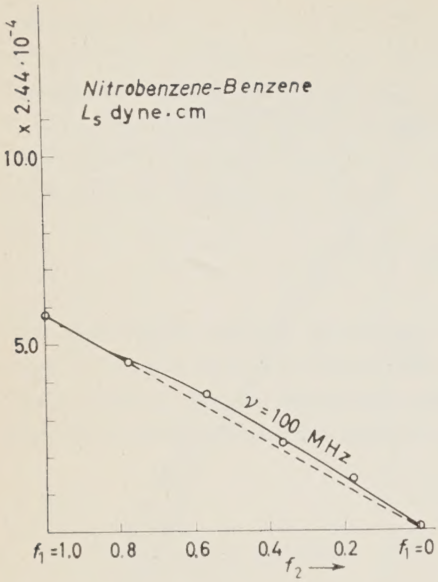

Fig. 6.

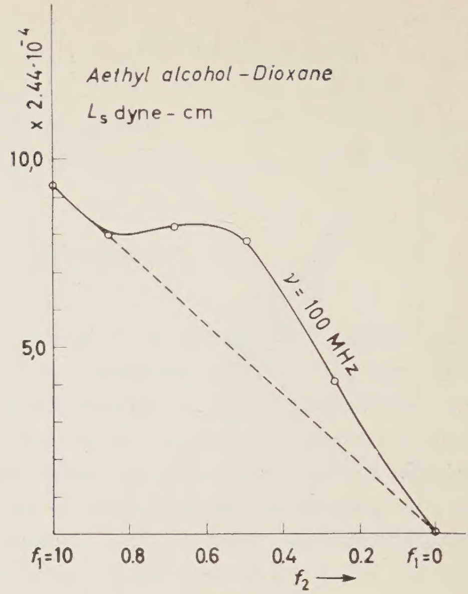

Fig. 7.

As it appears from the measurements made for solutions of acetic acid-benzene, methylic alcohol-benzene and ethylic alcohol-benzene, as the percentage

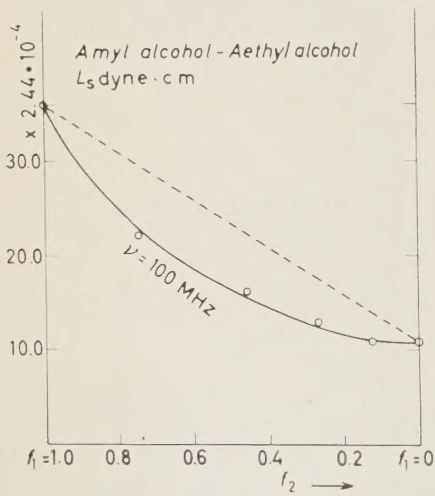

Fig. 8.

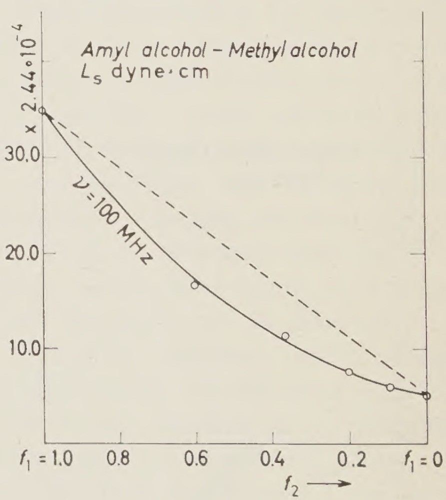

Fig. 9.

of the polar liquid in the non-polar one decreases, a maximum is noted in the behaviour of the momenta for a concentration which corresponds, nearly always to about 70% of the polar liquid.

As is known, this maximum is explained by the fact that pure liquids are remarkably associated, and that the presence of the non-polar component causes the decrease of the association and therefore of the number of free dipoles, which results, consequently, in an increase of the mechanical momentum.

Furthermore the rotational mechanical momenta have been determined for the ethylic alcohol-dioxane solution, that is, for a solution of a polar liquid in a non-polar one different from benzene. The behaviour of the momenta, at the variation of the concentration is practically the same as that found for the solution of ethylic alcohol-benzene, except that it shows a less accentuated maximum, and a lower strength of the dioxane at the decrease of the association.

However it must be noted that by using dioxane rather than benzene, we find that the maximum has a different position in relation to the concentration. Such maximum, for the various liquids, results always at the same value of the concentration.

Moreover the rotational mechanical momenta were also determined for solutions of two polar liquids, such as amylic alcohol-ethylic alcohol and amylic alcohol-methylic alcohol.

For such solutions, as the percentage of the liquid with highest electrical dipolar momentum decreases, the mechanical momenta observed also show a decrease which is less than that expected considering a proportionality.

This fact proves the increase in the liquid association process.

RIASSUNTO

Nel presente lavoro sono stati determinati i momenti meccanici di rotazione di alcune soluzioni di liquidi polari in non polari e soluzioni di liquidi ambedue polari al variare della concentrazione in campi elettrici rotanti a frequenza molto elevata (100 MHz). Per talune soluzioni l'andamento dei momenti meccanici è quello di una costante diminuzione al variare della concentrazione, mentre per altre si osserva un massimo nell'andamento dei momenti quasi, sempre per una concentrazione del liquido polare che corrisponde all'incirca al 70% di quest'ultimo.

IL NUOVO CIMENTO Vol. XIX, N. 1 1° Gennaio 1961

Magnetic Mirrors in the Milky Way Galaxy (*).

L. Marshall

Brookhaven National Laboratory - Upton, N. Y.

(ricevuto il 15 Luglio 1960)

Summary. — It is shown that the present day velocity distribution of the Milky Way Galaxy amplifies the magnetic field in the galactic arms by stretching the existing lines of force in such a way as to produce magnetic mirrors in the regions between 4 and 10 kps radius. The strength of the mirrors is increasing with time so that, effectively, a mirror of given strength seems to be moving out along the arm. It is suggested that these mirrors, fixed at constant radius but effectively moving, are important in production of cosmic rays, and it is shown that the appropriate constants relating to the mirrors are compatible with a Fermi accelerator mechanism of first order dependence on effective mirror velocity. The energy for this process is derived from differential rotation energy of which there is an adequate supply.

1. – Introduction.

It is the purpose of this paper to show that a cosmic ray acceleration device may be inferred from the known characteristics of the Milky Way Galaxy. These include *a*) a magnetic field directed along the arms of the Galaxy, and whose magnitude is known in the neighborhood of the sun, *b*) a velocity distribution and mass distribution for matter in the disc as a function of radius, different from a rigid rotation. It is noted that almost any cylindrically symmetric velocity distribution except that of a rigid rotation will produce magnetic mirrors.

(*) Work performed under the auspices of the U. S. Atomic Energy Commission.

a) That the magnetic field lies in the plane of the Galaxy is the conclusion of DAVIS and GREENSTEIN (1) and SPITZER and TUKY (2), based on measurements of W. A. HILTNER (3) and of HALL and MIKESELL (4) who discovered polarization of starlight transmitted through interstellar dust and gas. Further measurements of HILTNER (5) showed the magnetic field in the vicinity of the earth to be approximately parallel to the spiral arm of the Galaxy. An argument of DAVIS (6) interpreting the average deviation from parallelism of the field in terms of the lateral hydromagnetic velocity of the lines of force gave the value of the field $\sim 10^{-5}$ G. A similar analysis of CHANDRASEKHAR and FERMI (7) according to which the root mean square velocity of turbulence was equated to the velocity of irregular oscillatory motion of the field yielded a value of $7 \cdot 10^{-6}$ G for the magnetic field in the galactic arm near the sun.

b) The velocity distribution for matter in the disc of the Galaxy has been determined by KWEE, MULLER, and WESTERHOUT (8), by H. C. VAN DE HULST, C. A. MULLER and J. H. OORT (9), as a function of radius. It may be fitted by the expression

$$(1) \qquad \frac{v}{\varrho} = 88\,(\exp[-x])\left(\cos^3 x + \frac{1}{2}\sin^3 x\right)\,(\text{km/s kps})\,,$$

where v is the tangential velocity, ϱ is the radius in kps, and $x = \varrho/12$ kps. In Table I are listed experimental values of v/ϱ and, for comparison, also some calculated values.

Because the tangential velocity decreases with increasing radius after 6 kps radius, it follows that the arms of the Milky Way Galaxy are trailing and are winding up with time. Some other galaxies are known to wind up: for example, D. S. EVANS (10) has obtained data to show that this is true for NGC 253.

(1) L. DAVIS Jr.: *Phys. Rev.*, **81**, 890 (1951).
(2) L. SPITZER and J. TUKEY: *Astrophys. Journ.*, **114**, 187 (1951).
(3) W. A. HILTNER: *Science*, **109**, 165 (1949); *Astrophys. Journ.*, **109**, 471 (1949); *Phys. Rev.*, **78**, 170 (1950).
(4) J. S. HALL and A. H. MIKESELL: *Astron. Journ.*, **54**, 187 (1949): Pub. U. S. Naval Obs. 17, N Part 1 (1950).
(5) W. A. HILTNER: *Astrophys. Journ.*, **114**, 241 (1951).
(6) L. DAVIS Jr. and J. L. GREENSTEIN: *Astrophys. Journ.*, **114**, 206 (1951).
(7) S. CHANDRASEKHAR and E. FERMI: *Astrophys. Journ.*, **118**, 113 (1953).
(8) K. K. KWEE, C. A. MULLER and G. WESTERHOUT: *B.A.N.*, **12**, no. 458, 211 (1954).
(9) H. C. VAN DE HULST, C. A. MULLER and J. H. OORT: *B.A.N.*, **12**, no. 452, 117 (1954).
(10) D. S. EVANS: *Month. Not. Roy. Astr. Soc.*, **116**, 659 (1956).

TABLE I.

ϱ (kps)	(v/ϱ) (km/s kps)		v (km/s) experimental
	experimental	calculated	
3	66	63	196
5	44	45	215
6	36	39	224
7.5	23	23	207
10	19	19	190
12	—	15	174
14	—	12	160

DE VAUCOULEUR ([11]) gives a history of the accumulation of evidence that galaxies are winding up, and has made new measurements on 17 galaxies producing some evidence for each one to show it to be rotating with trailing arms, *i.e.* winding up.

2. – Amplification of magnetic fields of galactic windup.

Except for the perturbation caused by turbulence, the field stays directed along the arm and otherwise moves as the arm moves, being practically attached to the matter in the arm for the lifetime of the Galaxy, a well-known consequence of the high conductivity of galactic matter (A. SCHLÜTER ([12]), and L. BIERMANN ([13])).

The arms of the Galaxy and therefore the lines of force are not quite circular but instead have a slight pitch, *i.e.* dependence on radius. As a consequence, the arms and the lines of force contained in them are growing longer with time as they wind up. Consider for example a line of force which has distance R from the galactic center at an arbitrary angle ϑ. At a slightly larger angle, $\vartheta + \theta$, the line of force crosses the radius vector at $R + r$. But the velocity of the matter to which it is tied depends on the radius. Consider now two segments of the same line of force lying in a region where $R \sim 6$ kps. A segment of the line of force at R is moving faster than a segment at $R + r$, and the distance between the two pieces increases with time; $d = (\Delta v)t$, where Δv is the difference in velocities. So the line of force must be stretching and

([11]) G. DE VAUCOULEURS: *Astrophys. Journ.*, **127**, 487 (1958).
([12]) A. SCHLÜTER: *Zeits. Naturfor.*, **5a**, 72 (1950).
([13]) L. BIERMANN: *Ann. Rev. Nucl. Sci.*, **2**, 349 (1953).

growing longer, which means that kinetic energy of differential rotation is being changed to magnetic energy and stored in the arms. This process will continue until the entire Galaxy rotates as a rigid wheel, after which the magnetic field can no longer be increased by this method of amplification. For a discussion of amplifications of magnetic field by stretching of lines of force, see for example, W. ELSASSER ([14]).

The stretching mechanism produces an increase in magnetic field which is directly proportional to the increase in length of an arm, as can be shown by a simple argument. Let H_0 be the field in an arm and let $\pi x^2 H_0$ = total number of lines of force in the arm. Assume an arm to have a circular cross-section of radius x, and consider a cylindrical segment of arm of length S. Because as yet we do not know how to make or break the lines of force, we shall assume here 1) that the total flux stays constant with time and further assume 2) that the arm behaves as an incompressible fluid. Then as the segment of arm elongates from S to $S+s$, the radius of the cylindrical segment changes from x to $x-\varepsilon$. Requirement of constant total flux gives

$$H_0 \pi x^2 = H\pi (x-\varepsilon)^2 \,. \tag{2}$$

Requirement (2) gives

$$\pi x^2 S = \pi (x-\varepsilon)^2 (S+\varepsilon) \,. \tag{3}$$

The ratio of (3) to (2) gives

$$H/H_0 = (S+s)/S \,. \tag{4}$$

That is, the field strength increases in proportion to the length of arm. The magnetic energy density $\sim H^2$ and on this account increases as the square of the length of the arm.

3. – Increase of magnetic field as a function of time.

Intermediate types of galaxies like the Milky Way closely resemble hyperbolic spirals and can be represented as

$$\left\{\begin{aligned} &\varrho\theta = vt \,, \\ &\theta = t(v/\varrho) = 88t(\exp[-x])(\cos^3 x + \tfrac{1}{2}\sin^3 x) \,, \end{aligned}\right. \tag{5}$$

where θ is given in radians, t in billions of years, $x = (\varrho/12 \text{ kps})$, and ϱ is in kps.

([14]) W. ELSASSER: *Rev. Mod. Phys.*, **28**, no. 2, 147 (1956).

Consider what happens if at $t=0$ the original galactic arm lies along a radius vector and consequently has a magnetic field with only a radial component. Let the arm be divided into segments each having the same length. After time t, each segment of the arm still has its initial average radius but has rotated through some angle θ which is different depending on the corresponding values of v/ϱ. Segments at smaller radii have rotated through larger angles than have segments at larger radii. That is, because v/ϱ is decreasing with ϱ, then also θ decreases with ϱ. So the arm which once lay along a radius now has become a spiral, and its magnetic field, originally directed radially, now has both a radial and a tangential component. The radial component stays constant with time, whereas the tangential component grows with time in proportion to the increasing length of arm.

The length of an arm for $0 \leqslant r \leqslant 1$ kps is given by

$$(6)\qquad S=\int_0^R [(\mathrm{d}\varrho)^2+\varrho^2(\mathrm{d}\theta)^2]^{\frac{1}{2}}=\int_0^R \mathrm{d}\varrho[1+\varrho^2(\mathrm{d}\theta/\mathrm{d}\varrho)^2]^{\frac{1}{2}}=R\int_0^1 \mathrm{d}x[1+x^2(\mathrm{d}\theta/\mathrm{d}x)^2]^{\frac{1}{2}},$$

into which may be substituted $\mathrm{d}\theta/\mathrm{d}x$, the derivative of (5).

$$(7)\qquad \frac{\mathrm{d}\theta}{\mathrm{d}x}=-88t\exp[-x]\left|\cos^2 x(1+3\sin x)+\frac{1}{2}\sin^2 x(1-3\cos x)\right|=$$
$$=-88tF(x)\,.$$

For short lapses of time, when $x^2(\mathrm{d}\theta/\mathrm{d}x)^2$ is small compared with unity, the parenthesis may be expanded:

$$(8)\qquad S/R=\int_0^1 \mathrm{d}x\left[1+\frac{1}{2}x^2(\mathrm{d}\theta/\mathrm{d}x)^2\right]=1+\frac{1}{2}\int_0^1 x^2\left(\frac{\mathrm{d}\theta}{\mathrm{d}x}\right)^2\mathrm{d}x=1+\frac{1}{2}88^2t^2\int_0^1 xF(x)^2\,\mathrm{d}x\,.$$

For large t, $x^2(\mathrm{d}\theta/\mathrm{d}x)^2>1$, and the integral reduces to

$$(9)\qquad S/R=\int_0^1 x\,\mathrm{d}\theta=88t\int_0^1 xF(x)\,\mathrm{d}x\,.$$

It follows that when the Galaxy first begins to wind, the magnetic field first increases with t^2. But a simple numerical evaluation shows that after a lapse of time $\sim 5\cdot 10^8$ years the magnetic field increases $\sim t$.

Numerical integration of equation (6) gives the values of S/R shown in Table II. These values of S/R are directly equal to the amplification of the magnetic field H during the lapse of time t.

TABLE II. – *Average amplification* ($0 < R < 12$ kps).

S/R	$t \cdot 10^9$ year
3.0	0.1
8.9	0.3
28.3	1.0

The amplification of magnetic field at a radius $R - \varepsilon < r < R + \varepsilon$ from the center of rotation is given for large t by

$$S/R = 88t \int_{R^-}^{R^+} x F(x)\,\mathrm{d}x \,. \tag{10}$$

Numerical integration, putting $t = 5 \cdot 10^8$ years gives the values shown in Table III, where the values of H have been normalized to $H = 5.4 \cdot 10^{-6}$ G at the earth. One sees that in the neighborhood of the sun ($r = 8$ kps), the the field amplification is larger than the average amplification from 0 to 12 kps.

TABLE III.

x	R (kps)	($t = 5 \cdot 10^8$ year)	
		H/H_0	H (gauss)
$0 \div 0.1$	0.6	2.5	$1.4 \cdot 10^{-6}$
$0.1 \div 0.2$	1.8	8.5	5.5
$0.2 \div 0.3$	3.0	14	6.0
$0.3 \div 0.4$	4.2	18	7.7
$0.4 \div 0.5$	5.4	20	8.5
$0.5 \div 0.6$	6.6	20	8.5
$0.6 \div 0.7$	7.8	19	8.0
$0.7 \div 0.8$	9.0	16.5	7.0
$0.8 \div 0.9$	10.2	13.5	5.7
$0.9 \div 1.0$	11.4	10	4.2

The radial dimensions of any arbitrary initial feature of mass distribution and magnetic field are preserved by the motion described in Table I, but are deformed in such a way as to gradually become smeared over a larger and larger angle.

The reason for considering the effects on magnetic field amplification caused by Galactic rotation during a relatively short time interval $\sim 5 \cdot 10^8$ years is that if one assumes the experimental velocity dependence has obtained throughout the lifetime of the Galaxy, one finds that the spacing of arms in the neighborhood of the sun, 9 kps, is 0.14 kps, but the galactic structure deduced by M. SCHMIDT (15) shows about 1.3 kps between arms.

This lack of agreement may indicate that some radial velocity components exists for $r < 2$ kps (like those reported by VAN WOERDEN, RONGOOR, and OORT (16)).

In any case it suffices for the present argument to consider here only magnetic field amplifications resulting from motion during $t = 5 \cdot 10^8$ years. *a*) Assume that $5 \cdot 10^8$ years ago, the magnetic field had a constant value everywhere in the arm. Then the amplified magnetic field distribution today is given in Table III, and shows that magnetic mirrors exist, as will be discussed below. *b*) If on the other hand, we assume that at $5 \cdot 10^8$ years ago, the magnetic fields had different values at different places in the galaxy, it follows that the same amplification will cause the existence of even more magnetic mirrors. *c*) There is only one case in which no mirrors can exist today, and that is, if the initial magnetic field distribution had been exactly such that the resulting amplification cancelled out all fluctuations and made it constant today. This chance has a very low probability, and we shall ignore it in what follows. Let us assume, for the sake of simplicity, that the amplification acts on an originally constant magnetic field. The same arguments will go through even if the original fields fluctuated from place to place.

4. – Existence of magnetic mirrors in the galactic arms.

In Table III, it is shown that as a result of rotation for $5 \cdot 10^8$ years the magnetic field of an arm increases as a function of radius from a value of 1.4 μG at 0.6 kps to a maximum of 8.5 μG at 6.0 kps, and falls again at large radii, being, for example, 4.2 μG at 11.4 kps.

The fact that the magnetic field goes through a maximum value at about 6 kps means that the lines of force are closer together there than they are at larger or smaller radii, and on this account form two magnetic mirrors, placed back to back, one facing along the arm in the direction which leads to the center, and the other facing along the arm in the direction which leads away

(15) M. SCHMIDT: *B.A.N.*, no. 475, 247 (1957).
(16) H. VAN WOERDEN, W. RONGOOR and J. CORT: *Compt. Rend.*, **244**, 1691 (1957).

from the center. We may mention again that if the amplification acts on an originally non-uniform field distribution, more mirrors will result.

In effect the mirror moves; for r large, a region of constant mirror strength moves along the arm in the direction to go out of the galaxy, and for r small, such a region moves in the direction which leads to the galactic center.

To obtain an expression for mirror velocity we wish to find r and t such that

$$(H)_{R+r,\,T+t} = (H)_{R,\,T}\,. \tag{11}$$

One may substitute in this equation, assuming $\varrho^2(\mathrm{d}\theta/\mathrm{d}\varrho)^2 \gg 1$

$$\frac{H}{H_0} = \frac{s}{\Delta r} = \frac{\mathrm{d}}{\mathrm{d}r}\left(\frac{v}{r}\,t\right),$$

$$\left[r\,\frac{\mathrm{d}}{\mathrm{d}r}\left(\frac{v}{r}\,t\right)\right]_{R+r,\,T+t} = \left[r\,\frac{\mathrm{d}}{\mathrm{d}r}\left(\frac{v}{r}\,t\right)\right]_{R,\,T},$$

from which one finds

$$\frac{r}{R} \simeq \left[\frac{v}{R} - \left(\frac{\mathrm{d}v}{\mathrm{d}r}\right)_R\right]\frac{t}{T}\left[\frac{v}{T} + R\left(\frac{\mathrm{d}^2v}{\mathrm{d}r^2}\right)_R\right]^{-1}.$$

In time t, the position of constant mirror strength has moved from R to $R+r$. The velocity of the mirror V_m then is given by

$$v_m = -\,v\left[1 - \frac{R}{v}\left(\frac{\mathrm{d}v}{\mathrm{d}r}\right)_R\right]^2\left[1 + \frac{R^2}{v}\left(\frac{\mathrm{d}^2v}{\mathrm{d}r^2}\right)_R\right]^{-1}. \tag{12}$$

The mirror velocity, evaluated numerically for the Milky Way Galaxy, is given in Table IV. One concludes that to a particle moving with the local tangential velocity v in a region of $r \sim 6$ kps the magnetic mirror appears to be moving along the arm with velocity $\sim v$, in a direction to go out of the Galaxy.

TABLE IV.

r (kps)	v (km/s)	Calculated $\lvert V_m \rvert$ (km/s)	r (kps)	v (km/s)	Calculated $\lvert V_m \rvert$ (km/s)
1	132	—	6	224	128
2	172	57	7	226	176
3	196	61	8	218	230
4	210	86	9	207	207
5	215	107	10	190	182

5. – Fermi accelerator in the Galaxy.

The existence of magnetic mirrors as an intrinsic part of galactic structure automatically provides that head-on collisions shall dominate. Let us make the most pessimistic assumption, namely that the hydromagnetic waves go in both directions with equal probability and with a random distribution of amplitudes and wavelengths up to the maximum sizes allowed by the width of the galactic arm. Then on the average, a particle colliding with them gains no energy when it is totally reflected by them. Define a co-ordinate system moving with the local average tangential velocity v, namely so that the average velocity of hydromagnetic waves with respect to that system is zero. Now, however, the intrinsic mirror moves in this co-ordinate system, with velocity, $\sim v$, in such a direction as if to go out of the arm. Consequently, particles moving into the arm and colliding with the intrinsic mirror always gain energy upon total reflection in this mirror. Then the energy gain depends in first order on the quantity $v_{\text{mirror}}/v_{\text{particle}}$.

We have then in the outer regions of the galactic arm a flux of hydromagnetic waves mainly moving in such a direction as eventually to arrive at the galactic center. They gradually are damped as they spiral in, for the most part losing energy to cosmic ray particles. They form a set of magnetic mirrors of random distribution of strengths, and with amplitudes gradually decreasing as they come into the arm, and moving mainly in one direction with hydromagnetic velocity V_a given by (see, for example, ALFVÉN [17])

$$V_a = \sqrt{\frac{H^2}{4\pi d}},$$

where d is the local mass density, and H is the local field strength. Both H and d increase as the wave moves into the arm and to the mirror velocity stays roughly constant at $\sim 2\cdot 10^6$ cm/s. This is the velocity with which the mirrors move in a frame of reference rotating with the Galaxy.

Opposed to this set of magnetic mirrors moving in, is the built-in magnetic mirror in the galactic arm, which reaches its maximum strength at 6 kps radius. In addition its strength is increasing with time; consequently it is equivalent to a mirror of constant strength moving outward along the arm, toward the set of incoming mirrors, with velocity $V_m = v$, where v is the local tangential velocity, about $2\cdot 10^7$ cm/s.

We now see that there exists in a natural way, as a consequence of the differential rotation of the Galaxy, a Fermi accelerator composed of two sets

([17]) H. ALFVÉN: *Cosmical Electrodynamics* (Oxford, 1950).

of mirrors, which relatively speaking, move always toward each other, and yet never come together. Because they move toward each other, particles in the region between them and spiralling along the lines of force that connect them, collide alternately with each mirror.

6. – First order moving mirror Fermi accelerator.

A charged particle spiralling in the region of the sun bounces back and forth between the two mirrors, gaining energy on each galactic mirror collision. The rate of gaining energy is first order in the quantity $a = (V_{\text{mirror}}/v_{\text{particle}})$ because all collisions with the built-in galactic mirror are head on. Although an energetic particle, or one whose velocity vector is nearly parallel to the field direction, may penetrate (E. FERMI [18]) several smaller hydromagnetic waves as it spirals out along a line of force, eventually it will meet a wave w_0 sufficiently strong to reverse it and reflect it back into the arm with a gain or loss in energy $\mathrm{d}E$.

According to the well-known Fermi cosmic accelerator hypothesis, the rate at which a particle gains energy E is given by

$$\frac{\mathrm{d}E}{\mathrm{d}t} = \frac{aE}{T_1}\,, \qquad \text{where } a = (V_{\text{mirror}}/v_{\text{particle}})\,, \tag{13}$$

and $T_1 = d/v$ is the time to travel between mirrors, d being the distance between the mirrors. In the pessimistic case discussed above, when collision with hydromagnetic wave mirrors produces reversal of direction but no average energy gain, T_1 is the time for a particle to make a round trip from the intrinsic mirror and back to it again, and d is the corresponding distance.

The rate of loss of charged particles is given by

$$\frac{\mathrm{d}N}{\mathrm{d}t} = -\frac{N}{T_2}\,, \tag{14}$$

where N is the density of particles, $T_2 = L/v$ is the lifetime, and L is the distance for a particle to be removed from the cosmic ray spectrum by a catastrophic process. Then

$$N/N_0 = E^{-(T_1/aT_2)}\,.$$

[18] E. FERMI: *Phys. Rev.*, **75**, 1169 (1949); *Astrophys. Journ.*, **119**, 1 (1954).

Three conditions may now be mentioned, first that the power of E must be 1.5 in order to agree with the experimentally observed cosmic ray spectrum:

$$\frac{T_1}{aT_2} = \frac{d}{aL} = 1.5 \,. \tag{15}$$

Secondly, we require the catastropic mean free path L to be small compared with both $5\cdot10^{25}$ cm and $4\cdot10^{24}$ cm, the mean free paths for nuclear collision of high energy protons and of Fe nuclei respectively (MORRISON, OLBERT and ROSSI [19]). We take for protons $L=5\cdot10^{25}$ and discuss the situation with Fe ions later.

And thirdly, the distance between mirrors, d, should be larger than the hydromagnetic wave length λ. Also, λ should sometimes be large enough to bend and accelerate cosmic ray particles up to the highest energies presently known, namely 10^{18} eV. That is, λ should be larger than the Larmor radius (cp/eH) for these particles in the field of $7\cdot10^{-6}=H$ G,

$$d>\lambda>(cp/eH)=(10^{18})(1.6\cdot10^{-12})/(4.8\cdot10^{-10})(7\cdot10^{-6}) \qquad d>5\cdot10^{20}\text{ cm}\,. \tag{17}$$

From (15), (16) and (17) one finds for protons

$$a=\frac{d}{1.5L}>\frac{5\cdot10^{20}}{1.5\cdot5\cdot10^{25}}=0.7\cdot10^{-5}\,.$$

We may compare this value of a, required for acceleration, with that corresponding to the two sets of mirrors, the hydromagnetic waves having characteristic velocity $\sim2\cdot10^{6}$ cm/s, with minor variations depending on the square root of local field strength and density, and the mirror in the galactic arms having approximately the tangential velocity of motion of the galaxy, varying from $2.0\cdot10^{7}$ cm/s at 9 kps radius to $1.3\cdot10^{7}$ at 6 kps radius.

For completely relativistic particles, a is $0.5\cdot10^{-4}$ for the hydromagnetic mirror, and $0.7\cdot10^{-3}$ for the mirror of the arm. One sees that the value of a for the galactic mirror appears sufficiently large to meet the above requirement.

It would seem from the rough analysis given here that the two sets of mirrors approaching each other in the galactic arm have properties such that they can accelerate particles to the highest energies yet observed in the cosmic ray spectrum. (We must, of course, recognize the existence of the magnetic halo of the Galaxy as a region able to contain such high energy particles for long periods of time, as has been discussed by MORRISON [20]).

[19] P. MORRISON, S. OLBERT and B. ROSSI: *Phys. Rev.*, **94**, 440 (1954).
[20] P. MORRISON: *Rev. Mod. Phys.*, **29**, 235 (1957).

7. – Randomizing machinery.

The condition that particles are reflected at a mirror is $\sin^2\theta = B/B_0$, namely that a particle whose velocity vector makes an angle with the magnetic field vector B, is reflected when it has traveled into a region of field strength B_0. Now the mirrors discussed above have an increase of field $(B-B_0)/B_0 = 10^{-1}$ in a distance of 1 turn at $r = 9$ kps. The change in magnetic field $\Delta H/H$ corresponding to $d \sim 5\cdot 10^{20}$ cm $= 0.12$ kps is therefore

$$\left[\frac{\Delta H}{H}\right]_d = \frac{d}{2\pi r}\cdot\left[\frac{\Delta H}{H}\right] = \frac{0.12}{2\pi\cdot 9}\left[\frac{\Delta H}{H}\right] \simeq 2\cdot 10^{-4}\,.$$

Consequently only those particles having angle θ close to 90° are reflected in distance, d, namely

$$\cos^2\theta \sim \Delta\theta^2 \simeq \left[\frac{\Delta H}{H}\right]_d \simeq 2\cdot 10^{-4}\,,$$

$$\Delta\theta \sim 1.4\cdot 10^{-2}\,.$$

The fraction of particles reflected per trip is proportional to the solid angle containing their velocity vectors;

$$\tfrac{1}{2}\sin\theta\,\Delta\theta \sim \tfrac{1}{2}\Delta\theta \sim \tfrac{1}{2}(1.4\cdot 10^{-2}) \sim 0.7\cdot 10^{-2}\,.$$

That is, 99% of the particles are not mirror reflected unless a perturbation occurs which alters the orientation of the velocity vector to the magnetic field direction.

A strong perturbation, able to randomize the values of θ is furnished by the ion clouds around the stars strewn along the galactic arms. The light output from an average star is sufficient to ionize gas around it to a radius of $\sim 10^{18}$ cm, creating a sphere of ionized material of sufficient density and kinetic energy that it acts as a superconductor and pushes the galactic magnetic field lines out of itself. Therefore, to every such average star there corresponds a bump in the nearby lines of magnetic field, of length and amplitude $\sim 10^{18}$ cm. This is a distance commensurable with the Larmor radius of particles of cosmic ray energies and consequently able to randomize their corresponding velocity to field angles.

The radius R of ionized cloud around a star is computed as follows. Let N_p be density of protons (or electrons). The magnetic field is expelled when

$$N_p\left[\frac{1}{2}\,M_p v^2\right] \geqslant \frac{H^2}{8\pi}$$

namely when kinetic energy density of ions is greater than or equal to energy density of the galactic magnetic field.

To find N_p in a steady state condition around a star, write

$$\frac{dN_p}{dt} = \frac{I}{h\nu}\sigma_{\gamma p} N_p - N_p N_e \sigma_{ep} V_e = 0 ,$$

where I is the energy flux from the star, of photons, of average energy $h\nu$ having energy sufficient to ionize hydrogen, $\sigma_{\gamma p}$ and σ_{ep} are cross-sections for photoionization and for electron-proton recombination respectively, and v_e is electron velocity. Because $N_p = N_e$, it follows that

$$N_p = \frac{I}{h\nu}\frac{\sigma_{\gamma p}}{\sigma_{ep}}\frac{1}{v_e} .$$

At distance R from a star of energy output I, this is given by

$$I = \frac{I_0}{4\pi R^2}\frac{1}{30} ,$$

where the factor 1/30 is put in to take into account that only 1/30 of the energy output of the star is in the form of photons of 3 000 Å, namely energetic enough to ionize hydrogen. The value of I_0 is taken to be $3.8 \cdot 10^{33}$ erg/s. One finds that $R \leqslant 10^{18}$ cm.

The effective cross-section for a magnetic collision is $\sigma = \pi R^2$, and the length for such a collision is

$$\Lambda = \frac{1}{N_s \sigma} ,$$

where N_s is the density of stars $= 3.5 \cdot 10^{-56}$. Then $\Lambda = 10^{19}$ cm. It follows that in a path $d \sim 5 \cdot 10^{20}$ cm for minor collision, a particle makes 50 collisions with average sized bumps in the galactic magnetic field, so that the orientation of its velocity vector the magnetic field direction is well randomized between energy gaining collisions, correspondingly particles of all velocity components in the direction of the magnetic field have equal probability to be reflected by the mirror, namely 1% in distance d.

The effective distance d for mirror reflection is consequently 100 times longer, namely $5 \cdot 10^{22}$ cm, corresponding to a required value of $\alpha = 0.7 \cdot 10^{-3}$ for protons, this requirement is still in agreement with the value of α of the hydromagnetic mirrors, for protons, but not for Fe ions.

One should point out that the energy which this accelerator transforms into cosmic ray energy is coming from the differential energy of rotation of the

Galaxy on one hand (the major source, apparently), and to a much smaller extent from the turbulent energy of gas clouds in the halo, which produces the hydromagnetic waves that eventually arrive in the galactic arm. Local turbulence in the neighborhood of the sun does not give a measure of this last quantity.

The differential energy of rotation is sufficient to provide the energy for cosmic ray production. Its density given approximately by

$$\int_{4}^{14\,\text{kps}} \varrho v \left(\frac{\mathrm{d}v}{\mathrm{d}r}\right) \mathrm{d}r = (10^{-24}\ \text{g/cm}^3)(2\cdot 10^7\ \text{cm/s})(1\cdot 10^6\ \text{cm/s kps})(10\ \text{kps}) \simeq$$

$$\simeq 10^{-10}\ \text{erg/cm}^3\,.$$

The present day cosmic ray energy production requires 10^{-12} erg/10^7 years. The present day differential rotation energy is able to supply that for 10^9 years. The availability of energy of rotation has been pointed out before, *e.g.* by MORRISON ([20]).

* * *

The author is indebted to Professor BENGT STRÖMGREN for many conversations, and grateful to professor ROBERT OPPENHEIMER for a pleasant stay at the Institute for Advanced Study, where this paper was written.

RIASSUNTO (*)

Si mostra che l'attuale distribution di velocità della Via Lattea amplifica il campo magnetico nei bracci galattici stirando le esistenti linee di forza in modo da formare specchi magnetici nella regione fra 4 e 10 kps di raggio. La forza degli specchi cresce col tempo cosicchè, in effetti, uno specchio di forza data sembra muoversi verso l'esterno lungo il braccio. Si avanza l'ipotesi che questi specchi, fissi ad un raggio costante ma che in effetti si muovono, abbiano importanza nella produzione dei raggi cosmici, e si mostra che le opportune costanti riferentisi agli specchi sono compatibili con un meccanismo acceleratore di Fermi con dipendenza di primo ordine dalle velocità effettive dello specchio. L'energia per questo processo è derivata dall'energia differenziale di rotazione di cui si ha un rifornimento adeguato.

(*) *Traduzione a cura della Redazione.*

IL NUOVO CIMENTO Vol. XIX, N. 1 1° Gennaio 1961

Mesic Decays of Hypernuclei from K⁻-Capture.

II. Branching Ratios in the Charged Mesic Decay Modes of $^3H_\Lambda$, $^4H_\Lambda$, $^4He_\Lambda$ and $^5He_\Lambda$ (†).

R. G. Ammar (*), R. Levi Setti and W. E. Slater (**)

The Enrico Fermi Institute for Nuclear Studies, The University of Chicago - Chicago, Ill.

S. Limentani (***), P. E. Schlein (**) and P. H. Steinberg (**)

Northwestern University - Evanston, Ill.

(ricevuto il 18 Luglio 1960)

Summary. — Branching ratios in the charged mesic decay modes of hyperfragments with charge $Z \leqslant 2$ and mass number $A \leqslant 5$ are presented here, based on a total of 162 events. Such relative frequencies are relevant in discussing the consequences of charge independence, the $\Delta T = \frac{1}{2}$ rule as applied to hypernuclei, and the spin dependence of the Λ-nucleon interaction. In particular, the ratio R_4 of (π^--recoil) with respect to all π^- decays for $^4H_\Lambda$ was found to be $R_4 = 0.67^{+0.06}_{-0.05}$, where the errors represent statistical uncertainties only. Comparing this with the curves of R_4 *vs.* (p/s) calculated by Dalitz and Liu ([6]) on the two assumptions ($J = 0, 1$) regarding the spin of $^4H_\Lambda$, we conclude that the value $J = 0$ is more probable, as already suggested ([3,6]) on the basis of our preliminary data. If this spin assignment is accepted, following the above authors ([6]), one may infer that for the ratio of p- to s-wave amplitude in the charged decay of the free Λ, $0.45 \leqslant p/s \leqslant 1.4$. Finally, although they should have the same general configuration as the π^- events, no examples of decays involving either the emission of a π^+ or a charged lepton have been identified in the present sample.

(†) Research at the University of Chicago was supported by the U. S. Air Force Office of Scientific Research, Contract no. AF 49(638)-209. Research at Northwestern University was supported by the National Science Foundation and by the U. S. Atomic Energy Commission through Argonne National Laboratory subcontract.

(*) Now at Northwestern University, Evanston, Ill.

(**) Now at University of California, Los Angeles 24, Cal.

(***) Now at Lawrence Radiation Laboratory, Univ. of California, Berkeley, Cal.

(**) Now at Johns Hopkins University, Baltimore 18, Md.

(**) Now at University of Maryland, College Park, Md.

1. – Introduction.

In Part I (EFINS-NU collaboration [1]) we were primarily concerned with presenting precise values of the Λ-binding energy (B_Λ) for various hypernuclides. Events selected for this purpose did not necessarily represent an unbiased subset of the total population. In addition it was not possible at that time, on the basis of a single scan, to evaluate such quantities as the relative efficiency of detecting different decay modes. With the completion of a rescan of the stacks it is now possible to discuss the branching ratios in the decays of several hypernuclides.

There is considerable interest in a systematic determination of the relative frequencies for various decay modes of a given hypernuclide in which a charged pion is emitted. Such frequencies are relevant in discussing the consequences of the spin dependence of the Λ-nucleon interaction, charge independence, and of the $\Delta T = \frac{1}{2}$ rule as applied to hypernuclei, and have been the subject of several theoretical investigations [2-9]. In particular the frequencies R_3, R_4 of the π-r modes

$$ {}^3\mathrm{H}_\Lambda \to \pi^- + {}^3\mathrm{He} \tag{1} $$

and

$$ {}^4\mathrm{H}_\Lambda \to \pi^- + {}^4\mathrm{He} \tag{2} $$

relative to the totality of π^- decays for ${}^3\mathrm{H}_\Lambda$ and ${}^4\mathrm{H}_\Lambda$ respectively may in principle be used to infer the spins J_3, J_4 of these hypernuclides. It was first pointed out by DALITZ [2] that R_3 and R_4 are sensitive functions of the spin J_3 and J_4 as well as of the relative amount of s and p wave amplitude in the decay of the free Λ. For example (1) can proceed only through the p channel if the spin $J_3 = \frac{3}{2}$, while (2) may proceed only through the s (p) channel accordingly as $J_4 = 0$ (1). Detailed calculations of this dependence $R(J, p/s)$ have been discussed by several authors [3,4,6-8] Thus a knowledge of R

(1) R. G. AMMAR, R. LEVI SETTI, S. LIMENTANI, P. E. SCHLEIN, W. E. SLATER and P. H. STEINBERG: *Nuovo Cimento*, **15**, 181 (1960).
(2) R. H. DALITZ: *Rep. Progr. Phys.*, **20**, 163 (1957).
(3) R. H. DALITZ: *Phys. Rev.*, **112**, 605 (1958).
(4) R. H. DALITZ and B. W. DOWNS: *Phys. Rev.*, **111**, 967 (1958).
(5) R. H. DALITZ: *Rev. Mod. Phys.*, **31**, 823 (1959).
(6) R. H. DALITZ and L. LIU: *Phys. Rev.*, **116**, 1312 (1959).
(7) M. LEON: *Phys. Rev.*, **113**, 1604 (1959).
(8) L. E. PICASSO and S. ROSATI: *Nuovo Cimento*, **11**, 711 (1959).
(9) M. S. SWAMI and B. M. UDGAONKAR: *Nuovo Cimento*, **14**, 836 (1959).

together with p/s (or J) is useful in determining J (or p/s). Our preliminary determinations of R_3 and R_4 have already been reported by DALITZ ([10]). The final values reported at this time are essentially unchanged.

2. – Emulsion stack and scanning.

The exposure and calibration of the stacks have been described in I ([1]); of additional interest is the blob density g_0 at minimum ionization (300 MeV/c μ^-). This ranged approximately between 12 and 19 blobs/100 μm for the various sections of the stacks, which consisted of 1200 μm Ilford K-5 (EFINS stack) and 600 μm L-4 and K-5 pellicles (NU stack).

All our events were found by area-scanning that region where the K^- were expected to come to rest. This strip had a width of ~ 2.5 cm in the beam direction and extended 15 cm (length of the stack) normal to the beam.

The data in Part I came from the first scan; at that time we confined our attention primarily to the collection of those mesic hyperfragments which could be detected under low magnification using a dry objective (diameter of the field of view ~ 1200 μm). The additional data included here come from the «second scan»: this differs from the first primarily in that each K^- star was carefully examined under high resolution and each prong traced until it came to rest or left the pellicle. Thus, only hyperfragments which are produced and decay in a single pellicle are considered here.

Approximately $2\cdot10^{-4}$ K^- stars with at least one prong were examined in each stack. A total of 388 charged mesic decays at rest (EFINS 223, NU 165) have been found. These figures do not necessarily represent the true yield since due account has not been taken of the effect of finite pellicle thickness. The loss due to the finite pellicle thickness is of order 1% for the EFINS stack which consisted of the relatively thick 1200 μm pellicles (*).

3. – Detection biases.

3·1. *Scanning efficiency.* – Table I illustrates typical configurations which are encountered in the decay at rest of the hypernuclides under investigation. The π-r events consist of a short recoil together with a colinear lightly ionizing

([10]) R. H. DALITZ: *Reports of the Kiev Conference on High Energy Physics* (1959).

(*) In connection with another investigation, the grey and black prongs of the K^- stars in the EFINS stack were subsequently followed to their end in neighboring pellicles. Only 3 charged mesic hyperfragments were found ($2\ {}^3H_\Lambda$, $1\ {}^4H_\Lambda$). These events are included in the distributions of Figs. 2, 3 and 5, but are not included in the statistics for the determination of R_3 and R_4.

pion. In contrast to this configuration, the other modes often have a fairly long black track in addition to a π^- and recoil and hence one might expect them to be more readily detected.

TABLE I. – *Typical configurations encountered in the decays at rest of* $^{3,4}H_\Lambda$, $^{4,5}He_\Lambda$.

Decay mode	$\sim$ Pion range (cm)	$\sim g/g_0$	$\sim$ Recoil range (μm)	$\sim \sigma(Q)$ (MeV)
$^3H_\Lambda \to \pi^- + {}^3He$	2.6	1.6	8	0.8
$^4H_\Lambda \to \pi^- + {}^4He$	3.9	1.3	8	1
other H_Λ decays	< 2 (*)	1.7÷3	0÷100 (**)	0.7 (**)
He_Λ	< 2 (***)	1.7÷3	0÷ 35 (***)	0.6

(*) See Fig. 2 for the distribution of π^- ranges.
(**) See Fig. 5 for the distribution of the recoil momenta.
(***) See [12].
(**) For decays not involving neutrons.

From the number of coincidences in the several scans it is possible to determine the scanning efficiencies for various decays. In Table II, these are shown separately for the EFINS and NU stacks respectively. It is seen that there is not a large preferential bias against detecting the π-r modes relative to the others. For purposes of comparison this table also includes the efficiency for detecting π-r decays of hypernuclides with mass number $A > 5$ in which the recoil range is ~ 2 μm and which are perhaps the least conspicuous hyperfragment decays. We are of course not considering these decays here.

TABLE II. – *Scanning efficiencies for various decay configurations.*

Decay configuration	Scanning efficiency	
	EFINS	NU
a) π-r ($A \leqslant 4$)	0.97 ± 0.03	0.91 ± 0.07
b) π-r ($A > 5$)	0.89 ± 0.07	~ 1.0
c) others	0.96 ± 0.02	0.96 ± 0.03
d) $\dfrac{\text{efficiency for } a)}{\text{efficiency for } c)}$	1.02 ± 0.04	0.95 ± 0.08

3.2. « *Undetectable events* ». – The scanning efficiency determined above is to be understood as referring to events detected in at least one scan, truly « undetectable » events being missed in all scans. For example there may be a bias against detecting the π-r hydrogen decays in flight. For this reason and because we are unable to determine the extent of this loss with our present statistics, we considered only decays at rest. This corresponds to a rejection of only $\sim 2\%$ of the events.

3.2.1. Loss due to unfavourable geometry. – One might expect certain decays, by virtue of their specific geometry, to be less readily detectable, *e.g.* π-r events in which the pion is emitted directly forward or backward with respect to the hyperfragment track as well as other decays in which the pion may be obscured by the hyperfragment track. In exploring such a possibility, we consider the space angle θ between the direction of motion of

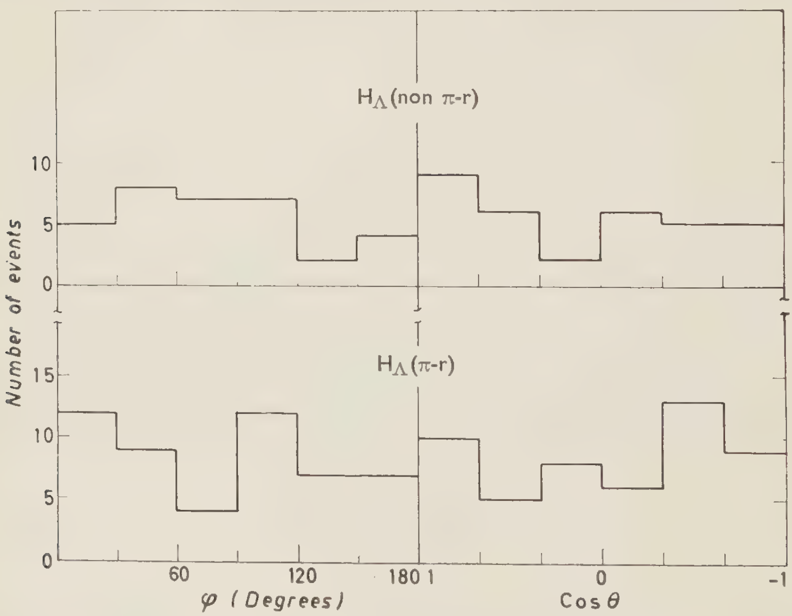

Fig. 1. - Distributions of the angle φ (projected in the emulsion plane) and θ (space angle) between the direction of motion of the hyperfragment and the direction of emission of the pion, for H_Λ events.

the π and hyperfragment at the decay point as well as φ, the projection of this angle in the plane of the emulsion. Fig. 1 gives the distributions over these angles both for the π-r and for the non-π-r events. Within our statistics, no appreciable loss is apparent for either type of events.

3.2.2. Loss due to ionization fluctuation. – Obviously, only those events are included here, for which the charged pion was detected. As seen from Section **2**, and Table I, the pions from *e.g.* $^4H_\Lambda(\pi\text{-r})$ may have rather low mean blob densities at emission (as low as ~ 16 blobs/100 μm) Due to statistical fluctuations there may be cases in which the pion track in the neighborhood of the decay is not well defined. Such an effect could in principle cause a preferential loss of these events, which would then be classified as potential π^0-decays (« hooks »). This possibility is not necessarily covered by scanning and geometrical losses discussed above.

A systematic examination of a large majority of « hooks » was carried out in connection with an investigation of π^0-decays (11). As a result of this search, which covered only $\frac{3}{4}$ of the stacks and $\frac{2}{3}$ of the recoil solid angle, it was found that $\sim 10\%$ of the $^4H_\Lambda$ (π-r) had been initially classified as hooks. Extrapolating to the total emulsion volume and solid angle we estimate that $\sim 5\%$ may still be undetected. We believe that this recovery and extrapolated loss adequately describe such an effect.

4. – Identification biases.

The general method of analysis here differs from that adopted in Part I. To avoid possible biases it is now important to assign an identity to every event without regard to obtaning precise binding energies which, for this experiment, are assumed to be given. Thus those events for which the pion did not come to rest in the stack (« incomplete events ») were included (see Section **4**.1). Furthermore, the usual kinematic analysis used in I was augmented by the following auxiliary means of identification (Section **4**.2): *Range distribution of the hyperfragment track* (**4**.2.1), *direct charge and mass measurements of hypernuclei* (**4**.2.2), *energy released in the decay* (**4**.2.3).

4.1. *Incomplete events.* – Incomplete events were obtained when the pion could not be traced to the end of its range, because it interacted in flight, or left the stack. As seen from Table I, the pions from π-r decays have longer ranges than those from the other modes. The pion range (momentum) spectrum for H_Λ is shown in Fig. 2. The corresponding distribution for He_Λ has already been given elsewhere (12). Because of the longer path length, the two-body modes may be expected to lead more frequently to an incomplete con-

(11) R. G. Ammar: *Nuovo Cimento*, **14**, 1226 (1959).
(12) R. G. Ammar, R. Levi Setti, S. Limentani, P. E. Schlein, W. E. Slater and P. H. Steinberg: *Nuovo Cimento*, **13**, 1156 (1959).

figuration. Approximately 15% of the events we considered here are incomplete, and it was therefore necessary to include them in the statistics.

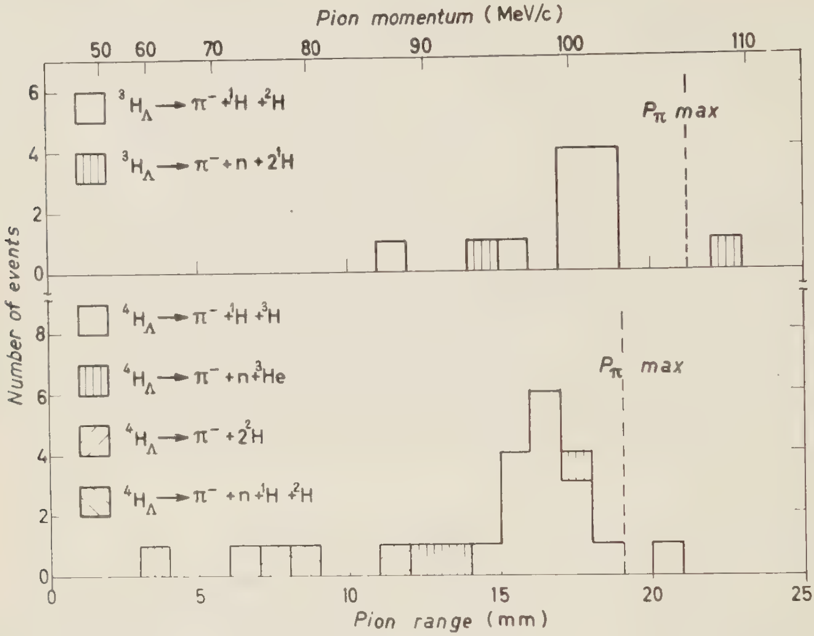

Fig. 2. – Pion range (momentum) distribution from the non-π-r-decay modes of $^3H_\Lambda$ and $^4H_\Lambda$ for those events with hyperfragment track longer than 50 μm.

In assigning an identity to these events we resorted, in favorable cases, to ionization measurements (blob density) as a function of range on the *incomplete* tracks. In addition, charge and mass measurements were made on the *hyperfragment* tracks whenever possible as an aid in the hyperfragment identification (see Section 4.2.2); from such information it is sometimes possible to infer whether the *incomplete* tracks represent pions or nuclear particles, thus distinguishing between mesic decays and the non-mesic ones or other background events. The inferred pion momentum (not very sensitive to the blob density measurements) was then used in the kinematic analysis of the decay. Such events obviously do not yield a reliable B_Λ value.

The incomplete events were identified in all but two cases. Both of these have configurations typical of the π-r decays of H_Λ, but because the « pion » tracks were steep, the blob density could yield no precise information. We conclude that they are most probably π-r decays of $^4H_\Lambda$ since the known frequency of these decays relative to the π-r decays of $^3H_\Lambda$, in our stack, is 10:1. Moreover, the probability of such a configuration being simulated by a background event is very small.

4·2. *Auxiliary means of identification.*

4·2.1. Hyperfragment range distribution. – Certain « heavy » hypernuclei (mass number $A > 5$) may simulate the decay modes of the « light »

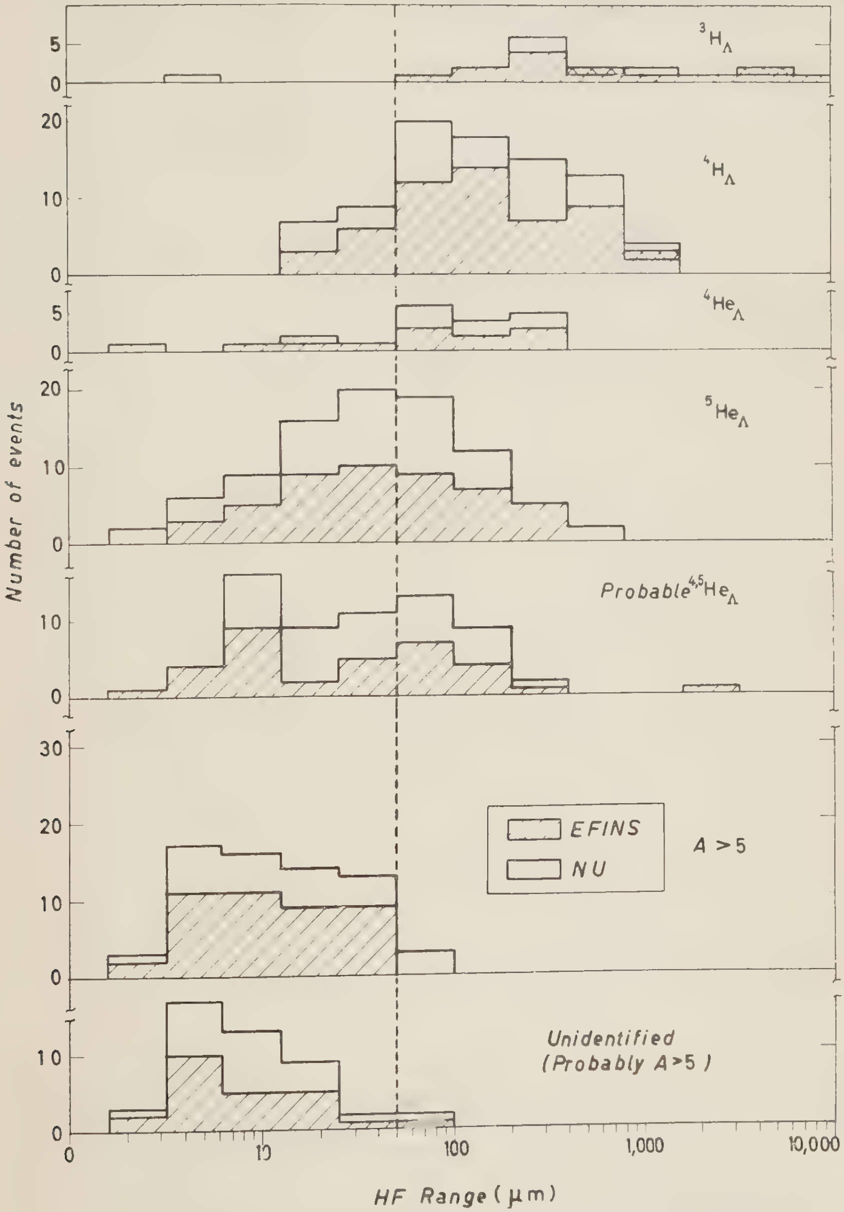

Fig. 3. – Range distribution of 396 hyperfragments in a single pellicle, decaying by π^- modes. Three additional events, contained in more than one pellicle, are shown by cross hatching (see footnote, Sect. 2).

ones ($A<5$), and it is therefore desirable to exclude them. Fig. 3 gives the range (R_c) distribution for all hyperfragments which come to rest in a single pellicle. As can be seen the spectrum for the « heavy » hypernuclei cuts off rather sharply at $\sim 50\ \mu m$ (only 5% exceed this range). On the other hand 85% of the ${}^{3,4}H_\Lambda$ and 50% of the ${}^{4,5}He_\Lambda$ yield ranges in excess of this value. Thus in the determination of R_3 and R_4 we consider only events with connecting tracks longer than $50\ \mu m$. In addition, for $R_c > 50\ \mu m$, one may, under favorable conditions, attempt a charge discrimination from profile measurements as described in (I). There are a total of 162 « light » hyperfragments which exceed this range. Applying only momentum balance in the decay process, we were able to assign an identity to 121 of these events (7 ${}^3H_\Lambda$, 61 ${}^4H_\Lambda$, 15 ${}^4He_\Lambda$, 38 ${}^5He_\Lambda$). Of the 41 ambiguous events, 12 are clearly ${}^{4,5}He_\Lambda$ (from momentum balance in the decay) which however cannot be individually identified as either ${}^4He_\Lambda$ or ${}^5He_\Lambda$. However it is possible to analyse them statistically from a knowledge of the separate range distribution for each species. *From Fig. 3 it follows that for* $R_c > 50\ \mu m$ *the relative proportion of* ${}^4He_\Lambda$ *to* ${}^5He_\Lambda$ *is* 15 : 38.

Of the remaining 29 events only 3, all $Z = 1$, had sufficiently long tracks (> 2 mm) to permit a mass discrimination from gap-length measurements. On this basis, the 3 events were all assigned $A = 3$, the measurements deviating from the value expected for $A = 4$ by > 1 standard error. Further corroborating evidence for this assignment will be discussed in Section 4.2.3.

We measured the charge Z of the remaining 26 hyperfragment tracks whenever possible (22 cases). Numerous events of known identity were also measured for purposes of comparison; details of these calibrations have been described elsewhere [1,13]. On the basis of the profile measurements we assigned 13 events to $Z = 2$, 9 to $Z = 1$, while 4 events could not be charge-identified.

Thus, in summarizing, we are able to classify the 41 ambiguous events as follows: 25 ${}^{4,5}He_\Lambda$ (7 ${}^4He_\Lambda$, 18 ${}^5He_\Lambda$), 3 ${}^3H_\Lambda$, 9 ${}^{3,4}H_\Lambda$, and 4 unidentified. In order to make a more specific assignment as to mass number or decay mode, it is necessary to consider the energy release in the decay.

4.2.3. Energy release in the decay. – Of the 16 (= 3 + 9 + 4) hyperfragments which could have unit charge, one is incomplete (it was identified as ${}^3H_\Lambda$ (π-r) solely on the basis of mass measurements in Section 4.2.2). The other 15 are all complete events and therefore suitable for analysis on the basis of the energy released in the decay.

[13] R. G. AMMAR: *Suppl. Nuovo Cimento*, **15**, 181 (1960).

The energy release for each decay mode of H_Λ is shown in Table III, the B_Λ's for $^3\mathrm{H}_\Lambda$ and $^4\mathrm{H}_\Lambda$ having been taken to be 0.12 MeV and 2.20 MeV respectively. The typical standard error $\sigma(Q)$ to be associated with decays not involving neutrons are indicated in Table I [1]. For the non-π-r decays in this category, $\sigma(Q) \simeq 0.7$ MeV, being somewhat higher if neutrons are emitted, the value depending on the specific configuration.

TABLE III. – *Decay modes of* $^3\mathrm{H}_\Lambda$ *and* $^4\mathrm{H}_\Lambda$.

Hypernuclide	Decay mode	$\sim Q$ (MeV)	EFINS complete	EFINS incomplete	EFINS total	NU complete	NU incomplete	NU total
$^4\mathrm{H}_\Lambda$	$\pi^-+{}^4\mathrm{He}$	55.2	18	9	27	10	7+(2)	19
	$\pi^-+{}^1\mathrm{H}+{}^3\mathrm{H}$	35.4	4+(5)	2+(1)		2+(2)	—	
	$\pi^-+\mathrm{n}+{}^3\mathrm{He}$	34.6	3	—		1	—	
	$\pi^-+{}^2\mathrm{H}+{}^2\mathrm{H}$	31.4	1	—	17	1	—	6
	$\pi^-+{}^1\mathrm{H}+{}^2\mathrm{H}+\mathrm{n}$	29.1	1	—		—	—	
	$\pi^-+2{}^1\mathrm{H}+2\mathrm{n}$	26.9	—	—		—	—	
$^3\mathrm{H}_\Lambda$	$\pi^-+{}^3\mathrm{He}$	42.9	4	—	4	—	1	1
	$\pi^-+{}^1\mathrm{H}+{}^2\mathrm{H}$	37.5	5	—	7	3	—	3
	$\pi^-+2{}^1\mathrm{H}+\mathrm{n}$	35.2	1	1		—	—	

Only those events are included for which the hyperfragment track is longer than 50 μm and comes to rest within a single pellicle.

The numbers in parenthesis correspond to events of ambiguous kinematical identification, which have been classified on the basis of the criteria discussed in Sect. 4.2.

The above 15 events consist essentially of only a pion and a long prong, the recoil being either invisible or too short to be identified from momentum balance. Fig. 4 shows a histogram of the Q's for these events on the assumption that the second prong is a proton; any other assumption as to the identity of this prong leads to inconsistencies (*e.g.* large momentum unbalance, larger Q's than are permissible, etc.). Those events with Q values in excess of ~ 37 MeV (approximately 2σ from the next higher permissible Q) have all (7)

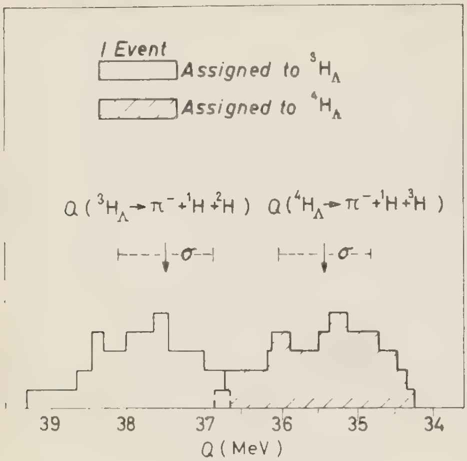

Fig. 4. – Histogram of the visible energy release for 15 H_Λ events in which essentially only a pion and a proton track are vis ble (short or undetectable recoil, see Sect. 4·2.3).

been assigned to ${}^3H_\Lambda$ (π-p-r). Indeed, on this assignment, the recoil momenta are all $\leqslant 30$ MeV/c, and are not expected to result in visible recoils.

The remaining 8 events in this figure (shaded region) may be either ${}^4H_\Lambda$ (π, p, r) or ${}^3H_\Lambda$ (π, p, p, n) which, as seen in Table III, have the same Q, and are «unidentifiable».

4·3. « *Unidentifiable* » H_Λ *events*. – In all the 8 «unidentifiable» events referred to above, the vector sum of the pion and proton momenta (equal and opposite to the recoil momentum) is always small (<30 MeV/c) and moreover points approximately antiparallel to the proton direction. Hence, if these events represent the decay ${}^4H_\Lambda$ (π, p, r) the recoil ${}^3H$ (with range $\leqslant 1.5$ μm) could be obscured by the long black proton track and thus be undetected.

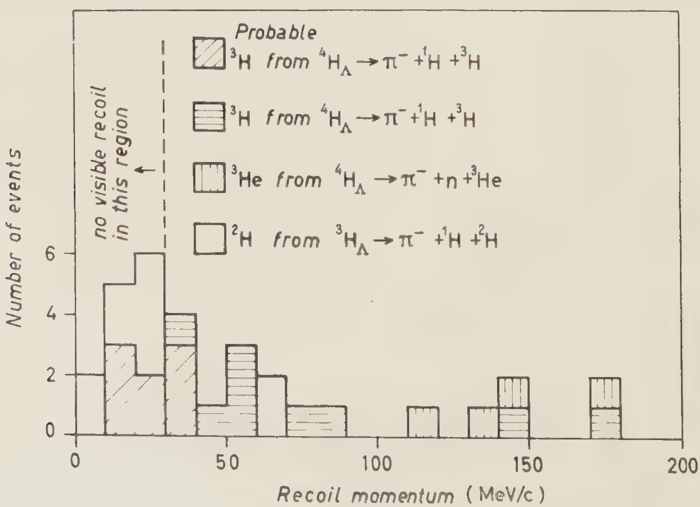

Fig. 5. – Distribution of the recoil momenta from the non-π-r decay of ${}^{3,4}H_\Lambda$ events.

In addition, as can be seen from Fig. 5, the distribution of recoil momenta from known ${}^4H_\Lambda$ extends down into this region and the assignment of all the 8 events to ${}^4H_\Lambda$ would be quite consistent with the rest of the distribution.

On the other hand it is unlikely that all 8 events represent the decay $^3H_\Lambda$ (π, p, p, n), since in this case two particles (p, n) are to share the missing momentum. Thus, in the absence of a peculiar mechanism, it is improbable that the charged particle (p) should always *a*) carry off little momentum, or *b*) point along the longer black proton track, and hence be obscured.

5. – Results and discussion.

A breakdown of the $^{3,4}H_\Lambda$ events according to their decay modes is shown in Table III, where complete and incomplete events are shown separately, and the EFINS and NU data are compared. The figures in parenthesis refer to the 8 events discussed in Section 4.2.3, all of which have been assigned to $^4H_\Lambda$. In accordance with the arguments presented there, this is the most likely assignment, and they have been included in Figs. 2 and 3 as such, although one cannot exclude the possibility that a small number of these may be $^3H_\Lambda$.

Computing R_3, R_4, taking into account the necessary corrections, (*e.g.* scanning efficiency) we find:

$$R_3 = 0.33^{+0.10}_{-0.13}\,, \tag{3}$$

$$R_4 = 0.67^{+0.06}_{-0.05}\,. \tag{4}$$

Table IV*a* gives a breakdown of the He_Λ events with $R_c > 50\ \mu m$. In

TABLE IV. – *Decay modes of* $^4He_\Lambda$ *and* $^5He_\Lambda$.

Hyper-nuclide	Decay mode	$\sim Q$ (MeV)	*a*) $R_c > 50$		*b*) $R_c > 20$		*c*) EFINS $1 < R_c \leq 20$	
			complete	incomplete	complete	incomplete	complete	incomplete
$^4He_\Lambda$	$\pi^- + {}^1H + {}^3He$	35.2	14+(7)	1	15+(9)	1+(1)	1+(1)	—
	$\pi^- + 2\,{}^1H + {}^2H$	29.7	—	—	—		1	
	$\pi^- + 3\,{}^1H + n$	27.5	—	—	1	—	—	—
$^5He_\Lambda$	$\pi^- + {}^1H + {}^4He$	34.5	36+(16)	2+(2)	56+(28)	5+(3)	16+(14)	1
	$\pi^- + {}^2H + {}^3He$	16.2	—	—	1	—	—	—

Numbers in parenthesis represent $^{4,5}He_\Lambda$ events which have been assigned to $^4He_\Lambda$ and $^5He_\Lambda$ respectively in proportion to the relative frequency of the identified decays of $^4He_\Lambda$ and $^5He_\Lambda$ in a given R_c interval (see Sect. 4.2).

addition, Table IV*b* gives a similar compilation for $R_c > 20\ \mu\text{m}$ where we have been able to ascertain on an individual basis that none of the probable $A > 5$ events with $R_c > 20\ \mu\text{m}$ (see Fig. 3) could be He_Λ. Finally in order to display a rare decay mode of $^4\text{He}_\Lambda$, Table IV*c* includes all He_Λ events with $1\ \mu\text{m} < R_c \leqslant 20\ \mu\text{m}$ from the EFINS stack where again we could exclude any possible contamination from the probable $A > 5$ events.

In view of the importance of R_4 in deducing the spin of $^4\text{H}_\Lambda$ it is useful to discuss the various possible sources of systematic errors as well as their order of magnitude.

Several effects are of such a sign as to cause a systematic underestimate of R_4. In this connection the effect of the loss of π-r modes discussed in **3**'2 on R_4 is not expected to be appreciable. However, the assignment of all 8 unidentified H_Λ events to $^4\text{H}_\Lambda$ (see Section **4**'3) together with the preceding effect may introduce a systematic error.

On the other hand there is a competing effect of opposite sign which tends to result in an overestimate of R_4. The decay:

$$^4\text{H}_\Lambda \to \pi^- + \text{n} + {}^3\text{He} \tag{5}$$

results in only two charged particles in which, moreover, the momentum distribution for the recoil (^{3}He) may extend down to low values where the efficiency for detecting the configuration is rather small. No appreciable loss is expected for ^{3}He momenta > 50 MeV/c corresponding to ranges $> 2\ \mu\text{m}$ since, as can be seen from Table I, the efficiency of detecting π-r decays of $A > 5$ hypernuclei (which have typical recoil ranges $\sim 2\ \mu\text{m}$) is not appreciably different from that for other modes. For momenta > 50 MeV/c the frequency of (5) relative to that of

$$^4\text{H}_\Lambda \to \pi^- + \text{p} + {}^3\text{H} \tag{5'}$$

is observed to be 4:7. It is however somewhat hazardous to estimate the loss of events (5) with recoil momenta $\leqslant 50$ MeV/c by an extrapolation on events (5′) in the same momentum interval together with the assumption that the relative frequency of (5) to (5′) is a constant independent of recoil momentum (*). Such low recoil momenta correspond essentially to the decay of a quasi free Λ and in the limit of a truly free decay (5′) would correspond to the primary decay process

$$\Lambda \to \pi^- + \text{p}\,, \tag{6}$$

(*) R. H. DALITZ: private communication.

while (5) would then be possible only as a two step process. In the absence of certain knowledge concerning the momentum dependence of the ratio (5):(5′) we have made no attempt to correct for a possible loss of events (5) with low recoil momenta.

In conclusion we note that the various systematic errors tend toward cancellation and their net effect could probably be best taken into account by increasing the error limits on R_4 by about 40%. The error limits on R_4 which are shown in (4) and Fig. 6 are purely statistical and have not been so increased.

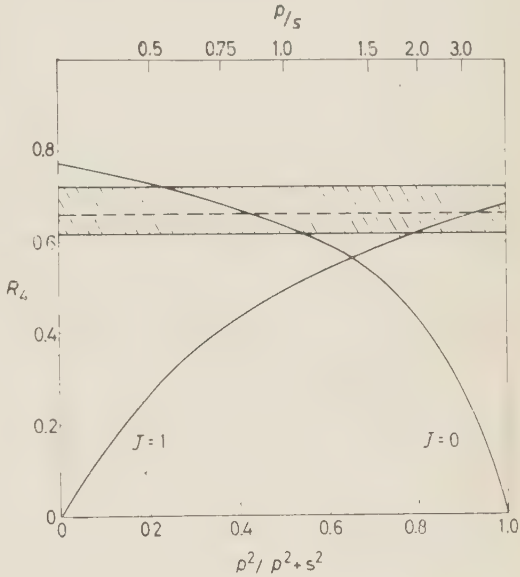

Fig. 6. – The value $R_4 = 0.67^{+0.06}_{-0.05}$ is indicated in the shaded region. The curves of R_4 *vs.* p/s are those calculated by DALITZ and LIU [6], for the two assumptions ($J = 0$, 1) regarding the spin of $^4H_\Lambda$.

6. – Conclusions.

Due to the large uncertainty in the value for R_3 it is not possible to draw stringent conclusions concerning say the spin of $^3H_\Lambda$ except to the extent that the data are consistent with the conclusions concerning the Λ-nucleon interaction which may be inferred from R_4. Clearly it is necessary to increase the statistics by at least an order of magnitude before attempting a serious comparison with the theoretical calculations.

The situation for $^4H_\Lambda$ is somewhat more promising. Fig. 6 shows the curves calculated by DALITZ and LIU [6] for the two assumptions ($J = 0$ or 1) for the spin of $^4H_\Lambda$. The experimental value of R_4, together with its statistical error is also shown. In order to discriminate between $J = 0$ and $J = 1$, it is necessary to have additional information concerning the p/s ratio in Λ-decay. Using the experimental data on the up-down asymmetry in the free Λ-decay, DALITZ has shown [3] that $0.45 \leqslant p/s \leqslant 2.25$, where the limits correspond to the assumption that the polarization of the Λ in these experiments is $\leqslant 70\%$. With reference to Fig. 6 it can be seen that, with these rest ictions on p/s, $J = 0$ is more probable, the value for R_4 lying (at its closest) ~ 1 standard deviation from the curve for $J = 1$. Using these data, a similar conclusion has

already been arrived at by DALITZ and LIU (6) and is further supported by arguments given there concerning the maximum permissible p/s ratio consistent with experimental data on the non-mesic/mesic ratio (14) in the decay of light hypernuclei.

If one accepts this spin assignment ($J=0$) it is possible to impose narrower limits (6) on p/s viz.,

$$0.45 \leqslant p/s \leqslant 1.4\,. \tag{7}$$

The upper limit obtains when allowance is made for a value of R_4 lower than the observed one by two standard deviations. An increase of the standard deviation on R_4 by 40%, suggested (Section **5**) in order to take into account possible systematic errors in the experiment would increase the above limit by only 0.2. Possible uncertainties in the theoretical curve of Fig. 6 could however affect the present assignment of limits to the p/s ratio.

We would like to mention explicitly the absence of the following two decays: *a*) those involving π^+ emission and *b*) those emitting a charged lepton.

a) The absence of π^+ decays in our sample of light hyperfragments should be viewed in the light of the following considerations: for hypernuclei with $Z=1$ the π^+ is the only charged particle in the final state and hence there probably exists a severe bias against its detection. Of the $Z=2$ events, π^+ emission from $^5He_\Lambda$ is rather unlikely because it involves a breakup of the α-particle in the initial state. The frequency of π^+ emission for $^4He_\Lambda$ has been calculated by DELOFF *et al.* (15) using a virtual Σ^+ in the intermediate state; they predict a frequency of order 10^{-2} for π^+ relative to π^- decays for $^4He_\Lambda$. Hence our present total of approximately 30 $^4He_\Lambda$ events is not suited for testing such a prediction.

b) It is not possible to make a detailed experimental comparison of the frequency of leptonic decay for the free and bound Λ without taking into account such modifying effects as for example the Pauli principle. However, the absence of such decays in our present sample is unlikely to be consistent with the estimates (about 2 percent) made by FEYNMAN and GELL-MANN (16) for the free Λ. Indeed experimental results from Berkeley (17) have already in-

(14) W. F. FRY, J. SCHNEPS and M. S. SWAMI: *Phys. Rev.*, **106**, 1062 (1957); E. SILVERSTEIN: *Suppl. Nuovo Cimento*, **10**, 41 (1958); P. E. SCHLEIN: *Phys. Rev. Lett.*, **2**, 220 (1959); S. LIMENTANI P. E. SCHLEIN, P. H. STEINBERG and J. H. ROBERTS: *Bull. Am. Phys. Soc.*, **4**, 289 (1959).

(15) A. DELOFF, J. SZYMANSKI and J. WRZECIONKO: *Pol. Acad. Sci.*, Report no. 95/VII (1959).

(16) R. P. FEYNMAN and M. GELL-MANN: *Phys. Rev.*, **109**, 193 (1958).

(17) F. S. CRAWFORD jr., M. CRESTI, M. L. GOOD, G. R. KALBFLEISCH, M. L. STEVENSON and H. K. TICHO: *Phys. Rev. Lett.*, **1**, 377 (1958).

dicated that the observed frequency of leptonic decays for the free Λ may be considerably less than the theoretical estimate and our results are in essential qualitative agreement with such an observation.

* * *

We have profited from numerous discussions with Professors R. H. DALITZ and V. L. TELEGDI. Their suggestions and criticism during the course of the present investigation and help in the writing of the manuscript have been very much appreciated. The authors who carried out the present investigation at Northwestern University (S. L., P. E. S, P. H. S.) are particularly grateful to Professors L. BROWN and J. H. ROBERTS for their continuous help and guidance in the various stages of the present work.

N. CRAYTON, J. MOTT, P. SHRIVASTAVA at EFINS, D. ABELEDO, B. BUNKER, S. LINFIELD, R. TREVINO at NU gave considerable assistance in the measurements. To them and to the scanning teams at EFINS and NU we are greatly indebted. We wish to thank Dr. E. J. LOFGREN, Dr. H. HECKMANN and the Bevatron staff for their invaluable co-operation in the exposure of the stack.

RIASSUNTO

Si presentano in questo lavoro i rapporti di ripartizione tra i vari modi di decadimento con emissione di pioni carichi, per gli iperframmenti di carica $Z = 2$ e numero di massa $A \leqslant 5$, su un totale di 162 eventi. Tali frequenze relative sono importanti nel discutere le conseguenze dell'indipendenza di carica, della regola di selezione $\Delta T = \frac{1}{2}$, applicate agli ipernuclei, e della dipendenza di spin nell'interazione Λ-nucleone. In particolare, il rapporto R_4 dei decadimenti (π^--rinculo) rispetto al totale dei decadimenti con emissione di π^- per l'$^4H_\Lambda$ risulta $R_4 = 0.67^{+0.06}_{-0.05}$ dove i limiti d'errore rappresentano soltanto incertezze statistiche. Dal confronto con le curve che legano R_4 al valore del rapporto p/s, calcolate da DALITZ e LIU ([6]) per le due ipotesi ($J = 0, 1$) al riguardo dello spin dell'$^4H_\Lambda$, si conclude che il valore $J = 0$ è il più probabile, come già suggerito ([3,6]) in base ai nostri risultati preliminari. Se si accetta questo valore dello spin, seguendo gli autori citati ([6]), è possibile assegnare i seguenti limiti per il rapporto delle ampiezze d'onda p ed s nel decadimento della Λ libera in particelle cariche: $0.45 \leqslant p/s \leqslant 1.4$. Infine, nel presente gruppo di eventi, non si sono trovati esempi di decadimento con emissione di π^+ o di leptoni carichi, sebbene tali decadimenti non dovrebbero differire nelle loro caratteristiche esteriori da quelli in cui viene emesso un π^-.

IL NUOVO CIMENTO VOL. XIX, N. 1 1° Gennaio 1961

Effect of Final State Interactions on the (Σ^-, d) Capture Reactions (*).

YUNG YI CHEN

Physics Department, University of Maryland - College Park, Md.

(ricevuto il 23 Luglio 1960)

Summary. — The effects of the two neutron final state interaction in the reaction $\Sigma^- + d \to (\Lambda^0 \text{ or } \Sigma^0) + n + n$ are calculated using the impulse approximation with the assumption of S-wave absorption and even relative parity between hyperons. Comparing the results with those neglecting all final state interactions, one finds that the Σ^0 production can be enhanced by a factor ~ 6 while the Λ^0 production is increased by only $\sim 10\%$. The most recent experimental results on the branching ratio of the two hyperon-productions can now be fit with a less extreme assumption about the spin dependence of the transition matrix for the reaction $\Sigma^- + p \to \Sigma^0 + n$, although an appreciable amount of spin dependence is still required. The effect of the dineutron final state interaction on the Λ^0 momentum spectrum is calculated as a function of the spin dependence of the Λ^0 production process. The present experimental data, however, are not sufficient to determine this spin dependence.

1. – Introduction.

When Σ^- hyperons at rest are absorbed in deuterium, the reaction produces two neutrons together with a Λ^0 or Σ^0 hyperon. The most recent measurement on the Λ^0, Σ^0 branching ratio has been reported to be [1]:

$$\frac{\omega_{\Sigma^0}(d)}{\omega_{\Sigma^0}(d) + \omega_{\Lambda^0}(d)} = 0.037 \pm 0.022 \,, \tag{1}$$

(*) Research supported in part by the U. S. Atomic Energy Commission. This paper contains thesis research submitted to the University of Maryland Graduate School in partial fulfillment of the requirements for the M. S. degree (Phys. Dept. Tech. Report no. 176).

[1] O. DAHL, N. HORWITZ, D. MILLER and J. MURRAY: *Phys. Rev. Lett.*, **4**, 77 (1960).

where $\omega_Y(d)$ is the transition probability for the reaction

$$\Sigma^- + d \to Y + n + n \tag{2}$$

while the corresponding result for Σ^- absorption in hydrogen is (²)

$$\frac{\omega_{\Sigma^0}(p)}{\omega_{\Sigma^0}(p) + \omega_{\Lambda^0}(p)} = 0.33 \pm 0.05 \,. \tag{3}$$

Using the simple impulse approximation in which the Σ^- is pictured as interacting only with the proton, DAY, SNOW and SUCHER (³) have calculated the branching $\omega_{\Lambda^0}(d)/\omega_{\Sigma^0}(d)$ for several choices of spin-flip and spin-independent parameters in the S-wave interaction transition operator for the Σ reaction in hydrogen. The assumptions they made were: i) the reaction takes place from an S orbit of the (Σ^-, d) system (⁴); ii) the parity of both Λ^0 and Σ^0 relative to Σ^- is even; iii) all final state interactions are neglected so that the final two-neutron wave function can be taken as an antisymmetrized plane wave. The results indicate that almost the maximum possible spin dependence of the transition matrix for the reaction $\Sigma^- + p \to \Sigma^0 + n$ was required in order to fit the experimental data. It is the aim of this paper to show that the strong final state interaction between the two neutrons will substantially enhance the total production rate of Σ^0 hyperons in the (Σ^-, d) reaction so that a less extreme assumption about the spin dependence is required to fit the data.

2. – Final state interactions and calculations.

In reaction (2) all three particles produced are strongly interacting baryons with coupling constants of approximately the same order. No single pair of them can be isolated from the remaining particle. Therefore the simple two-body final state interaction formalism is not strictly applicable to this three-body problem. KARPLUS and RODBERG (⁵) have studied in detail the inelastic final state interaction between the hyperon and a nucleon produced in the (K^-, d) reaction. In this note, we shall consider only the effect of the known final state interaction between the identical neutrons. This effect alone will be shown to have a considerable effect on the Σ^0/Λ^0 ratio from the (Σ^-, d) reaction, and it is felt that this qualitative feature would still be present in

(²) R. R. ROSS: *Bull. Amer. Phys. Soc.*, **3**, 335 (1958).
(³) T. B. DAY, G. A. SNOW and J. SUCHER: *Phys. Rev. Lett.*, **2**, 468 (1959).
(⁴) T. B. DAY, G. A. SNOW and J. SUCHER: *Phys. Rev. Lett.*, **2**, 61 (1959).
(⁵) R. KARPLUS and L. S. RODBERG: *Phys. Rev.*, **115**, 1058 (1959).

a more rigorous three-body final state formalism which is beyond the scope of this paper.

Since the maximum momentum of the Σ^0 in the laboratory system is much less than that of the Λ^0 (36.62 MeV/c and 329.7 MeV/c) respectively, it is expected that the final state interaction between the two neutrons will play a more important role for the Σ^0 case, because from a phyiscal point of view low outgoing momenta will allow the particles to have longer time to interact with each other before they leave the region of mutual interaction.

We shall assume that the final state interaction between the two neutrons takes place in the S-state of relative orbital angular momentum only. This assumption is certainly justified for Σ^0 production because of the low amount of available energy in the system. As to the case of Λ^0 production, P-wave modification will affect the branching ratios very little since the final state interaction is not dominant here.

Within the framework of the impulse approximation, the matrix element for the reaction $\Sigma^- + \mathrm{d} \to \mathrm{Y} + \mathrm{n} + \mathrm{n}$ wille have the form [6]

$$M = \int \Psi^*_{\mathrm{nn}}(\boldsymbol{r}) \exp\left[-i\boldsymbol{q}\cdot\frac{\boldsymbol{r}}{2}\right] \langle \chi_{\Sigma^0}, \chi_{2\mathrm{n}} | t | \chi_{\Sigma^-}, \chi_{\mathrm{d}} \rangle \Psi^{\mathrm{d}}_{ns}(0)\, u_{\mathrm{d}}(\boldsymbol{r})\, \mathrm{d}\boldsymbol{r}\,, \tag{4}$$

where $u_{\mathrm{d}}(\boldsymbol{r})$ is the ground state Hulthen function of the deuteron [7], $\Psi^{\mathrm{d}}_{ns}(0)$ is the hydrogenic wave function for the Σ^- hyperon in the nS atomic orbit of the deuteron, and $\boldsymbol{q}$ is the hyperon momentum. The arguments in both functions are the relative co-ordinates in question. The χ's are the spin wave functions, with subscripts denoting the specific particle or system referred to. With assumptions i) and ii) as mentioned in Section **1**, and from general invariance considerations, the most general S-wave interaction transition operator for the Σ^- reaction in hydrogen may be written, for Σ^0 production, as

$$t = a_0 \mathbf{1}_{\Sigma^0\Sigma^-} \mathbf{1}_{\mathrm{np}} + a_1 \boldsymbol{\sigma}_{\Sigma^0\Sigma^-} \cdot \boldsymbol{\sigma}_{\mathrm{np}}\,.$$

Similarly, for Λ^0 production, the constants a_0, a_1 are replaced by constants b_0 and b_1.

The space wave function for the two neutrons can then be written as [8]

$$\Psi_{\mathrm{nn}}(\boldsymbol{r}) = \exp[i\boldsymbol{k}\cdot\boldsymbol{r}] + f_-(k)\,\frac{\exp[-ikr] - \exp[-\beta r]}{r}\,,$$

(6) A. Pais and S. B. Treiman: *Phys. Rev.*, **107**, 1396 (1957).
(7) $u_{\mathrm{d}}(\boldsymbol{r}) = N\,(\exp[-\alpha r] - \exp[-\beta' r])/r$ with $\alpha = 45.7$ MeV/c and $\beta' = 6.2\alpha$. Thus the normalization constant N can be written as $(\alpha\beta'(\alpha+\beta')/2\pi(\beta'-\alpha)^2)^{\frac{1}{2}}$.
(8) Y. Yamaguichi: *Phys. Rev.*, **95**, 1628 (1954).

where

$$f_\pm(k) = \frac{1}{\mp ik + k \operatorname{cotg} \delta} = \frac{1}{\mp ik + (-1/a + \frac{1}{2} r_0 k^2)},$$

is the S-wave scattering amplitude, and $\boldsymbol{k}$ represents the relative momentum of the two neutrons. β is determined by the condition that the S-part of the wave function gives the correct effective range at $k = 0$, hence β is defined by the relation

$$r_0 = \frac{3}{\beta} - \frac{4}{a\beta^2},$$

where $a = -2.37 \cdot 10^{-12}$ cm and $r_0 \simeq 2.65 \cdot 10^{-13}$ cm are the appropriate n-n singlet scattering length and effective range as deduced from n-p and p-p scattering.

The symmetrized and antisymmetrized space wave functions are respectively

$$\frac{1}{\sqrt{2}}(\exp[i\boldsymbol{k}\cdot\boldsymbol{r}] + \exp[-i\boldsymbol{k}\cdot\boldsymbol{r}]) + \sqrt{2}\,\frac{f_-(k)}{r}(\exp[-ikr] - \exp[-\beta r]),$$

and

$$\frac{1}{\sqrt{2}}(\exp[i\boldsymbol{k}\cdot\boldsymbol{r}] - \exp[-i\boldsymbol{k}\cdot\boldsymbol{r}]).$$

The total rate for the reaction $\Sigma^- + \mathrm{d} \to \mathrm{Y} + \mathrm{n} + \mathrm{n}$ is then given by

$$(5) \qquad \omega_{\mathrm{Y}}(\mathrm{d}) = \frac{2\pi}{6} |\Psi^{\mathrm{d}}_{ns}(0)|^2 \sum_{\substack{i,f \\ \text{spins}}} \int \frac{\mathrm{d}\boldsymbol{q}\,\mathrm{d}\boldsymbol{k}}{(2\pi)^6}\, \delta(E_f - E_i) \cdot$$
$$\cdot \left| \int \Psi^*_{\mathrm{nn}}(\boldsymbol{r}) \exp\frac{-i\boldsymbol{q}\cdot\boldsymbol{r}}{2} \langle \chi_{\Sigma^0}, \chi_{2\mathrm{n}} | t | \chi_{\Sigma^-}, \chi_{\mathrm{d}} \rangle u_{\mathrm{d}}(\boldsymbol{r})\, \mathrm{d}\boldsymbol{r} \right|^2.$$

The final q-integration is performed numerically and the final values of the antisymmetric and symmetric space integrals will be represented by I^0 and I^e respectively [9] (see Appendix).

Note that without final state interaction between the two neutrons I^e will be reduced to the first six terms of eq. (A.1), denoted by I^e_p, while I^0 remains the same.

Then

$$(6) \qquad \omega_{I^0}(\mathrm{d}) = \frac{M_{\mathrm{n}}}{\pi} N^2 |\Psi^{\mathrm{d}}_{ns}(0)|^2 (I^e + 2I^0) |a_1|^2 + I^0 |a_0|^2],$$

where M_{n} is the neutron mass.

([9]) YUNG Y. CHEN: Phys. Dept. Tech. Report no. 176, University of Md. (1960).

3. – Results and discussion.

The values of the integrals I^0 and I^e are listed in Table I using the same arbitrary scale. One can notice that the (n, n) final state interaction enhances I^e for Σ^0 production by a factor ~ 6 while the integral I^e for Λ^0 production

TABLE I. – *Relative numerical values of space integrals.*

	Λ^0 production	Σ^0 production
I^0	1.195	0.000392
I^e_p	1.775	0.03796
I^e	2.206	0.2363
I^e/I^e_p	1.243	6.225

is increased by only about 20%. In order to compare with experiment, the branching ratio $\omega_{\Lambda^0}(\mathrm{d})/\omega_{\Sigma^0}(\mathrm{d})$ is written as

$$\frac{\omega_{\Lambda^0}(\mathrm{d})}{\omega_{\Sigma^0}(\mathrm{d})} = \frac{\omega_{\Lambda^0}(\mathrm{d})}{\omega_{\Lambda^0}(\mathrm{p})}\cdot\frac{\omega_{\Lambda^0}(\mathrm{p})}{\omega_{\Sigma^0}(\mathrm{p})}\cdot\left(\frac{\omega_{\Sigma^0}(\mathrm{d})}{\omega_{\Sigma^0}(\mathrm{p})}\right)^{-1},$$

where $\omega_{\Lambda^0}(\mathrm{p})/\omega_{\Sigma^0}(\mathrm{p})$ can be obtained from the experimental value, *i.e.*, $2.03^{+0.54}_{-0.12}$. To get an expression for the other two factors we have to calculate the transition rate for the case when the Σ^- hyperon is absorbed in hydrogen. In this case one finds

$$\omega_{\Sigma^0}(\mathrm{p}) = \frac{q_{\Sigma^0}\mu_{\Sigma^0\mathrm{n}}}{\pi}|\Psi^{\mathrm{H}}_{ns}(0)|^2(|a_0|^2+3|a_1|^2),$$

with a similar expression for $\omega_{\Lambda^0}(\mathrm{p})$.

The values of $\omega_{\Lambda^0}(\mathrm{d})/\omega_{\Sigma^0}(\mathrm{d})$ with and without the final state interaction for some limiting choices of the parameters a_0, a_1, b_0, b_1 are given in Table II. On comparing Table II with the results obtained by DAY *et al.*, one first observes that for the plane wave approximation a difference of about 12% exists when the β'-term in the deuteron wave function is neglected, since the cross terms contribute substantially to the integrals even though $\beta' = 6.2\alpha$.

Table II also shows that the branching ratio $\omega_{\Lambda^0}(\mathrm{d})/\omega_{\Sigma^0}(\mathrm{d})$ varies very little between the two extreme values for the ratio $b_0:b_1$ (1:0 and 0:1), *i.e.*, the total Λ^0 production is not sensitive to the spin-dependence of the transition matrix. Thus, to fit the experimental value of $\omega_{\Lambda^0}(\mathrm{d})/\omega_{\Sigma^0}(\mathrm{d}) \simeq 26$, the ratio

TABLE II. – *Branching ratios with and without final state interaction.*

(Σ^0) $a_0:a_1$	(Σ^0) $b_0:b_1$	$\dfrac{\omega_{\Lambda^0}(\mathrm{d})}{\omega_{\Sigma^0}(\mathrm{d})}$ (*) $\begin{pmatrix}\text{plane wave}\\ \text{approximation}\end{pmatrix}$	$\dfrac{\omega_{\Lambda^0}(\mathrm{d})}{\omega_{\Sigma^0}(\mathrm{d})}$ (*) $\begin{pmatrix}\text{with final}\\ \text{state interaction}\end{pmatrix}$
1:0	1:0	1286	1286
0:1	0:1	45.2	8.15
0:1	1:0	38.9	6.36

(*) All numbers are for a mass difference of 4.45 MeV between the Σ^0-and Σ^--hyperons.

between a_0 and a_1 can be solved for these two values of $b_0:b_1$, with the result of 3.07 to 1 and 2.58 to 1 respectively. Hence the experimental results can now be fitted with a less extreme assumption about the spin dependence of the transition matrix for the reaction $\Sigma^- + p \to \Sigma^0 + n$, although an appreciable amount of spin dependence is still required. If one were to include the (Σ^0, n) final state interaction in the impulse approximation, this could further depress the observed number of Σ^0's via the reaction $\Sigma^0 + n \to \Lambda^0 + n$. In this case one may again be forced to an extreme spin dependence for the reaction $\Sigma^- + p \to \Sigma^0 + n$, *i.e.*, $a_0:a_1$ near 0:1.

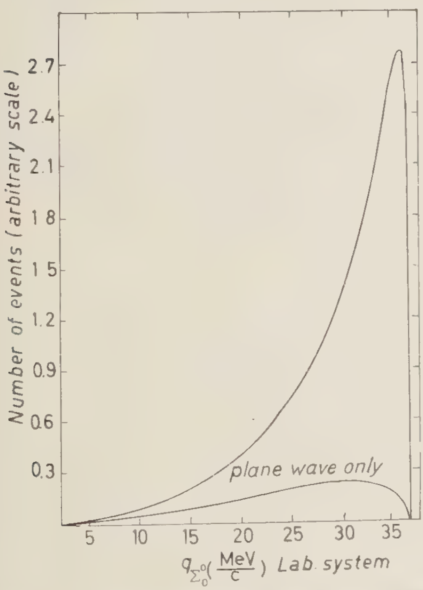

Fig. 1. – Comparison of the partial Σ^0 momentum spectra with and without S-wave final state interaction between the two neutrons in the spin singlet state.

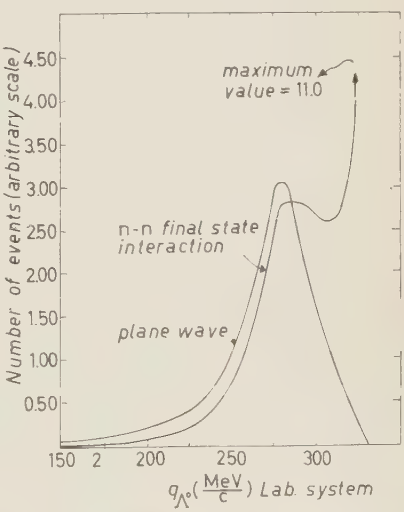

Fig. 2. – Comparison of the partial Λ^0 momentum spectra with and without S-wave final state interaction between the two neutrons in the spin singlet state.

In Fig. 1 and 2 the partial momenta spectra of Σ^0 and Λ^0 production with and without S-wave final state interaction between the two neutrons in their

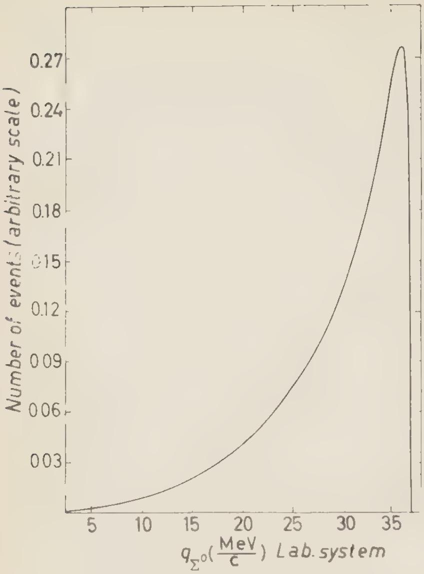

Fig. 3. – Total Σ^0 momentum spectrum with an appropriate choice of spin dependence for the (Σ^-, p) transition operator so as to fit the experimental data, *i.e.* $a_0 : a_1 = 3 : 1$.

spin singlet state are compared, *i.e.*, the area under each curve is exactly proportional to the integral I^e or I^e_p respectively. The Σ^0 spectrum with the final state interaction is smooth with a well defined maximum, while the Λ^0 spectrum has a pronounced dip in the region between $q_{\Lambda^0} \simeq 280$ MeV/c and $q_{\Lambda_0} \simeq 315$ MeV/c. This particular phenomenon can be understood if we consider the spectrum as a superposition of two parts, plane wave and final state interaction contributions separately. From Fig. 2, the smooth plane wave curve has its maximum at $q_{\Lambda^0} = 281.4$ MeV/c (when $k = q_{\Lambda^0}/2$); then the production rate steadily decreases to zero, but meanwhile the final state interaction does not become predominant until after $q_{\Lambda^0} = 310$ MeV/c. Thus there exists an overall decrease in the number of Λ's produced in the above mentioned region.

In Fig. 3, the complete momentum spectrum of Σ^0 production has been plotted with $a_0 : a_1 = 3 : 1$ as an intermediate choice. Its shape hardly differs any from that of Fig. 1, except for the fact that it is reduced by a factor of 10; but this is what we would have expected since $I^0 \ll I^e$. Also, we have calculated in Fig. 4 the complete Λ^0-momentum spectrum for the maximum effect of final state interaction, *i.e.*, $b_0 : b_1 = 0 : 1$. It is clear from this figure that a determination with very good resolution of the upper end of the Λ^0-momentum spectrum can yield some information about the spin dependence of the transition matrix for the reaction $\Sigma^- + p \to \Lambda^0 + n$.

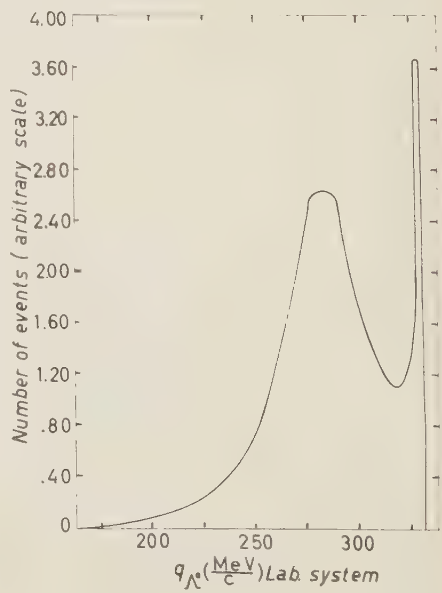

Fig. 4. – Total Λ^0 momentum spectrum with the maximum effect of final state interaction, *i.e.* $b_0 : b_1 = 0 : 1$.

In Fig. 5, the complete Λ^0 momentum spectrum for the interval $q_{\Lambda^0} = 200$ MeV/c to $q_{\Lambda^0} = 345$ MeV/c is calculated with an approximate experimental momentum uncertainty of ± 15 MeV/c and compared with the ob-

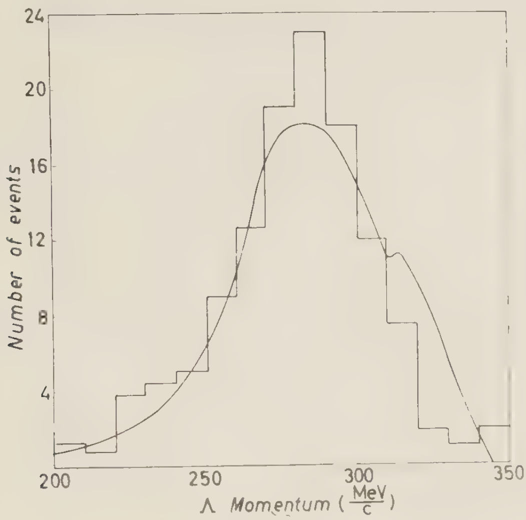

Fig. 5. – Comparison of the observed Λ^0 momentum spectrum with the prediction of the impulse model including S-wave final state interaction between the two neutrons. The theoretical curve has folded in an approximate experimental momentum uncertainty of ± 15 MeV/c. The two curves have the same number of events in the Σ momentum interval from 200 MeV/c to 345 MeV/c.

served spectrum [1]. The theoretical curve and experimental idiogram are so normalized that they include the same number of events in the above momentum interval. This theoretical curve, which includes a maximum two neutron final state interaction, does not give quite as good a fit to the experimental data as does the simple plane wave calculation [1]. However, much more experimental data would be required to substantially narrow the range of the parameters $b_0 : b_1$ that describe the spin dependence of the Σ^-, Λ^0 transition matrix.

* * *

The author wishes to extend his most sincere thanks to Prof. G. A. Snow for his continuous advice and encouragement in the preparation of this paper. Thanks are also due to Dr. T. B. Day and Dr. J. Sucher for their helpful assistance and many valuable suggestions.

Appendix

In evaluating the integrals I^e and I^0 of eq. (6), we shall keep the β'-terms in the deuteron wave function. Then

$$(\text{A.1})\qquad I^e = \int_0^{q_{\max}} \mathrm{d}q \left\{kq^2 \left[\frac{1}{[\alpha^2+(k+q/2)^2][\alpha^2+(k-q/2)^2]} + \right.\right.$$

$$+ \frac{1}{[\beta'^2+(k+q/2)^2][\beta'^2+(k-q/2)^2]} - \frac{1}{kq(\beta'^2-\alpha^2)}\cdot$$

$$\cdot\log\frac{[\alpha^2+(k+q/2)^2][\beta'^2+(k-q/2)^2]}{[\alpha^2+(k-q/2)^2][\beta'^2+(k+q/2)^2]} + \frac{1}{2kq(\alpha^2+q^2/4+k^2)}\log\frac{\alpha^2+(k+q/2)^2}{\alpha^2+(k-q/2)^2} +$$

$$+ \frac{1}{2kq(\beta'^2+q^2/4+k^2)}\log\frac{\beta'^2+(k+q/2)^2}{\beta'^2+(k-q/2)^2} - \frac{1}{kq(\alpha^2+\beta'^2+2k^2+q^2/2)}\cdot$$

$$\cdot\log\frac{[\alpha^2+(k+q/2)^2][\beta'^2+(k+q/2)^2]}{[\alpha^2+(k-q/2)^2][\beta'^2+(k-q/2)^2]}\Bigg] + \frac{1}{[((r_0/2)k^2-1/a)^2+k^2]}\cdot$$

$$\cdot\Bigg[k\Bigg(\mathrm{tg}^{-1}\frac{q/2+k}{\alpha} + \mathrm{tg}^{-1}\frac{q/2-k}{\alpha} - \mathrm{tg}^{-1}\frac{q/2+k}{\beta'} - \mathrm{tg}^{-1}\frac{q/2-k}{\beta'} -$$

$$- \mathrm{tg}^{-1}\frac{q}{2(\alpha+\beta)} + \mathrm{tg}^{-1}\frac{q}{2(\beta'+\beta)}\Bigg)^2 + \left(\frac{r_0}{2}k^2-\frac{1}{a}\right)\Bigg(\mathrm{tg}^{-1}\frac{q/2+k}{\alpha} + \mathrm{tg}^{-1}\frac{q/2-k}{\alpha} -$$

$$- \mathrm{tg}^{-1}\frac{q/2+k}{\beta'} - \mathrm{tg}^{-1}\frac{q/2-k}{\beta'} - \mathrm{tg}^{-1}\frac{q}{2(\alpha+\beta)} + \mathrm{tg}^{-1}\frac{q}{2(\beta'+\beta)}\Bigg)\cdot$$

$$\left.\left.\cdot\log\frac{[\alpha^2+(k+q/2)^2][\beta'^2+(k-q/2)^2]}{[\alpha^2+(k-q/2)^2][\beta'^2+(k+q/2)^2]} - \frac{k}{4}\left(\log\frac{[\alpha^2+(k+q/2)^2][\beta'^2+(k-q/2)^2]}{[\alpha^2+(k-q/2)^2][\beta'^2+(k+q/2)^2]}\right)^2\right]\right\},$$

$$(\text{A.2})\qquad I^0 = \int_0^{q_{\max}} kq^2\,\mathrm{d}q \left\{\frac{1}{[\alpha^2+(k+q/2)^2][\alpha^2+(k-q/2)^2]} + \right.$$

$$+ \frac{1}{[\beta'^2+(k+q/2)^2][\beta'^2+(k-q/2)^2]} - \frac{1}{kq(\beta'^2-\alpha^2)}\cdot$$

$$\cdot\log\frac{[\alpha^2+(k+q/2)^2][\beta'^2+(k-q/2)^2]}{[\alpha^2+(k-q/2)^2][\beta'^2+(k+q/2)^2]} - \frac{1}{2kq(\alpha^2+q^2/4+k^2)}\log\frac{\alpha^2+(k+q/2)^2}{\alpha^2+(k-q/2)^2} -$$

$$- \frac{1}{2kq(\beta'^2+q^2/4+k^2)}\log\frac{\beta'^2+(k+q/2)^2}{\beta'^2+(k-q/2)^2} +$$

$$\left. + \frac{1}{kq(\alpha^2+\beta'^2+2k^2+q^2/2)}\log\frac{[\alpha^2+(k+q/2)^2][\beta'^2+(k+q/2)^2]}{[\alpha^2+(k-q/2)^2][\beta'^2+(k-q/2)^2]}\right\}.$$

RIASSUNTO (*)

Gli effetti della interazione dello stato finale a due neutroni nella reazione $\Sigma^- + d \to (\Lambda^0 \text{ o } \Sigma^0) + n + n$ vengono calcolati usando l'approssimazione dell'impulso col presupposto dell'assorbimento dell'onda S e della parità relativa pari fra gli iperoni. Confrontando i risultati con quelli ottenuti trascurando tutte le interazioni con gli stati finali, si trova che la produzione dei Σ^0 può essere accresciuta di un fattore di ~ 6 mentre la produzione dei Λ^0 viene aumentata solo di $\sim 10\%$. I più recenti risultati sperimentali sul rapporto di branching della produzione di due iperoni possono ora essere approssimati con una ipotesi meno estremista sulla dipendenza dallo spin della matrice di transizione per la reazione $\Sigma^- + p \to \Sigma^0 + n$, per quanto si richieda ancora un grado apprezzabile di dipendenza dallo spin. L'effetto dell'interazione dello stato finale del dineutrone sullo spettro del momento del Λ^0 si calcola in funzione della dipendenza dallo spin del processo di produzione Λ^0. I dati sperimentali attuali tuttavia non sono sufficienti a determinare questa dipendenza dallo spin.

(*) *Traduzione a cura della Redazione.*

IL NUOVO CIMENTO Vol. XIX, N. 1 1° Gennaio 1961

On the Vibration Spectrum of a Disordered Linear Lattice – I.

J. MAHANTY (*)

Department of Physics, University of Maryland - College Park, Md.

(ricevuto il 1° Agosto 1960)

Summary. — In this paper the average eigenfrequency equation of a disordered two-component linear chain is derived by a direct algebraic method. It is shown that the moments of the frequency spectrum can be evaluated easily from this equation.

1. – Introduction.

The vibrational properties of disordered lattices are of considerable interest from both theoretical and practical standpoints. Though the exact solution of the problem of evaluating the frequency distribution function has proved rather elusive, a number of interesting techniques have been developed and used for obtaining approximate solutions. Among the papers published recently on the disordered linear chain mention may be made of the ones by HORI [1-3] who used the method of transfer matrices, and by DOMB and others [4,5] who used the moment trace method of Montroll [6]. MARADUDIN

(*) Permanent address: Physics Dept., Panjab University, Chandigarh.

(1) J. HORI and T. ASAHI: *Progr. Theor. Phys.*, **17**, 523 (1957).

(2) J. HORI: *Progr. Theor. Phys.*, **18**, 367 (1957).

(3) J. HORI: *Progr. Theor. Phys.*, **23**, 475 (1960).

(4) C. DOMB, A. A. MARADUDIN, E. W. MONTROLL and G. H. WEISS: *Phys. Rev.* **115**, 18 (1959).

(5) C. DOMB, A. A. MARADUDIN, E. W. MONTROLL and G. H. WEISS: *Phys. Rev.*, **115**, 24 (1959).

(6) E. W. MONTROLL: *Journ. Chem. Phys.*, **10**, 218 (1942); **11**, 481 (1943).

and WEISS (7) have made use of the transfer matrix method to obtain the behaviour of the frequency distribution function for $\omega \to 0$, and have also given an upper bound for the frequencies.

The object of this note is methodological. It will be shown that it is possible to obtain the average eigenfrequency equation of a disordered linear chain with two types of atoms by a direct algebraic method. This leads to an easy method for the evaluation of the moments, which turn out to be the same as the ones evaluated by DOMB *et al.* It is also possible to obtain a closed integral expression for the eigenvalue equation. In this form it is suitable for perturbation theoretic treatment.

2. – Mathematical preliminaries.

We will consider the case of a linear lattice with nearest neighbour interactions. The method of transfer matrices of ASAHI and HORI (1,2) will be used and the notation will substantially be the same as in their first paper, with the modifications introduced by MARADUDIN and WEISS (7).

It has been shown by ASAHI and HORI (1,2) that associated with each atom of mass M_i in the linear lattice, there exists a 2×2 transfer matrix $(I+T_i)$ where the explicit form of the matrix is given by

$$I+T_i=J_i=\begin{pmatrix} 1 & 1 \\ -\dfrac{M_i\omega^2}{\gamma} & 1-\dfrac{M_i\omega^2}{\gamma}\end{pmatrix}, \tag{2.1}$$

where γ is the nearest neighbour force constant.

The entire lattice consisting of r atoms each of mass M_1 and $(N-r)$ atoms each of mass M_2 can be considered as a unit cell. When the arrangement of atoms is randomized, the average eigenvalue equation is

$$\langle \operatorname{Tr} H\rangle = 2\,, \tag{2.2}$$

where H is the product of r matrices of type J_1 and $(N-r)$ matrices of type J_2, and the averaging is done with respect to all the distinct permutations amongst the N matrices.

Since J_1 does not commute with J_2, all the distinct permutations of r matrices of type J_2 can be obtained as the coefficient of z^r in the expression

$$(J_2+zJ_1)^N\,.$$

(7) A. A. MARADUDIN and G. H. WEISS: *Journ. Chem. Phys.*, **29**, 631 (1958).

The average eigenvalue equation is, therefore,

$$\frac{1}{\binom{N}{r}} \operatorname{Tr}\{\text{Coefficient of } z^r \text{ in } (J_2+zJ_1)^N\} = 2\,. \tag{2.3}$$

3. – Evaluation of the trace.

The matrix $(J_2+zJ_1)\equiv L$ is a 2×2 matrix and satisfies its characteristic equation

$$L^2 - L\{2(1+z)-(x_2+zx_1)\}+(1+z)^2 I = 0\,, \tag{3.1}$$

where $x_i = M_i\omega^2/\gamma$.

Let

$$L^N = f_N L - g_N I\,. \tag{3.2}$$

Using equation (3.1), we obtain

$$L^{N+1} = [f_N\{2(1+z)-(x_2+zx_1)\}-g_N]L - f_N(1+z)^2 I$$

and from this,

$$f_{N+1} = f_N\{2(1+z)-(x_2+zx_1)\}-g_N\,, \tag{3.3a}$$

$$g_{N+1} = f_N(1+z)^2\,. \tag{3.3b}$$

These difference equations can be solved by the method of generating functions. Let

$$F(s) = \sum_{\nu=0}^{\infty} f_\nu s^\nu \tag{3.4a}$$

and

$$G(s) = \sum_{\nu=0}^{\infty} g_\nu s^\nu\,. \tag{3.4b}$$

The initial conditions are $f_0=0$, $g_0=-1$. Multiplying equation (3.3) by s^{N+1} and summing over all values of N, and after some simplification we obtain

$$F(s) = \frac{s}{1-\{2(1+z)-(x_2+zx_1)\}s+s^2(1+z)^2}\,, \tag{3.5a}$$

and

$$G(s) = \frac{\{2(1+z)-(x_2+zx_1)\}s-1}{1-\{2(1+z)-(x_2+zx_1)\}s+s^2(1+z)^2}\,. \tag{3.5b}$$

The average eigenvalue equation becomes

$$(3.6)\qquad \frac{1}{\binom{N}{r}}\{\text{Coefficient of } s^N \text{ and } z^r \text{ in } \operatorname{Tr}[F(s)L-G(s)I]\}=2\,.$$

We can expand $\operatorname{Tr}[F(s)L-G(s)I]$ as follows. For small s and finite z,

$$\operatorname{Tr}[F(s)L-G(s)I]=1+\frac{1-s^2(1+z)^2}{[1-s(1+z)]^2-s(x_2+zx_1)}=$$

$$=1+[1+s(1+z)]\sum_{\nu=0}^{\infty}(-1)^\nu\frac{s^\nu(x_2+zx_1)^\nu}{[1-s(1+z)]^{2\nu+1}}=$$

$$=1+[1+s(1+z)]\sum_{\nu=0}^{\infty}(-1)^\nu s^\nu(x_2+zx_1)^\nu\sum_{\mu=0}^{\infty}\frac{(2\nu+\mu)!}{(2\nu)!\,\mu!}s^\mu(1+z)^\mu\,.$$

The coefficient of s^p in the double series is

$$\sum_{\nu=0}^{p}(-1)^\nu\frac{(\nu+p)!}{(2\nu)!\,(p-\nu)!}(x_2+zx_1)^\nu(1+z)^{p-\nu}\,.$$

So, the coefficient of s^N in the trace is

$$\sum_{\nu=0}^{N}(-1)^\nu\frac{(\nu+N)!}{(2\nu)!\,(N-\nu)!}(x_2+zx_1)^\nu(1+z)^{N-\nu}+$$

$$+\sum_{\nu=0}^{N-1}(-1)^\nu\frac{(\nu+N-1)!}{(2\nu)!\,(N-\nu-1)!}(x_2+zx_1)^\nu(1+z)^{N-\nu}=$$

$$=(-1)^N(x_2+zx_1)^N+\sum_{\nu=0}^{N-1}(-1)^\nu\frac{(\nu+N-1)!\,2N}{(2\nu)!\,(N-\nu)!}(x_2+zx_1)^\nu(1+z)^{N-\nu}\,.$$

The coefficient of z^r in the above expression is obtained in a straightforward manner. Finally, substituting for $x_i=M_i\omega^2/\gamma$ we obtain the following expression:

$$(3.7)\qquad \text{Coefficient of } z^r \text{ and } s^N \text{ in } \operatorname{Tr}[F(s)L-G(s)I]=$$

$$=(-1)^N\binom{N}{r}\frac{M_2^{N-r}M_1^r}{\gamma^N}\omega^{2N}+\sum_{\nu=0}^{N-1}(-1)^\nu\frac{(\nu+N-1)!\,2N}{(2\nu)!\,(N-\nu)!}\left\{\sum_{p=r'}^{p=r''}\binom{\nu}{p}\binom{N-\nu}{r-p}M_2^{\nu-p}M_1^p\right\}\frac{\omega^{2\nu}}{\gamma^\nu}.$$

The upper limit r'' for the summation over p is given by $r''=r$ when $r<\nu$ and $r''=\nu$ when $r>\nu$. The lower limit r' is given by $r'=0$ when $r\leqslant N-\nu$ and $r'=r+\nu-N$ when $r>N-\nu$.

The average eigenvalue equation is, therefore,

$$\begin{aligned}(3.8)\qquad \omega^{2N} + \Bigg[\sum_{r=0}^{N-1} (-1)^{\nu-N} \frac{(\nu+N-1)!\,r!\,(N-r)!\,2N}{N!\,(2\nu)!\,(N-\nu)!}\,\cdot \\ \cdot\left\{\sum_{p=r'}^{p=r''} \binom{\nu}{p}\binom{N-\nu}{r-p} M_2^{\nu-p-N+r} M_1^{p-r}\right\}\frac{\omega^{r}}{\gamma^{\nu-N}}\Bigg] - \frac{(-1)^N 2\gamma^N}{M_2^{N-r} M_1^r} = 0\,.\end{aligned}$$

4. – Evaluation of the moments.

In a polynomial equation of the form

$$(4.1)\qquad x^n + \sum_{\nu=0}^{N-1} (-1)^{\nu-N} a_\nu x^\nu = 0\,,$$

the moments are easy to evaluate. The first moment, is

$$(4.2)\qquad n\mu_1 = \sum x_i = a_{N-1}\,.$$

The second moment is

$$(4.3)\qquad n\mu_2 \equiv \sum x_i^2 = a_{N-1}^2 - 2a_{N-2}\,.$$

The third moment is

$$(4.4)\qquad n\mu_3 \equiv \sum x_i^3 = a_{N-1}^3 - 3a_{N-1}a_{N-2} + 3a_{N-3}$$

and so on (*).

It is easy to use these formulae in equation (3.8) to obtain the first few moments. In the limit when N and r tend to infinity keeping the ratio $r/N = c$ constant, the moments are:

$$(4.5)\quad N\mu_1 = \sum \omega_i^2 = 2N\gamma\left[\frac{c}{M_1} + \frac{1-c}{M_2}\right],$$

$$(4.6)\quad N\mu_2 = \sum \omega_i^4 = 2N\gamma^2\left[\left\{\frac{c}{M_1} + \frac{1-c}{M_2}\right\}^2 + 2\left\{\frac{c}{M_1^2} + \frac{1-c}{M_2^2}\right\}\right],$$

$$(4.7)\quad N\mu_3 = \sum \omega_i^6 = 4N\gamma^3\left[2\left\{\frac{c}{M_1^3} + \frac{1-c}{M_2^3}\right\} + 3\left(\frac{c}{M_1} + \frac{1-c}{M_2}\right)\left(\frac{c}{M_1^2} + \frac{1-c}{M_2^2}\right)\right].$$

(*) A table of these formulae can be found in *Smithsonian Mathematical Formulae and Tables of Elliptic Functions*, p. 3 (Washington D. C., 1947).

It is possible to write the coefficients in the eigenfrequency equation in a compact form by using the following artifice. The sum

$$\sum_{p=r'}^{p=r''} \binom{\nu}{p} \binom{N-\nu}{r-p} M_2^{\nu-p} M_1^{p} ,$$

in equation (3.7) can be written in the form

$$(4.8) \qquad \lim_{y\to 1} \sum_{p=0}^{\nu} \sum_{k=0}^{N-\nu} \binom{\nu}{p} M_1^p M_2^{\nu-p} \binom{N-\nu}{k} y^k \, \delta(p+k-r) =$$

$$= \lim_{y\to 1} \frac{1}{2\pi} \int_0^{2\pi} \mathrm{d}\varphi \sum_{p=0}^{\nu} \sum_{k=0}^{N-\nu} \exp[i(p+k-r)\varphi] \binom{\nu}{p} M_1^p M_2^{\nu-p} \binom{N-\nu}{k} y^k$$

$$= \lim_{y\to 1} \frac{1}{2\pi} \int_0^{2\pi} \mathrm{d}\varphi \exp[-ir\varphi] (M_2 + M_1 \exp[i\varphi])^{\nu} (1 + y \exp[i\varphi])^{N-\nu}$$

$$= \frac{1}{2\pi} \int_0^{2\pi} \mathrm{d}\varphi \exp[-ir\varphi] (M_2 + M_1 \exp[i\varphi])^{\nu} (1 + \exp[i\varphi])^{N-\nu} .$$

This can be substituted in equation (3.8) to give us, with some rearrangement of terms,

$$(4.9) \quad \left[\binom{N}{r}\right]^{-1} \left[\frac{1}{2\pi} \int_0^{2\pi} \mathrm{d}\varphi \exp[-ir\varphi] \left\{ \sum_{\nu=0}^{N} \frac{(-1)^{\nu}}{N+\nu} \binom{N+\nu}{2\nu} \left(\frac{M_2 + M_1 \exp[i\varphi]}{1+\exp[i\varphi]} \right)^{\nu} \left(\frac{\omega^2}{\gamma} \right)^{\nu} \right\} \cdot \right.$$

$$\cdot 2N(1 + \exp[i\varphi]^N) - 2 = 0 .$$

The coefficients of the various powers of ω^2 are now reduced to simple integrals. If we substitute

$$(4.10) \qquad \left(\frac{M_2 + M_1 \exp[i\varphi]}{1 + \exp[i\varphi]} \right) \frac{\omega^2}{\gamma} = 4 \sin^2 [\eta(\varphi, \omega)] ,$$

(where $\eta(\varphi, \omega)$ can be complex) equation (4.9) can be written in the form

$$(4.11) \qquad \frac{1}{\pi} \int_0^{2\pi} \mathrm{d}\varphi \exp[-ir\varphi] (1 + \exp[i\varphi])^N [\cos(2N\eta) - 1] = 0 .$$

In the case when the difference between the masses vanishes, this reduces

to the usual equation

$$\cos\left(2N \sin^{-1} \frac{\omega\sqrt{M}}{2\sqrt{\gamma}}\right) = 1 . \tag{4.12}$$

When the difference is small, one can use a perturbation theory to equation (4.11) to find the change in the frequency distribution function due to disordering, starting from a regular lattice of atoms the mass of each of which equals the mean mass. This will be discussed in a subsequent note.

* * *

The author is indebted to Dr. A. A. MARADUDIN for his interest in this work.

RIASSUNTO (*)

In questo scritto si deriva con un metodo algebrico diretto l'equazione dell'autofrequenza media di una catena lineare disordinata con due componenti. Si mostra che gli impulsi dello spettro di frequenza possono essere facilmente calcolati con questa equazione.

(*) *Traduzione a cura della Redazione.*

IL NUOVO CIMENTO Vol. XIX, N. 1 1° Gennaio 1961

The Polarization of the Proton from the Process $\gamma + p \to p + \pi^0$ in the Region of the Higher Resonances.

R. QUERZOLI, G. SALVINI and A. SILVERMAN (*)

Laboratori del C.N.R.N. - Frascati

(ricevuto il 18 Agosto 1960)

Summary. — The polarization of the recoil proton in the photoproduction process $\gamma + p \to p + \pi^0$ has been measured with the beam of the Frascati electrosynchrotron at an angle of 90° in the c.m. system, in the energy interval (500 ÷ 900) MeV. A counter technique has been used, and the polarization of the proton was revealed by the left to right asymmetry in the elastic scattering of the protons in a carbon target. The experimental results are given in Table III and in Fig. 10. A definite polarization is found, always of the same sign and equal to $-0.4 \pm .14$, $0.63 \pm .23$, $-0.6 \pm .25$, $-0.57 \pm .12$, $-0.38 \pm .09$, $-0.5 \pm .17$, $-0.5 \pm .22$ at the γ-ray energies of 560, 610, 650, 700, 750, 800, 850 MeV respectively. The discussion of these experimental results, together with the data of angular dstributions, allows to conclude that they are in agreement with the hypothesis that the second resonance is a transition $(E_1, d^{\frac{3}{2}})$ and the third one is a transition $(E_2, f^{\frac{5}{2}})$.

1. – Introduction.

The single photoproduction of pions in the energy interval (500 ÷ 1100) MeV has been measured in the last three years, with several contributes from the electron-synchrotron of Caltech and Cornell University, and only more recently from the Frascati groups (1). The discovery of other maxima after

(*) Now at Cornell University.

(1) J. I. VETTE: *Phys. Rev.*, **111**, 622 (1958); R. M. WORLOCK: *Phys. Rev.*, **117**, 537 (1960); M. HEIMBERG, W. M. MCCLELLAND, F. TURKOT, W. M. WOODWARD, R. R. WILSON and D. M. ZIPOY: *Phys. Rev.*, **110**, 1208 (1958); I. W. DE WIRE, H. E. JAKSON and R. LITTAUER: *Phys. Rev.*, **110**, 1208 (1958); P. C. STEIN and K. C. ROGERS: *Phys. Rev.*, **110**, 1209 (1958); F. P. DIXON and R. L. WALKER: *Phys. Rev. Lett.*, **1**, 142 (1958).

the well known resonance at 300 MeV has stimulated the investigation on the behaviour of the differential cross-section and of the polarization of the recoil nucleon. The polarization is particularly interesting in the case of the neutral photoproduction $\gamma+\text{p}\rightarrow\text{p}+\pi^0$.

We report in the present paper an experiment to measure the polarization of the recoil proton in this reaction.

Generally speaking the interest in the polarization of the recoil proton comes from the following arguments, which hold as long as the process may be described in the general frame of quantum mechanics, with a transition matrix which is a sum of the contributing multipole transitions, each with a total angular momentum, a given parity, and a definite isotopic spin value:

a) There is polarization of the recoil proton only when at least two different states are present.

b) The polarization may indicate the relative parity of the states: in particular the polarization is absent for the protons emitted at 90° in the center of mass system, if two states are present with the same parity.

From *a*), *b*) one deduces that the measurements of the polarization at 90° in the center of mass may contribute to find out those γ-ray energies where only one state can describe the pion-nucleon system, and may contribute to determine the relative parity of the interfering states. The interest of the polarization has been recently underlined by SAKURAY [2] as a method to establish the parity of the second resonance.

We have measured the polarization of the protons at 90° c.m. in order to get an information which is very useful to establish which multipole transition can describe the photo-production phenomena in the region (500 ÷ 1000) MeV of the incident γ-rays.

The polarization of the protons has been measured until now up to a maximum of 700 MeV by STEIN [3].

2. – Experimental disposition.

The aim of the present experiment is then the measurement of the polarization of the recoil protons from the reaction

$$\gamma+\text{p}\rightarrow\text{p}+\pi^0\,.$$

[2] J. J. SAKURAI: *Phys. Rev. Lett.*, **1**, 258 (1958).
[3] P. C. STEIN: *Phys. Rev. Lett.*, **2**, 473 (1959).

To get the polarization we measure the left to right asymmetry in the scattering of protons from carbon at different angles between 14° and 16°.

The experimental disposition is given in Fig. 1. The counters 1, 2 ... 10 are plastic scintillation counters which detect the proton; the Čerenkov counter

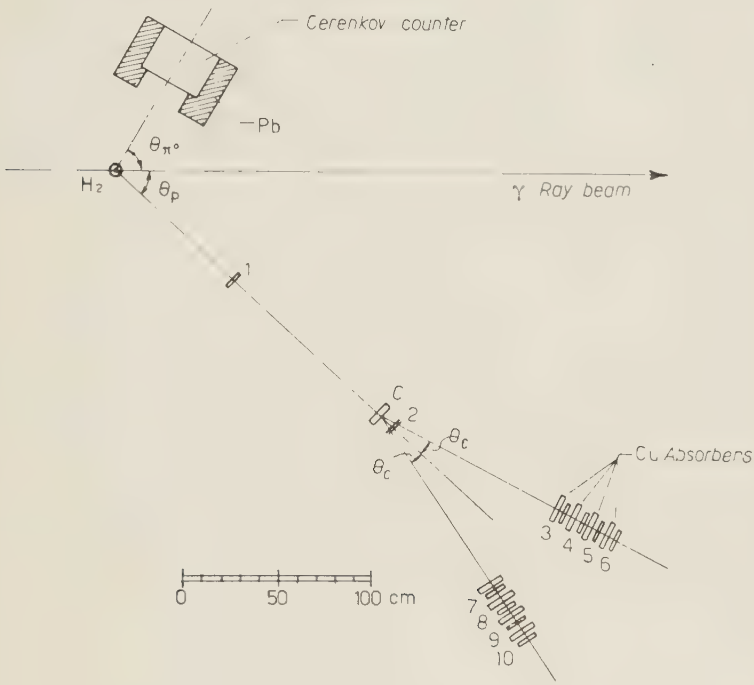

Fig. 1. – General disposition of the scintillation and Čerenkov counters.

Dimensions of the counters.

No.	Width (cm)	Height (cm)	Thickness (cm)
1	9	14	0.5
2	10	25	1.2
3– 7	12.5	25	1.2
4– 8	12.5	25	1.2
5– 9	12.5	25	1.2
6–10	15.0	28	1.2

detects the π^0-meson through its decay γ-rays. We indicate by C the carbon scatterer, whose thickness was changed according to the proton energy; Cu are the copper absorbers which define the range of the proton energy.

We were counting at the same time four kinds of coincidences:

$$(\text{Cer},\ 1,\ 2,\ 3,\ 4,\ -5) = L_{\text{II}}\,; \qquad (\text{Cer},\ 1,\ 2,\ 3,\ 4,\ 5,\ -\ 6) = L_{\text{I}}\,;$$

$$(\text{Cer},\ 1,\ 2,\ 7,\ 8,\ -9) = R_{\text{II}}\,; \qquad (\text{Cer},\ 1,\ 2,\ 7,\ 8,\ 9,\ -10) = R_{\text{I}}\,,$$

it is therefore possible to measure two different energy intervals of the protons, corresponding to two different energy intervals of the γ's.

Discrimination of the protons against the pions is guaranteed by the required coincidence with the Čerenkov counter as well as by pulse height discrimination in counters 2, 3, 7.

The block diagram of our electronics is given in Fig. 2.

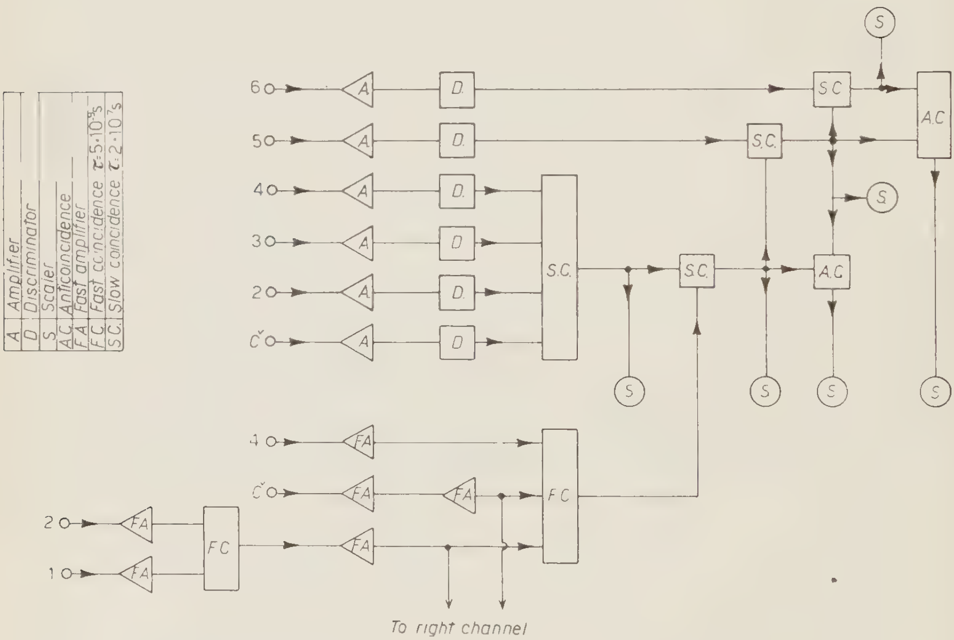

Fig. 2. – Block diagram of the electronics for the left channel.

By *F.C.* we indicate fast coincidences, with a resolving time of around 5 ns. The pulses arriving to the discriminators D are on the contrary rather slow (time arouns 200 ns) so that it is easy to realize a precise height pulse discrimination. As shown in Fig. 2, the anticoincidences $L_{\text{I}}L_{\text{II}}$ are obtained as the differences between the coincidences (Čer, 1, 2, 3, 4), (Čer, 1, 2, 3, 4, 5), (Čer, 1, 2, 3, 4, 5, 6) in order to reduce dead time effects. As a check we also register the three coincidences in each telescope.

All the measurements reported in this paper have been taken on the protons emitted at an angle of 42° degrees in the laboratory system which corresponds to an angle close to 90° in the center of mass system for all our energies (see Table I).

The choice of the dimensions and the distances of the counters and of the angle of scattering from the carbon is made on the basis of the measured elastic cross-sections and analyzing power of protons in carbon. In Fig. 3 we report the cross-section for elastic scattering from carbon for protons of different energies (the incident beam is unpolarized), according to the work of many authors (4-7).

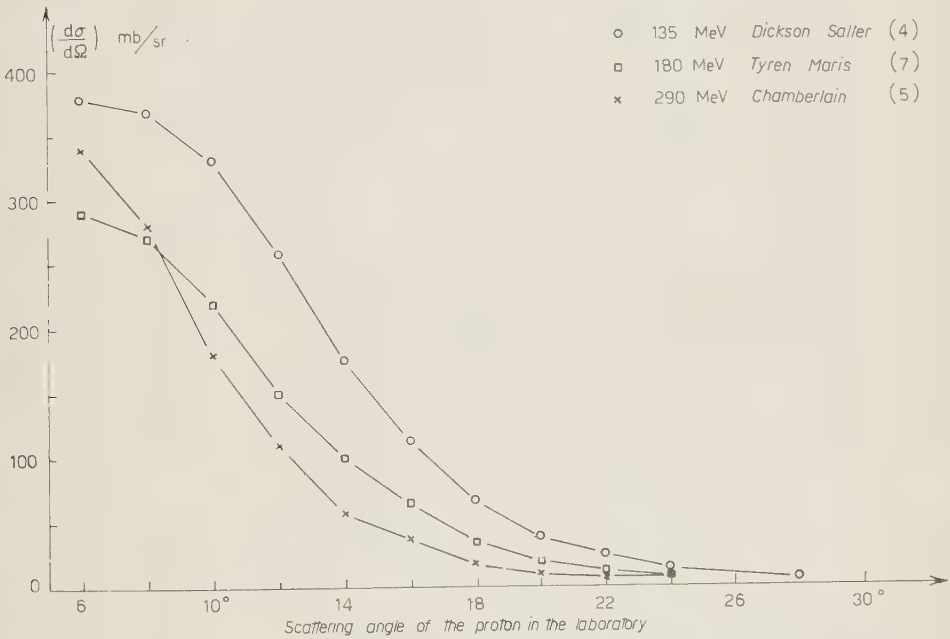

Fig. 3. – Differential cross section for elastic scattering of protons of different kinetic energies on carbon (polarization zero, left=right).

In Fig. 4 we report the corresponding analyzing power for the same energies of the protons. We define the analyzing power P_c in the usual way,

(4) J. M. DICKSON and D. C. SALTER: *Nuovo Cimento*, **6**, 235 (1957); R. ALPHONCE, A. JOHANSSON and G. TIBELL: *Nucl. Phys.*, **3**, 185 (1957).

(5) O. CHAMBERLAIN, E. SEGRÈ, R. D. TRIPP, C. WIEGAND and T. YPSILANTIS: *Phys. Rev.*, **102**, 1659 (1956).

(6) E. M. HAFNER: *Phys. Rev.*, **111**, 297 (1958); K. GOTOW: NYO-2352 (University of Rochester, 1959).

(7) H. TYREN and A. J. MARIS: *Nucl. Phys.*, **3**, 52 (1957) and **4**, 662 (1957).

TABLE I.

E_γ	E_m	ΔE_γ	$\theta_{p\,c.m.}$	T	C (g/cm²)	θ_c	no. 1	left	right	left	right	R/L_{unc}	$-\varepsilon_{unc}$	$-\varepsilon$
1	2	3	4	5	6	7	8	9	10	11	12	13	14	15
560	650	70	90.7 ± 5.2	129 ÷ 155	3.7	16.5	yes	230	365	7.6 ± 0.50	11.4 ± 0.8	1.5 ± 0.14	0.20 ± 0.07	0.25 ± 0.09
700	830	95	91.4 ± 5.2	180 ÷ 216	8.08	14°	no	194	398	16.9 ± 1.4	32.4 ± 2.5	1.92 ± .22	0.33 ± .07	0.42 ± .10
							yes	124	251	19.0 ± 1.7	38.4 ± 2.4	2.02 ± .22		
750	870	110	91.7 ± 5.2	195 ÷ 238	8.08	14	no	161	284	18.8 ± 1.5	29.4 ± 2.1	1.69 ± .19	0.26 ± .09	0.30 ± .12
800	930	118	92.2 ± 5.2	214 ÷ 258	8.08	14	yes	216	392	10.7 ± 1.1	20.0 ± 1.0	1.87 ± .21	.30 ± .09	0.37 ± .13
850	990	130	92.5 ± 5.2	236 ÷ 276	8.08	14	no	139	234	7.6 ± 0.8	12.9 ± 1.0	1.7 ± .22	.26 ± .10	0.32 ± .14

TABLE II.

E_γ	E_m	ΔE_γ	$\theta_{p\,c.m.}$	T	C (g/cm²)	θ_c	no. 1	left	right	left	right	R/L_{unc}	$-\varepsilon_{unc}$	$-\varepsilon$
1	2	3	4	5	6	7	8	9	10	11	12	13	14	15
475	650	75	90.7 ± 5.2	93 ÷ 129	3.7	16.5	yes	1368	1424	42.5 ± 1.8	43.9 ± 1.6	1.03 ± .06	0 ± 0.03	—
610	830	84	90.9 ± 5.2	144 ÷ 180	8.08	14°	no	527	749	40.1 ± 4.4	62.7 ± 3	1.56 ± .19	0.25 ± 0.07	0.42 ± 0.18
							yes	194	325	26.1 ± 3.3	47.9 ± 3.2	1.84 ± .28		
650	870	90	91.1 ± 5.2	162 ÷ 195	8.08	14	no	284	476	28.8 ± 2.1	47.5 ± 2.6	1.65 ± .15	0.25 ± 0.07	0.41 ± 0.17
700	930	92	91.4 ± 5.2	180 ÷ 214	8.08	14	yes	355	666	18.1 ± 1.4	35.2 ± 1.4	1.95 ± .17	0.32 ± 0.08	0.50 ± 0.19
750	990	110	91.7 ± 5.2	192 ÷ 236	8.08	14	no	478	754	26.0 ± 1.5	40.0 ± 1.7	1.52 ± .11	0.21 ± 0.05	0.31 ± 0.1

Columns meaning. - **1**: central energy of the γ's; **2**: energy of the synchrotron; **3**: energy width; **4**: proton c.m. angle; **5**: kinetic energy of the proton; **6**: carbon thickness; **7**: carbon scattering angle; **8**: counter 1 present or not; **9** (**10**): total number of protons in the left (right) telescope (not yet corrected for accidentals and background); **11** (**12**): frequency of the left (right) telescope; **13**: ratio right to left; **14**: asymmetry $-\varepsilon_{unc}$; **15**: the same corrected for inelastic scattering: $-\varepsilon = (R - L)/(R + L)$.

as the asymmetry:

$$(1)\qquad \varepsilon = \frac{\text{Left} - \text{Right}}{\text{Left} + \text{Right}},$$

for an incident beam of polarization $+1$.

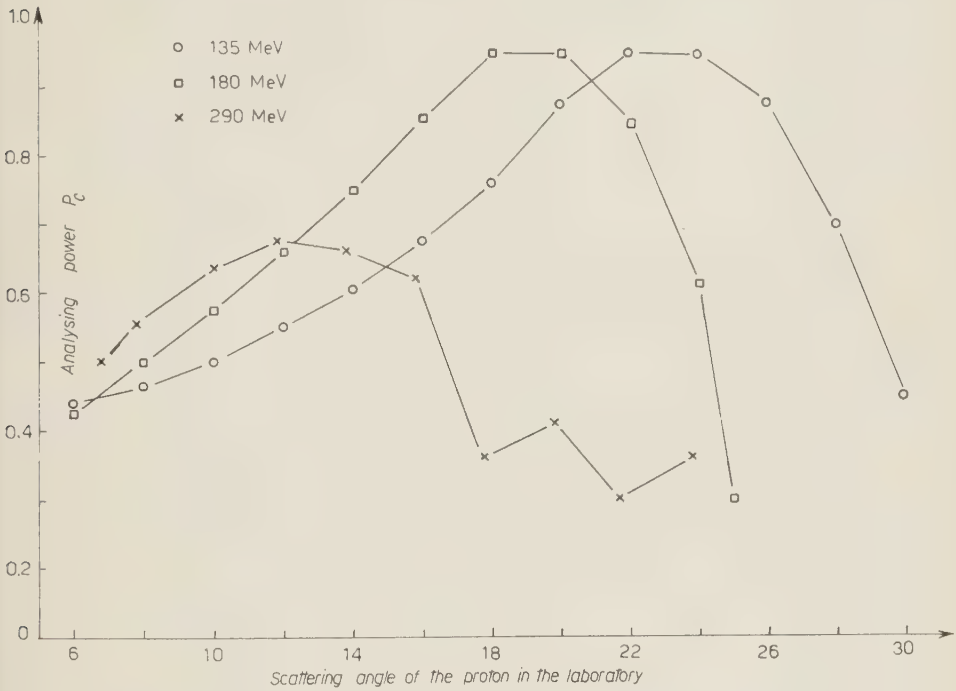

Fig. 4. – Analysing power of carbon for protons of different kinetic energies (polarization $+1$ of the incident beam; the same authors as in Fig. 3).

The choice of the scattering angle and of the dimensions of the hydrogen target and of the counters has to take into account the following features of the proton-carbon interactions:

— The elastic cross-section is a steep function of the angle (increasing for smaller angles).

— There is a definite maximum of the analyzing power at rather low values of the elastic cross-section.

— The Rutherford diffusion has to be taken into account in the choice of the scattering angle.

— The analysing power of the Carbon decreases with $\cos\varphi$, φ being the angle between the photoproduction plane and the plane of scattering in the carbon.

Fig. 5 gives, as an example, a graph where in the ordinate there is the product of the time T of counting multiplied by ΔP^2, being ΔP the error in the measurement of the polarization of the proton; in the abscissa there is the angle of scattering of the proton in carbon.

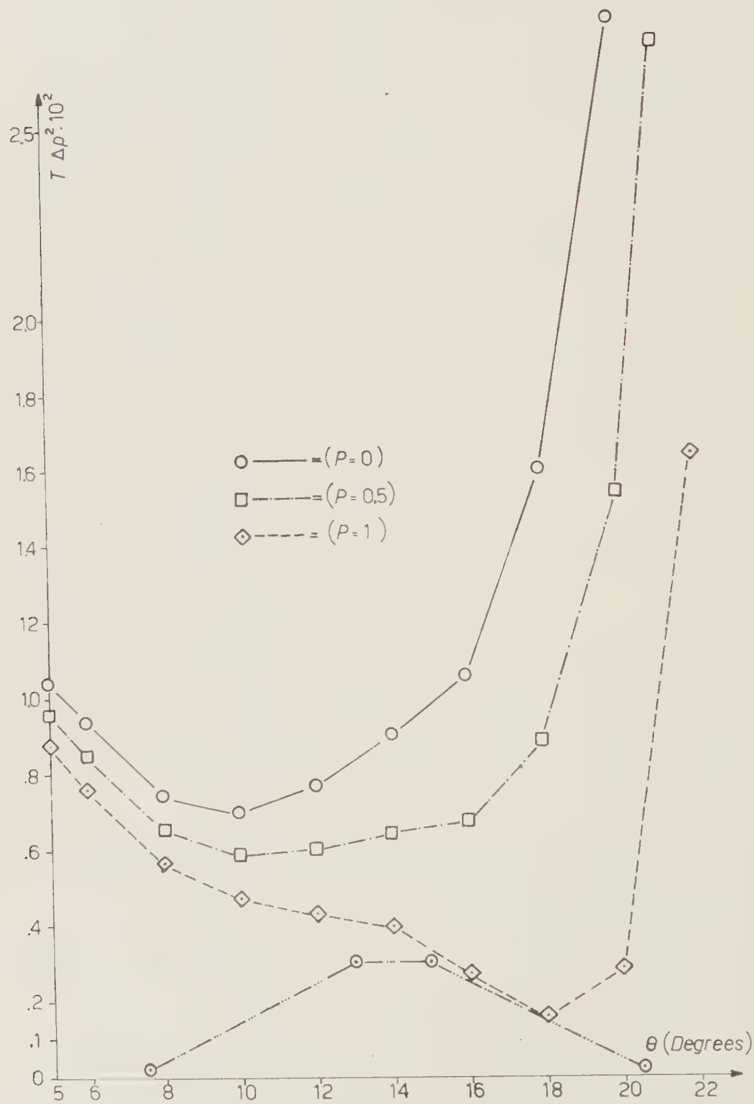

Fig. 5. – The product $T\Delta P^2$ *versus* the elastic scattering angle in carbon of 180 MeV protons. Below the curves the angular resolution of our telescope is given.

The graph has been drawn for an energy of the proton of 180 MeV. It clearly shows that the minimum time, for a given error ΔP, is displaced toward

an angle smaller than the angle corresponding to the maximum value of the analysing power; this being due to the fast decrease of the scattering cross-section *versus* the scattering angle. The graph of Fig. 5 does not take into account the contribution of the Rutherford scattering. With the help of graphs of this type the average angle and the horizontal dimensions of the counters have been chosen. The geometrical angular resolution we used is reported in arbitrary units in the same Fig. 5 at the bottom.

The vertical dimensions of the counters are larger than the horizontal dimensions, but with the general condition that $\cos\varphi \leqslant 0.8$.

In Table I are reported the values of the elastic scattering angles θ_c we have chosen at different proton energies.

The hydrogen target is similar to the type already in use at Cornell University: the hydrogen container is a cylindrical vessel with a vertical axis. The diameter is 7.4 cm, and it is 8.7 cm high. The wall is a foil of stainless steel plus mylar, with a total thickness per wall of 22 mg/cm². The vessel is contained in a cylindrical stainless steel vacuum chamber; mylar windows (3 mg/cm²) for the γ-rays and the protons are prepared in the chamber. Thin aluminum radiation shields are disposed between the vessel and the wall of the chamber. The diameter of our γ-ray beam at the target, is 4.5 cm. This dimension is defined by a lead collimator 18 mm in diameter; the collimator is at 2.3 m from the internal target (0.5 mm Ta) and 3.5 m from the H_2 target.

In Fig. 6 we give as an example the kinematical situation of our measurements. The rectangles are determined by the thickness of the copper absorbers we have chosen and by the dimensions of the counters.

The three rectangles which have been drawn refer to energies of 560, 700, 800 MeV for the γ-ray beam. Fig. 6 makes clear the reason why we preferred to use anticoincidences to define the energy of the protons, rather than limiting this energy by the top of the γ-ray beam: in this latter case one would have a proton flux on the carbon which is larger at smaller angles: this gives rise to an asymmetry between the two telescopes, even if the laboratory differential cross-section for photoproduction does not change with the angle θ.

The proton flux on the carbon scatterer may differ from point to point; as we explain later, we have masured the differential flux of the protons at each energy, as a function of the angle of emission θ.

The Čerenkov counter is made with a lead glass cylinder 18 cm thick and with a diameter of 35 cm. Light is collected by three photomultipliers in parallel, type 6364, which are in direct contact with the glass.

In front of the Čerenkov counter is a lead shield which reduces its opening to a diameter of 25 cm. It is possible, because of the rather high energy of our pions, to cut by a discriminator the height of the pulses from the Čerenkov, so that most of the charged pions do not enter the coincidences. This helps to avoid a possible contamination by neutrons in our proton telescopes.

Part of our measurements have been made with a different Čerenkov counter: a cylinder of lucite with a lead converter in front 8 mm thick.

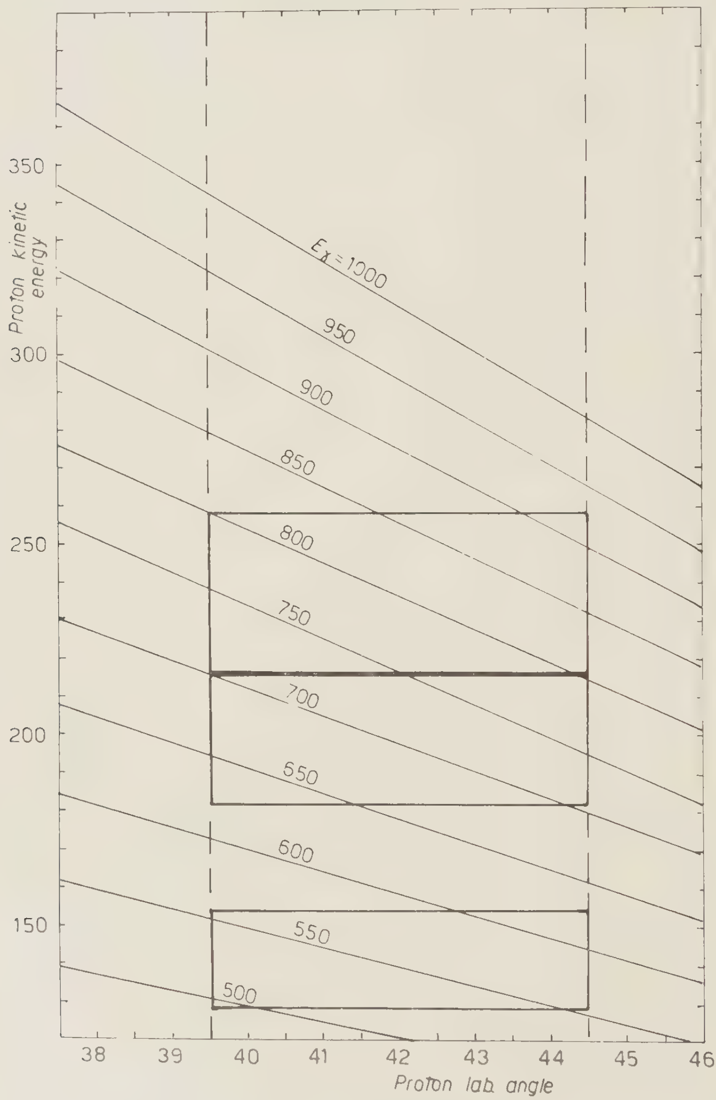

Fig. 6. – Proton kinematics in the process $\gamma + p \to p + \pi^0$. In the rectangles are the angles and the energies of the protons detected in the measurements at 560, 700, 800 MeV of the γ, respectively (first energy channel).

Counter 1 has been added in order to avoid the possibility that a neutron coming from a charged pion photoproduction may arrive to the carbon, pro-

duce a proton in a quasi-elastic collision, and be detected as a scattered proton in our coincidences.

The discussion of the results have confirmed to us that the presence of counter number 1 was not strictly necessary.

We have therefore included in our results some measurements which were taken without counter 1 in position.

3. – Measurements and controls.

The measurements for each γ-ray energy were taken in the following order. First, one of the two telescopes (for instance that at the right) is aligned with the hydrogen target and with counter number 1, and the thresholds of the discriminators of counters 4, 5, 6 are fixed to a level corresponding to an energy loss of at least 3 MeV in the scintillator. Second, on the basis of a photographic analysis of the height of the pulses, the levels of the discriminators of counters 1, 2, 3 are fixed, so that they certainly count the protons and only a very small percent of the pions. The further discrimination against the pions is made by the Čerenkov counter.

Third, the threshold of the Čerenkov counter is fixed to a value, that makes the counting rate quite independent from its voltage.

Similar preliminary measurements are made on the telescope at the left, and by alternatively aligning the right and the left telescope we verify that the counting rate is the same within statistics (usually within 4%).

After these controls have been made the two telescopes are finally set at the chosen scattering angle and the measurements start. Measurements with and without liquid hydrogen in the target, and with delays on the Čerenkov counter, on the counters 1 and 2, on the counters 4 and 8 are taken in order to measure accidentals. Every three to four hours each telescope is aligned to check that the counting rates are equal.

At each chosen γ-ray energy the distribution of the proton flux on the carbon scatterer was made: this measurement is necessary to deduce the polarization from the measured left to right ratio.

To do this, a counter (number 11 which is 2.5 cm large and 25 cm high) is placed just in front of the carbon, in line with the hydrogen target and one of the two telescopes; thus we measure the coincidences between counter 11 and the telescope plus Čerenkov for three different positions of counter 11 in front of the carbon. This gives the change of the proton flux with the angle θ of the recoil protons emitted from the hydrogen; in this way the possible different efficiency of the Čerenkov at different angles is automatically taken into account. The results of these measurements are reported for a few energies in Fig. 7.

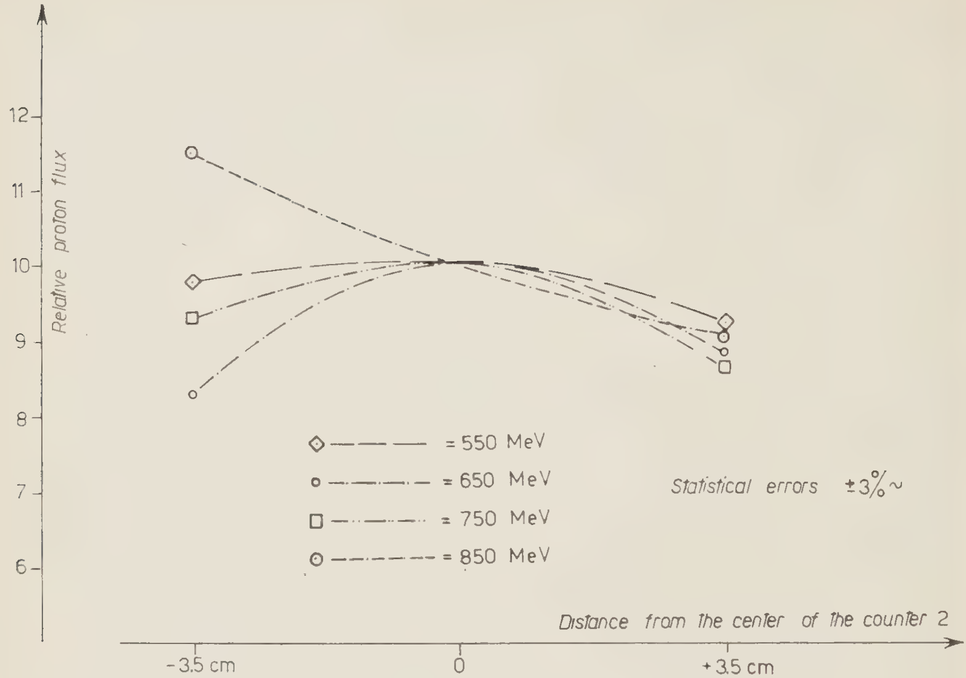

Fig. 7. – Differential proton flux at different positions of counter 11.

One of the main difficulties in our measurements is due to the fast dependence of the proton-carbon elastic cross-section on the angle: as a consequence any local difference in efficiency of our large counters may give rise to an apparent asymmetry. To be safe from this effect some further controls were made:

a) Measurements heve been taken of the protons scattered from the carbon at different angles between 0° and 16°, to the left and to the right, at energies for which the proton flux arriving to the carbon was rather uniform. In this way we could make sure that the angle zero coincides with the symmetry axis of our system, for those small angles for which the polarization effect is negligible, and that the two telescopes are really equivalent also where the proton intensity changes very fast with the angle.

b) Measurements have been made with the carbon substituted by an equivalent amount of lead, and placing the telescopes at angles of four to six degrees. Considering the large contribution of the Rutherford scattering and the lower analyzing power of the lead, we should expect equal counting for the two telescopes. The good results of these control measurements strongly contribute to increase our confidence in our results.

4. – Results.

Our results are reported in Tables I, II. Table I refers to the high energy channels R_{I} and L_{I}, and Table II reports the results from the low energy channels R_{II} and L_{II}: E_γ is the average energy of the photons producing the protons; E_m is the maximum energy on the γ-rays spectrum; ΔE_γ is the energy interval of the photons which contains 75% of the counted protons. $\theta_{p\,c.m.}$ is the average angle of the emitted protons in the center of mass.

T is the energy interval of the protons. C is the thickness of the scattering carbon. θ_c is the average scattering angle of the protons in carbon. Column 8 specifies if the counter one is in position or not. Columns 9 and 10 give the total number of protons scattered to the left and to the right, not yet corrected for accidentals and background. Columns 11 and 12 give the intensity of the protons scattered to the right and to the left respectively, per 10^{13} equivalent quanta, corrected for accidentals and background. In column 13 the ratio is given between the right and the left intensity, and in column 14 the asymmetry is given, defined as

$$\varepsilon_{unc}=\left(\frac{L-R}{L+R}\right)_{unc}.$$

The results of columns 11, 12, 13, 14 are already corrected for empty hydrogen target and for accidentals, but they have not been corrected yet for the contribution of the inelastic collisions. This contribution is calculated in Section 5. When the contribution of the inelastic events is subtracted, we finally obtain the correct value ε of the asymmetry. This value is given in column 15.

During the measurements the average intensity of our collimated γ-rays beam was of the order of $2.5\cdot10^{11}$ equivalent quanta per minute.

5. – Analysis of the data. Corrections.

In order to get the value of the polarization P from the measured left to right asymmetry, one must introduce a number of corrections. We give a list of those we took into consideration. The correction c) is the most important of the group.

a) Empty target corrections and accidentals.

b) Unwanted detection of other processes than the single neutral pion photoproduction.

c) Interactions of the recoil protons in the copper absorbers.

d) Different proton flux at different points in the carbon, that is in different points in counter number 2.

e) Inelastic collisions of the protons on carbon. The protons emitted in the photoproduction process, which initially have an energy higher than the energy defined in the two channels of our telescopes, may undergo in the carbon an inelastic collision which reduces their energy, and may therefore enter one of the two proton channels. The left to right asymmetry of the protons in these inelastic collisions is definitely smaller than in the elastic ones; as a consequence the inelastic processes, if not subtracted, have a tendency to reduce the total analysing power of the Carbon.

We describe in the following the method we used to estimate the corrections, when we decided we had to take them into account.

Estimate of correction *a*). The large intensity of our machine makes the quality of our electronics quite important. With our fast coincidences, and by properly clipping the Čerenkov and the other counters we succeeded to reduce the accidentals to about 10%. The empty target events were about 5%. These spurious events were immediately subtracted from our counting rates.

Estimate of corrections *b*), *c*). We did not introduce any correction for these effects. In fact many checks made it clear that we were really counting single π_0 events: the excitation curve of our protons, the size of the pulses in our counters, the resulting value of the absolute cross-section, etc. The analysis of the possible kinematical conditions, together, with any reasonable assumption on the differential cross-section, brought us to the conclusion that the contribution to our measurements of the double production of pions may be disregarded. We also did not introduce any correction for the interactions of the protons in the copper absorbers: this effect is symmetric in the two telescopes, and only may slightly change the definition in energy of our channels.

Estimate of correction *d*). The differential flux of the protons in the Carbon has been measured by the 2.5 cm counter as described in Section **3**. The correction for this lack of symmetry is taken into account when we deduce the polarization of the recoil protons with the Montecarlo method (see Section **6**).

Estimate of correction *e*). All our information on the quality of the carbon as an analyzer for measuring the polarization of the protons comes to us from other experiments, in particular from the synchrocyclotron experiments [4-7]. These experiments give us the left to right asymmetry and the differential cross-section in the elastic collisions of protons on carbon at different energies. It is necessary, to use these results, to subtract from the elastic events those which are due to the inelastic collisions in carbon, for which the cross section and the left to right asymmetry is unfortunately not as well known. After this subtraction has been done, we can make the estimate

of the analysing power of our system in respect of the protons which have been elastically scattered in our telescopes and which have entered our channels.

The correction may in principle be applied on the following lines. Call $(d^2\sigma/d\alpha\, dT)_{in}$ the differential cross-section for an inelastic collision of a proton on carbon, when it loses an energy T and is scattered at an angle α; call E the energy of the incident proton. Call $d\sigma/d\alpha$ the differential cross-section for elastic collision of protons on carbon. Each one of our telescopes detects protons of a given $\Delta E = E_2 - E_1$ energy interval (actually there are, as we said in Section 2, two energy channels per telescope, and our calculation has been made for each of them).

Call $N(E)\, dE$ the number of protons of energy $E - dE$ emitted from the hydrogen and arriving to the carbon. With these definitions, the number N_{el} of protons elastically scattered at the angle α when the proton flux arrives to the carbon is

$$N_{el} = n_c \Delta\Omega \int_{E_1}^{E_2} \frac{d\sigma}{d\alpha} N(E)\, dE \,, \tag{2}$$

$\Delta\Omega$ being the solid angle of our telescopes, and n_c the number of carbon nuclei per square centimeter.

The number N_{inel} of protons inelasticaly scattered is

$$N_{inel} = n\, \Delta\Omega \left[\int_{E_2}^{E_{max}} N(E)\, dE \int_{E-E_2}^{E-E_1} \left(\frac{d^2\sigma}{d\alpha\, dT}\right)_{in} dT + \int_{E_1}^{E_2} N(E)\, dE \int_{0}^{E-E_1} \left(\frac{d^2\sigma}{d\alpha\, dT}\right)_{in} dT \right], \tag{3}$$

where E_{max} is the maximum energy of the protons for the given maximum energy of the beam.

Should the value of $(d^2\sigma/dT\, d\alpha)_{in}$ be assumed to be independent of T in our energy interval $(E - E_1) - (E - E_2)$, then the ratio of the inelastic collisions to the elastic ones may be written as

$$\frac{N_{in}}{N_{el}} = \frac{(E_2 - E_1) \int_{E_2}^{E_{max}} (d^2\sigma/d\alpha\, dT)_{in} N(E)\, dE + \int_{E_1}^{E_2} (E - E_1)(d^2\sigma/d\alpha dT)_{in} N(E) dE}{\int_{E_1}^{E_2} (d\sigma/d\alpha) N(E)\, dE} . \tag{4}$$

The integrals contain the proton spectrum $N(E)\, dE$, which can be expressed by the differential cross-section in the laboratory system for photoproduction $dS/d\theta$, the efficiency C of the Čerenkov counter and the derivative dE_γ/dE of the energy of the producing photon *versus* the proton energy E at our fixed laboratory angle.

If we disregard the contribution of the inelastic collisions inside the channel, that is the second integral in the numerator of (4), formula (4) becomes

$$(5)\qquad \frac{N_{\text{in}}}{N_{\text{el}}} = (E_2 - E_1)\,\frac{\int_{E_2}^{E_{\max}} (\mathrm{d}^2\sigma/\mathrm{d}\alpha\,\mathrm{d}T)_{\text{in}}(C/E_\gamma)(\mathrm{d}S/\mathrm{d}\theta)(\mathrm{d}E_\gamma/\mathrm{d}E)\,\mathrm{d}E}{\int_{E_1}^{E_2} (\mathrm{d}\sigma/\mathrm{d}\alpha)(C/E_\gamma)(\mathrm{d}S/\mathrm{d}\theta)(\mathrm{d}E_\gamma/\mathrm{d}E)\,\mathrm{d}E},$$

where θ is the angle of emission of the proton of energy E from the hydrogen target.

The quantity C is a function of E, and has been calculated by us for our geometry, while $\mathrm{d}S/\mathrm{d}\theta$ is known from previous experiments [1].

The ratio (5) may be therefore calculated provided that the functions $(\mathrm{d}^2\sigma/\mathrm{d}\alpha\,\mathrm{d}T)_{\text{in}}$, $\mathrm{d}S/\mathrm{d}\alpha$ are known. It is just the limited knowledge of $(\mathrm{d}^2\sigma/\mathrm{d}\alpha\,\mathrm{d}T)_{\text{in}}$ that makes the estimate of (5) somewhat uncertain.

The value of $(\mathrm{d}^2\sigma/\mathrm{d}\alpha\,\mathrm{d}T)_{\text{in}}$ has been measured by TYRON and MARIS [7] in the angular region of $5^\circ \div 49^\circ$ (which includes the values interesting for our telescopes), at a kinetic energy of the protons of 185 MeV, and in the energy interval $0 < T < 35$ MeV.

This nice piece of information is unfortunately limited to the energy $E = 185$ MeV. The value of $(\mathrm{d}^2\sigma/\mathrm{d}\alpha\,\mathrm{d}T)_{\text{in}}$ exhibits a few peaks, clearly connected to some known carbon levels, for $0 < T < 15$ MeV, and varies in the limits $0.5 < \mathrm{d}^2\sigma/\mathrm{d}\alpha\,\mathrm{d}T < 1.5$ mb·sr·MeV for values of T between 15 and 35 MeV.

The only information at energies $E > 200$ MeV has been indirectly deduced from some absorption measurements of CHAMBERLAIN and co-workers [5]. We have interpreted their results as an indication that $\mathrm{d}^2\sigma/\mathrm{d}\alpha\,\mathrm{d}T \approx .7$ mb·sr·MeV at $E = 300$ MeV, and $20 < T < 150$ MeV.

The function $(\mathrm{d}^2\sigma/\mathrm{d}\alpha\,\mathrm{d}T)_{\text{in}}$ and the polarization af the protons may be considered rather well known in the region of the low energy levels of the carbon.

Having at disposal this limited amount of information, we calculated our correction for the inelastic events using formula (5). The function $(\mathrm{d}^2\sigma/\mathrm{d}\alpha\,\mathrm{d}T)_{\text{in}}$ has been assumed to be of the form

$$\left(\frac{\mathrm{d}^2\sigma}{\mathrm{d}\alpha\,\mathrm{d}T}\right)_{\text{in}} = \frac{552 - E}{338}\ \text{mb}\cdot\text{sr}\cdot\text{MeV},$$

and valid in the energy interval $(130 \div 300)$ MeV (this value is in agreement with the results at 185 and 300 MeV).

As we said, in formula (5) the contribution of the integral

$$\int_{E_1}^{E_2} (E - E_1)\left(\frac{\mathrm{d}^2\sigma}{\mathrm{d}\alpha\,\mathrm{d}T}\right)_{\text{in}} N(E)\,\mathrm{d}E,$$

given in (4) has been disregarded. This corresponds to include among the elastic collisions the quasi elastic ones, for which $T < (E_2 - E_1)$. The average value of T is in this case $\bar{T} \leqslant (E_2 - E_1)/3$, the equality being valid for a constant value of $(\mathrm{d}^2\sigma/\mathrm{d}\alpha\,\mathrm{d}T)_{\text{in}}$, which is not true, the cross-section being generally larger for smaller values of T. In our case we have $T \leqslant 10$ MeV, and one does not introduce an appreciable error assuming for these excitation energies a polarization comparable with that from the elastic collisions.

Let us call A the ratio $N_{\text{in.el}}/N_{\text{el}}$. Once the value of A is known, it is possible to get the correct value of the asymmetry ε:

$$\varepsilon = (1 + A)\varepsilon_{\text{unc}}\,.$$

In Tables I and II the values of ε_{unc} and the values of ε (columns 14 and 15) for different proton energies are given.

An alternative way is offered to us in order to estimate the contribution of the inelastic collisions, or at least to verify the validity of our corrections. As explained in Section 2 we have the possibility to measure protons of a given energy interval $E_2 - E_1$ in channel I or in channel II. The left to right asymmetry of the protons of a given energy has to be the same, independently from the channel where they are revealed, but for the contribution of the inelastic collisions, which are relatively more in the second channel and have a tendency to reduce the asymmetry ε_{unc} in this channel. Once the corrections for the inelastic collisions have been made with the method we outlined above, we shall have the same value of ε, inside the statistical errors, for protons of the same energy interval, independently from their channel. The check is quite efficient, due to the different distance of the two channels from the top energy of the protons.

The results of this check confirm our method. In Table III and in Fig. 8 we added together the asymmetries resulting from the first as well as from the second channel.

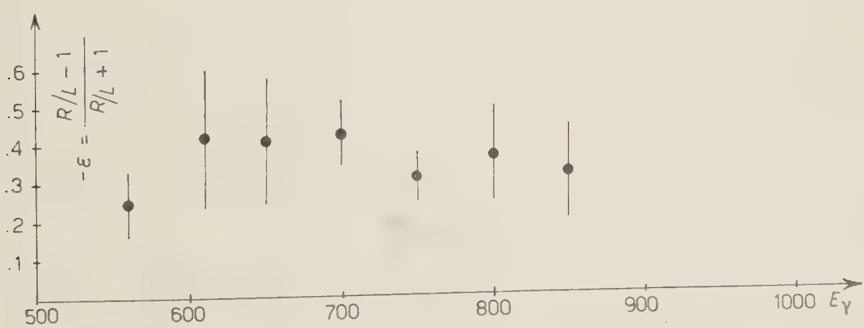

Fig. 8. – The asymmetry ε *versus* the energy of the photons (the intensity is always lower at the telescope closer to the γ-ray beam).

TABLE III. – *The asymmetry to be expected according to the Montecarlo method for $P = -1$ and for $P = 0$, the experimental value of ε and the corresponding value of the polarization of the recoil proton.*

E	ε_c $(P=-1)$	ε $(P=0)$	ε	P
560	0.64	0.01	-0.25 ± 0.09	$-0.4\ \pm0.14$
610	—	—	-0.42 ± 0.18	-0.63 ± 0.23
650	0.69	0	-0.41 ± 0.17	$-0.6\ \pm0.25$
700	—	—	-0.43 ± 0.09	-0.57 ± 0.12
750	0.82	0	-0.31 ± 0.07	-0.38 ± 0.09
800	—	—	-0.37 ± 0.13	$-0.5\ \pm0.17$
850	0.68	-0.04	-0.32 ± 0.14	$-0.5\ \pm0.22$

6. – The computation of the polarization P from the corrected asymmetry.

Let us call $P_c(\alpha)$ the analysing power of the carbon at the angle α, that is the asymmetry $\varepsilon=(L-R)/(L+R)$ for an incident proton beam of polarization $+1$. Let us call P the polarization of the recoil protons we are measuring. As well known, the relation holds:

$$\varepsilon = P_c(\alpha)\,P\,. \tag{6}$$

Relation (6) is exactly valid at a definite angle α.

In an extended telescope a range of angles α is interested and the value of P_c is an average obtained from an integration on all possible angles α. The integration has been performed on the following lines.

Let us consider as an « elementary » telescope, that element of our telescope which detects a proton emitted from a given point of the H_2 target and scattered in a given point of the carbon with given angles α and φ (φ is the angle among the photoproduction plane and the plane determined by the proton lines of flight before and after the collision in the carbon, that is the scattering plane: α is the angle among these two lines of flight).

We have divided the counters M, N (see Fig. 9) in $4\times 8=32$ elements, and in the calculation each element is replaced by its center. We have calculated the probability $F_{L,R}$ for having a proton emitted from the H_2 target, scattered in the carbon, and reaching a given element i of the counter at the left or at the right. This implies integration over all the possible positions in the H_2 target and in the carbon. The H_2 target may be approximated by a short segment along the γ-rays direction.

By this approximations the probability for the proton to get the i-th ele-

ment of the counter is given by an expression of the type

$$(7)\qquad (F_i)_{L,R}=\iint K\left[\left(\frac{\mathrm{d}\sigma}{\mathrm{d}\Omega}\right)_{L,R}\right]\mathrm{d}\xi\,\mathrm{d}S;\qquad K\frac{\mathrm{d}\sigma}{\mathrm{d}\Omega}(\alpha,\varphi)=I_i\,,$$

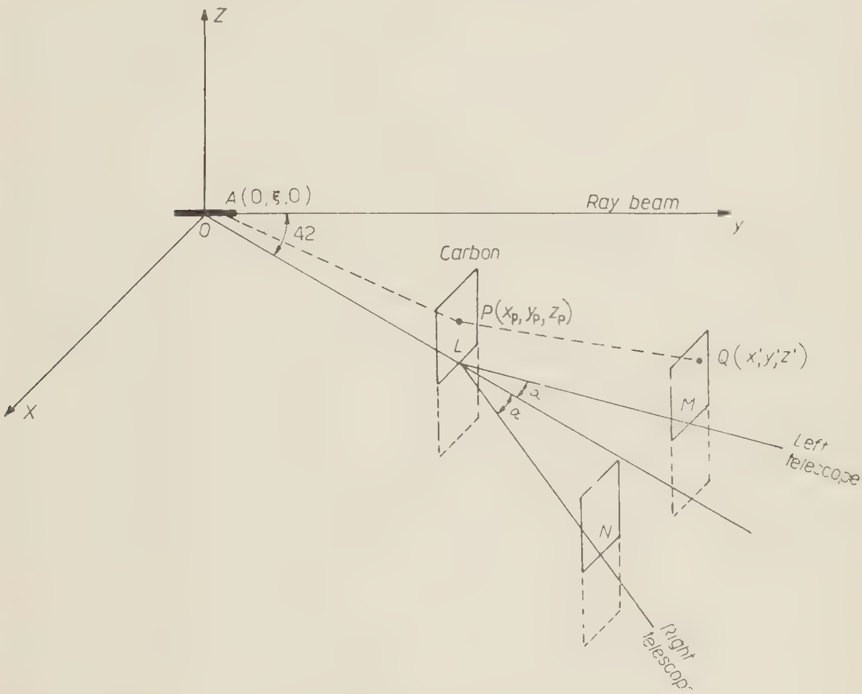

Fig. 9. – A view of our disposition to indicate the variables we used to calculate the polarization by the Montecarlo method.

where the factor K was introduced to take into account the difference in proton flux on the carbon from point to point, $\mathrm{d}S$ represents the elementary surface surrounding the point on the carbon where the scattering takes place, ξ is the co-ordinate on the hydrogen target. The integral (7) has been computed by the Montecarlo method.

The function $\mathrm{d}\sigma/\mathrm{d}\Omega$ is the differential elastic cross-section in carbon, which is different at the left and at the right for polarized protons; it is given by

$$\left(\frac{\mathrm{d}\sigma}{\mathrm{d}\Omega}\right)_L=\left(\frac{\mathrm{d}\sigma}{\mathrm{d}\Omega}\right)_{AV.}[1+PP_c(\alpha)\cos\varphi]\quad\text{at the left}\,,$$

$$\left(\frac{\mathrm{d}\sigma}{\mathrm{d}\Omega}\right)_R=\left(\frac{\mathrm{d}\sigma}{\mathrm{d}\Omega}\right)_{AV.}[1-PP_c(\alpha)\cos\varphi]\quad\text{at the right}\,.$$

The total flux of protons at the left and at the right is obtained by adding each contribution F_i as given in (7):

$$F_L = \sum_{i=1}^{32} (F_i)_L\,, \qquad F_R = \sum_{i=1}^{32} (F_i)_R\,.$$

The final asymmetry is given by

$$\varepsilon = \frac{F_L - F_R}{F_L + F_R}\,.$$

The relation between the asymmetry ε and the proton polarization is linear, and in order to have it, it is enough to estimate the value of ε for $P = -1$ and for $P = 0$. If the proton flux on the carbon is uniform, it evidently has to be $\varepsilon = 0$ for $P = 0$. In the other cases an approximate calculation of ε for $P = 0$ was made, by dividing the carbon in three parts, and using the experimental results on the proton flux in carbon we already reported.

For $P = -1$ the integral (7) has been computed by the FINAC electronic computer of the Istituto Nazionale del Calcolo, using the following method. One point (ξ, S) within the limits of the integral was extracted at random, and the value of the function $I_i(\xi, S)$, as given in (7) was calculated. After a sufficient number of random extractions N, we can evaluate the mean value of I_i:

$$\bar{I}_i = \frac{\sum_1^N {}_l\, I_{i,l}(\xi, S)}{N}\,.$$

The product $\bar{I}_i \cdot V_{\xi,S}$, $V_{\xi,S}$ being the volume within which we integrate, gives the Montecarlo value of the integral given in (7).

7. – The sign and the value of the polarization.

We have found a right/left ratio larger than one in all our measurements, and we made our measurements at the right of the γ-ray beam (see Fig. 1). The intensity of the protons scattered from the carbon is therefore lower at the telescope which is closer to the γ-ray beam. By knowing the analyzing power of the carbon, we can say that most of our protons emitted from the hydrogen target have the spin down. If we define the sign of the polarization by the vector $(\boldsymbol{n})$ as we show in formula (9), then the sign of our polarization results to be negative.

In Table III we give the results on the polarization: the energy of the γ-ray beam is given in column 1; the asymmetry ε as resulting from the Montecarlo method when the incident protons have polarization $P=-1$ is given in column 2; the same for $P=0$ in column 3; column 4 reports the experimental value we found for the asymmetry (which is negative according to our definition), and finally we give in column 5 the value we found of the polarization of the recoil protons.

The value of the polarization P as a function of the γ-ray energy is also given in Fig. 10.

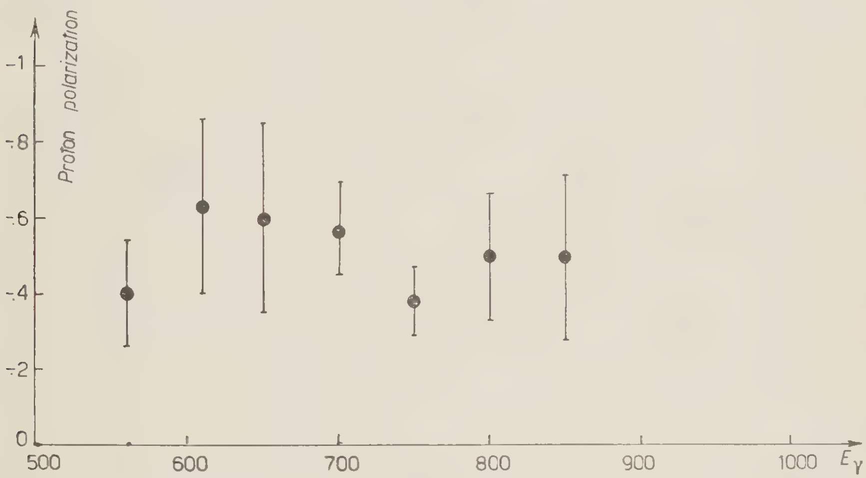

Fig. 10. – The polarization P of the recoil proton at 90° c.m. *versus* the γ-ray energy.

We remark that our results at 700 MeV and 550 MeV are in agreement with the results of STEIN (3).

8. – Discussion of our results.

A general discussion of the experimental results in photoproduction has been recently made by PEIERLS (8), and we shall refer to his work.

In particular this author has given a general table of the angular distributions and polarizations in photoproduction, and we will make use of his results.

His assignements have been done on the basis of π^+ and π^0 photoproduction, and of the polarization up to 700 MeV; his attribution of the states is reported

(8) R. F. PEIERLS: *Phys. Rev.*, **118**, 325 (1960).

in the Table IV. We shall see that our results agree with his general assigments, but differ in the possible estimate of the relative amplitudes of the levels.

TABLE IV. – *Quantum numbers describing the three photoproduction resonances.*

Level	l	Y	w	λ^+	λ^0	T
A	1	$\frac{3}{2}$	+	—	—	$\frac{3}{2}$
B	1	$\frac{3}{2}$	—	+	—	$\frac{1}{2}$
C	2	$\frac{5}{2}$	+	+	—	$\frac{1}{2}$

l = multipole order; Y = total angular momentum; w = parity; T = isotopic spin; λ^+ and λ^0 = sign of the multipole amplitude for π^+ and π^0 photoproduction, respectively.

The most interesting characteristic of our results is that the polarization remains rather high from 550 MeV up to 850 MeV, as if at each energy two or more interfering states, with a resulting polarization of negative sign, were present. In particular no minimum of the polarization appears around 700 MeV.

We must therefore look for those states who can describe the already known results of the differential cross-sections for neutral and positive pions, and which can produce a polarization of negative sign in the notations of Peierls, and rather constant in our range of energies.

a) Assignement of the levels on the basis of the sign of the polarization. – In the hypothesis that the three states A, B, C with the attributions specified in Table IV are present, the expression of the polarization becomes

$$P(\theta) = \frac{1}{\mathrm{d}\sigma/\mathrm{d}\Omega}\{-4AB\sin(\delta_A-\delta_B) - 5\sqrt{3}xAC\sin(\delta_A-\delta_C) + \\ + \sqrt{3}BC(x^2-2)\sin(\delta_B-\delta_C)\}\sin\theta(\boldsymbol{n}), \tag{8}$$

with $x = \cos\theta$.

$(\boldsymbol{n})$ is a unit vector normal to the production plane, which we define as

$$\boldsymbol{n} = \frac{\boldsymbol{k}\wedge\boldsymbol{q}}{|\boldsymbol{k}\wedge\boldsymbol{q}|}, \tag{9}$$

$\boldsymbol{k}$, $\boldsymbol{q}$ being the momenta of the incoming photon and the outgoing pion in the c.m. system. $\mathrm{d}\sigma/\mathrm{d}\Omega$ is the photoproduction cross-section for π^0 production; it is given by

$$\frac{\mathrm{d}\sigma}{\mathrm{d}\Omega} \sim \frac{1}{2}A^2(5-3x^2) + B^2\left(\frac{5}{2}-\frac{3}{2}x^2\right) + \frac{3}{2}C^2(1+6x^2-5x^4) - \\ -2ABx\cos(\delta_A-\delta_B) + \sqrt{3}AC(1-3x^2)\cos(\delta_A-\delta_C) + \\ + \sqrt{3}\,BC(6x-4x^3)\cos(\delta_B-\delta_C).$$

$A\exp[i\delta_A]$, $B\exp[i\delta_B]$, $C\exp[i\delta_C]$ are the amplitudes of the levels producing the first, second, third resonance respectively. A, B, C may be positive or negative, and we restrict therefore the phases δ to lie between 0 and π.

Our experimental results refer to $x=0$, and in this case the AC term is zero in (8). The two remaining interference terms AB, BC both give a negative polarization, if we assume for A, B, C the sign of the multipole amplitude λ_0 which has been proposed in Table IV.

This negative sign of the polarization both at the left and the right of the second resonance is in agreement with our experimental results (Fig. 10, Table III). According to them and in agreement with Table IV, B must have opposite parity with A and with C and therefore B is an E_1, $d^{\frac{3}{2}}$ transition, and C is an E_2, $f^{\frac{5}{2}}$ transition. The attribution of B agrees with the experimental results of STEIN (3), and also with the recent theoretical considerations of MALLOY (9) and of PELLEGRINI and STOPPINI (10).

b) On the amplitude of the levels at different energies. – The analysis of Peierls has been done under the hypothesis that polarization is small or absent above 700 MeV. This was indicated by some preliminary measurements quoted by him, which do not seem to agree with our present results. In fact (see Fig. 10) we find a definite negative polarization and this result may somewhat change the discussion as developed before.

It is reasonable to assume that the amplitude of C is negligible below 700 MeV. In fact there is no evidence of appreciable terms x^4 in the angular distributions below 800 MeV, this implying that at least at 700 MeV, $C^2 \ll A^2+B^2$. In this case the high polarization we observe at 700, 750 MeV must be due, according to (7), to the interference AB: that is, the amplitude A of the first resonance extends beyond 700 MeV. When the energy increases the contribution of the AB interference decreases, but at the same time the interference BC comes out and this can explain our experimental result that the polarization remains rather constant up to 850 MeV. Our statistical uncertainties do not allow to establish if there is a real minimum around 750 MeV.

Just to fix our ideas we tried to calculate the polarization on the following hypotheses: amplitude A vanishes only after 800 MeV; amplitude B has a maximum at 700 MeV and an extension corresponding to a width of the second resonance of about 120 MeV; the amplitude C starts from 700 MeV and has a maximum at 1100 MeV. In these hypotheses and with reasonable assumptions on the phasis we found values of the polarization at different energies which are consistent with our results.

While we believe in the qualitative indications that we derived from our results, we do not consider convenient to try to get more quantitative results,

---

(9) J. O. MALLOY: private communication.

(10) C. PELLEGRINI and G. STOPPINI: *Nuovo Cimento*, 17, 269 (1960).

because we realise that, with the present large statistical errors in the measurements of the polarization and of the differential cross-section, it is not yet possible to obtain in an unambiguous way the value of the amplitudes of the multipole states also supposing that only states A, B, C are contributing in this range of energies. It is certain that more refined work remains to be done in this energy interval. In particular for the polarization, it may be interesting to examine the function $P(\theta)$ at other angles than $\theta = 90°$.

In conclusion, the present results agree with the hypotheses that:

1) The three states A, B, C corresponding to the first, second, third resonance, seem to be sufficient to explain the single π^0 photoproduction in the range of energies $(500 \div 900)$ MeV. This may be simply due to the poor accuracy of the existing measurements.

2) The three states A, B, C have multipole order l, total angular momentum J, parity w, sign, isotopic spin, as assigned in Table IV.

3) The resonance A extends its amplitude rather beyond 700 MeV (for instance up to 800 MeV).

4) The resonance C has an amplitude of the same order as B, and starts to be important from 750 MeV on.

* * *

The authors express their gratefulness to Dr. GIORGIO GHIGO and the whole Synchrotron staff for the useful discussions and the continuous co-operation.

They are also grateful to Dr. CORRADO MENCUCCINI for his substantial help during the development of this work; to Dr. ANGELO TURRIN and his group for assistance in developing the program for the electronic computer; to Dr. CLAUDIO PELLEGRINI and GHERARDO STOPPINI for useful discussions.

RIASSUNTO

È stata misurata la polarizzazione dei protoni di rinculo nella reazione $\gamma + p \to p + \pi^0$, usando il fascio γ dell'elettrosincrotrone di Frascati; le misure sono eseguite ad un angolo corrispondente a 90° nel sistema del baricentro, nell'intervallo di energia γ di $(500 \div 900)$ MeV. Si è usata una tecnica di contatori; la polarizzazione dei protoni è ricavata dall'asimmetria nella diffusione elastica, a sinistra e a destra, dei protoni contro carbonio. I risultati sperimentali sono dati in Tab. III e in Fig. 10. È stata trovata polarizzazione diversa da zero, sempre dello stesso segno, a tutte le energie misurate e precisamente: $P = -0.4 \pm .14$ a 560 MeV; $P = -0.63 \pm 0.23$ a 610 MeV; $P = -0.6 \pm 0.25$ a 650 MeV; $P = -0.57 \pm 0.12$ a 700 MeV; $P = -0.38 \pm 0.09$ a 750 MeV; $P = -0.5 \pm 0.17$ a 800 MeV; $P = -0.5 \pm 0.22$ a 850 MeV. La discussione di questi risultati sperimentali, insieme a quelli sulle distribuzioni angolari, porta alla conclusione che essi sono in accordo con l'ipotesi che la seconda risonanza sia una transizione $(E_1, d_{\frac{3}{2}})$ e la terza sia una transizione $(E_2, f_{\frac{5}{2}})$.

Unitarity and the Mandelstam Representation (*).

R. W. Lardner
St. John's College - Cambridge

(ricevuto il 20 Agosto 1960)

Summary. — The three particle terms in the unitarity expansion for a scattering amplitude are examined on the assumption that the relevant production amplitudes satisfy single dispersion relations. It is shown that they can be made to satisfy the Mandelstam representation within the freedom which seems to be allowed by the unitary equation. The proof is extended to the four particle terms.

1. – Introduction.

Mandelstam (1) and Kibble (2) have recently examined the two-particle terms in the unitarity equation for a scattering amplitude, and have shown, on the basis of single dispersion relations for the scattering amplitudes appearing in these terms, that they satisfy Mandelstam's representation. In this note we consider the same problem for the three-particle terms. The motivation behind this investigation was the discovery of the surprising lack of analyticity of production amplitudes in perturbation theory (3). These restrictions, however, proved irrelevant: it turns out that single dispersion relations for five-point amplitudes are sufficient to guarantee that the three-particle terms satisfy double dispersion relations, provided we allow ourselves to make a judicious choice of cuts.. We show, in fact, that the absorptive part satisfies a single dispersion relation, which has been shown by Mandelstam (1) to be equivalent to two-variable relations for the total amplitude.

In Section **2** we consider the kinematics of the three-particle terms and in Section **3** we reduce the terms to a form in which some of the integrations

(*) This work was supported in part by the United States Air Force, Air Research and Development Command, European Office.

(1) S. Mandelstam: *Phys. Rev.*, **112**, 1344 (1958).

(2) T. W. B. Kibble: *Phys. Rev.*, **117**, 1159 (1960).

(3) M. Fowler, P. V. Landshoff and R. W. Lardner, *Nuovo Cimento*, **17**, 956 (1960).

can be performed. Unlike the one- and two-particle terms, this reduced form still contains a δ-function, which leads to the interesting situation of having an integration round a non-null contour on a torus. The methods of POLKINGHORNE and SCREATON ([4]) can be extended to this case, and they give all the pinch singularities. However, a new type of singularity arises due to the degeneracy of the torus, and it is this that takes the place of the missing end-point singularities. It is shown that the cuts associated with this singularity can be so chosen as to make the amplitude have only real singularities.

In Section 5 the proof is extended to the four particle terms.

In what follows we employ the following notation. Let $\{p_i\}$ be the particle 4-momenta associated with any process. We denote scalar invariants by

$$s_{kl} = (\pm p_k \pm p_l)^2$$
$$(+ \text{ for ingoing, } - \text{ for outgoing}).$$

We also use the shorthand, for scalars x, y, z

$$k(x, y, z) = x^2 + y^2 + z^2 - 1 - 2xyz\,.$$

2. – Kinematics.

We consider a process in which incoming particles 1, 2 (4-momenta p_1, p_2) go, through intermediate particles 5, 6, 7, into final particles 3, 4 (Fig. 1, 2). Then in the centre of mass system of the incoming particles we can write

$$(1)\qquad \begin{cases} p_1 = (E_1, \boldsymbol{q}_1)\,, & p_2 = (E_2, -\boldsymbol{q}_1)\,, \\ p_3 = (E_3, \boldsymbol{q}_3)\,, & p_4 = (E_4, -\boldsymbol{q}_3)\,, \\ p_5 = (E_5, \boldsymbol{q}_5)\,, & p_6 = (E_6, -\boldsymbol{q}_5 - \boldsymbol{q}_7)\,, \quad p_7 = (E_7, \boldsymbol{q}_7)\,, \end{cases}$$

with the energy $s_{12}^{\frac{1}{2}} = E_1 + E_2 = E_3 + E_4 = E_5 + E_6 + E_7$.

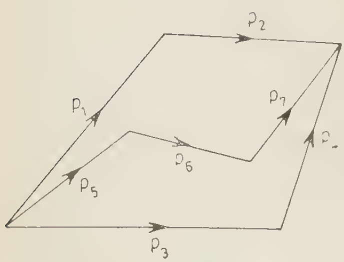

Fig. 1. – Momentum diagram for three-particle terms.

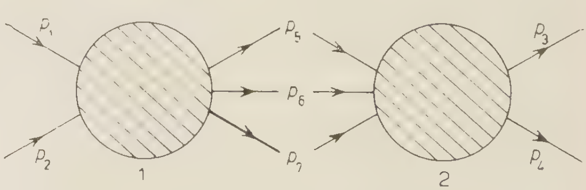

Fig. 2. – Graph representing the three-particle terms.

([4]) J. C. POLKINGHORNE and G. R. SCREATON: *Nuovo Cimento*, 15, 289 (1960).

A simple calculation then gives the E_i, $\boldsymbol{q}_i$ in terms of scalar invariants

$$(2)\qquad \begin{cases} E_1 = \dfrac{1}{2s_{12}^{\frac{1}{2}}}\,(s_{12} + m_1^2 - m_2^2)\,, \\ q_1^2 = \dfrac{1}{4s_{12}}\,[s_{12} - (m_1 + m_2)^2][s_{12} - (m_1 - m_2)^2]\,, \end{cases}$$

and similarly for E_2, E_3, E_4 and q_3^2;

$$(3)\qquad \begin{cases} E_7 = \dfrac{1}{2s_{12}^{\frac{1}{2}}}\,(s_{12} + m_7^2 - s_{56})\,, \\ q_7^2 = - m_7^2 + E_7^2\,, \end{cases}$$

and similarly for E_5, q_5^2. Defining $z_{ij} = \cos(\boldsymbol{q}_i, \boldsymbol{q}_j)$ we have

$$(4)\qquad 2q_1 q_7 z_{27} = s_{27} - m_2^2 - m_7^2 + \frac{1}{2s_{12}}\,(s_{12} + m_2^2 - m_1^2)(s_{12} + m_7^2 - s_{56})\,,$$

and similar expression for $z_{\;7}$, z_{35}, z_{15} and z_{13}.

Finally we have

$$(5)\qquad p_6^2 - m_6^2 = 2q_5 q_7 (z_{57} - \lambda)\,,$$

where

$$\lambda \equiv \frac{1}{2q_5 q_7}\left\{s_{12} + m_6^2 - s_{56} - s_{67} - \frac{1}{2s_{12}}\,(s_{12} + m_5^2 - s_{67})(s_{12} + m_7^2 - s_{56})\right\},$$

and λ is independent of $z_{27}, \ldots, z_{15}$ and z_{13}.

It will be more convenient to work with Φ, Ψ, defined by

$$(6)\qquad \begin{cases} z_{15} = z_{13} z_{35} + (1 - z_{13}^2)^{\frac{1}{2}}(1 - z_{35}^2)^{\frac{1}{2}} \cos\Phi\,, \\ z_{47} \quad\;\; z_{21} z_{27} + (1 - z_{21}^2)^{\frac{1}{2}}(1 - z_{27}^2)^{\frac{1}{2}} \cos\Psi\,, \end{cases}$$

in place of z_{15}, z_{17}. Then, taking a representative co-ordinate system with, say, $\boldsymbol{q}_1 = q_1(1,0,0)$ and $\boldsymbol{q}_3 = q_3(z_{13}, \sqrt{1 - z_{13}^2}, 0)$ we obtain

$$(7)\qquad \begin{aligned} z_{57} = z z_{27} z_{35} - z(1 - z_{27}^2)^{\frac{1}{2}}(1 - z_{35}^2)^{\frac{1}{2}} \cos\Phi \cos\Psi + (1 - z^2)^{\frac{1}{2}} \cdot \\ \cdot [z_{27}(1 - z_{35}^2)^{\frac{1}{2}} \cos\Phi + z_{35}(1 - z_{27}^2)^{\frac{1}{2}} \cos\Psi] + (1 - z_{27}^2)^{\frac{1}{2}}(1 - z_{35}^2)^{\frac{1}{2}} \sin\Phi \sin\Psi\,, \end{aligned}$$

where we write $z \equiv z_{13} = z_{24}$.

3. – The three particle terms.

For physical values of s_{12} and z (*i.e.*, z real, $|z| \leqslant 1$), the three particle term in the unitarity equation can be reduced (see Appendix I) to

$$(8)\qquad A^{(3)}(s_{12}, z) = \frac{1}{8s_{12}} \int \mathrm{d}s_{56}\,\mathrm{d}s_{67} \int\limits_{-1}^{1} \mathrm{d}z_{27}\,\mathrm{d}z_{35} \int\limits_{0}^{\pi} \mathrm{d}\Phi\,\mathrm{d}\Psi\,\delta(z_{57}-\lambda)\cdot$$
$$\cdot M_1^*(s_{12}, z_{27}, z_{15}, s_{56}, s_{67})\cdot M_2(s_{12}, z_{47}, z_{35}, s_{56}, s_{67})\,,$$

with z_{15}, z_{17} given in terms of Φ, Ψ by (6). We are interested in the analytic properties of $A^{(3)}$ as a function of z for real s_{12}; the z-dependence in (8) comes only from the z_{15}- and z_{47}-dependences of $M_1^* M_2$ and from the argument of the δ-function, so that in order to isolate the dependence of $A^{(3)}$ on z we must make some assumption about the behaviour of M_1 and M_2 as functions of z_{15} and z_{47}. We assume that they are analytic in the cut-planes of these variables, with real cuts, so that

$$(9)\qquad M_1^* = \frac{1}{\pi}\int\limits_{\infty}^{\infty} \frac{A_1^*(z'_{15})}{z'_{15}-z_{15}}\,\mathrm{d}z'_{15}\,,\qquad M_2 = \frac{1}{\pi}\int\limits_{-\infty}^{\infty} \frac{A_2(z'_{47})}{z'_{47}-z_{47}}\,\mathrm{d}z_{47}\,,$$

and we suppose normal thresholds — *i.e.*, the ranges of integration lie completely outside $|z'| < 1$. Substitution from (6) into (9) and of the result into (8) gives

$$(10a)\qquad A^{(3)}(s_{12}, z) = \frac{1}{8\pi^2 s_{12}} \int \mathrm{d}s_{56}\,\mathrm{d}s_{67} \int\limits_{-\infty}^{\infty} \mathrm{d}z'_{17}\,\mathrm{d}z'_{15} \int\limits_{-1}^{1} \mathrm{d}z_{27}\,\mathrm{d}z_{35}\,\chi(z, z_{27}, z_{35}, z'_{17}, z'_{15}, \lambda)\cdot$$
$$\cdot A_1^*(s_{12}, z_{27}, z'_{15}, s_{56}, s_{67})\cdot A_2(s_{12}, z_{35}, z'_{47}, s_{56}, s_{67})\,,$$

where

$$(10b)\qquad \chi = \int\limits_{0}^{\pi} \frac{\mathrm{d}\Phi\,\mathrm{d}\Psi\,\delta(z_{57}-\lambda)}{[z'_{15}-zz_{35}-(1-z^2)^{\frac12}(1-z_{35}^2)^{\frac12}\cos\Phi][z'_{47}-zz_{27}-(1-z^2)^{\frac12}(1-z_{27}^2)^{\frac12}\cos\Psi]}\,,$$

with z_{57} given by (7).

4. – Singularities of χ.

i) Then for physical z,

$$\chi = \int\limits_{0}^{\pi} \frac{\mathrm{d}\Phi\,\mathrm{d}\Psi\,\delta\{f(\Phi, \Psi)\}}{F(\Phi, \Psi)}\,,$$

where we can write $F(\Phi, \Psi) = g(\Phi)h(\Psi)$. Firstly we investigate the form of $f(\Phi, \Psi) = 0$; changing variables to $x = \cos\Phi$ and $y = \cos\Psi$, taking the $\sin\Phi\sin\Psi$ term over to the r.h.s. and squaring both sides gives a quartic in x and y which has the following properties: any line x (or y) = constant meets the curve twice at infinity; its asymptotes are

$$(11)\qquad y = \frac{1 - zz_{27}}{(1-z^2)^{\frac{1}{2}}(1-z_{27}^2)^{\frac{1}{2}}} \quad\text{and}\quad y = \frac{-1 - zz_{27}}{(1-z^2)^{\frac{1}{2}}(1-z_{27}^2)^{\frac{1}{2}}},$$

and similar one parallel to $x = 0$; and it has two pairs of tangents in each direction, all of which lie between the asymptotes, and two pairs of which are the lines $x = \pm 1$, $y = \pm 1$. We conclude that the curve is as shown in Fig. 3, or a rotation of this through 90°. If $|\lambda| > 1$, the second two pairs of tangents are complex, so that the closed loop, Γ, is missing in this case.

The form of the complex surface $f(x, y) = 0$ has been obtained in a similar case by TARSKI [5]; we merely remark that it can be regarded as a torus, with two surfaces joining Γ to each infinite arc.

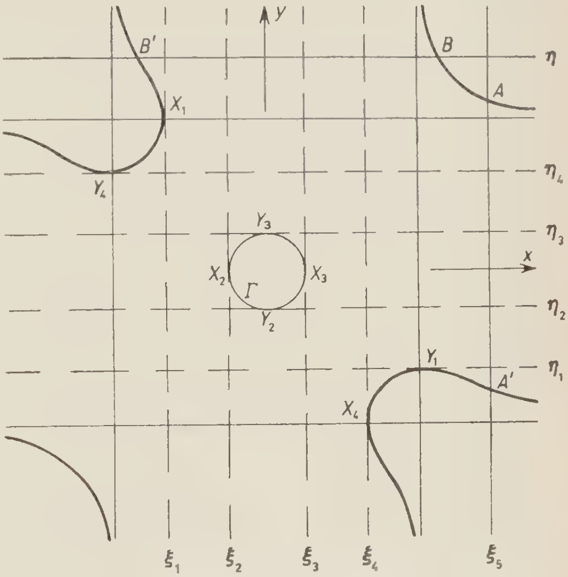

Fig. 3. – Plot of $f(x, y) = 0$; general case.

In all possible configurations, the only part of the curve lying inside the square region bounded by $x = \pm 1$, $y = \pm 1$ (*i.e.*, the region of integration) is Γ, which is therefore the integration contour for χ; if $|\lambda| > 1$, none of the curve lies inside the square, so $\chi = 0$ (*i.e.*, the domain over which the s_{56}, s_{67} integrations are performed must be limited to $|\lambda| \leqslant 1$).

ii) With this definition we can now continue χ to unphysical values of z: as z varies, the torus moves about continuously in the complex x–y space, and we vary the integration contour continuously with it. As singularities of the integrand approach the contour, we deform it away from them on the surface of the torus. This gives an analytic continuation by the generalization

([5]) J. TARSKI: *Journ. Math. Phys.*, **1**, 149 (1960).

of Cauchy's theorem to Riemann surfaces. A singularity of χ results from this being impossible, *i.e.*, from two coalescing singularities pinching the contour (we note that there can be no end-point singularities). This, by the results of Polkinghorne and Screaton ([4]), implies an extremum of $F(\Phi, \Psi)$ on $f = 0$; introducing Lagrange multipliers, we have

$$\text{(12)} \qquad \begin{cases} F = gh = 0\,, \\ F_\Phi|_{f=0} = 0 \quad \text{gives} \quad g_\Phi h + \lambda f_\Phi = 0\,, \\ F_\Psi|_{f=0} = 0 \quad \text{gives} \quad g h_\Psi + \lambda f_\Psi = 0\,, \end{cases}$$

which are satisfied by

$$\text{(13)} \qquad \begin{cases} (a) \quad g = g_\Phi = 0 \to k(z, z_{35}, z'_{15}) = 0\,, \\ (b) \quad h = h_\Psi = 0 \to k(z, z_{27}, z'_{47}) = 0\,, \\ (c) \quad g = f_\Psi = 0 \to k(\lambda, z_{27}, z'_{15}) = 0\,, \\ (d) \quad h = f_\Phi = 0 \to k(\lambda, z_{35}, z'_{47}) = 0\,, \\ (e) \quad g = h \;\; = 0 \to (z_{35}z'_{47} + z_{27}z'_{15}) - z(z_{27}z_{35} + z'_{47}z'_{15}) + \\ \qquad\qquad + \sqrt{k(z, z_{35}, z'_{15})k(z, z_{27}, z'_{47})} - \lambda(1 - z^2) = 0\,. \end{cases}$$

The remaining possibility of a singularity is the degeneracy of the surface at a singular point; we return to this later.

Transforming to x, y

$$\text{(14)} \qquad \chi = \int_{-1}^{1} \frac{\mathrm{d}x\,\mathrm{d}y\,\delta\{f(x, y)\}}{g(x)\,h(y)\sqrt{(1 - x^2)(1 - y^2)}}\,.$$

There are thus singularities of the integrand at $x^2 = 1$, $y^2 = 1$, *i.e.*, at those points X_i, Y_i (cf. Fig. 3) which lie on $x, y = \pm 1$. If any of these lies on Γ we deform the integration contour round it. The direction of deformation does not affect the physical values of the function since the singularity appears only with the power $-\frac{1}{2}$ in the integrand. It will affect the position of the cuts, but, as we shall see later, only in a trivial way. We draw lines ξ, η at $f(x) = 0$, $g(y) = 0$ respectively, meeting the curve in AA', BB', which are the remaining singular points of the integrand. The singularity (a) arises from the coincidence of A and A' at a singular X_i; similarly for (b); (c) arises from the coincidence of A and A' at a non-singular X_i; similarly (d); (e) arises from the coincidence of one of A, A' with one of B, B'.

iii) We now wish to continue in the z-plane to a singularity of χ, and see whether the singularities do, in fact, pinch the contour. However, the

singularities of χ lie outside the physical region, and there is some difficulty in visualizing the movement of the torus in four dimensions. So instead we first decrease z'_{15}, say, below its integration range so that the singularity occurs for physical z, and then continue along the singular surface back to the given value of z'_{15}; during this latter movement there is no opportunity for the coincident singularities to change from pinching to non-pinching, or vice-versa, except that we might pass over a cut which will produce a discontinuity of behaviour.

Reducing z'_{15} moves ξ to the left (we take $z'_{15} > -1$ originally) and leaves everything else unchanged. Eventually A and B coincide; this cannot possibly pinch Γ, so we conclude (c) does not occur. Further reduction of z'_{15} makes A, A' coincide at X_4, and this also is non-singular; it gives type (a) if ξ_4 is $x=1$, type (c) otherwise. Still further reduction makes A, A' move round the surface of the torus (in opposite directions, since the y's at A, A' are the complex conjugate roots of a real equation) and finally converge at X_3. If ξ_3 is $x=1$, then whichever way we have deformed the contour round the stationary singularity, one of the coincidences must pinch it; if ξ_3 is not $x=1$, then A, A' themselves pinch the contour. Hence both (a) and (c) occur in this case.

Therefore the singularity $z'_{15}-zz_{35}=\pm(1-z^2)^{\frac{1}{2}}(1-z_{35}^2)^{\frac{1}{2}}$ (*i.e.*, (a)) occurs if and only if $x=\pm 1$ touches Γ, and vice-versa for the the (c)-type singularity $z'_{15}-\lambda z_{27}=\pm(1-\lambda^2)^{\frac{1}{2}}(1-z_{27}^2)^{\frac{1}{2}}$. Similarly for (b), (d). The singularity (e) does not occur for certain combinations of z, z'_{47}, z'_{15}. However, since it occurs only for real z under our assumptions on z'_{15}, z'_{47} we do not consider it further.

To find if Γ touches $x=\pm 1$ or not, we solve $f(\pm 1, \bar{y})=0$ and examine whether $|\bar{y}|\lesssim 1$. The transition occurs when $f(\pm 1, \pm' 1)=0$, when a pair of tangents $y=\text{const}$ coincide. This equation is symmetric in x and y, so the coincidence of a pair of tangents in one direction is accompanied by a coincidence in the other. The solution of $f(\pm 1, \pm' 1)=0$ can readily be found to be

$$(15)\qquad (f)\ \ \theta\mp\theta_{35}\mp'\theta_{27}\pm''\alpha=0\,,$$

where we write

$$(16)\qquad z=\cos\theta\,,\qquad z_{27,35}=\cos\theta_{27,35}\,,\qquad \lambda=\cos\alpha\,.$$

At $f(+1\ -1)=0$, say, the curve is as in Fig. 4. In the neighbourhood of V (which is a singularity of the integrand) the surface degenerates into a cone, so that the integraton contour must pass through V; hence χ has a singularity at (f), and the branches of this determine the presence or absence of the singularites (a) ... (d). (See Appendix II).

iv) For each pair of roots of (a) and (c), the cuts of (f) divide the z-plane into two regions: one in which (c) is singular, containing part of the physical region, the other, containing the rest of the physical region, in which (a) is singular. For definiteness we consider the positive roots of (a), (c). The relevant (f)-singularities then correspond to a coincidence of X_3 and X_4.

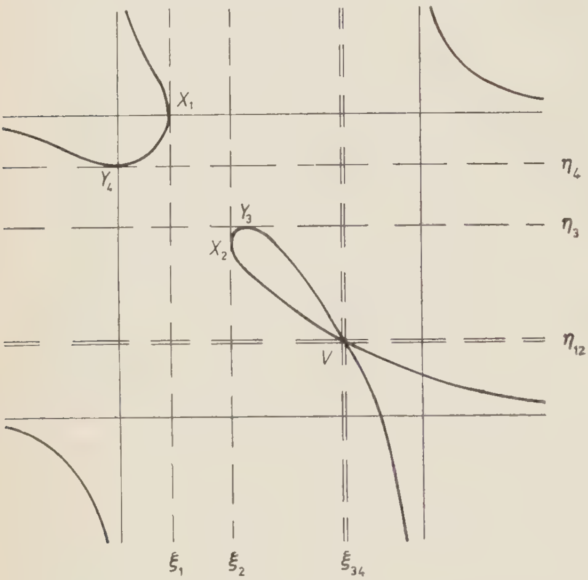

Fig. 4. – Plot of $f(x, y) = 0$; coincident case.

To determine the exact positions of the cuts, we follow a small contour, γ, round an (f)-type singularity, F, from a point P where (a_+) is singular to a point Q where (c_+) is singular. As we move, we also vary z'_{15} in such a way that

$$(17)\quad \frac{z_{15} - zz_{35}}{(1-z^2)^{\frac{1}{2}}(1-z_{35}^2)^{\frac{1}{2}}} = 1 + \varepsilon\,,$$

so that in $z - z'_{15}$-space we move along a surface parallel and near to the singular surface (a_+); to reach the singular surface, we merely let $\varepsilon \to 0$. The plane $x = 1$ always touches the torus, so the intersections A, A' are distance apart $0(\varepsilon^{\frac{1}{2}})$; as $\varepsilon \to 0$ they always stay close together—they cannot, for instance, circumnavigate the torus—and converge at a singular X_i. This does not pinch the integration contour at Q, and cannot do so as we move away from Q, unless and until we cross a cut.

As we move round γ from Q to P, X_3 and X_4 change places round the torus, the direction in which they change depending on the half plane in which we move on γ. During this movement we allow the contour to slide round the surface, so that at Q it meets X_3 which is not $x = 1$ and at P it meets the new X_3 which *is* now $x = 1$. The side of the torus that the contour moves on is determined by the half plane of γ.

Since we are keeping close to the surface a_+ the points A, A' move round the torus with the singularity at $x = +1$. Hence the two possible limits at P differ by having all these three singularities on different sides of the contour. So the cut starting from F can be split into three cuts, where we allow one singularity to cross the contour at once. Between the outer two of these cuts, a^+ becomes singular. Since we know that a^+ is singular at all real points

such as Q to one side of F, this region between the cuts must contain the real axis. Apart from this it is arbitrary. We therefore choose this region to be an arbitrarily narrow strip about the real axis (*).

This definition creates certain difficulties in that if the strips overlap, the values of χ on the physical region are not the boundary values of any analytic function. One certainly knows that this fact as well as the arbitrariness in the position of the cuts must be removed by later integrations, so that one might hope that the final result for $A^{(3)}$ is independent of the choice of cuts. But there remains the criticism that it is dangerous to cut off completely the physical region.

The situation then is: the roots of (a), (b) are only singular when they occur arbitrarily close to the real axis; (c), (d) occur for all z except in the strip; z at (e) and (f) is always real for the other variables in their integration ranges. Then integrating $\chi(\zeta)/\zeta - z$ along a contour round the strips and including the upper and lower semi-circles gives that χ has an integral representation which approximates as closely as desired to a spectral integral along the real axis (it can be seen that as $z \to \infty$, $\chi \sim \text{const}/z^2$, so that the semicircle contributions are zero; the singularities (c) and (d), being independent of z, can be included in the spectral function).

Interchanging orders of integration now shows that $A^{(3)}$ also has htis property.

5. – Higher terms.

The n-particle term in the unitarity equation is

$$A^{(n)} = \int M_1^* M_2 \prod_{k=5}^{n+4} \mathrm{d}^4 p_k\, \delta(p_k^2 - m_k^2)\, \delta\big(p_1 + p_2 - \sum_5^{n+4} p_k\big)\,. \tag{18}$$

Again, we transform the p_5, p_7 integrations to integrations over the invariants p_5^2, s_{35}, s_{15}, $s_5 \equiv (p_5 - p_1 - p_2)^2$ and p_7^2, s_{27}, s_{47} and s_7, and perform the p_6-integration by means of the energy-momentum conservation δ-function. The other integrations we transform to

$$p_k \to p_k^2\,, \qquad (p_k + p_5)^2 = s_{5k}\,, \qquad (p_k + p_7)^2 = s_{7k}\,, \qquad (p_k - p_1 - p_2)^2 = s_k\,.$$

This gives a complete set of invariants for the two functions M_1 and M_2. The

(*) *Note added in proof*: It is hoped to give a complete discussion of this argument in a later paper.

total Jacobian is the product of the separate Jacobians, and as before, in terms of centre of mass variables, these are given by

$$\left\{\frac{\partial(p_5^2 \dots s_5)}{\partial(p_{50} \dots p_{53})}\right\}^2 = -\,2^8 s_{12} q_1^2 q_3^2 q_5^2 k(z, z_{35}, z_{15}) ,$$

similarly for p_7, and

$$\left\{\frac{\partial(p_k^2 \dots s_k)}{\partial(p_{k0} \dots p_{k3})}\right\}^2 = -\,2^8 s_{12} q_5^2 q_7^2 q_k^2 k(z_{57}, z_{5k}, z_{7k}) .$$

Performing the p_k^2-integrations, we are left with

$$(19) \qquad A^{(n)} = 2^{n-1}\int M_1^* M_2\, \delta(p_6^2 - m_6^2)\cdot \frac{\mathrm{d}s_{15}\,\mathrm{d}s_{35}\,\mathrm{d}s_5\,\mathrm{d}s_{27}\,\mathrm{d}s_{47}\,\mathrm{d}s_7 \prod_8^{n+4} \mathrm{d}s_{5k}\,\mathrm{d}s_{7k}\,\mathrm{d}s_k}{(2^4 s_{12}^{\frac{1}{2}})^{n-1} q_1 q_2 q_3 q_4 q_5^{n-2} q_7^{n-2}\left[k(z, z_{35}, z_{15})\, k(z, z_{27}, z_{47}) \prod_{k=8}^{n+4} - k(z_{57}, z_{5k}, z_{7k})\right]^{\frac{1}{2}}} .$$

For the centre of mass variables, (2) and (4) for z_{13} still hold, in place of (3) we have

$$(3') \qquad E_k = \frac{1}{2s_{12}^{\frac{1}{2}}}\,(s_{12} + m_k^2 - s_k) ,$$

and in place of (4), for $k = 8, \dots, n+4$,

$$(4') \qquad 2q_k q_5 z_{k5} = s_{k5} + m_k^2 + m_5^2 - (s_{12} + m_k^2 - s_k)(s_{12} + m_5^2 - s_5)/4s_{12} ,$$

and similarly for z_{k7}. Transforming the s_{kl}-integrations to integrations over z_{kl}, we have

$$(20) \quad A^{(n)} = \frac{1}{(2s_{12}^{\frac{1}{2}})^{n-1}}\int M_1^* M_2\, \delta(p_6^2 - m_6^2)\cdot \frac{q_5\,\mathrm{d}z_{15}\,\mathrm{d}z_{35}\,\mathrm{d}s_5\, q_7\,\mathrm{d}z_{27}\,\mathrm{d}z_{47}\,\mathrm{d}s_7 \prod_{k=8}^{n+4} q_k\,\mathrm{d}z_{5k}\,\mathrm{d}z_{7k}\,\mathrm{d}s_k}{\left[k(z, z_{35}, z_{15})\, k(z, z_{27}, z_{47}) \prod_{k=8}^{n+4} - k(z_{57}, z_{5k}, z_{7k})\right]^{\frac{1}{2}}} ,$$

$$(21) \quad p_6^2 - m_6^2 = \Big(s_{12}^{\frac{1}{2}} - {\sum_5^{n+4}}' E_k\Big)^2 - \Big({\sum_5^{n+4}}' \mathbf{q}_k\Big)^2 - m_6^2$$ (where by $\sum'$ we mean that the $k=6$ term is not included),

$$= 2q_5 q_7(\lambda - z_{57}) - \sum_{i,j}\sum_{8}^{n+4} \mathbf{q}_i \mathbf{q}_j .$$

where λ depends only on the q_k, s_k, z_{5k}, z_{7k} and masses, and is independent of z_{15}, z_{35}, z_{27}, z_{47} and z.

For the four-particle term, the last term in (21) is not present. This gives

$$A^{(4)} = \frac{1}{2^4 s_{12}^{\frac{3}{2}}} \int M_1^* M_2 q_8 \frac{\mathrm{d}z_{58}\,\mathrm{d}z_{78}\,\mathrm{d}s_5\,\mathrm{d}s_7\,\mathrm{d}s_8}{[-k(\lambda, z_{58}, z_{78})]^{+\frac{1}{2}}} \cdot \frac{\mathrm{d}z_{15}\,\mathrm{d}z_{35}\,\mathrm{d}z_{27}\,\mathrm{d}z_{47}\,\delta(\lambda - z_{57})}{[k(z, z_{35}, z_{15})\,k(z, z_{27}, z_{47})]^{\frac{1}{2}}}, \tag{22}$$

on substituting λ for z_{57} in the first term. If we now assume a spectral representation for M_1, M_2 in z_{15}, z_{47} respectively, the z_{15}- and z_{47}-integrations can be performed, giving exactly the same function χ as the three-particle terms.

For higher terms, the presence of $\boldsymbol{q}_i\boldsymbol{q}_j$ terms in (21) (which can be expressed in terms of z_{57} by relations similar to (7) in which z is replaced by z_{57}) makes the algebra of the problem prohibitively difficult.

6. – Conclusion.

We conclude that the three- and four-particle terms in the unitarity equation for the scattering amplitude satisfy the Mandelstam representation, on the assumption that the five- and six-point processes satisfy single dispersion relations. It should be emphasized that this result is independent of any perturbation theory calculations.

* * *

I am indebted to Dr. J. C. Polkinghorne for his continued help and to Mr. M. Fowler and Mr. P. V. Landshoff for many discussions on the topic of this paper. I would also like to thank the University of Cambridge for the award of the W. A. Meek scholarship and St. John's College and the Department of Scientific and Industrial Research for studentships.

Appendix I

For physical s_{12}, z, the three-particle terms (Fig. 2) are defined by

$$A^{(3)}(s_{12}, z) = \int M_1^*(s_{12}, s_{27}, s_{76}, s_{65}, s_{51})\, M_2(s_{34}, s_{47}, s_{76}, s_{65}, s_{53}) \cdot$$
$$\cdot\, \mathrm{d}^4p_5\, \mathrm{d}^4p_6\, \mathrm{d}^4p_7\, \delta(p_5^2 - m_5^2)\, \delta(p_6^2 - m_6^2)\, \delta(p_7^2 - m_7^2)\, \delta^{(4)}(p_5 + p_6 + p_7 - p_1 - p_2), \tag{A.1}$$

summed over all possible groups of internal masses, m_5, m_6, m_7. We consider the contribution from any one such group. We perform, say, the p_6-integration

by the energy-momentum conservation δ-function, and, following KIBBLE (2), transform the p_5, p_7 integrations to integrations over invariants by means of the variable changes:

$$p_5 \to p_5^2\,, \quad (p_5-p_3)^2 = s_{35}\,, \quad (p_5-p_1)^2 = s_{51}\,, \quad (p_5-p_1-p_2)^2 = s_{67}\,.$$

$$p_7 \to p_7^2\,, \quad (p_7-p_2)^2 = s_{27}\,, \quad (p_7-p_4)^2 = s_{47}\,, \quad (p_7-p_1-p_2)^2 = s_{56}\,,$$

Jacobian: $\partial(p_5^2 \ldots s_{67})/\partial(p_{50} \ldots p_{53}) = 2^4 |p_5, -p_3, -p_1, -p_1-p_2| = D_5$, say.
Then

$$D_5^2 = 2^4 \begin{vmatrix} 2m_5^2 & s_{35}-m_3^2-m_5^2 & s_{15}-m_1^2-m_5^2 & s_{67}-s_{12}-m_5^2 \\ s_{35}-m_3^2-m_5^2 & 2m_3^2 & m_1^2+m_3^2-s_{13} & s_{12}+m_3^2-m_4^2 \\ s_{15}-m_1^2-m_5^2 & m_1^2+m_3^2-s_{13} & 2m_1^2 & s_{12}+m_1^2-m_2^2 \\ s_{67}-s_{12}-m_5^2 & s_{12}+m_3^2-m_4^2 & s_{12}+m_1^2-m_2^2 & 2s_{12} \end{vmatrix} =$$

$$= -2^8 s_{12} q_1^2 q_3^2 q_5^2 k(z, z_{35}, z_{15})$$

obtained by subtracting multiples of the last column from each of the others to obtain 3 zeros in the last row, then using (2), (3) and (4). A similar result holds for D_7: The transformations are 2 to 1, so we must multiply by 4; the range of integration is such that $k(z, z_{35}, z_{15})$ and $k(z, z_{27}, z_{47})$ are always negative, and s_{56}, s_{67} over the range determined by the positiveness of the three internal energies. So, after performing the p_5^2, p_7^2 integrations, (A.1) becomes

$$\text{(A.2)} \qquad A^{(3)} = \frac{1}{2^6 s_{12}} \int M_1^* M_2 \delta(p_6^2 - m_6^2) \frac{\mathrm{d}s_{35}\,\mathrm{d}s_{15}\,\mathrm{d}s_{67}\,\mathrm{d}s_{27}\,\mathrm{d}s_{47}\,\mathrm{d}s_{56}}{q_1 q_2 q_3 q_4 q_5 q_7} \cdot$$
$$\cdot [k(z, z_{27}, z_{47}) k(z, z_{35}, z_{15})]^{-\frac{1}{2}}\,.$$

We transform by (4) to integrations over the z's using

$$\frac{\partial(z_{35}, z_{15})}{\partial(s_{35}, s_{15})} = \frac{1}{4 q_1 q_3 q_5^2}\,, \quad \text{etc.}\,,$$

and at the same time remove z_{15}, z_{47} if favour of Φ, Ψ by (6), giving

$$\text{(A.3)} \qquad A^{(3)} = \frac{1}{4 s_{12}} \int \mathrm{d}s_{56}\,\mathrm{d}s_{67} \int_{-1}^{1} \mathrm{d}z_{27}\,\mathrm{d}z_{35} \int_0^{\pi} \mathrm{d}\Phi\,\mathrm{d}\Psi\, q_5 q_7 M_1^* M_2 \delta(p_6^2 - m_6^2)\,,$$

which, on substituting from (5) gives eq. (8).

APPENDIX II

In order to illustrate the structure of χ obtained in Sect. 4 (iii) we calculate χ in two special cases and show that it does have exactly the structure indicated there.

(i) $z_{27}=1$

$$\chi=\int_0^{\pi}\mathrm{d}\Phi\,\mathrm{d}\Psi\,\frac{\delta\{zz_{35}-\lambda-(1-z^2)^{\frac12}(1-z_{35}^2)^{\frac12}\cos\Phi\}}{[z'_{15}-zz_{35}-(1-z^2)^{\frac12}(1-z_{35}^2)^{\frac12}\cos\Phi][z'_{47}-z]}=$$

$$=\frac{\pi}{[z'_{15}-\lambda][z'_{47}-z]}\int_0^{\pi}\delta\{f(\Phi)\}\,\mathrm{d}\Phi\,,$$

with

$$f(\Phi)=zz_{35}-\lambda-(1-z^2)^{\frac12}(1-z_{35}^2)^{\frac12}\cos\Phi\,,$$

$$\frac{1}{f_\Phi}\Big|_{f=0}=\frac{1}{\sqrt{k(\lambda,z,z_{35})}}\,.$$

$f(\Phi)=0$ has a real root provided $\left|\dfrac{zz_{35}-\lambda}{(1-z^2)^{\frac12}(1-z_{35}^2)^{\frac12}}\right|<1\,,$

(A.4) *i.e.*, provided $k(z,z_{35},\lambda)<0\,,$
i.e., provided $\cos(\alpha+\theta_{35})<\cos\theta<\cos(\alpha-\theta_{35})\,.$

Thus

$$\chi=\frac{\pi}{[z'_{15}-\lambda][z'_{47}-z]}\,\frac{1}{\sqrt{k(\lambda,z,z_{35})}}\,,\qquad\text{provided (A.4) holds}$$
$$=0,\qquad\text{otherwise}\,.$$

(ii) $z=1$

$$\chi=\frac{1}{[z'_{15}-z_{35}][z'_{47}-z_{27}]}\int_0^{\pi}\mathrm{d}\Phi\,\mathrm{d}\Psi\,\delta\{z_{27}z_{35}-\lambda-(1-z_{27}^2)^{\frac12}(1-z_{35}^2)^{\frac12}\cos(\Phi+\Psi)\}\,.$$

The remaining integral gives only an (f)-type singularity or zero, and we always have (a) and (b) singular.

RIASSUNTO (*)

Si esaminano i termini a tre particelle nello sviluppo dell'unitarietà per un'ampiezza di scattering nella supposizione che le notevoli ampiezze di produzione soddisfino alle relazioni di dispersione singola. Si mostra che è possibile portarle a soddisfare la rappresentazione di Mandelstam entro i limiti della libertà che appare concessa dalla equazione unitaria. La prova si estende anche ai termini a quattro particelle.

(*) *Traduzione a cura della Redazione.*

IL NUOVO CIMENTO Vol. XIX, N. 1 1° Gennaio 1961

The Determination of a Local or Almost Local Field from a Given Current (*).

H. Araki (**), R. Haag and B. Schroer

Department of Physics, University of Illinois - Urbana, Ill.

(ricevuto il 24 Agosto 1960)

Summary. — It is shown that one cannot construct a local quantum field theory from a current operator which is a local polynomial of a free field. Secondly, the current of a local theory has to be complete or else the elastic scattering vanishes. These results do not depend in any essential way on the requirement of strict locality for the field but are only slightly modified if one allows « almost local » fields. The conditions which the current operator has to satisfy to ensure the existence of a local or almost local field are given.

1. – Introduction.

To date the only known models of consistent local, Lorentz invariant quantum field theories are those in which the field $A(x)$ is a local function of a free field $A_0(x)$, for instance

$$A(x) = \sum_1^N c_n :A_0^n(x): . \tag{1}$$

The double dots denote the Wick product [1]. Wightman [2] has shown that

(*) Supported in part by the United States Office of Naval Research.

(**) On leave of absence from Department of Nuclear Engineering, Kyoto University, Kyoto, Japan.

[1] A. Houriet and A. Kind: *Helv. Phys. Acta*, **22**, 319 (1949); G. C. Wick: *Phys. Rev.*, **80**, 268 (1950).

[2] A. S. Wightman: *Problèmes mathématiques de la théorie quantique des champs* (Paris lectures, 1958).

expression (1) is indeed a quantum field with the usually required properties viz.:

1) it is an operator-valued distribution;

2) it transforms covariantly under the Lorentz group;

3) it satisfies local commutativity

(2) $$[A(x), A(y)] = 0 \qquad \text{for space-like } x-y \text{ (3)};$$

4) If $c_1 = 1$ it satisfies the asymptotic condition in the trivial manner

(3) $$A^{\text{in}}(x) = A^{\text{out}}(x) = A_0(x)\,.$$

Due to (3) the S-matrix is the identity and hence these models are relatively empty. In order to obtain more interesting models Wightman (4) proposed to consider (1) not as the field but as the current of the theory. The field would then be determined from

(4) $$(\Box - m^2)\, A(x) = j(x)\,,$$

with

(5) $$j(x) = \sum_2^N c_n :A_0^n(x):$$

together with the locality requirement (2). In other words, one has to find an incoming field such that

(6) $$A(x) = A^{\text{in}}(x) - \int \Delta_R(x-x')\, j(x')\, \mathrm{d}x'\,,$$

satisfies (2). Wightman and Epstein (5) have shown by a discussion of the analytic properties of vacuum expectation values that in the simplest case, namely $j = :A_0^2:$, such a «local integration» of (4) is not possible.

We shall generalize their result by other methods in the following way:

1) If j is complete (6) theorems due to Borchers (7) imply that eqs. (4), (5) and (2) together mean $S = 1$.

(3) We use in this paper short hand notation, treating $A(x)$ as if it were a proper operator. The way in which this has to be understood in an exact mathematical sense is described in ref. (2).

(4) A. S. Wightman: *Kiev Conference on High Energy Physics* (1959).

(5) A. S. Wightman and S. T. Epstein: to be published.

(6) For the definition see Sect. 2.

(7) H. J. Borchers: *Nuovo Cimento*, **15**, 784 (1960).

2) If j is incomplete we show in Section **3** that at least all processes with 2 incident particles must have zero cross-section. The latter result is not limited to the special models (5) but holds generally for incomplete j.

3) The direct calculation of the scattering cross-section by means of the reduction formula gives a non zero result for the polynomial (5). This means then that (2), (4) and (5) are not compatible. These results do not depend in any essential way on the requirement of strict locality for the field but concern only the behavior of the theory for large distances in space (see Section **5**).

2. – The case of complete j and Borchers' theorems.

We consider—as usual in this kind of structure analysis—the Hilbert space formed by the states of a single type of spinless particles with mass m. We shall be concerned with various covariant operator fields in this Hilbert space (A, A^{in}, A^{out} j, A_0) and employ the following terminology:

i) A field $A(x)$ is called local if (2) holds.

ii) Tho fields A and B are called *local relative to* each other if

$$[A(x), B(y)] = 0 \qquad \text{for space-like } x-y. \tag{7}$$

iii) A field $B(x)$ is called *complete* is there are no bounded operators other than multiples of the identity which commute with all polynomals of B (8).

iv) Let the field B be complete and local. Consider all fields (covariant operator-valued distributions) C_1, C_2, ... which are local relative to B. The set of these fields will be called the *Borchers class of* B (9).

The two results of Borchers' paper (7) which we shall use are:

Theorem 1. – All fields in one Borchers class are local and local relative to each other.

(8) By a polynomial of B we mean an expression of the form

$$cI + \sum_k \int f_k(x_1 \dots x_k) B(x_1) \dots B(x_k) \, \mathrm{d}x_1 \dots \mathrm{d}x_k ,$$

with suitable test functions f_k (class S).

(9) Due to theorem 1 a complete field can belong only to one Borchers class. Incomplete fields may possibly be members of several Borchers classes.

Theorem 2. – All fields in one Borchers class (which satisfy the asymptotic condition in the sense of [10]) have the same incoming and the same outgoing field and hence lead to the same S-matrix (*).

In the integration problem (2), (4), (5) we know that A_0 and j are local relative to each other due to (5) and that A and j are local relative to each other because of (2) and (4). Therefore, if j is complete, theorem 1 implies that A is local relative to A_0. The three fields A, A_0 and j belong to the Borchers class of A_0. According to the second theorem

$$A^{\text{in}} = A_0 ; \qquad S = 1 . \tag{8}$$

3 – The consequences of incompleteness of j.

The case of incomplete j will be discussed quite generally, *i.e.*, without referring to the special models (5). In the first part of this section we shall make extensive use of the concept of « almost local fields » [11]. The definition is as follows. If B is the field in question consider the vacuum expectation values $\langle 0 | B(x_1) \dots B(x_n) | 0 \rangle$ and their linked cluster decomposition (Ursell expansion) which leads to the « truncated functions » $(B(x_1) \dots B(x_n))_T$. The field is called « almost local » if these truncated functions decrease faster than any power of the distance between the points with increasing separation in space-like directions and if they do not increase for large separations in time-like directions. It will always be assumed that the field is covariant with respect to the translation group in space-time but not necessarily that it is covariant with respect to Lorentz rotations. Two fields B and C are called « almost local relative to each other », if the vacuum expectation values of all mixed products between B's and C's have the property described above.

We denote the single particle state with momentum $\boldsymbol{p}$ by $|\boldsymbol{p}\rangle$ and use the abbreviations

$$B_{\boldsymbol{p}}(t) = \int \left(\sqrt{\boldsymbol{p}^2 + m^2}\, B(\boldsymbol{x}, t) - i\dot{B}(\boldsymbol{x}, t)\right) \exp\left[i\boldsymbol{p}\boldsymbol{x}\right] \mathrm{d}^3 x ; \qquad B_{\boldsymbol{p}}(0) = B_{\boldsymbol{p}} ,$$

$B^+_{\boldsymbol{p}}(t)$ is the adjoint of $B_{\boldsymbol{p}}(t)$. Note that for a free field

$$B_{\boldsymbol{p}}(t) \exp\left[-i\sqrt{\boldsymbol{p}^2 + m^2}\, t\right] = B_{\boldsymbol{p}}$$

[10] H. LEHMANN, K. SYMANZIK and W. ZIMMERMANN: *Nuovo Cimento*, **1**, 205 (1955).

(*) *Note added in proof.* – We have discarded an irrelevant normalization factor which drops out if our definition of the incoming field (equation (9)) is adopted.

[11] R. HAAG: *Phys. Rev.*, **112**, 669 (1958).

is independent of t and represents the creation operator for a particle with momentum $\boldsymbol{p}$.

The counterpart of Borchers' second theorem for almost local fields is

Theorem 3. – *a*) If B is almost local and

$$\langle 0|B(x)|0\rangle = 0 , \qquad \langle \boldsymbol{p}|B(x)|0\rangle \neq 0 ;$$

then an incoming field satisfying

$$(\Box - m^2) B^{\text{in}}(x) = 0 , \qquad [B^{\text{in}}(x), B^{\text{in}}(y)] = i\Delta(x-y)$$

is obtained by [12]

$$(9) \qquad \begin{cases} \lim\limits_{t\to-\infty} B_{\boldsymbol{p}}(t) \exp[-i\sqrt{\boldsymbol{p}^2+m^2}\, t] = B_{\boldsymbol{p}}^{\text{in}} \langle \boldsymbol{p}|B(0)|0\rangle , \\ \lim\limits_{t\to-\infty} B_{\boldsymbol{p}}^{+}(t) \exp[-i\sqrt{\boldsymbol{p}^2+m^2}\, t] = B_{\boldsymbol{p}}^{\text{in}+} \langle 0|B(0)|\boldsymbol{p}\rangle . \end{cases}$$

A corresponding statement holds for the limit $t\to+\infty$ which yields B^{out}.

b) If B and C are almost local relative to each other then

$$(10) \qquad B^{\text{in}} = C^{\text{in}} .$$

Eq. (9) is a short hand notation for the following precise statement: First one has to integrate (9) with a smooth test function $f(\boldsymbol{p})$. Then the limits exist in the sense of weak convergence in a certain domain $\mathscr{D}_1$. In other words the equalities are true for matrix elements between states ψ and ψ' one of which has to belong to $\mathscr{D}_1$ while the other one may be arbitrary. The domain $\mathscr{D}_1$ includes the states

$$\int f(x_1 \dots x_n) B^{\text{in}}(x_1) \dots B^{\text{in}}(x_n)\, dx_1 \dots dx_n |0\rangle$$

for all test functions $f(x_1 \dots x_n)$ of class S.

The proof of this theorem may be taken from ref. [11]. One has to remark that the definition of « almost local » was slightly narrower there but that this is of no consequence to any argument in the proof. The relation between the assumptions used in Theorem 3 and those in Borchers' second Theorem [13]

[12] It is not proved that B^{in} is complete. If it is not complete then the existence of the limit (9) and the equality $C^{\text{in}}=B^{\text{in}}$ are established only for matrix elements between states of the subspace which is generated by B^{in} from the vacuum.

[13] Compare also W. ZIMMERMANN: *Nuovo Cimento*, **4**, 597 (1958).

has not been completely clarified. Obviously Theorem 3 is more general in some respects but there is no complete proof yet that every «local» field is also «almost local» [14].

We shall need for our discussion the following consequence of Theorem 3.

Theorem 4. – If B is an incomplete covariant field which is almost local relative to a field A and if A^{in} is complete, then

$$\langle \boldsymbol{p} | B(x_1) \dots B(x_n) | 0 \rangle = 0 \tag{11}$$

for all $\boldsymbol{p}$, n and arbitrary configurations of the points $x_1 \dots x_n$.

Proof. If (11) is not satisfied then there exists a test function $h(x_1 \dots x_n)$ with support in a finite region of space for which

$$\langle \boldsymbol{p} | \int h(x_1 \dots x_n) B(x_1) \dots B(x_n) \, \mathrm{d}x_1 \dots \mathrm{d}x_n | 0 \rangle \neq 0 \,,$$

for at least some range of the momentum $\boldsymbol{p}$. Define

$$\begin{aligned} C(x) = \int h(x - x_1 \dots x - x_n) B(x_1) \dots B(x_n) \, \mathrm{d}x_1 \dots \mathrm{d}x_n - \\ - \langle 0 | \int h(x - x_1 \dots x - x_n) B(x_1) \dots B(x_n) | 0 \rangle \, \mathrm{d}x_1 \dots \mathrm{d}x_n \,. \end{aligned} \tag{12}$$

Then C is «almost local» relative to B and $\langle 0 | C(0) | 0 \rangle = 0$. Thus, according to Theorem 3 we can use C to construct $A^{\text{in}}(\boldsymbol{p})^+$ for all $\boldsymbol{p}$ for which $\langle \boldsymbol{p} | C(0) | 0 \rangle \neq 0$. Since B was assumed to be covariant we can easily find an almost local field C' with $\langle \boldsymbol{p} | C'(0) | 0 \rangle \neq 0$ for any prescribed $\boldsymbol{p}$ by a suitable Lorentz rotation of C.

If there exists a bounded operator T which commutes with all polynomials of B [8] then we have

$$\langle \psi | T A_{\boldsymbol{p}}^{\text{in}+} | \psi' \rangle = \langle \psi | A_{\boldsymbol{p}}^{\text{in}+} T | \psi' \rangle \,, \tag{13}$$

$$\langle \psi | T A_{\boldsymbol{p}}^{\text{in}} | \psi' \rangle = \langle \psi | A_{\boldsymbol{p}}^{\text{in}} T | \psi' \rangle \,, \tag{14}$$

for ψ, ψ' in $\mathscr{D}_1$ and for all p. If A^{in} is complete one easily finds that T must be a multiple of the identity by using the above mentioned properties of $\mathscr{D}_1$. Thus, if (11) is not true then B is complete.

[14] See G. F. Dell'Antonio and P. Gulmanelli: *Nuovo Cimento*, 7, 38 (1959); H. Araki: *Ann. Phys.*, in press.

We now return to the problem posed in the introduction and use Theorem 4 for $n=3$. If j is incomplete, then for instance

$$\langle 0|j(x_1)j(x_2)j(x_3)|\boldsymbol{p}\rangle = 0 . \tag{15}$$

Since

$$A^{\text{out}}(x) - A^{\text{in}}(x) = \int \Delta(x-y)j(y)\,dy . \tag{16}$$

(15) can also be written

$$\langle 0|j(x)j(y)|\boldsymbol{p}_1\boldsymbol{p}_2^{\text{in}}\rangle = \langle 0|j(x)j(y)|\boldsymbol{p}_1\boldsymbol{p}_2^{\text{out}}\rangle . \tag{17}$$

We introduce the projection operator P on the subspace which is generated from the vacuum by the application of bilinear expressions of j. Then (17) may be written

$$P|\boldsymbol{p}_1\boldsymbol{p}_2^{\text{in}}\rangle = P|\boldsymbol{p}_1,\boldsymbol{p}_2^{\text{out}}\rangle . \tag{18}$$

On the other hand, using the reduction formula we get for an arbitrary state Φ:

$$\begin{aligned}(19)\quad \langle \boldsymbol{p}_1'^{\text{out}}\boldsymbol{p}_2'|\Phi\rangle &= \langle \boldsymbol{p}_1'^{\text{in}}\boldsymbol{p}_2'|\Phi\rangle + \frac{1}{(2\pi)^3}\int dx\,dy \exp[-i(p_1'x+p_2'y)](\Box_y - m^2)\cdot \\ &\cdot\langle 0|[A(y), j(x)]\theta(x-y)|\Phi\rangle = \langle \boldsymbol{p}_1'^{\text{in}}\boldsymbol{p}_2'|\Phi\rangle + \frac{1}{(2\pi)^3}\int dx\,dy \exp[-i(p_1'x+p_2'y)]\cdot \\ &\cdot\langle 0|[j(y), j(x)]\theta(x-y)|\Phi\rangle + R ,\end{aligned}$$

where R involves the difference between $(\Box_y - m^2)[A(y)j(x)]\theta(x-y)$ and $[j(y), j(x)]\theta(x-y)$ and thus is a polynomial in its dependence on one of its arguments as will be discussed below.

We now decompose the scattering matrix element in the following manner

$$\langle^{\text{out}}\boldsymbol{p}_1\boldsymbol{p}_2|\boldsymbol{p}_1\boldsymbol{p}_2^{\text{in}}\rangle = \langle^{\text{out}}\boldsymbol{p}_1\boldsymbol{p}_2|P|\boldsymbol{p}_1\boldsymbol{p}_2^{\text{in}}\rangle + \langle^{\text{out}}\boldsymbol{p}_1\boldsymbol{p}_2|1-P|\boldsymbol{p}_1\boldsymbol{p}_2^{\text{in}}\rangle .$$

For the first term on the right hand side we use (18) to replace the superscript « out » by « in », for the second term we use (19) with $\Phi = (1-P)|\boldsymbol{p}_1^{\text{in}}\boldsymbol{p}_2\rangle$. Due to the definition of P the expression with the retarded commutator of $j(x)$, $j(y)$ vanishes in the latter term, leaving only

$$\langle \boldsymbol{p}_1'^{\text{out}}\boldsymbol{p}_2'|\boldsymbol{p}_1^{\text{in}}\boldsymbol{p}_2\rangle = \langle \boldsymbol{p}_1'^{\text{in}}\boldsymbol{p}_2'|\boldsymbol{p}_1^{\text{in}}\boldsymbol{p}_2\rangle + R . \tag{20}$$

Due to invariance requirements R may be written in the form

$$R = \delta(p_1+p_2-p_1'-p_2')\,T(s_1, s_3) . \tag{21}$$

We use the three Lorentz invariants

$$s_1 = -(p_1 - p_2')^2 ; \quad s_2 = -(p_1 - p_1')^2 ; \quad s_3 = -(p_1 + p_2)^2 \tag{22}$$

which are related by

$$s_1 + s_2 + s_3 = 4m^2 . \tag{23}$$

Since j and A are local and local relative to each other the difference between $(\Box_y - m^2)[j(x), A(y)]\theta(x-y)$ and $\theta(x-y)[j(x), j(y)]$ has support only at $x = y$ and therefore the components of p_1' can appear in R only in the form of a polynomial the coefficients of which may be arbitrary functions of p_1, p_2. According to (21), (22), (23) then

$$T(s_1, s_3) = \sum_0^n a_k(s_3)\, s_1^k = \sum_0^n b_k(s_3) s_2^k , \tag{24}$$

$$a_k(s) = (-1)^k \sum_{l \geqslant k} \binom{l}{k} (4m^2 - s)^{l-k} b_l(s) . \tag{25}$$

We prove now that the $a_k(s_3)$ must also be polynomials. To do this we use the following established properties of the scattering amplitude of a local theory ([15]). If s_2 is kept fixed and its value lies in a certain interval I then T as a function of s_3 is the boundary value of an analytic function $f(z_3, s_2)$ for z_3 approaching the real value s_3 from the upper half plane. This function is regular in the whole z_3 plane with the exception of poles and cuts on the real axis and it satisfies the crossing relation

$$f(z_3, s_2) = f(4m^2 - s_2 - z_3, s_2) . \tag{26}$$

Choose $N+1$ distinct values of s_2 in the interval I, say $s_2^{(\lambda)}$, $\lambda = 0 \dots N$. The matrix $M_{\lambda k} = (s_2^{(\lambda)})^k$, $(\lambda, k = 0, 1 \dots N)$ has an inverse since its determinant (the van der Monde determinant) does not vanish if the $s_2^{(\lambda)}$ are distinct. Thus $b_k(s_3)$ is the boundary value of the function

$$b_k(z_3) = \sum_\lambda f(z_3, s_2^{(\lambda)})\, M_{k\lambda}^{-1} , \tag{27}$$

which is analytic in the whole plane apart from poles and cuts on the real

([15]) N. N. BOGOLIUBOV and D. V. SHIRKOV: *Introduction to the Theory of Quantized Fields* (New York, 1959); H. J. BREMERMANN, R. OEHME and J. G. TAYLOR: *Phys. Rev.*, **109**, 2178 (1958); H. LEHMANN: *Nuovo Cimento*, **10**, 579 (1958); *Suppl. Nuovo Cimento*, **14**, 153 (1959).

axis. Because of (25) also a_k is the boundary value of such an analytic function $a_k(z_3)$ and (by the edge of the wedge theorem for example)

$$f(z_3, s_2) = \sum_k a_k(z_3)(4m^2 - s_2 - z_3)^k . \tag{28}$$

One can therefore make an analytic continuation of the crossing relation (26) in the second argument and obtains

$$\sum_0^N a_k(z_3)\, z_1^k = \sum_0^N a_k(z_1)\, z_3^k . \tag{29}$$

Again, choosing $N+1$ distinct points $z^{(\lambda)}$ off the real axis and defining the matrix $L_{\lambda k} = (z^{(\lambda)})^k$, we obtain

$$a_k(z) = \sum L^{-1}_{k\lambda} a_j(z^{(\lambda)}) z^j$$

which shows that a_k is a polynomial.

Since it is also known ([15]) that the imaginary part of the function $f(z_3, s_2)$ must vanish in a certain interval on the real axis of z_3 we can conclude that the imaginary part of the scattering amplitude has to vanish for all values of s_3, s_1 and hence by the optical theorem that T itself must vanish.

The final result is: if in an asymptotically complete local field theory the current is incomplete, then the elastic scattering cross-section vanishes.

4. – The conditions for « local integrability » of j.

In this section we show first that a current operator of form (5) cannot be associated with a local field, *i.e.*, that eqs. (2), (4), (5) are not compatible. Secondly we give conditions which assure the local integrability of a general complete j.

In the special case of models (5) we have seen that if local integration is possible at all then the 2-particle scattering cross-section must vanish. Because of (16) this is equivalent to

$$\tilde{j}(p)\,|\boldsymbol{p}'\rangle = 0 \qquad \text{for } p \text{ on the mass shell,} \tag{30}$$

where $\tilde{j}(p)$ is the 4-dimensional Fourier transform of $j(x)$. Inserting (5) one immediately sees that this is violated unless $c_n = 0$ for $n > 2$. The only case which remains to discuss is therefore

$$j = {:}A_0^2{:} \,. \tag{31}$$

This is just the case treated in ref. (5). The inconsistency of this model may also be demonstrated in the following way which does not make use of any of the results of previous sections. On the one hand eq. (31) holds for this model. Thus the imaginary part of the scattering amplitude vanishes and hence by the optical theorem the whole scattering amplitude must vanish. On the other hand, applying the reduction formula one has

$$T(p_1'p_2';\, p_1p_2) =$$
$$= \int \exp\left[-i\left(p_2 + \frac{p_1 - p_1'}{2}\right)x\right] \langle \boldsymbol{p}_1' | \left[j\left(\frac{x}{2}\right), j\left(-\frac{x}{2}\right)\right] |\boldsymbol{p}_1\rangle \,\theta(x)\,\mathrm{d}x + \text{polynomial}\,.$$

Inserting (31) this gives, apart from irrelevant constants

$$T = (m^2 - s_1)^{-1} + (m^2 - s_3)^{-1} + \sum_1^N a_k(s_2)s_1^k\,. \tag{32}$$

where the a_k are unknown arbitrary functions. It is evident (for instance by looking at the singularities of T as a function of s_1 for fixed s_2) that T cannot be made to vanish by any choice of the functions a_k. This completes the inconsistency proof for the eqs. (2, (4), (5).

We shall formulate now conditions for the local integrability of a given current. We restrict ourselves to the case of a complete j since this is the only physically reasonable one. Due to (4) and the first Borchers theorem A is local if and only if it is local relative to j. Consider the distributions

$$\langle 0|j(x_1)\,\dots\,j(x_n)A(x)|0\rangle = -\int \Delta_R(x-y)\langle 0|j(x_1)\,\dots\,j(x_n)j(y)|0\rangle\,\mathrm{d}y\, + \tag{33}$$
$$+ \int \langle 0|j(x_1)j(x_2)\,\dots\,j(x_n)\rangle|\boldsymbol{p}\rangle\,\exp\left[-ipx\right]\delta(p^2+m^2)\,\mathrm{d}p\,.$$

Remark that the right hand side can be evaluated if j is given because the single particle states $|\boldsymbol{p}\rangle$ are uniquely defined by their transformation properties without reference to the unknown field A^{in}. If A is local relative to j then the distribution (33) must be the boundary value of a function which is analytic in the union of the permuted extended tubes (17) and this function

---

(16) The fact that direct application of the reduction formula gives a non zero result for the scattering amplitude in the model $j = :A_0^2:$ was brought to our attention by A. S. WIGHTMAN.

(17) D. HALL and A. S. WIGHTMAN: *Dan. Mat. Phys. Medd.*, **31**, no. 5 (1957); R. JOST: *Helv. Phys. Acta*, **30**, 409 (1957).

is uniquely determined by (33) because of the edge of the wedge theorem [18]. Conversely, if the right hand side of (4.7) is the boundary value of such an analytic function then the matrix elements

$$\langle 0 | j(x_1) \dots j(x_m) A(x) j(x_{m+1}) \dots j(x_n) | 0 \rangle \tag{34}$$

may be defined as appropriate boundary values of this same analytic function. The field A obtained in this way will then be local relative to j and hence local itself [19].

The condition for local integrability of a complete and local j is therefore that the right hand side of (33) be (for all n) the boundary value of an analytic function which is regular in the union of the permuted extended tubes. A condition of type (33) was used in ref. (5). The point of our remark here is that because of Borchers' first theorem it suffices to satisfy the analyticity condition for those functions which have only one factor A.

5. – Almost local fields.

In order to get some insight into the physical aspects of the question discussed one has to ask to what degree the results depend on the requirement of strict locality. We shall therefore drop the commutation relations (2) and require instead that the field be almost local as defined in Section **3**. It is easy to see that most previous results are unaffected by this substitution.

Suppose that j is complete and of form (5). If A is almost local then due to (4) it is almost local relative to j. Also it is immediately seen that j defined by (5) is almost local relative to A_0. Also any field of form

$$\int h(x - x_1 \dots x - x_n)\, j(x_1) \dots j(x_n)\, \mathrm{d}x_1 \dots \mathrm{d}x_n\,,$$

with h having support only in a finite region of space time is almost local relative to A_0. One can find such a field, symbolically denoted by $(jj \dots j)$ which has non-vanishing matrix elements between the vacuum and single particle states (j was assumed to be complete). Theorem 3 then says that

$$A^{\text{in}} = (jj \dots j)^{\text{in}} = A_0^{\text{in}} = A_0\,; \qquad S = 1\,.$$

(18) H. Bremermann *et al.* (15); F. J. Dyson: *Phys. Rev.*, **110**, 579 (1958); L. Garding and A. Beurling: to be published.

(19) It is, of course, not proved that the matrix elements of A given by (34) define an operator-valued distribution $A(f)$.

This is turn implies (30) which is not satisfied by any complete j of form (5). So a polynomial of type (5), if complete, cannot be the current of even an almost local field.

The discussion of the case of incomplete j is more complicated if we do not assume strict locality of A since then we cannot apply the results of dispersion theory which were used at the end of Section 3. However, Theorem 4 still implies that many S-matrix elements vanish if j is incomplete. We refrain from a further discussion of this case.

Let us consider now the determination of an almost local field from a given complete almost local current. The following remark is of interest in this context.

Theorem 5. – *a*) Two (complete) free fields which are not identical cannot be almost local relative to each other.

b) If j is complete then there can be not more than one almost local field of which j is the current.

This theorem is an obvious consequence of Theorem 3. In fact, the way in which the incoming field may be constructed from a complete j is already described in (9). Suppose for instance, as the simplest case, that

$$\langle \boldsymbol{p} | j(x) j(x') | 0 \rangle \neq 0 .$$

Then, for any fixed ξ take

$$B_\xi(x) = j(x+\xi) j(x-\xi) - \langle 0 | j(x+\xi) j(x-\xi) | 0 \rangle \tag{35}$$

and insert it in (9). This defines $A^{\text{in}} = B^{\text{in}}$ and then we obtain A from (6). There is a consistency condition, however. The difference $A^{\text{out}} - A^{\text{in}}$ so obtained must agree with (16). This gives the operator relation

$$\int \Box \{ (-m^2) B_\xi(x) - \langle \boldsymbol{p} | B_\xi(0) | 0 \rangle j(x) \} \exp [ipx] \, \mathrm{d}x = 0 ,$$

for p on the mass shell, or:

$$(p^2 + m^2) \tilde{j}(p - Q) \tilde{j}(Q) = \tilde{j}(p) F(p, Q) \tag{36}$$

for p on the mass shell, Q arbitrary.

$$F(q, Q) = -\int \langle \boldsymbol{p} | j(\xi) j(-\xi) | 0 \rangle \exp [i(p - 2Q)\xi] \, \mathrm{d}\xi = \frac{1}{16} \langle \boldsymbol{p} | j(0) \tilde{j}(-Q) | 0 \rangle . \tag{37}$$

This very powerful operator relation has to be satisfied if j shall be the current of an almost local field. In the absence of strict locality it replaces the analyticity requirement formulated at the end of the last section.

6. – Concluding remarks.

The results of this study are mainly negative. They demonstrate again the difficulty of relating a field with interaction to a free field. One may express this as the stability of Borchers' classes. They also show that already the requirement of macroscopic locality imposes exact and very stringent conditions on the field. Eq. (36) is an example of this but there are infinitely many similar and independent relations to be satisfied in general. In Section **5** eq. (36) is probably sufficient because it was assumed there that j is given and almost local.

On the positive side one may hope that the theorems collected here and the locality conditions derivable from them may prove useful for the structure analysis of Quantum Field Theory.

RIASSUNTO (*)

Si mostra che non si può costruire una teoria locale dei campi quantistici da un operatore di corrente che sia un polinomio locale di un campo libero. Inoltre la corrente di una teoria locale deve essere completa perchè altrimenti lo scattering elastico si annulla. Questi risultati non dipendono in modo essenziale dall'esigenza di stretta localizzazione del campo e si modificano solo lievemente se si considerano campi « quasi locali ». Si espongono le condizioni a cui l'operatore di corrente deve soddisfare per assicurare l'esistenza di campi locali o quali locali.

(*) *Traduzione a cura della Redazione.*

IL NUOVO CIMENTO Vol. XIX, N. 1 1° Gennaio 1961

Nucleus-Nucleus Reaction Cross Section at High Energy Collisions (*).

G. Alexander (**) and G. Yekutieli

Department of Physics, The Weizmann Institute of Science - Rehovoth

(ricevuto il 30 Agosto 1960)

Summary. — The nucleon-nucleus and nucleus-nucleus reaction cross sections at high energies for various elements are calculated according to the optical model as a function of σ_0, the effective nucleon-nucleon total cross section in nuclear matter. Use is made of the charge distributions of various nuclei recently obtained from electron scattering experiments. The results are compared with existing data of experiments using machine beams and cosmic ray particles. But for the very light nuclei, a general agreement is found for values of σ_0 differing only by a few percent from the free nucleon-nucleon total cross section.

1. – Introduction.

In recent years several experiments have been performed on high energy nucleus-nucleus interactions using the heavy component of the cosmic rays as the incident beam. The reaction cross-section of these interactions has been first described by Bradt and Peters (1) by a semiempirical formula

$$\sigma_{12} = \pi(R_1 + R_2 - 2\Delta R)^2 \text{ fermi}^2 ,$$

where R_1 and R_2 are the radii of the two nuclei and ΔR is the minimum overlapping required before an interaction takes place. With this expression of Bradt and Peters it was possible to predict interaction cross-sections of several heavy primaries in emulsion using $R = 1.45A^{\frac{1}{3}}$ fermi and $\Delta R = 0.86$ fermi.

(*) Sponsored in part by the Air Force Cambridge Research Center, Geophysical Research Directorate, of the Air Research and Development Command, United States Air Force, through its European Office.

(**) Also from the I.A.E.C. Laboratories, Rehovoth.

(1) H. L. Bradt and B. Peters: *Phys. Rev.*, **77**, 54 (1950); **80**, 943 (1950).

The Bradt and Peters formula, however, is independent of the effective nucleon-nucleon cross-section in nuclear matter and the shapes of the two colliding particles. The transparency of nuclear matter in nucleus-nucleus collisions has been considered by EISENBERG (2). Assuming that nuclei are spheres of radius $R = 1.3A^{\frac{1}{3}}$ fermi and of uniform density, and using, a m.f.p. of $\lambda = 5.0$ fermi, he was able to predict correctly reaction cross-sections of several heavy primaries in emulsion and lead.

The importance of the nucleus shape in calculating its reaction cross-section at high energy collisions was pointed out by WILLIAMS (3). He showed that the assumption of similarity between charge and matter distribution in nuclei yields correct reaction cross-sections in nucleon-nucleus collisions in the GeV region.

The accumulation of experimental data on high energy nucleus-nucleus interaction cross-sections at different energies increases the interest in studying the reaction cross-section as function of the effective nucleon-nucleon cross-section in nuclear matter.

The purpose of this paper is to calculate the reaction cross-section of high energy nucleus-nucleus collisions as function of the effective N-N cross-section in nuclear matter using a nucleons' distribution similar to the charge distribution obtained from electron scattering experiments. Following WILLIAMS we first calculate the nucleon-nucleus reaction cross-section of several nuclei and compare them to the available experimental data. In the second step we extend these calculations to the case of nucleus-nucleus interaction. These results are used to predict the interaction m.f.p. of cosmic ray nuclei in photographic emulsion and in air.

2. – Nucleon-nucleus reaction cross section.

According to the optical model (4,5) the reaction cross-section in high energy nucleon-nucleus collisions is given by

$$(2.1)\qquad \left\{\begin{aligned} &\sigma = 2\pi\int(1-\exp[-\sigma_0 S_T(b)])\, b\,\mathrm{d}b\,;\\ &S_T(b) = \int N_T([b^2+z^2]^{\frac{1}{2}})\,\mathrm{d}z\,,\end{aligned}\right.$$

(2) Y. EISENBERG: *Phys. Rev.*, **96**, 1378 (1954).

(3) R. W. WILLIAMS: *Phys. Rev.*, **98**, 1387, 1398 (1955); with A. E. BRENER: *Phys. Rev.*, **106**, 1020 (1957) and *Nuovo Cimento*, **16**, 762 (1960).

(4) S. FERNBACH, R. SERBER and T. B. TAYLOR: *Phys. Rev.*, **75**, 1352 (1949).

(5) R. J. GLAUBER: *High Energy Collision Theory* (Boulder, Colo., 1958) and *Physica*, **22**, 1185 (1956).

where σ_0 is the effective $\mathcal{N}$-$\mathcal{N}$ total collision cross-section and $N(r)$ is the nucleon's density distribution of the target nucleus. In the derivation of (2.1) it was assumed that the range of the nuclear forces, a, is much smaller than the nuclear radius R, and accordingly terms of the order of $(a/R)^2$ are neglected. For $a = 0.87$ fermi the magnitudes of the neglected terms are 15%, 7% and 1% in Helium Carbon and Lead nuclei respectively. An attempt to correct for the finite range of nuclear forces was made by CRONIN *et al.* (6) and WILLIAMS (3). They replaced the $N(r)$ in (2.1) by a modified density function obtained by folding the original nucleon distribution function into a gaussian function with the same range as that of the nuclear forces. According to WILLIAMS the use of a nucleons distribution function corrected for the finite range of nuclear forces increases the reaction cross-section (2.1) of intermediate nuclei by a few percents.

If the target nucleus is described by the independent particle model, σ_0 in (2.1) is equal to the free $\mathcal{N}$-$\mathcal{N}$ total collision cross-section, $\sigma_{\mathcal{N}\mathcal{N}}$. In this approximation all correlations between nucleons in the nucleus are neglected, and so is the effect of the exclusion principle. The effect of the Pauli principle can be described by replacing σ_0 in (2.1) by a new effective cross-section. It was a widely accepted assumption that the Pauli exclusion principle decrease the effective cross-section. It has been shown, however, by GLAUBER (5) that at high energies the effect of the exclusion principle could sometimes increase the effective $\mathcal{N}$-$\mathcal{N}$ collision cross-section in nuclear matter. According to GLAUBER

$$\sigma_F = \sigma_0 + \frac{4\pi}{5}\left(\frac{P}{P_F}\right)^2 \left[(\operatorname{Im} f(0))^2 - (\operatorname{Re} f(0))^2\right], \tag{2.2}$$

where P_F and P are the Fermi and the incident momentum respectively, and $f(0)$ is the forward scattering amplitude. It follows from (2.2) that for $(\operatorname{Im} f(0))^2 > (\operatorname{Re} f(0))^2$, σ_F is larger than $\sigma_{\mathcal{N}\mathcal{N}}$. The magnitude of $(\operatorname{Im} f(0))^2$ and $(\operatorname{Re} f(0))^2$ for 1.4 GeV neutrons can be estimated from the experiment of COOR *et al.* (7). With these values the Glauber formula (2.2) predicts an increase of 6% in the effective collision cross-section, above the free $\mathcal{N}$-$\mathcal{N}$ total collision cross-section.

Information on the shapes of nuclei can be obtained from electron nucleus scattering experiments at high energies. The analysis of these experiments yields the charge distribution of several nuclei (8,9). For the evaluation of

---

(6) J. CRONIN, R. COOL and A. ABASHIAN: *Phys. Rev.*, **107**, 1121 (1957).

(7) T. COOR, D. A. HILL, W. F. HORNYAK, L. W. SMITH and G. SNOW: *Phys. Rev.*, **98**, 1369 (1955).

(8) R. HOFSTADTER: *Ann. Rev. Nucl. Phys.*, **7**, 231 (1957).

(9) U MEYER-BERKHOUT, W K. FORD and A. E. S. GREEN: *Ann. Phys.*, **8**, 11 (1959).

(2.1) it will be assumed that the nucleon's distribution of a nucleus is similar to its charge distribution. The charge distribution of several nuclei deduced from electron scattering experiments are listed in Table I. Further on, it is assumed that these distributions properly normalized describe the nucleons' distribution of the same elements.

TABLE I. – *Charge distributions of nuclei.*

Elements	Model	Parameters	Reference
^{1}H	Point	—	—
^{4}He	Gaussian	$(r^2)^{\frac{1}{2}} = 1.61$ fermi	(*b*)
^{7}Li	Modified exponential	$(r^2)^{\frac{1}{2}} = 2.71$ fermi	(*a*)
^{9}Be	Harmonic-well	$(r^2)^{\frac{1}{2}} = 2.2$ fermi, $\alpha = \frac{2}{3}$	(*b*)
^{11}Be	Harmonic-well	$r_k = r_- = 1.55$ fermi, $\alpha = 1$	(*c*)
^{12}C	Harmonic-well	$(r^2)^{\frac{1}{2}} = 2.37$ fermi, $\alpha = \frac{2}{3}$	(*b*)
^{14}N	Harmonic-well	$r_k = r_- = 1.667$ fermi, $\alpha = \frac{5}{3}$	(*c*)
^{16}O	Harmonic-well	$(r^2)^{\frac{1}{2}} = 2.64$ fermi, $\alpha = 2.0$	(*b*)
^{28}Si	Gaussian-uniform	$g = 1.0$, $RA^{-\frac{1}{3}} = 1.12$ fermi	(*d*)
$A=30$	Fermi	$c = 3.38$ fermi, $z = 0.546$ fermi	(*e*)
^{40}Ca	Fermi	$c = 3.64$ fermi, $z = 0.568$ fermi	(*b*)
^{58}Ni	Fermi	$c = 4.28$ fermi, $z = 0.565$ fermi	(*b*)
^{80}Br	Fermi	$c = 4.62$ fermi, $z = 0.546$ fermi	(*e*)
^{108}Ag	Fermi	$c = 5.07$ fermi, $z = 0.546$ fermi	(*e*)
^{115}In	Fermi	$c = 5.24$ fermi, $z = 0.523$ fermi	(*b*)
^{207}P	Fermi	$c = 6.34$ fermi, $z = 0.546$ fermi	(*e*)

$f = 10^{-13}$ cm.
(*a*) R. HOFSTADTER: *Rev. Mod. Phys.*, **28**, 214 (1956).
(*b*) R. HOFSTADTER: *Ann. Rev. Nucl. Phys.*, 7, 231 (1957).
(*c*) U. MEYER-BERKHOUT, K. W. FORD and A. E. S. GREEN: *Ann. Phys.*, **8**, 119 (1959).
(*d*) R. H. HELM: *Phys. Rev.*, **104**, 1466 (1956).
(*e*) Interpolation.

Using the nucleons distribution function $N(r)$ as quoted in Table I, the reaction cross-sections (2.1) of several elements were numerically integrated on the WIEZAC electronic computor. The reaction cross-sections of each nucleus were calculated for nine different effective cross-sections $\sigma_0 = 20, 25, 30, 35, 40, 45, 50, 55$, and 60 mb.

The calculated cross-sections as function of σ_0 are plotted on Fig. 1. On the same figure the cross-sections of Al, S, Fe and Cu, found by interpolation are also given. The cross-sections of N, O, and Fe were already calculated by WILLIAMS (3). As was mentioned before, these calculations were corrected for the finite range of nuclear forces, and subsequently are higher by $(2 \div 5)\%$ than those plotted on Fig. 1.

The influence of the specific nuclear model chosen for ^{12}C was also examined. ^{12}C, for example, can be described equally well by several models, different from the one quoted in Table I. One of the models for ^{12}C, the so-called « Family II model » ([9]) was used to calculate the cross-section with the intention to examine the influence of the model on the reaction cross-section values. It was found that the cross-sections of model II fall slightly below the values obtained for ^{12}C as given in Fig. 1. The difference between the two values is 3 % at $\sigma_0 = 20$ mb and falls gradually below 1 % for $\sigma_0 > 45$ mb. Both the results of Williams and the last example show that minor modifications in the shape of the nucleus change its calculated cross-section values by a few percents only.

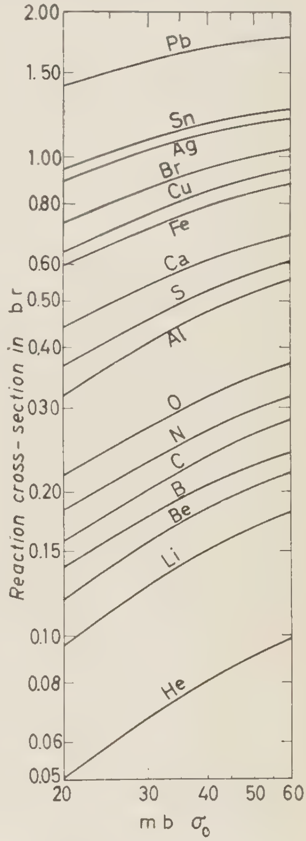

Fig. 1. – Nucleon-nucleus reaction cross sections.

Observations on the reaction cross-sections at high energy nucleon-nucleus collisions were made with cosmic ray particles and artificial accelerated beams. In Table II, some of the experimental results are compared with the calculated values of Fig. 1. For each observed cross-section in Table II (first column) the corresponding σ_0 obtained from Fig. 1 is given in the fourth column, while the measured free $\mathcal{N}$-$\mathcal{N}$ collision cross-section and its expected reaction cross-section are presented in the 5-th and 6-th columns respectively. The agreement between theory and experiment is better for artificial accelerated beams than for cosmic ray particles. We shall therefore first consider the machine results. According to the independent particle model, the effective σ_0, and the $\sigma_{\mathcal{N}\mathcal{N}}$ cross-sections should be equal. It is seen from Table II, that but for Iron and Copper there is a reasonable agreement between theory and experiment. The discrepancy in the case of the Iron and Copper is too large to be corrected neither by the finite range nor by the exclusion principle effects. Moreover, the first effect, and according to GLAUBER even the second, will only increase the discrepancy. It should however be pointed out that the reaction cross-section of Fe and Cu were found by interpolation and where not based on nucleon distributions derived directly from electron scattering experiments. More information on the shapes of these nuclei may furnish the explanation for their low observed reaction cross-sections.

The measured reaction cross-section values quoted in Table II are not ac-

TABLE II. – *Nucleon-nucleus reaction cross sections* (*a*).

Incident particle	Target	σ_{mb} observed	σ_{mb} effective	σ_{mb} measured	σ_{mb} expected
1.4 GeV neutrons (*b*)	Be	187 ± 12	43 ± 5	44.1	195
	C	201 ± 13	30 ± 5	43.9	245
	Al	414 ± 23	31 ± 5	43.9	480
	Cu	674 ± 34	23 ± 3	44.2	880
	Sn	1158 ± 63	40 ± 8	44.4	1200
	P	1727 ± 45	49 ± 8	44.8	1700
2.8 GeV protons (*c*)	C	230 ± 12	38 ± 5	39.5	235
	Fe	690 ± 28	29 ± 3	39.3	780
	P	1630 ± 75	36 ± 9	39.2	1665
3.0 GeV neutrons (*d*)	Al	430 ± 56	34 ± 9	39.1	460
	Cu	704 ± 140	25 ± 16	39.2	812
	P	1930 ± 300	100 ± 64	39.6	1670
4.5 GeV neutrons (*e*)	C	218 ± 8	34 ± 4	36.8	225
	Cu	638 ± 24	21 ± 5	37.1	820
	P	1660 ± 8	40 ± 2	37.5	1630
5.0 GeV neutrons (*f*)	C	235 ± 16	40 ± 8	36.8	225
	Al	381 ± 27	27 ± 5	~ 36.9	450
	Cu	586 ± 25	< 20	~ 37.1	820
	P	1670 ± 79	42 ± 9	~ 37.5	1630
C.R. $E \sim 4$ GeV (*g*)	Al	398 ± 11	30 ± 1	—	—
	Cu	899 ± 38	51 ± 2	—	—
	P	2050 ± 13	115 ± 8	—	—
C.R. $0.9 < E < 34$ GeV (*h*)	C	210 ± 15	32 ± 5	—	—
	Pb	1740 ± 90	52 ± 18	—	—
C.R. $15 < E < 50$ GeV (*i*)	C	256 ± 15	46 ± 6	—	—
	S	680 ± 100	82 ± 30	—	—
	Fe	790 ± 120	42 ± 30	—	—
	P	2150 ± 100	120 ± 30	—	—
C.R. $28 < E < 327$ GeV (*j*)	Fe	610 ± 40	22 ± 4	—	—

(*a*) σ_{pp} and $\sigma_{\mathcal{N}\mathcal{N}}$ up to 3 GeV were taken from F. F. CHEN, C. P. LEAVITT and A. M. SHAPIRO: *Phys. Rev.*, **103**, 211 (1956). For higher energies we used the σ_{pp} given by O. PICCIONI: *Proc. of the High Energy Geneva Conference* (1958) and $\sigma_{\mathcal{N}\mathcal{N}}$ given by (*f*).

(*b*) T. COOR, D. A. HILL, W. F. HORNYAK, L. W. SMITH and G. SNOW: *Phys. Rev.*, **98**, 1369 (1955).

(*c*) T. BOWEN, M. DI CORATO, W. H. MOORE and G. TAGLIAFERRI: *Nuovo Cimento*, **9**, 908 (1958).

(*d*) P. H. BARRETT: *Phys. Rev.*, **114**, 1374 (1959).

(*e*) J. H. ATKINSON, W. H. HESS, V. PEREZ-MENDEZ and R. W. WALLACE: *Phys. Rev. Lett.*, **2**, 168 (1959).

(*f*) J. H. ATKINSON: *Ph. D. Thesis*, UCRL-8966 (1959).

(*g*) M. S. SINHA and N. C. DAS: *Phys. Rev.*, **105**, 1587 (1957).

(*h*) R. B. GEGZAHANOV: *Soviet Physics, J.E.T.P.* **7**, 534 (1958).

(*i*) R. W. WILLIAMS: *Phys. Rev.*, **98**, 1393 (1955).

(*j*) A. E. BRENNER and R. W. WILLIAMS: *Phys. Rev.*, **106**, 1020 (1957).

curate enough to reveal variations due to small changes in $\sigma_{\mathcal{N}\mathcal{N}}$. For the same reason minor modifications of the shapes of the nuclei and the Pauli exclusion principle effect are still undetectable. The cosmic ray results were obtained in less favourable conditions and therefore are less accurate than the machine data. The observed reaction cross sections at cosmic ray energies are basically not different from those obtained by machines apart from the abnormal high cross-section of lead that seems to contradict the machine value. Hence it seems that the $\mathcal{N}$-$\mathcal{N}$ collision cross-section at cosmic ray energies is not appreciably different from the corresponding one at $(1\div5)$ GeV.

The reaction cross-sections expressed by (2.1) and plotted as a function of σ_0 in Fig. 1 for several elements, can be used for energetic incident particles other than nucleons, where σ_0 is the effective collision cross section in nuclear matter of that incident particle. The analysis of pion nucleus collisions is outside the scope of this work; however, general survey of pion-nucleus reaction cross-sections shows similar results as presented in Table II. One exception is the pion-Helium reaction cross-section measured in the He bubble chamber by BLOCK *et al.* [10]. They obtained a reaction cross-section of ~ 115 mb for 1.8 GeV negative pions in He. The total π-$\mathcal{N}$ collision cross-section at 1.8 GeV is ~ 30 mb, which corresponds according to Fig. 1 to a He-π reaction cross-section of 750 mb. The discrepancy between the prediction of formula (2.1) and the observed cross-section in the He case, may indicate that the assumptions and approximations used in the derivation of (2.1) are insufficient for nuclei with a small R as that of He.

3. – Nucleus-nucleus reaction cross-section.

The extension of (2.1) to an expression for the reaction cross-section σ_{IT} at high energy nucleus-nucleus collisions is:

$$\sigma_{IT} = 2\pi\int\left(1 - \exp\left[-\sigma_0 S_{IT}(b)\right]\right) b\,\mathrm{d}b\;, \tag{3.1}$$

where σ_0 is the effective cross-section in nuclear matter and

$$S_{IT}(b) = \int N_I\{[(x-b)^2 + y^2 + z'^2]^{\frac{1}{2}}\}\, N_T(r)\,\mathrm{d}x\,\mathrm{d}y\,\mathrm{d}z\,\mathrm{d}z'\;, \tag{3.2}$$

---

[10] M. BLOCK, B. BRUCKER, C. CHANG, T. KICHUCHI, C. MELTZER, F. ANDERSON, A. PEVSNER, H. COHN, E. HARTH, J. LEIFNER, G. BRAUTTI, C. FRANZINETTI and R. TOSI: *Nuovo Cimento*, **12**, 642 (1959).

$N_I(r)$ and $N_T(r)$ are the nucleons' distributions of the incident I, and target T, nuclei respectively. For an incident nucleon with point distribution $N_T(r)=\delta(r)$ formula (3.1) goes into (2.1).

The assumptions and approximations used in the derivation of (3.1) are the same as used in (2.1). Moreover, the Pauli exclusion principle will affect both the incident and the target nuclei, and hence the change of the effective cross-section will be increased. Similar considerations are applied to the finite range effect of nuclear forces.

Using the density distribution of Table I, the reaction cross-sections σ_{IT}, of several nuclei pairs were calculated. The reaction cross-section (3.1), (3.2) was integrated numerically on the WEIZAC electronic computor for nine values of $\sigma_0 = 20$, 25, 30, 35, 40, 45, 50, 55 and 60 mb. Only the results for $\sigma_0 = 20$, 30 and 40 mb are plotted in Figs. 2, 3 and 4 respectively. It is seen from these

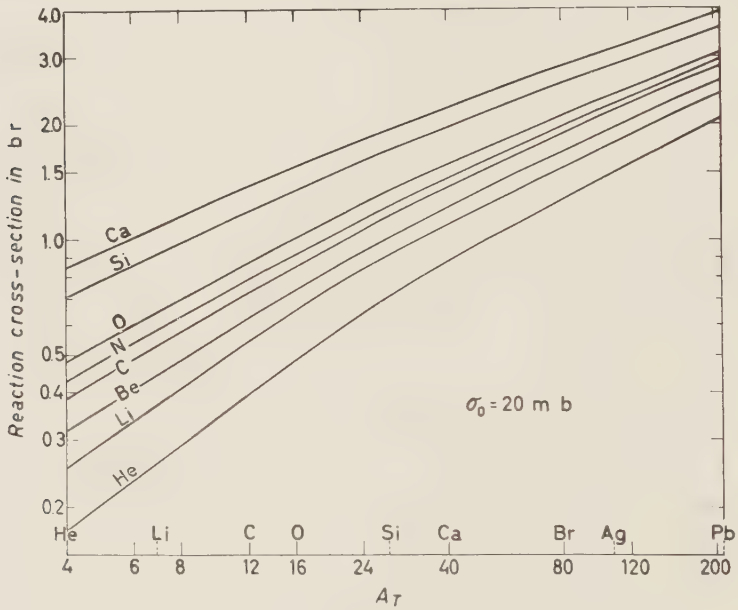

Fig. 2. – Nucleus-nucleus reaction cross sections: $\sigma_0 = 20$ mb.

figures that the cross-section values of different σ_0 are lying on a similar family of curves, hence other cross-section values for $20 < \sigma_0 < 60$ can be found from Figs. 2, 3 and 4 either by interpolation or by extrapolation.

At this point it is of interest to compare the cross-sections given by the empirical formula of Bradt and Peters [1]

$$\sigma_{IT} = \pi(1.45\,A_I^{\frac{1}{3}} + 1.45\,A_T^{\frac{1}{3}} - 1.7)^2 \text{ fermi}^2 \tag{3.3}$$

with the results of the present work. The Bradt and Peters cross-sections for incident He, C and Ca nuclei and different target nuclei are compared in Fig. 5

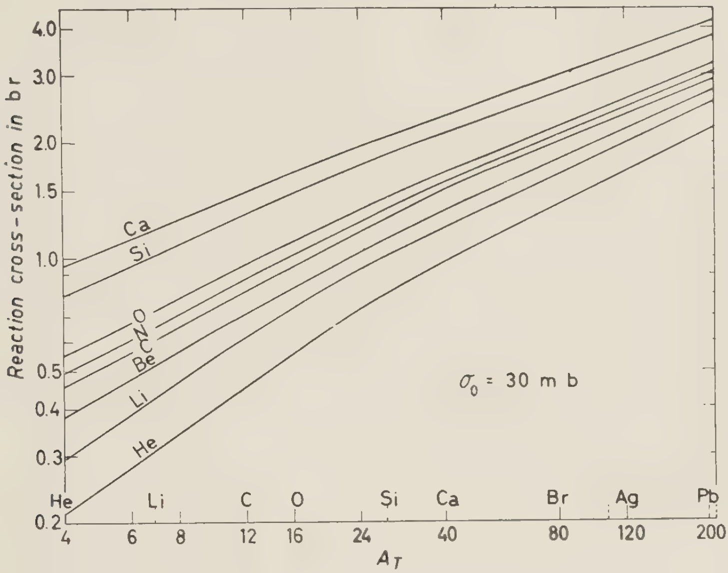

Fig. 3. – Nucleus-nucleus reaction cross sections: $\sigma_0 = 30$ mb.

with the corresponding values calculated by (3.1). Now the Bradt and Peters formula is independent of σ_0 and it is not at all evident that the cross-section

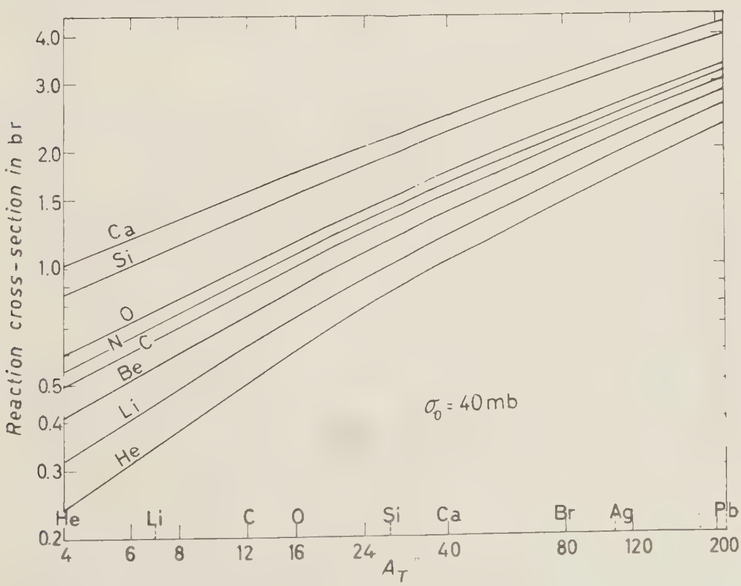

Fig. 4. – Nucleus-nucleus reaction cross sections: $\sigma_0 = 40$ mb.

derived from it can be compared with those obtained from (3.1) for a single σ_0 value. Indeed the best fit is obtained with the cross-sections of Bradt and Peters of He, C and Ca and the corresponding values of (3.1) calculated with three different $\sigma_0 = 30$, 25 and 20 mb respectively. As seen from Fig. 5 the Bradt and Peters formula agrees well with the present results for medium target nuclei, and incident nuclei with A between 4 and 40 corresponding to σ_0 that varies from 30 to 20 mb. However for light and heavy target nuclei the Bradt and Peters values are higher than those of the present work, *i.e.* 7 % for Ca–Pb up to 20 % For He–He.

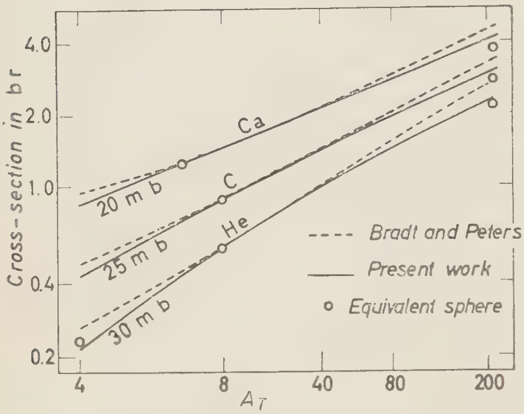

Fig. 5. – Comparison with the predictions of Bradt and Peters.

Some values calculated by (3.1) with the equivalent sphere model are also plotted on Fig. 5. In this model the nucleus is described by an uniform density sphere with an equivalent r.m.s. radius as found by electron scattering experiments (see reference ([8])). The plotted cross-section values in Fig. 5 are of He, C, and Ca calculated with $\sigma_0 = 30$, 25, and 20 mb respectively. We may conclude that the equivalent sphere cross-sections are nearer to the present work values than those derived from the Bradt and Peters formula.

4. – Reaction mean free path of cosmic ray particles in emulsion and air.

The cosmic radiation is today the only source of high energy heavy nuclei. Measurements of interaction m.f.p. of He and heavier elements were carried out in nuclear emulsion exposed to the C.R. at the top of the atmosphere. The results of these observations together with some m.f.p. values of protons obtained with artificially accelerated beams are summarized in Table III.

Helium after Hydrogen is the most abundant element in the C.R. and the only one for which a « pure » reaction m.f.p. has been measured. The reaction m.f.p. of heavier and less abundant elements has been measured in groups: *a*) « Light group » L = Li Be and B; *b*) « Medium group » M = C, N and O; *c*) « Heavy group » = all heavier nuclei.

The expected reaction m.f.p. values of H, He, Li, Be, B, C, N and O in emulsion, as function of the effective cross-section between 20 and 60 mb,

TABLE III. – *Reaction m.f.p. of energetic nuclei in emulsion.*

Incident particle	Energy per nucleon (GeV)	m.f.p. (g/cm²)	Expected m.f.p. for $\sigma_0 = 30$ mb	References
1. Protons	9	141 ± 3	143.5	(*a*)
2. Protons	6.2	146 ± 5	143.5	(*b*)
3. Protons	5.7	144 ± 16	143.5	(*c*)
4. α-particles (C.R.)	6	78.5 ± 8	85	(*d*)
5. α-particles (C.R.)	8	70.5 ± 15	85	(*e*)
6. α-particles (C.R.)	12	67.0 ± 4	85	(*f*)
7. α-particles (C.R.)	20	76.0 ± 7	85	(*g*)
8. α-particles (C.R.)	20	77.4 ± 7	85	(*h*)
9. « L » group (C.R.)	> 1.5	60.0 ± 5.7	59	(*i*)
10. « L » group (C.R.)	> 1.5	51.6 ± 6.1	59	(*j*)
11. « L » group (C.R.)	> 0.3	61.7 ± 9.4	59	(*k*)
12. « L » group (C.R.)	> 7.0	51.4 ± 7.2	59	(*h*)
13. « M » group (C.R.)	> 1.5	51.6 ± 3	50	(*i*)
14. « M » group (C.R.)	> 1.5	51.9 ± 3.8	50	(*j*)
15. « M » group (C.R.)	> 0.3	59.6 ± 6	50	(*k*)
16. « M » group (C.R.)	> 7.0	51.4 ± 7.2	50	(*h*)
17. « H » group (C.R.)	> 1.5	42.5 ± 4.1	35	(*i*)
18. « H » group (C.R.)	> 1.5	37.0 ± 3.1	35	(*j*)
19. « H » group (C.R.)	> 0.3	36.5 ± 4.8	35	(*k*)
20. « H » group (C.R.)	> 7.0	44.2 ± 4.5	35	(*h*)

(*a*) N. P. BOGACHEV, S. A. BUNJATOV, IU. P. MEREKOV and V. M. SIDEROV: *Sov. Phys. Dokl.*, **3**, 785 (1958).
(*b*) H. WINZELER, B. KLAIBER, W. KOCH, M. NIKOLIĆ and M. SCHNEEBERGER: preprint (1960).
(*c*) M. SCHEIN, D. H. HASKIN and R. G. GLASSER: *Nuovo Cimento*, **3**, 131 (1956).
(*d*) C. J. WADDINGTON: *Phil. Mag.*, **45**, 1312 (1956).
(*e*) F. HÄNNI: *Helv. Phys. Acta*, **29**, 281 (1956).
(*f*) M. V. APPA RAO, R. R. DANIEL and K. A. NEELAKANTAN: *Proc. Ind. Acad. Sci.*, A **43**, 181 (1956).
(*g*) M. M. SHAPIRO, B. STILLER and R. W. O'DELL: *Bull. Am. Phys. Soc.*, **1**, 319 (1956).
(*h*) E. LOHRMANN and M. W. TEUCHER: *Phys. Rev.*, **115**, 636 (1959).
(*i*) R. CESTER, A. DEBENEDETTI, C. M. GARELLI, B. QUASSIATI, L. TALLONE and M. VIGONE: *Nuovo Cimento*, **7**, 371 (1958).
(*j*) P. H. FOWLER, R. R. HILLIER and C. J. WADDINGTON: *Phil. Mag.*, **2**, 239 (1957); also V. Y. RAJOPADHYE and C. J. WADDINGTON: *Phil. Mag.*, **3**, 19 (1958).
(*k*) J. H. NOON and M. F. KAPLON: *Phys. Rev.*, **97**, 769 (1955).

are plotted in Fig. 6. In the same figure the m.f.p. values of L, M (– N) groups are also shown. In evaluating these m.f.p. values, the m.f.p. of the different elements of each group were weighted according to their composition, while the H group is represented by a representative nucleus of $A = 31$. The

reaction m.f.p. value of protons in nuclear emulsion is more sensitive to variation σ_0 in than it is for the other elements plotted in Fig. 6. The average logarithmic derivative $\langle d(\ln \partial)/d(\ln \sigma_0)\rangle$ between $\sigma_0 = 20$ mb and 60 mb of the re-

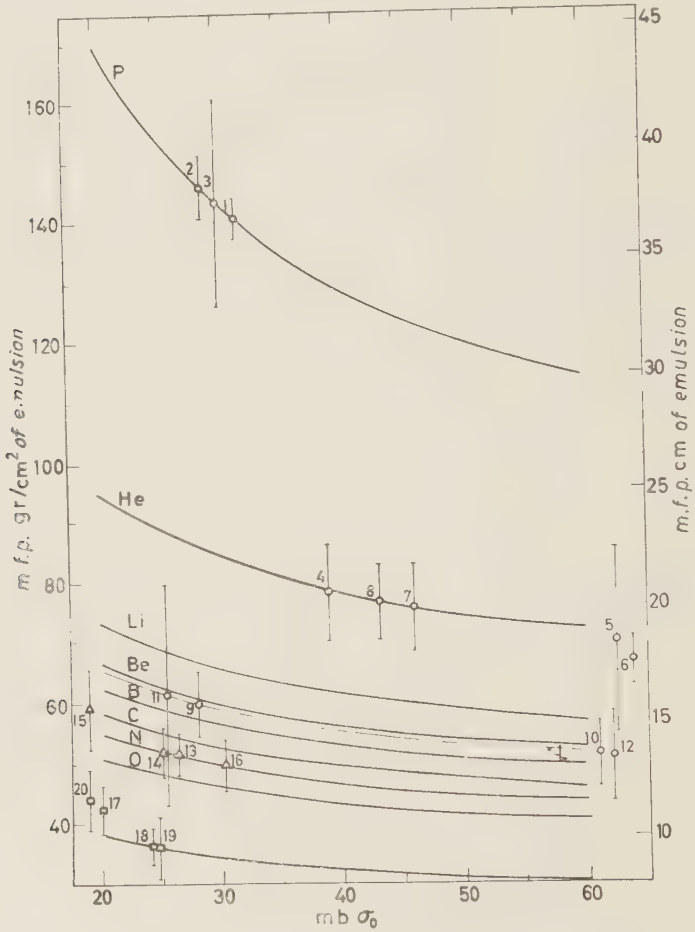

Fig. 6. – Reaction m.f.p. of cosmic ray particles in emulsion.

action m.f.p. in emulsion is 0.44; 0.26 and 0.21 for H, He, and C primaries respectively. This means that in order to detect a variation of 10 % in σ_0, the m.f.p. in emulsion of protons and heavier elements should be measured with accuracy better than 4 % and 2 % respectively. The results presented in Table III show that only some measurements on primary protons meet this requirement.

The observed m.f.p. values of Table III are also shown in Fig. 6. Each experimental m.f.p. value is drawn on the line corresponding to its identity.

The σ_0 of every observed value in Fig. 6 is the effective cross-section as obtained by (3.1).

The experimental m.f.p. of $(5\div9)$ GeV protons is $(143.5\pm4)\ \text{g/cm}^2$ corresponding to an effective cross-section of $\sigma_0=(30\pm5)$ mb, which is in good agreement with the free $\mathcal{N}$-$\mathcal{N}$ cross-section $\sigma=(32\pm8)$ mb measured at this range of energy [11].

Unfortunately there are some inconsistencies between the different observed m.f.p. values of heavy primaries in emulsion, that do not allow to combine together results from different experiments done in the same energy region. For this reason the statistical significance of these measurements is rather poor. The observed m.f.p. values are compared in Table III, with the expected values obtained with the same $\sigma_0=30$ mb as found for the $(5\div9)$ GeV protons in emulsion. It appears that the observed m.f.p. values of the L, M, H groups agree within the experimental errors with the predicted values obtained from (3.1) for $\sigma_0=30$ mb. All the values for α particles, however, seem to be shorter than the predicted ones, and agree better with the value of $\sigma_0=40$ mb. This discrepancy is in the same direction as found for the pion-Helium reaction cross-section, and it may indicate that the expression (3.1) like (2.1) in based on assumptions and approximations that are not valid for a nucleus as small as the α-particle. It will be very interesting to calculate the interaction m.f.p. of energetic α particles without neglecting effects due to the Pauli exclusion principle. At the same time the accuracy

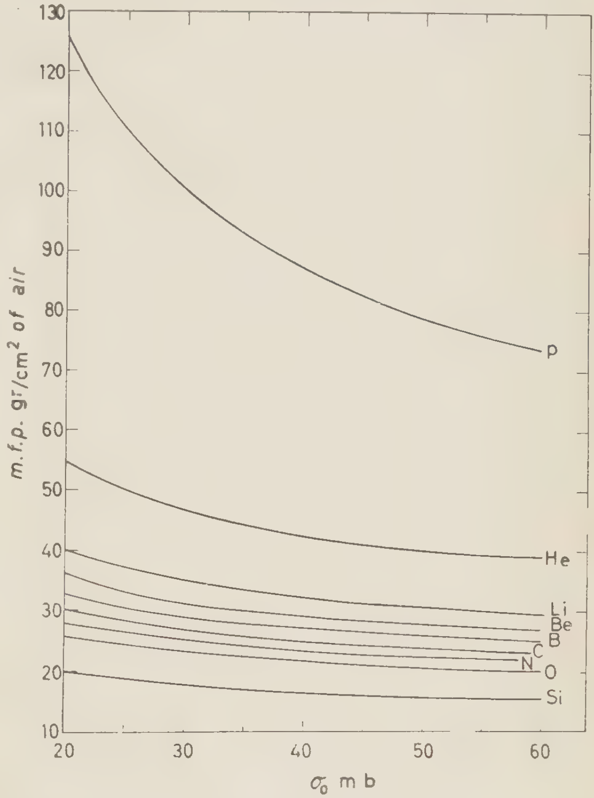

Fig. 7. – Reaction m.f.p. of cosmic ray particles in air.

([11]) O. Piccioni: *Proc. of the High Energy Geneva Conference* (1958).

of the reaction m.f.p. of cosmic ray He-primaries in emulsion should be improved to enable the detection of these small but interesting effects.

The discussion on the m.f.p. of energetic nuclei in photographic emulsion enables the predictions of the reaction m.f.p. of cosmic ray particles in air. The reaction m.f.p. values in air of the more abundant C.R. particles are plotted in Fig. 7 as functions of σ_0. The analysis of m.f.p. of protons in emulsion suggests a value of $\sigma_0=30$ mb, in Table IV are given the expected m.f.p. values of several C.R. particles in air for the same $\sigma_0 = 30$ mb values. In the same table the m.f.p. of He for $\sigma_0 = 40$ mb is also given.

TABLE IV. – *Reaction m.f.p. values of cosmic ray primaries in air for* $\sigma_0 = 30$ mb.

Element	H	He	Li	Be	B	C	N	O	Si
m.f.p. (g/cm^2 air)	100.5	47.2 42.51 (*)	35.1	31.7	29.5	27.2	25.5	23.4	17.5

(*) For $\sigma_0 = 40$ mb.

5. – Conclusions.

It may be concluded from this work that the optical model as expressed by (2.1) and (3.1) for the reaction cross-section of high energy nucleon-nucleus and nucleus-nucleus collisions is able to predict the existing experimental data on the assumptions that the effective collision cross-section in nuclear matter is equal to the free $\mathcal{N}$-$\mathcal{N}$ total collision cross-section, and that the nucleons' distribution in a nucleus is similar to its charge distribution. In deriving (2.1) and (3.1) the effects of both the finite range of nuclear forces and the correlations due to Pauli's exclusion principle were neglected. These effects influence the reaction cross-sections, in most of the cases, by a few percent only, and they are undetectable with the existing experimental means. For the same reason the observed cross-sections are not sensitive to minor variations in the effective cross-section σ_0 and to slight modifications in the shapes of the nuclei. The exceptions to the above conclusion are the cases of Iron and Helium.

The observed nucleon-Iron (same for the nucleon-Copper) reaction cross-section is significantly lower than the predicted one. However as the nucleons' density distribution used for the Iron was obtained by interpolation and not from electron scattering experiments, it could be that the discrepancy in this case is due to a marked deviation in the shape of the Iron nucleus. An electron-Iron scattering experiment yielding information on the nucleons' density distribution might throw light on this problem.

There are indications that the optical model treatment as expressed by (2.1) and (3.1) is inadequate for the Helium nucleus. It seems that both the observed pion-Helium cross-section and the reaction cross-section of α-particles in emulsion are larger than the predicted values. The reason for this effect could be the smallness of the Helium nucleus. Hence it will be worth-while to attempt a calculation of the reaction cross-section of Helium nuclei, without neglecting effects like the finite range of the nuclear forces and exclusion principle correlations, that have characteristic lengths of the order of the Helium nucleus size. At the same time it is very desirable to measyre both the reaction cross-section of high energy nucleons and pions in Helium bubble chamber and the interaction m.f.p. in emulsion of cosmic ray α-particles at different energies. These measurements have to be carried out accurately enough to reveal effects of a few percents.

As was mentioned earlier both theory and experiments, in the case of heavier nuclei, are not fine enough to reach final conclusion on the validity of the reaction cross-section (2.1) and (3.1). Changes in the effective collision cross-section σ_0 can be compensated by proper modification in the shape of the nuclei $N(r)$ while slight variations in both σ_0 and $N(r)$ are irrelevant to the experimental accuracy in order to detect dependence on σ_0, and effects of finite range and exclusion principle correlation. In the same time the optical model calculation has to be extended to include these effects.

RIASSUNTO (*)

Si calcolano secondo il modello ottico le sezioni d'urto nucleone-nucleo e nucleo-nucleo alle alte energie per vari elementi in funzione di σ_0, sezione d'urto effettiva nucleone-nucleone in materia nucleare. Si impiegano le distribuzioni di vari nuclei recentemente ottenute da esperienze di scattering elettronico. Si confrontano i risultati coi dati disponibili di esperienze eseguite sia coi fasci delle macchine acceleratrici sia coi raggi cosmici. Salvo che per i nuclei molto leggeri, si trova un accordo generale pei valori di σ_0 che differiscono solo di qualche percento dalla sezione d'urto totale per la collisione libera nucleone-nucleone.

(*) *Traduzione a cura della Redazione.*

IL NUOVO CIMENTO Vol. XIX, N. 1 1° Gennaio 1961

On the Density Field Description of a Boson System.

HONG-MO CHAN and J. G. VALATIN

Department of Mathematical Physics, University of Birmingham - Birmingham

(ricevuto il 5 Settembre 1960)

Summary. — The introduction of a density description through a field approach is discussed. Additional mathematical complications resulting from the appearance of powers of the δ-function can be avoided by means of a limiting process. The configuration space argument of Bogolubov and Zubarev is cast in an x-space form in which simple expressions are given. In the resulting representation the normalisation integral is defined by means of a weight function the expression of which is determined. The weight function establishes the connection between the rather different expressions of the two density field representations. Some simple cases are considered and a variational principle is formulated.

1. – Introduction.

The density $\varrho(x)$ can be introduced as a basic variable to describe a Boson system in two different ways, either by considering the field operator $\varrho(x) = \psi^*(x)\,\psi(x)$ and its conjugate which plays the role of a velocity potential, or through a configuration space approach on the line of a work by BOGOLUBOV and ZUBAREV (1). The present short note establishes the connection between the two approaches and attempts the clarification of a few points in their contents.

The density representation gives a rather non-conventional description of a quantum mechanical system and may prove to be a mathematical tool to a new kind of approximations. For a Boson system, the use of density variables may be of special interest, partly because of the connection of phonon

(1) N. N. BOGOLUBOV and D. N. ZUBAREV: *Sov. Phys.*, **1**, 83 (1955); *Žurn. Èksp. Teor. Fiz.*, **28**, 129 (1955).

excitations with changes in density, partly because the density description is related to hydrodynamic concepts and may be of help in considering hydrodynamic aspects, for instance problems related to quantum vortices.

The variable transformations which lead to the density description introduce new mathematical complications because of the improper character of the quantized field operators. Similar complications will be met in quantum field theory if one wants to introduce new kind of variables and a better understanding of these problems in the present simple non-relativistic theory seems of interest also in this connection.

2. – The density field and its conjugate.

A Boson system with two-body interactions can be described by means of a Hamiltonian

$$\mathscr{H} = T + V\,, \tag{1a}$$

$$T = -\frac{1}{2m}\int \mathrm{d}x\,\psi^*(x)\,\Delta\psi(x)\,, \qquad \hbar = 1, \tag{1b}$$

$$V = \frac{1}{2}\iint \mathrm{d}x\,\mathrm{d}x'\,\psi^*(x)\,\psi^*(x')\,V(x-x')\,\psi(x')\,\psi(x)\,, \tag{1c}$$

which is expressed in terms of a quantized field $\psi(x)$ and its conjugate $\psi^*(x)$. One can introduce the density field operator

$$\varrho(x) = \psi^*(x)\,\psi(x) \tag{2a}$$

and its conjugate $\varphi(x)$ by means of the transformation [2-4]

$$\psi(x) = \exp\left[i\varphi(x)\right]\varrho^{\frac{1}{2}}(x)\,, \qquad \psi^*(x) = \varrho^{\frac{1}{2}}(x)\,\exp\left[-i\varphi(x)\right]. \tag{2b}$$

If ψ is a c-number field, the transformation (2b) leads, with

$$\nabla\psi = \exp\left[i\varphi\right]\left(i\,\nabla\varphi\,\varrho^{\frac{1}{2}} + \frac{\frac{1}{2}\nabla\varrho}{\varrho^{\frac{1}{2}}}\right), \tag{2c}$$

([2]) L. de Broglie: *Journ. Phys.*, **8**, 225 (1927).
([3]) E. Madelung: *Zeits. Phys.*, **40**, 322 (1927).
([4]) T. Nishiyama: *Progr. Theor. Phys.*, **8**, 655 (1952); **9**, 245 (1953).

to the well-known « hydrodynamic » form of the kinetic energy

$$T = \frac{1}{2m}\left\{\int dx\,\varrho(\nabla\varphi)^2 + \int dx\,\frac{(\frac{1}{2}\nabla\varrho)^2}{\varrho}\right\}. \tag{2d}$$

$\varphi(x)$ plays the role of a velocity potential, and the energy depends only on its gradient defining the velocity field.

Wit a quantized operator $\psi(x)$, the transformation ($2b$) is not yet well-defined, since through the functions of the improper operators $\varrho(x)$, $\varphi(x)$ one introduces powers of the δ-function. A simple way of handling the resulting additional mathematical complications is to introduce a lattice space with a discrete set of points at a distance a instead of the continuum of points x. The mathematical operations are now well defined as they involve the Kronecker δ of the commutation relation

$$[\psi_x, \psi^*_{x'}] = \delta_{xx'} \tag{3a}$$

instead of the δ-function of the commutation relation

$$[\psi(x), \psi^*(x')] = \delta(x - x'). \tag{3b}$$

If a is much smaller than any length of physical interest, the introduction of the lattice space cannot influence the physical content of the theory. In the results one can go to the limit $a \to 0$ of the continuum. With ($3a$), the transformation ($2b$) corresponds to the standard introduction of amplitude and phase of creation and annihilation operators (5).

With this limiting process, one obtains from ($3b$) and ($2b$) the commutation relation

$$[\varphi(x), \varrho(x')] = -i\,\delta(x - x'). \tag{4a}$$

The kinetic energy operator ($1b$) is transformed into the form

$$\hat{\mathscr{T}} = \frac{1}{2m}\left\{-\int dx\left(\nabla\frac{\delta}{\delta\varrho(x)}\right)\varrho(x)\left(\nabla\frac{\delta}{\delta\varrho(x)}\right) + \int dx\,\frac{(\frac{1}{2}\nabla\varrho(x))^2}{\varrho(x)} + \frac{1}{2}\iint dx\,dx'\,\delta(x-x')\,\nabla^2\delta(x-x')\right\}, \tag{4b}$$

in which the symbolic notation

$$\varphi(x) = -i\,\frac{\delta}{\delta\varrho(x)} \tag{4c}$$

---

(5) P. A. M. DIRAC: *Proc. Roy. Soc.*, A **114**, 243 (1927); O. KLEIN and P. JORDAN: *Zeits. Phys.*, **45**, 751 (1927).

has been introduced, and the last term cancels singularities of the second term. The potential energy (1c) can be written in the form

(4d) $$\mathscr{V}=\frac{1}{2}\iint \mathrm{d}x\,\mathrm{d}x'\,V(x-x')\varrho(x)\left(\varrho(x')-\delta(x-x')\right).$$

In this representation the state vectors are functionals

(5a) $$\hat{\chi}=\hat{\chi}[\varrho(x)]$$

of the density $\varrho(x)$. In the lattice space approximation they are functions

(5b) $$\hat{\chi}=\hat{\chi}(\dots, n_x, \dots)$$

of the number operators n_x of the lattice points, which take non-negative integer values 0, 1, 2, ... The scalar product of two states $\hat{\chi}_1$ and $\hat{\chi}_2$ is then given by

(5c) $$(\hat{\chi}_1, \hat{\chi}_2)=\sum_{n_x}\hat{\chi}_1^*(\dots, n_x, \dots)\,\chi_2(\dots, n_x, \dots)\,,$$

where the summation extends over the values 0, 1, 2, ... of all the n_x.

With x continuous, the operator $\varrho(x)$ defined by (2a) still has the property that

(5d) $$\int_{\Omega_{x'}}\mathrm{d}x\,\varrho(x)$$

integrated over any finite volume $\Omega_{x'}$, around the point x' can take only integer values. The functional operations act on functionals of such operators. One can then accept one of two possible points of view. One can restrict the domain of definition of the functionals to take this feature of $\varrho(x)$ into account and keep a one-to-one correspondence of the state vectors with those expressed in terms of particle creation operators. This can be done most conveniently through a lattice space occupation number representation. Or one can extend the considerations to a wider class of functionals $\hat{\chi}=\hat{\chi}[\varrho(x)]$ without this restriction of the domain. In this way one introduces a redundancy of states, but also more freedom in the mathematical manipulations. The scalar product (5c) is then replaced by the functional integral

(5e) $$(\hat{\chi}_1, \hat{\chi}_2)=\int\delta\varrho(x)\,\hat{\chi}_1^*[\varrho]\,\hat{\chi}_2[\varrho]$$

which is to be extended over positive real functions $\varrho(x)$.

3. – Configuration space and density variables.

Another connection with a density field representation is obtained by starting from the configuration space description of the Boson system. This has been given by BOGOLUBOV and ZUBAREV [1] in terms of the Fourier transform

$$\varrho_k = \int \mathrm{d}x \exp[ikx]\,\varrho(x)\,.$$

The expressions are somewhat simpler in x-space where one obtains products instead of convolution integrals.

Tha Hamiltonian ($1a, b, c$) corresponds in configuration space to the operators

$$(6a) \qquad T = -\frac{1}{2m}\sum_i \Delta_i\,, \qquad V = \sum_{i<j} V(x_i - x_j)\,,$$

and to a wave equation

$$(6b) \qquad (T + V)\varphi(x_1, \ldots, x_N) = E\varphi(x_1, \ldots, x_N)\,.$$

The density operator is given by

$$(6c) \qquad \varrho(x) = \sum_{j=1}^{N} \delta(x - x_j)\,.$$

One can obtain a wave equation for a functional $\chi[\varrho(x)]$ of the density $\varrho(x)$ by requiring that the substitution ($6c$) into the functional should lead to the configuration space solution $\Phi(x_1, \ldots, x_N)$ of ($6b$), that is

$$(7a) \qquad \chi[\varrho(x)]\Big|_{\varrho(x) = \sum_{j=1}^{N}\delta(x - x_j)} = \Phi(x_1, \ldots, x_N)\,.$$

The configuration space wave function $\Phi(x_1, \ldots, x_N)$ obtained in this way is symmetric. This equation can be written in the form

$$(7b) \qquad (\mathscr{T} + \mathscr{V})\,\chi[\varrho(x)] = E\chi[\varrho(x)]\,,$$

where $\mathscr{V}$ is given by ($4d$) and the expression of the kinetic energy $\mathscr{T}$ is obtained by applying the Laplacian operator Δ_j on ($7a$), taking first functional derivatives $\delta/\delta\varrho(x)$ and then the derivative of ($6c$) with respecto to x_j. One obtains

in this way

$$(7c)\qquad \mathscr{T} = -\frac{1}{2m}\left\{\int \mathrm{d}x\,\Delta\varrho(x)\,\frac{\delta}{\delta\varrho(x)} + \int \mathrm{d}x\,\varrho(x)\left(\nabla\varrho(x)\,\frac{\delta}{\delta\varrho(x)}\right)^2\right\}.$$

The second term can be symmetrized.

A solution of the functional differential equation (7*b*) gives by (7*a*) a solution of the wave equation (6*b*). The connection between functionals $\chi[\varrho]$ and configuration space wave functions $\Phi(x_1, \ldots, x_N)$ is, however, not a one-to-one correspondence, as there are functionals for which the substitution (6*c*) gives identically zero. Since the Hamiltonian commutes with the number operator

$$(7d)\qquad N = \int \mathrm{d}x\,\varrho(x)\,,$$

a solution of (7*b*) multiplied by an arbitrary functional $C[\int \mathrm{d}x\,\varrho(x)]$ is still a solution. One can obtain functionals $\chi[\varrho]$ corresponding to a definite number N of particles, by projecting a solution of (7*b*) to the corresponding subspace, in multiplying it by a δ-function of $N - \int \mathrm{d}x\,\varrho(x)$. The representation of Bogolubov and Zubarev refers to such subspaces. On the other hand, the equation (7*b*) has solutions which have the same functional dependence for any value of N apart from this δ-function factor and this is a favourable feature in describing large systems.

4. – Weight function and the correspondence between the two representations.

The form of the kinetic energy operator (7*c*) is non-Hermitian. The scalar product

$$(8a)\qquad (\chi_1, \chi_2) = \int \delta\varrho(x)\,\chi_1^*[\varrho]\,\chi_2[\varrho]\exp[-W[\varrho]]\,,$$

of two functionals χ_1, χ_2 is to be defined, therefore, with a weight function $\exp[-W[\varrho]]$ in such a way as to make the expectation value of the kinetic energy $\mathscr{T}$

$$(8b)\qquad (\chi, \mathscr{T}\chi) = (\mathscr{T}\chi, \chi)$$

real. (8*a*) becomes of the form (5*e*) by means of a transformation

$$(8c)\qquad \hat{\chi}[\varrho] = \chi[\varrho]\exp[-\tfrac{1}{2}W[\varrho]]$$

which means for any functional operator $\mathscr{B}$ a transformation of the form

$$\hat{\mathscr{B}} = \exp[-\tfrac{1}{2}W]\mathscr{B}\exp[\tfrac{1}{2}W]\,. \tag{8d}$$

The functional differential operator $\delta/\delta\varrho(x)$ is transformed by (8d) into

$$\frac{\delta}{\delta\varrho(x)} + \frac{1}{2}\frac{\delta W}{\delta\varrho(x)}\,,$$

and the non-Hermitian terms of the kinetic energy (7c) disappear through (8d) if the equation

$$\nabla\frac{\delta W}{\delta\varrho(x)} = \frac{\nabla\varrho(x)}{\varrho(x)} = \nabla\log\varrho(x) \tag{9a}$$

is satisfied. This has the solution

$$W[\varrho] = \int dx\{\varrho(x)\log\varrho(x) - \varrho(x)\} \tag{9b}$$

to which a multiple of $\int dx\,\varrho(x)$ could be added. The weight function $W[\varrho]$ of (8a) is then given by (9b). The argument for its derivation can be made more rigorous by a detailed investigation of the equation (8b).

If one calculates the functional integral in (8a) by a limiting process after a subdivision of x-space, the weight factor factorizes into a product form with respect to the integration variables ϱ_x,

$$\exp[-W[\varrho]] = \prod_x \varrho_x^{-\varrho_x}\exp[\varrho_x]\,. \tag{9c}$$

The effect of the weight factor is to cut down the contributions from large values of $\varrho(x)$.

Transforming the kinetic energy $\mathscr{T}$ of (7c) by means of (8d), (9b) one finds the expression (4b) of $\hat{\mathscr{T}}$. The potential energy (4d) remains unchanged under this transformation. The transformation (8c, d) with the expression (9b), establishes in this way the connection between the state vectors and operators of the two density field representations obtained from the field description and from the configuration space argument (7a). The form of the kinetic energy operator is rather different in the two representations. At the two descriptions result from rather different approaches the obtained relationship is not a trivial one.

5. – Discussion.

In the density variables, the interaction energy $\mathscr{V}$ is a simple quadratic expression and the complications of the dynamics are reflected in the form of the kinetic energy. A simple linearization of the non-linear terms of the kinetic energy, obtained in replacing $\varrho(x)$ by its average ϱ_0, leads as shown by BOGOLUBOV and ZUBAREV, to a system of independent excitations with an energy spectrum $E_k = \sqrt{\varepsilon_k(\varepsilon_k + 2\varrho_0 V_k)}$, where $\varepsilon_k = k^2/2m$ and V_k is the Fourier transform of $V(x-x')$. As this spectrum corresponds to the weak coupling limit, one would like to hope that one will be able to find better approximations.

As the complications of the method are related to the form of the kinetic energy, some insight in the description might be gained by constructing the eigenstates of the kinetic energy operator. These represent the energy states of a non-interacting Bose gas.

The lowest eigenvalue 0 of the kinetic energy operator $\mathscr{T}$ of (7c) corresponds to the functional $\chi_0[\varrho] = 1$, and a complete set of eigenstates is given by the functionals

$$1\,, \tag{10a}$$

$$\int \mathrm{d}x \exp[ikx]\varrho(x)\,, \tag{10b}$$

$$\iint \mathrm{d}x_1\,\mathrm{d}x_2 \exp\left[i(k_1x_1 + k_2x_2)\right]\varrho_2(x_1, x_2)\,, \tag{10c}$$

$$\cdots\cdots\cdots\cdots\cdots\cdots$$

$$\int\!\cdots\!\int \mathrm{d}x_1 \ldots \mathrm{d}x_n \exp\left[i(k_1x_1 + \ldots + k_nx_n)\right]\varrho_n(x_1, \ldots, x_n)\,, \tag{10d}$$

where

$$\varrho_n(x_1, \ldots, x_n) = \tag{10e}$$
$$= \varrho(x_1)\left[\varrho(x_2) - \delta(x_1 - x_2)\right] \ldots \left[\varrho(x_n) - \delta(x_1 - x_n) - \ldots - \delta(x_{n-1} - x_n)\right].$$

These can still be multiplied by an arbitrary factor $C[\int \mathrm{d}x\, \varrho(x)]$ and should be multiplied by $\delta(N - \int \mathrm{d}x\, \varrho(x))$ to represent the states of an N particle system. By means of the substitution $\varrho(x) = \sum_{j=1}^{N} \delta(x - x_j)$, one obtains from (10a-d) the symmetric configuration space wave functions

$$1\,, \tag{11a}$$

$$\sum_{j=1}^{N} \exp[ikx_j]\,, \tag{11b}$$

(11c)
$$\sum_{i \neq j=1}^{N} \exp\left[i(k_1 x_i + k_2 x_j)\right],$$

. . . .

(11d)
$$\sum_{i_1 \neq \ldots \neq i_n = 1}^{N} \exp\left[i(k_1 x_{i_1} + \ldots + k_n x_{i_n})\right],$$

which represent states with all particles in the zero momentum state, or with 1, 2, ..., n particles with momenta k_1, k_2, ..., k_n excited. The substitution of $\varrho(x) = \sum_{j=1}^{N} \delta(x - x_j)$ in the expression (10e) of $\varrho_n(x_1, \ldots, x_n)$ gives identically zero for $n > N$. The multiple density functions $\varrho_n(x_1, \ldots, x_n)$ represent those polynomials of $\varrho(x)$ which remain well-defined after the substitution leading to the configuration space wave functions. All functionals $\chi[\varrho]$ to be considered must have this property.

The free particle solutions of an N-particle system in the Hermitian density representation $\hat{\chi}[\varrho]$ are obtained with (8c), (9b) on multiplying (10a-d) by

(12a)
$$\hat{\chi}_0^N[\varrho] = \exp\left[-\tfrac{1}{2} W_0 \varrho\right] \delta\left(N - \int \mathrm{d}x\, \varrho\right).$$

If one goes over to the lattice space with creation operators ψ_x^*, the density operator $\varrho(x)$ is replaced by the occupation number operator n_x with eigenvalues 0, 1, 2, ... The zero momentum state of a particle is related to a linear combination of all ψ_x^* with equal coefficients, and the state of N particles in the zero momentum state to the N-th power of this linear combination. In forming this N-th power, the term $(\psi_{x_1}^*)^{n_{x_1}} \ldots (\psi_{x_m}^*)^{n_{x_m}}$ with $n_{x_1} + \ldots + n_{x_m} = N$, $n_x = 0, 1, 2, \ldots$ occurs

$$\frac{N!}{\prod_x n_x!}$$

times.

With the definition (5c) of the norm, the state of N Bosons in the zero momentum state will be given in the n_x occupation number representation by the function

(12b)
$$\hat{\chi}_x^N[\ldots, n_x, \ldots] = \left(\frac{N!}{\prod_x n_x!}\right)^{\frac{1}{2}} \delta_{N, n_{x_1} + \ldots + n_{x_m}}.$$

By application of particle creation operators formed with $\psi_x^* = n_x^{\frac{1}{2}} \exp[i\varphi_x]$ one obtains from (12b) the states (10b-d), multiplied by a factor $\hat{\chi}_0^N$, with $\varrho(x)$ replaced by n_x and $\delta(x - x')$ by $\delta_{xx'}$.

With

$$\left(\prod_x n_x!\right)^{-\frac{1}{2}} = \exp\left[-\tfrac{1}{2}\sum_x \log(n_x!)\right] \tag{12c}$$

the relationship between (12b) and (12a), (9b) is reminescent of the Sterling formula and indicates the combinatorial origin of the weight factor.

A complete set of eigenstates can be constructed also in the case of independent particle motion in an external field. The solutions are sufficiently different from those in the free particle case to give some indications of general character and are given in an Appendix.

Assuming in general an exponential form

$$\chi_0[\varrho] = \exp[A[\varrho]]$$

for the lowest eigenstate of the Hamiltonian of a system with interactions one obtains a functional equation for $A[\varrho]$. A given $A[\varrho]$ corresponds to a given interaction energy, in general to many-body interactions. One can try to construct soluble models on the line of the work of COESTER and HAAG [6] and ARAKI [7].

Some types of wave function become very simple in the density variables. The configuration space wave function

$$\Phi = \prod_{i>j} \varphi(x_i - x_j) \tag{13a}$$

results from

$$\chi[\varrho] = \exp\left[\frac{1}{2}\iint \mathrm{d}x\,\mathrm{d}x'\,\boldsymbol{\varphi}(x-x')\,\varrho(x)[\varrho(x') - \delta(x-x')]\right], \tag{13b}$$

with $\varphi(x-x') = \exp[\boldsymbol{\varphi}(x-x')]$ through the substitution (7a). If $\chi_0[\varrho]$ describes the ground state of the system, Feynman's phonon excitations in which the ground state wave function is multiplied by a factor $\sum_{j=1}^{N} \exp[ikx_j]$ corresponds to a multiplication of $\chi_0[\varrho]$ by a factor (10b). The type of excitations with a back flow considered by FEYNMAN and COHEN [8] which is described in configuration space by

$$\sum_{i=1}^{N} \exp[ikx_i] \exp\left[i\sum_{j\neq i} g(x_i - x_j)\right] \Phi_0(x_1, \ldots, x_N) \tag{13c}$$

[6] F. COESTER and R. HAAG: *Phys. Rev.*, **117**, 1137 (1960).
[7] H. ARAKI: *Ph. D. Thesis* (Princeton, 1960).
[8] R. P. FEYNMAN and M. COHEN: *Phys. Rev.*, **102**, 1189 (1956).

result from a functional

$$\chi[\varrho] = \int \mathrm{d}x \exp\,[ikx]\,\varrho(x) \exp\left[i\int \mathrm{d}x'\, g(x-x')\,\varrho(x')\right] \chi_0[\varrho]\,. \tag{13d}$$

A starting point to investigate properties of the ground state could be by means of a variational principle in which a definite functional dependence of $\chi_0[\varrho]$ is assumed and the expectation value of the Hamiltonian is minimized with respect to variations of the functions in the trial functional, the normalization of the state vector being kept fixed. This will not be attempted here. It should be only mentioned that by means of partial integrations which lead to cancellations of terms the kinetic energy can be transformed into a more convenient form, and the expectation value of the Hamiltonian can be written as

$$\langle \mathscr{T} + \mathscr{V} \rangle = \int \delta\varrho(x) \exp\,[-W[\varrho]] \left\{ \frac{1}{2m} \int \mathrm{d}x\, \varrho(x)\, \nabla \frac{\delta\chi^*}{\delta\varrho(x)}\, \nabla \frac{\delta\chi}{\delta\varrho(x)} + \right.$$
$$\left. + \iint \mathrm{d}x\, \mathrm{d}x'\, V(x-x')\, \varrho(x)[\varrho(x') - \delta(x-x')]\chi^*\chi \right\}. \tag{14a}$$

This is to be varied under the supplementary condition

$$\int \delta\varrho(x) \exp\,[-W[\varrho]]\,\chi^*\chi = \text{const}\,. \tag{14b}$$

* * *

For helpful discussions thanks are due to Professor A. THELLUNG, Professor R. E. PEIERLS and Dr. G. V. CHESTER.

APPENDIX

The operator $\sum_{j=1}^{N} U(x_j)$ of configuration space corresponds in the density representation to

$$\mathscr{U} = \int \mathrm{d}x\, U(x)\, \varrho(x)\,, \tag{15a}$$

and the functionals $\chi[\varrho]$ describing the energy states of a system of bosons

moving independently in an external potential $U(x)$ satisfy the equation

$$\{\mathcal{T}+\mathcal{U}\}\,\chi[\varrho] = E\,\chi[\varrho]\,. \tag{15b}$$

Including a constant in the potential in such a way that the ground state $\chi_0[\varrho]$ should correspond to $E=0$, and substituting

$$\chi_0[\varrho] = \exp\,[A[\varrho]]\,, \tag{15c}$$

one obtains

$$A[\varrho] = \int \mathrm{d}x\,\boldsymbol{\varphi}(x)\,\varrho(x)\,, \tag{15d}$$

where $\varphi(x) = \exp\,[\boldsymbol{\varphi}(x)]$ is a solution of the equation

$$\left\{-\frac{1}{2m}\,\Delta + U(x)\right\}\varphi(x) = 0\,. \tag{15e}$$

The functional (15c, d) corresponds in configuration space to the wave function

$$\Phi_0(x_1, \dots, x_N) = \prod_i \exp\,[\boldsymbol{\varphi}(x_i)] = \prod_i \varphi(x_i)\,. \tag{15f}$$

that is to a state in which all particles are in the state $\varphi(x)$.

The functional

$$\chi[\varrho] = \int \mathrm{d}x\, f(x)\,\varrho(x)\,\chi_0[\varrho]\,, \tag{16a}$$

is a solution of (17b), if

$$\left\{-\frac{1}{2m}\,\Delta + U(x)\right\}\big(f(x)\,\varphi(x)\big) = E\big(f(x)\,\varphi(x)\big)\,. \tag{16b}$$

(16a) corresponds to the configuration space wave function

$$\sum_{j=1}^{N} f(x_j)\prod_i \varphi(x_i)\,, \tag{16c}$$

and represents a state in which one particle is in the excited state $f(x)\varphi(x)$. With solutions $f_1(x), \dots, f_n(x)$ of (16b) which correspond to excited states $f_1(x)\varphi(x), \dots, f_n(x)\varphi(x)$, (15$b$) has the general solution

$$\chi[\varrho] = \int \mathrm{d}x_1 \dots \mathrm{d}x_n\, f_1(x_1) \dots f_n(x_n)\,\varrho_n(x_1, \dots, x_n)\,\chi_0[\varrho]\,, \tag{16d}$$

where $\varrho_n(x_1, ..., x_n)$ is given by (10e). In configuration space, this corresponds to the symmetric wave function

$$\sum_{j_1 \neq ... \neq j_n = 1}^{N} f_1(x_{j_1}) \ldots f_n(x_{j_n}) \prod_{i=1}^{N} \varphi(x_i) \; . \tag{16e}$$

The free particle solutions result by writing $\boldsymbol{\varphi}(x) = 0$, $\varphi(x) = 1$.

RIASSUNTO (*)

Si discute l'introduzione di una descrizione della densità con una trattazione di campo. Le complicazioni matematiche addizionali provenienti dall'apparizione delle potenze della funzione δ possono venire evitate con l'uso di un procedimento limitativo. Il ragionamento sullo spazio di configurazione di Bogolubov e Zubarev è esposto per mezzo di uno spazio x in cui si danno espressioni semplici. Nella rappresentazione risultante l'integrale di normalizzazione è definito con una funzione peso, di cui si determina l'espressione. La funzione peso mette in relazione le espressioni alquanto diverse delle due rappresentazioni di campo della densità. Si considerano alcuni casi semplici e si formula un principio variazionale.

(*) *Traduzione a cura della Redazione.*

IL NUOVO CIMENTO Vol. XIX, N. 1 1° Gennaio 1961

Lie Equations for a Lee Model.

E. R. Caianiello (*)
University of Maryland - College Park, Md. (**)

S. Okubo
Istituto di Fisica Teorica dell'Università - Napoli

(ricevuto il 7 Settembre 1960)

Summary. — The renormalization in configuration space of a slight generalization of the Lee model is discussed, as an example of general procedures (1) which seem to be applicable also to more general cases than the present one. The replacement of ordinary with finite-part integrals removes consistently all ultraviolet infinities and permits to write the Lie equations of the renormalization group, the solution of which yields the familiar relations between unrenormalized and renormalized parameters.

1. – Introduction.

1·1. – We discuss in this work the renormalization of the Lee model (with minor modifications) in configuration space, as a first example of general procedures which were described elsewhere (1). Our interest in the Lee model is only incidental, as it does not seem legitimate, also in the light of the present treatment, to infer general conclusions from its behavior; we shall not, therefore, touch here upon the well-known problems that arise in its detailed

(*) On leave from the Istituto di Fisica Teorica, Università di Napoli.

(**) Physics Department Technical Report no. 185. This research was sponsored in part by the U.S.A.F.O.S.R. and by the U.S. Army (through its European Office).

(1) E. R. Caianiello: *Nuovo Cimento*, **13**, 637 (1959); **14**, 185 (1959); E. R. Caianiello, A. Campolattaro and B. Preziosi: *Nuovo Cimento*, in print (referred to in text as I, II, III, resp.). See also references quoted in these works.

study, nor on the related questions connected with the nature of the Lie equations of the renormalization group, which are the starting point of our analysis. Our aim is rather to present, in more detail than it was possible before, the general formalism which is required by our method for investigations of this nature, in a shape that may be immediately generalized to more realistic models; there is thus the hope that a similar study may be attempted for electrodynamics. The essential feature of this approach is that it separates completely the problems of renormalization from those of actual computation of physical quantities; the first can be exactly studied from the Lie equations of the renormalization group [1], the second are automatically taken care of by the replacement of ordinary with suitably defined finite-part integrals.

We shall show how this procedure works in detail on the example of a Lee model, which is obtained from the original model [2] by extending it to contain graphs with arbitrarily time-ordered vertices (of the same topology); this slight generalization, which is introduced merely to expedite computations, improves the correspondence of the model with the actual theory and does not alter the nature of the results. There is every reason, however, to believe that radical changes might be introduced by the consideration of graphs of more general topology, and also by couplings to meson fields other than the neutral scalar.

A well-known difficulty which is met in a study of the Lee model in configuration space is that the causal propagation of a particle of infinite mass is not a well-defined concept. This shows up in the fact that the non-relativistic propagator (xy) is given, both for V and N particles ($V \rightleftarrows N+K$), by

$$(xy)_{V,N} \simeq \theta(x^0 - y^0)\,\delta^3(\boldsymbol{x}-\boldsymbol{y}) \exp\left[-im_{V,N}(x^0-y^0)\right], \tag{1}$$

which does not have singularities in its time part. This apparent inconsistency can however be easily avoided by a careful use of limiting processes, by calculating, that is, with a theory in which the mass is finite, so that causal behavior can be correctly formulated, and then taking, if it is so desired, the mass to be very large or infinite.

We shall find it convenient to cast the exact Lee model in a shape that permits that all perturbative expansions be written, formally, with the same algorithms which apply to ordinary mesodynamics [1]; we shall then add, merely for computational ease, also the graphs which correspond to time orderings of the vertices which are forbidden by the original model.

---

[2] T. D. Lee: *Phys. Rev.*, **95**, 1329 (1954); G. Källèn and W. Pauli: *Dan. Mat. Fys. Medd.*, **30**, no. 7 (1955).

1·2. – We use the notation established in ref. (1). The Lagrangian density

$$\mathscr{L} = g(\bar{N}V)K^+ + g(\bar{V}N)K\,, \tag{2}$$

$$(V \rightleftarrows N + K)$$

can be written, with the introduction of an isotopic spin, as

$$\mathscr{L} = g\sum_{\mu=1,2}\bar{\psi}\tau_\mu\psi\cdot\varphi_\mu\,, \tag{3}$$

where

$$\left\{\begin{array}{l}
\psi = \begin{pmatrix} V \\ N \end{pmatrix}, \qquad \varphi_1 = K\,, \qquad \varphi_2 = K^+; \\[2mm]
\varrho_1 = \tau_+ = \dfrac{\tau_1 + i\tau_2}{2}\,, \qquad \varrho_2 = \tau_- = \dfrac{\tau_1 - i\tau_2}{2}; \\[2mm]
\tau_V = \dfrac{1+\tau_3}{2}\,, \qquad \tau_N = \dfrac{1-\tau_3}{2}; \\[2mm]
\varrho_1\tau_V = \varrho_2\tau_N = \tau_N\varrho_1 = \tau_V\varrho_2 = 0; \\[1mm]
\varrho_1\tau_N = \tau_V\varrho_1 = \varrho_1\,, \qquad \varrho_2\tau_V = \tau_N\varrho_2 = \varrho_2; \\[1mm]
\varrho_i\tau_V\varrho_i = \varrho_i\tau_N\varrho_i = 0\,, \qquad \varrho_1\tau_V\varrho_2 = \varrho_2\tau_N\varrho_1 = 0; \\[1mm]
\varrho_1\tau_N\varrho_2 = \tau_V\,, \qquad \varrho_2\tau_V\varrho_1 = \tau_N\,.
\end{array}\right. \tag{4}$$

To the cost of some additional combinatories, of course, all the considerations that follow could be made starting directly from (2): the form (3) is however more convenient in view of future extensions of this work.

The propagation kernels $K_{N_0P_0}$ are given by:

$$K_{N_0P_0} = K\begin{pmatrix} x_1 \dots x_{N_0} \,| & \\ & |\, t_1 \dots t_{P_0} \\ y_1 \dots y_{N_0} \,| & \end{pmatrix} = \tag{5}$$

$$= \sum_{N(P_0)} \frac{\lambda^N}{N!}\int \mathrm{d}\xi_1 \dots \int \mathrm{d}\xi_N\, \varrho^1 \dots \varrho^N \begin{pmatrix} x_1 \dots x_{N_0}\, \xi_1 \dots \xi_N \\ \\ y_1 \dots y_{N_0}\, \xi_1 \dots \xi_N \end{pmatrix} [t_1 \dots t_{P_0}\, \xi_1 \dots \xi_N]\,,$$

where we have put

$$\lambda = ig\,, \tag{6}$$

$$(xy) = \tau_V\theta(x^0 - y^0)(xy)_V + \tau_N\theta(x^0 - y^0)(xy)_N\,, \tag{7}$$

$$[t_i t_j] = [\varepsilon_{\mu_i\mu_j}\theta(t_i^0 - t_j^0) + \varepsilon_{\mu_j\mu_i}\theta(t_j^0 - t_i^0)][t_i t_j]_K\,, \tag{8}$$

with $\varepsilon_{11}=\varepsilon_{22}=\varepsilon_{21}=0$, $\varepsilon_{12}=1$, $\varrho^i=\varrho^{\mu_i}_{\alpha_i\beta_i}$, etc., as in ref. (1). It is easily verified that with the choice (4), (7), (8) the kernels (5) contain all, and only, the graphs of the original Lee model. Once these graphs are written, graphs with arbitrarily time-ordered vertices are included by replacing, in (7) and (8), $\theta(x^0-y^0)(x,y)_{\text{V,N}}$ and $\theta(t_i^0-t_j^0)[t_i,t_j]_{\text{K}}$ respectively with $(x,y)_{\text{V,N}}$ and $[t_i,t_j]_{\text{K}}$.

1·3. – Our analysis is based upon the equations (I-23, 24, 25):

$$\frac{\partial K_{N_0P_0}}{\partial\lambda}=\int\mathrm{d}\xi\,\varrho^\xi K\left(\begin{matrix}x_1\,\dots\,x_{N_0}\\ \\ y_1\,\dots\,y_{N_0}\end{matrix}\,\middle|\,\xi t_1\,\dots\,t_{P_0}\right),\tag{9}$$

$$\frac{\partial K_{N_0P_0}}{\partial m_{\text{V}}}=-i\int\mathrm{d}\xi\,\tau^\xi_{\text{V}} K\left(\begin{matrix}\xi x_1\,\dots\,x_{N_0}\\ \\ \xi y_1\,\dots\,y_{N_0}\end{matrix}\,\middle|\,t_1\,\dots\,t_{P_0}\right),\tag{10}$$

$$\frac{\partial K_{N_0P_0}}{\partial m_{\text{N}}}=-i\int\mathrm{d}\xi\,\tau^\xi_{\text{N}} K\left(\begin{matrix}\xi x_1\,\dots\,x_{N_0}\\ \\ \xi y_1\,\dots\,y_{N_0}\end{matrix}\,\middle|\,t_1\,\dots\,t_{P_0}\right),\tag{11}$$

$$\frac{\partial K_{N_0P_0}}{\partial(m^2_{\text{K}})}=-\frac{i}{2}\int\mathrm{d}\xi\,K\left(\begin{matrix}x_1\,\dots\,x_{N_0}\\ \\ y_1\,\dots\,y_{N_0}\end{matrix}\,\middle|\,\xi\xi t_1\,\dots\,t_{P_0}\right),\tag{12}$$

$$((\xi\xi)=[\xi\xi]=0)\,,$$

which we shall also write, for short, as

$$\frac{\partial K_{N_0P_0}}{\partial\lambda_i}=\int\mathrm{d}\xi\,H^i\left(\xi\,\middle|\begin{matrix}x_1\,\dots\,x_{N_0}\\ \\ y_1\,\dots\,y_{N_0}\end{matrix}\middle|\,t_1\,\dots\,t_{P_0}\right)=\int\mathrm{d}\xi\,H^i_{N_0P_0}(\xi)\,,\tag{13}$$

with $\lambda_1=\lambda$, $\lambda_2=m_{\text{V}}$, $\lambda_3=m_{\text{N}}$, $\lambda_4=m^2_{\text{K}}$, where the r.h.s. is defined by the r.h.s.'s of (9)–(12).

These equations must be brought into the form

$$\frac{\partial\overline{K}_{N_0P_0}}{\partial\overline{\lambda}_i}=\rfloor\,\mathrm{d}\xi\,\overline{H}^i_{N_0P_0}(\xi)\,,\tag{14}$$

where all barred symbols refer to renormalized quantities (we remind that by this we mean that all infinities of ultraviolet origin are disposed of correctly; $\overline{\lambda}$, $\overline{m}_{\text{V}}$, etc., acquire the role of indeterminate parameters, the values of which will be determined by comparison of theory with experiment, *i.e.*, by an additional finite renormalization).

The passage from (13) to (14) is achieved by replacing ordinary integrals

with finite-part integrals, symbolically expressed by

$$\int \mathrm{d}\xi_h = \underset{\xi}{\Big\lceil} \mathrm{d}\xi_h + D_\xi^h \,, \tag{15}$$

which remove all, and only, the divergences arising from confluence of ξ_h with a fixed ξ. Several, among the host of possible prescriptions (15) are described in II. We use here finite-part integrals defined so as to satisfy (III.3),

$$D_\xi^{h,\dots,m+1} \underset{\xi}{\Big\lceil} \mathrm{d}\xi_m = \underset{\xi}{\Big\lceil} \mathrm{d}\xi_h D_\xi^{h-1,\dots,m} - D_\xi^{h,\dots,m+1} D_\xi^m + D_\xi^h D_\xi^{h-1,\dots,m} + D_\xi^{h,\dots,m} \,, \tag{16}$$

where $D_\xi^{h,\dots,1}$ contains all, and only, the divergent contributions due to simultaneous confluence of $\xi_1, \dots, \xi_h$ with ξ; all integrands are symmetric functions of $\xi_1, \dots, \xi_N$.

2. – Removal of divergences.

2·1. – It was proved in II and III that the replacement (15) changes the r.h.s. of (13) into infinite sums, which we may write for short with the symbolic notation (cf. (III-13′))

$$\int \mathrm{d}\xi\, H^i_{N_0P_0}(\xi) = \int \mathrm{d}\xi \exp[\lambda \hat{\underset{\sim}{\mathscr{D}}}_\xi] H^{i(\xi)}_{N_0P_0}(\xi) \,, \tag{17}$$

where $H^{i(\xi)}_{N_0P_0}(\xi)$ denotes that it is calculated from (5) after replacing $\int \mathrm{d}\xi_h$ with $\underset{\xi}{\Big\lceil} \mathrm{d}\xi_h$, and the symbolic exponential operator is defined by the convention (which could be immediately transcribed into functional-derivative notation)

$$(\hat{\underset{\sim}{\mathscr{D}}}_\xi)^h H^{i(\xi)}_{N_0P_0}(\xi) = \hat{\mathscr{D}}_\xi^{h,\dots,1} \varrho^1 \dots \varrho_\xi^h H^{i(\xi)} \left(\xi \left\| \begin{matrix} x_1 \dots x_{N_0} & \xi_1 \dots \xi_h \\ y_1 \dots y_{N_0} & \xi_1 \dots \xi_h \end{matrix} \right| t_1 \dots t_{P_0}\, \xi_1 \dots \xi_h \right) , \tag{18}$$

where $\hat{\mathscr{D}}_\xi^{h\dots 1}$ is formed from the divergent parts which occur in (16), in the way specified by (III.6).

The discussion in II-2 shows that the whole problem reduces to the computation of the « divergent cores », one for each parameter of the theory, which can be concisely expressed, after (17), as

$$C_{n,p}^{(\lambda_i)} = \underset{}{\Big\lceil} \mathrm{d}\xi \left[\exp[\lambda \underset{\sim}{\mathscr{D}}_\xi] H^i \left(\xi \left| \begin{matrix} \mathring{u}_1 \dots \mathring{u}_n \\ \mathring{v}_1 \dots \mathring{v}_n \end{matrix} \right| \mathring{w}_1 \dots \mathring{w}_p \right) \right]_{\lambda=0} , \tag{19}$$

where $\underset{\sim}{\mathscr{D}}_\xi$ is defined by (16) and (III.7). Thus, for instance,

$$(20)\qquad C^{(\lambda_i)}_{n,p} = C^{(\lambda)}_{n,p} = \int \mathrm{d}\xi\, \varrho^\xi \sum_{M(P+1)} \frac{\lambda^M}{M!}\, \mathscr{D}_\xi^{M\dots 1} \varrho^1 \dots \varrho^M \begin{pmatrix} \mathring{u}_1 \dots \mathring{u}_n & \xi\xi_1 \dots \xi_M \\ \mathring{v}_1 \dots \mathring{v}_n & \xi\xi_1 \dots \xi_M \end{pmatrix} \cdot [\xi\xi_1 \dots \xi_M\ \mathring{w}_1 \dots \mathring{w}_p]\,,$$

etc..

2'2. – It is easy to see, as in the discussion in II-2, that the only non-vanishing divergent cores, if any, may be those for which

$$(21)\qquad \begin{cases} (\lambda_1): & 4M - 3(M+1-n) - 2\cdot\frac{1}{2}(M+1-p) \leqslant 0\,, \quad i.e.\ \ 3u + p \leqslant 4\,, \\ (\lambda_2, \lambda_3): & 3n + p \leqslant 3\,, \\ (\lambda_4): & 3n + p \leqslant 2\,. \end{cases}$$

The restrictions (21) are the same as in electrodynamics; everything that has been said thus far applies to any field theory. The special nature of the Lee model imposes many additional restrictions; the most obvious is that, because of (7), all cores with $n=0$ vanish identically (no closed loops survive in the determinants of their expansions). We have, therefore, to examine only $C^{(\lambda_1)}_{1,0}$, $C^{(\lambda_2)}_{1,0}$, $C^{(\lambda_3)}_{1,0}$, $C^{(\lambda_1)}_{1,1}$. In order to evaluate these, he remark first that all determinants in the expansions reduce to:

$$(22)\qquad \sigma_i^\xi \varrho^1 \dots \varrho^M \begin{pmatrix} \mathring{u} & \xi\xi_1 \dots \xi_M \\ \mathring{v} & \xi\xi_1 \dots \xi_M \end{pmatrix} = (-1)^{M-1} \sum_{P_{M+1}} (u\xi_{j_1})\, \varrho^{j_1} (\xi_{j_1}\xi_{j_2})\, \varrho^{j_2} \dots \varrho^{j_M}{}^{-1} (\xi_{j+1} v)\,,$$

where we have put $\sigma_1 \equiv \varrho$, $\sigma_2 \equiv \tau_V$, $\sigma_3 \equiv \tau_N$, and $\sum_{P_{M+1}}$ is the sum over all permutations $j, \dots, j_{M+1}$ of $0, 1, \dots, M$ ($\xi_0 \equiv \xi$; $\varrho^0 \equiv \sigma_i^\xi$); it follows further from (4), (7), (8), (16), (III-7) and the considerations made in III-3 that the only terms that *might* survive, out of the whole expansions (19), are those which correspond to graphs of type:

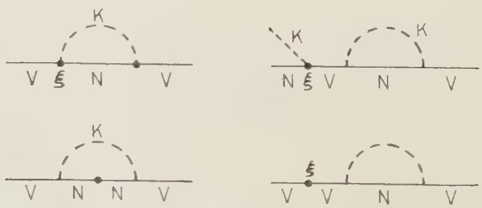

Fig. 1.

All terms in the expansions (19) with $M > 2$ vanish therefore identically. This leaves us with

$$(23)\qquad C^{(\lambda)}_{1,0} \equiv \lambda \,⌈\, \mathrm{d}\xi\, \mathscr{D}^1_\xi \varrho^\xi \varrho^1 \begin{pmatrix} \overset{\circ}{u}\,\xi\,\xi_1 \\ \\ \overset{\circ}{v}\,\xi\,\xi_1 \end{pmatrix} [\xi\xi_1] =$$

$$= \lambda\tau_{\mathrm{V}} \,⌈\, \mathrm{d}\xi\, D^1_\xi \{[\xi\xi_1]_{\mathrm{K}} [(u\xi)_{\mathrm{V}} (\xi\xi_1)_{\mathrm{N}} (\xi, v)_{\mathrm{V}} + (u\xi_1)_{\mathrm{V}} (\xi_1\xi)_{\mathrm{N}} (\xi v)_{\mathrm{V}}]\} =$$

$$= \lambda a \tau_{\mathrm{V}} (uv) + \lambda a (m_{\mathrm{V}} + 2m_{\mathrm{N}}) \frac{\partial(uv)}{\partial m_{\mathrm{V}}},$$

where

$$(24)\qquad a = \frac{i}{(2\pi)^4} \int \mathrm{d}^4\eta \,\frac{1}{(\eta^2 + i\varepsilon)^2} \exp[iC\eta^2], \qquad (c > 0);$$

the factor $\exp[iC\eta^2]$ in (24) removes a spurious divergence at infinity, as it was discussed in III, and the calculation is simplest if use is made of the equation

$$(\gamma\partial + m)(xy) = i\,\delta(x - y)\,.$$

The operation $⌈\mathrm{d}\xi$ acts, for $u \neq v$, like ordinary integration (cf. I and II).

« Acc'dental » cancelation of terms gives

$$(25)\qquad C^{(\lambda)}_{1,1} \equiv \frac{\lambda^2}{2} \,⌈\, \mathrm{d}\xi\, \varrho^\xi \varrho^1 \varrho^2 \mathscr{D}^{21}_\xi \begin{pmatrix} \overset{\circ}{u}\,\xi\,\xi_1\,\xi_2 \\ \\ \overset{\circ}{v}\,\xi\,\xi_1\,\xi_2 \end{pmatrix} [\xi\xi_1\xi_2 w] \equiv 0\,,$$

$$(26)\qquad C^{(m_{\mathrm{V}})}_{1.0} \equiv -i\,\frac{\lambda^2}{2} \,⌈\, \mathrm{d}\xi\, \tau^\xi_{\mathrm{V}} \varrho^1 \varrho^2 \mathscr{D}^{21}_\xi \begin{pmatrix} \overset{\circ}{u}\,\xi\,\xi_1\,\xi_2 \\ \\ \overset{\circ}{v}\,\xi\,\xi_1\,\xi_2 \end{pmatrix} [\xi_1\xi_2] \equiv 0\,,$$

while

$$(27)\qquad C^{(m_{\mathrm{N}})}_{1.0} \equiv -i\,\frac{\lambda^2}{2} \,⌈\, \mathrm{d}\xi\, \tau^\xi_{\mathrm{N}} \varrho^1 \varrho^2 \mathscr{D}^{21}_\xi \begin{pmatrix} \overset{\circ}{u}\,\xi\,\xi_1\,\xi_2 \\ \\ \overset{\circ}{v}\,\xi\,\xi_1\,\xi_2 \end{pmatrix} [\xi_1\xi_2] =$$

$$= i\,\frac{\lambda^2}{2}\,\tau_{\mathrm{V}} \,⌈\, \mathrm{d}\xi\, \mathscr{D}^{21}_\xi [(u\,\xi_1)_{\mathrm{V}} (\xi_1\xi)_{\mathrm{N}} (\xi\,\xi_2)_{\mathrm{N}} (\xi_2\,v)_{\mathrm{V}} + (u\,\xi_2)_{\mathrm{V}} (\xi_2\xi)_{\mathrm{N}} (\xi\,\xi_1)_{\mathrm{N}} (\xi_1\,v)_{\mathrm{V}}] [\xi_1\xi_2]_{\mathrm{K}} =$$

$$= i\lambda^2 \frac{\partial(uv)}{\partial m_{\mathrm{V}}} D^{21}_\xi [(\xi_1\xi)_{\mathrm{N}} (\xi\xi_2)_{\mathrm{N}} [\xi_1\xi_2]_{\mathrm{K}}] = \frac{i\lambda^2}{\pi^2 (2\pi)^4}\cdot$$

$$\cdot \frac{\partial(uv)}{\partial m_{\mathrm{V}}} D^{21}_\xi \left[\frac{\gamma^\mu\gamma^\nu(\xi_1 - \xi)^\mu (\xi_2 - \xi)^\nu}{[(\xi_1 - \xi)^2 + i\varepsilon']^2 [(\xi_2 - \xi)^2 + i\varepsilon'']^2 [(\xi_1 - \xi_2)^2 + i\varepsilon''']}\right] = \lambda^2 a \frac{\partial(uv)}{\partial m_{\mathrm{V}}}\,.$$

(For the computation of (27), remark that in it D^{21}_ξ reduces to $D^2_\xi \int \mathrm{d}\xi_1$.)

2'3 – Collecting our results, and proceeding as in II, we find

$$\frac{\partial K_{N_0P_0}}{\partial\lambda}=\int \mathrm{d}\xi\,\varrho^{\xi}K\left(\begin{matrix}x_1\dots x_{N_0}&\xi\\ y_1\dots y_{N_0}&\xi\end{matrix}\middle|\,\xi\;t_1\dots t_{P_0}\right)+ \tag{28}$$

$$+\sum_{N(P_0)}\frac{\lambda^N}{N!}\int\mathrm{d}\xi_1'\int\mathrm{d}\xi_N'\,\varrho^{1'}\dots\varrho^{N'}\sum_{\sigma_r}(-1)^{p(i,j)}C^{(\lambda)}_{1,0}\begin{pmatrix}\mathring{i}''\\ \mathring{j}''\end{pmatrix}\begin{pmatrix}\mathring{i}_1'\dots \mathring{i}_{N_0+N-1}'\\ \mathring{j}_1'\dots \mathring{j}_{N_0+N-1}'\end{pmatrix}[\xi_1'\dots\xi_N'\,t_1\dots t_{P_0}]\,,$$

where $\sum_{c_r}$ is over all combinations i'', i' of $x_1\dots x_{N_0}\xi_1'\dots\xi_N'$ and j'', j' of $y_1\dots y_{N_0}\xi_1'\dots\xi_N'$, of relative parity $p(i,j)$. After (23), and due modification of (I-30) to account for the factor τ_{V} in the first term at r.h.s. of (23) (take half the sum of (I-30), computed once by rows first and once by columns first, and observe that $\tau_{\mathrm{V}}\varrho_\mu+\varrho_\mu\tau_{\mathrm{N}}=\varrho_\mu$), (28) becomes

$$\left[\left(1-\frac{a\lambda^2}{2}\right)\frac{\partial}{\partial\lambda}-\lambda a\,(m_{\mathrm{V}}+2m_{\mathrm{N}})\frac{\partial}{\partial m_{\mathrm{V}}}\right]K_{N_0P_0}= \tag{29}$$

$$=\frac{a\lambda}{2}N_{\mathrm{V}}\cdot K_{N_0P_0}+\int\mathrm{d}\xi\,\varrho^{\xi}K\left(\begin{matrix}x_1\dots x_{N_0}&\xi\\ y_1\dots y_{N_0}&\xi\end{matrix}\middle|\,\xi\;t_1\dots t_{P_0}\right),$$

where N_{V} is the total number of initial and final V external lines contained in $K_{N_0P_0}$.

In an entirely analogous manner we find

$$\frac{\partial K_{N_0P_0}}{\partial m_{\mathrm{V}}}=-i\int\mathrm{d}\xi\,\tau_{\mathrm{V}}^{\xi}K\left(\begin{matrix}\xi\;x_1\dots x_{N_0}\\ \xi\;y_1\dots y_{N_0}\end{matrix}\middle|\,t_1\dots t_{P_0}\right), \tag{30}$$

$$\frac{\partial K_{N_0P_0}}{\partial(m_{\mathrm{K}}^2)}=-\frac{i}{2}\int\mathrm{d}\xi\,K\left(\begin{matrix}x_1\dots x_{N_0}\\ y_1\dots y_{N_0}\end{matrix}\middle|\,\xi\,\xi_1 t\dots t_{P_0}\right), \tag{31}$$

$$\left[\frac{\partial}{\partial m_{\mathrm{N}}}-a\lambda^2\frac{\partial}{\partial m_{\mathrm{V}}}\right]K_{N_0P_0}=-i\int\mathrm{d}\xi\,\tau_{\mathrm{N}}^{\xi}K\left(\begin{matrix}\xi\;x_1\dots x_{N_0}\\ \xi\;y_1\dots y_{N_0}\end{matrix}\middle|\,t_1\dots t_{P_0}\right). \tag{32}$$

3. – Lie equations.

3'1. – We can now apply to the equations (29)–(32) the technique outlined in II. Let

$$K_{N_0P_0}=A_{N_0P_0}(\lambda_i)\widetilde{K}_{N_0P_0} \tag{33}$$

and determine $A_{N_0P_0}$ so as to remove the first term at r.h.s. of (29); this yields

$$(34)\qquad \begin{cases} \dfrac{\partial A_{N_0P_0}}{\partial m_{\mathrm{V}}} = \dfrac{\partial A_{N_0P_0}}{\partial (m_{\mathrm{K}}^2)} = 0\,, \\ \left[\left(1-\dfrac{a\lambda^2}{2}\right)\dfrac{\partial}{\partial\lambda} - a\lambda(m_{\mathrm{V}}+2m_{\mathrm{N}})\dfrac{\partial}{\partial m_{\mathrm{V}}}\right](\log A_{N_0P_0}) = \dfrac{a\lambda}{2}N_{\mathrm{V}}\,, \\ \left[\dfrac{\partial}{\partial m_{\mathrm{N}}} - a\lambda^2\dfrac{\partial}{\partial m_{\mathrm{V}}}\right]A_{N_0P_0} = 0\,, \end{cases}$$

which show that $A_{N_0P_0}$ is a function of λ only, such that

$$(35)\qquad \left(1-\frac{a\lambda^2}{2}\right)\frac{\partial(\log A_{N_0P_0})}{\partial\lambda} = \frac{a\lambda}{2}N_{\mathrm{V}}\,,$$

which is solved by

$$(36)\qquad A_{N_0P_0} = Z_{\mathrm{V}}^{N_{\mathrm{V}}/2}\,,$$

$$(37)\qquad Z_{\mathrm{V}} = \frac{C_z}{1-(a/2)\lambda^2}\,,$$

where C_z is a constant to be determined.

3·2 – The equations for $\widetilde{K}_{N_0P_0}$ are:

$$(38)\qquad \left[\left(1-\frac{a\lambda^2}{2}\right)\frac{\partial}{\partial\lambda} - a\lambda(m_{\mathrm{V}}+2m_{\mathrm{N}})\frac{\partial}{\partial m_{\mathrm{V}}}\right]\widetilde{K}_{N_0P_0} = \mathscr{D}^{(\lambda)}\widetilde{K}_{N_0P_0} =$$
$$= Z_V^{\frac{1}{2}}\int d\xi\,\varrho^{\xi}\widetilde{K}\left(\begin{matrix} x_1 \dots x_{N_0} & \xi \\ y_1 \dots y_{N_0} & \xi \end{matrix}\middle|\, \xi\; t_1 \dots t_{P_0}\right),$$

$$(39)\qquad \frac{\partial\widetilde{K}_{N_0P_0}}{\partial m_{\mathrm{V}}} = -iZ_{\mathrm{V}}\int d\xi\,\tau_{\mathrm{V}}^{\xi}\widetilde{K}\left(\begin{matrix} \xi & x_1 \dots x_{N_0} \\ \xi & y_1 \dots y_{N_0} \end{matrix}\middle|\, t_1 \dots t_{P_0}\right),$$

$$(40)\qquad \frac{\partial\widetilde{K}_{N_0P_0}}{\partial(m_{\mathrm{K}}^2)} = -\frac{i}{2}\int d\xi\,\widetilde{K}\left(\begin{matrix} x_1 \dots x_{N_0} \\ y_1 \dots y_{N_0} \end{matrix}\middle|\, \xi\xi t_1 \dots t_{P_0}\right),$$

$$(41)\qquad \left[\frac{\partial}{\partial m_{\mathrm{N}}} - a\lambda^2\frac{\partial}{\partial m_{\mathrm{V}}}\right]\widetilde{K}_{N_0P_0} = \mathscr{D}^{(m_{\mathrm{N}})}\widetilde{K}_{N_0P_0} = -i\int d\xi\,\tau_{\mathrm{N}}^{\xi}\widetilde{K}\left(\begin{matrix} \xi & x_1 \dots x_{N_0} \\ \xi & y_1 \dots y_{N_0} \end{matrix}\middle|\, t_1 \dots t_{P_0}\right).$$

The Lie equations of the renormalization group (in which the role of parameter is played by the quantity a defined by (24), which can assume arbitrary values because it is changed by a finite amount by any alteration of the

prescription for the evaluation of finite-part integrals) are now immeditaely obtained by requiring that the change of variables

$$\bar{\lambda}_i = \bar{\lambda}_i(\lambda_j) \qquad (i, j = 1, \ldots, 4) \tag{42}$$

and of functions

$$\widetilde{K}_{N_1 P_0}(\lambda_i) = \bar{K}_{N_0 P_0}(\bar{\lambda}_i) \tag{43}$$

reduce the equations (38)–(41) to the form (14). They are:

$$\left\{\begin{array}{ll} \mathscr{D}^{(\lambda)}(\bar{\lambda}) = Z^{\frac{1}{2}}_{-\mathrm{V}}, & \mathscr{D}^{(\lambda)}(\overline{m}_{\mathrm{V}}) = \mathscr{D}^{(\lambda)}(\overline{m}_{\mathrm{N}}) = \mathscr{D}^{(\lambda)}(\overline{m}^2_{\mathrm{K}}) = 0\,, \\ \mathscr{D}^{(m_N)}(\overline{m}_{\mathrm{N}}) = 1\,, & \mathscr{D}^{(m_{\mathrm{N}})}(\bar{\lambda}) = \mathscr{D}^{(m_{\mathrm{N}})}(\overline{m}_{\mathrm{V}}) = \mathscr{D}^{(m_{\mathrm{N}})}(\overline{m}^2_{\mathrm{K}}) = 0\,, \\ \dfrac{\partial \overline{m}_{\mathrm{V}}}{\partial m_{\mathrm{V}}} = Z_{\mathrm{V}}; & \dfrac{\partial \bar{\lambda}}{\partial m_{\mathrm{V}}} = \dfrac{\partial \overline{m}_{\mathrm{N}}}{\partial m_{\mathrm{V}}} = \dfrac{\partial (\overline{m}^2_{\mathrm{K}})}{\partial m_{\mathrm{V}}} = 0\,, \\ \dfrac{\partial (\overline{m}^2_{\mathrm{K}})}{\partial (m^2_{\mathrm{K}})} = 1; & \dfrac{\partial \bar{\lambda}}{\partial (m^2_{\mathrm{K}})} = \dfrac{\partial \overline{m}_{\mathrm{V}}}{\partial (m^2_{\mathrm{K}})} = \dfrac{\partial \overline{m}_{\mathrm{N}}}{\partial (m^2_{\mathrm{K}})} = 0\,, \end{array}\right. \tag{44}$$

which are immediately seen to be compatible, and are solved by (reinstating g in place of λ (6))

$$\left\{\begin{array}{l} \overline{m}_{\mathrm{K}} = m_{\mathrm{K}} + c_{\mathrm{K}}; \qquad \overline{m}_{\mathrm{N}} = m_{\mathrm{N}} + c_{\mathrm{N}}\,, \\ \overline{m}_{\mathrm{V}} = c_z \dfrac{m_{\mathrm{V}} - a g^2 m_{\mathrm{N}}}{1 + (a/2) g^2} + c_{\mathrm{V}}\,, \\ \bar{g} \;\; = Z^{\frac{1}{2}} g + c_\lambda\,, \\ Z_{\mathrm{V}} = \dfrac{c_z}{1 + (a/2) g^2}\,. \end{array}\right. \tag{45}$$

The constants c_{K}, etc., can be determined by imposing that, in the limit $g \to 0$, the fields become free. This gives

$$\left\{\begin{array}{l} \overline{m}_{\mathrm{K}} = m_{\mathrm{K}}; \qquad \overline{m}_{\mathrm{N}} = m_{\mathrm{N}}; \\ \overline{m}_{\mathrm{V}} = \dfrac{m_{\mathrm{V}} - a g^2 m_{\mathrm{N}}}{1 + (a/2) g^2}\,, \\ \bar{g} \;\; = \dfrac{g}{\sqrt{1 + (a/2) g^2}}; \qquad Z_{\mathrm{V}} = \dfrac{1}{1 + (a/2) g^2}\,. \end{array}\right. \tag{46}$$

It is apparent from (24) that a is a real positive constant (divergent, in the transition from ordinary to finite-part integrals, if no cut-off is introduced).

We find thus the familiar result

$$0 \leqslant Z_V \leqslant 1\,, \qquad g^2 = \frac{\bar{g}^2}{1-(a/2)\bar{g}^2}\,. \tag{47}$$

A discussion of deeper points, which would take the lead from the rather remarkable mathematical properties of the Lie equations (44), would not be very profitable in the present case, which is too distant from situations of concrete interest; it is better postponed, therefore, until more realistic instances are treated with this method.

* * *

The first named author expresses his warm thanks to Prof. J. S. TOLL for his most kind hospitality at his Department.

RIASSUNTO

Viene studiata la rinormalizzazione nello spazio della configurazione di una leggera variante del modello di Lee, come esempio di applicazione di metodi generali (1) la cui validità sembra estendersi a casi assai più generali. La sostituzione di integrali ordinari con integrali a parte finita rimuove in modo consistente tutte le divergenze ultravioletti e permette di scrivere le equazioni di Lie del gruppo di rinormalizzazione, risolvendo le quali si trovano le note relazioni tra parametri non rinormalizzati e parametri rinormalizzati.

IL NUOVO CIMENTO Vol. XIX, N. 1 1° Gennaio 1961

The Effect of a Pion-Pion Interaction on Low-Energy Meson-Nucleon Scattering - II.

J. Bowcock, N. Cottingham and D. Lurié
CERN - Geneva

(ricevuto l'8 Settembre 1960)

Summary. — Using the formalism developed in a previous paper we investigated the consequences of a pion-pion interaction on low energy pion-nucleon phase shifts. By confining our considerations to the isotopic spin flip combination of waves we are able to isolate the effects due to a pion-pion interaction in the $T=1$ state. We find that such an interaction is definitely necessary to give agreement with experiment and that a simple resonance in the $J=1$, $T=1$ state gives a good fit to the data.

1. – Introduction.

In this paper we shall discuss the effect of a pion-pion interaction on some aspects of pion-nucleon scattering. We shall attempt in particular to answer the question of whether from the experimental data on pion-nucleon scattering one can find evidence for a pion-pion interaction in the $T=1$ state. We shall also investigate if a $J=1$, $T=1$ resonance between two pions is capable of giving a satisfactory fit to the data.

The formalism we shall use has already been developed in a previous paper (1) (which we shall refer to as I) and is a dispersion treatment based on the Cini-Fubini approximation to the Mandelstam representation (2). In the comparison of the results of this theory with the experimental phase shift we shall consider the isotopic spin-flip combination $(T=\frac{1}{2})-(T=\frac{3}{2})$ since this combination depends only on a π-π interaction in the $T=1$ state, being unaffected by π-π interactions in even parity states ($T=0, 2$). Furthermore it

(1) J. Bowcock, N. Cottingham and D. Lurié: *Nuovo Cimento*, **16**, 918 (1960).
(2) M. Cini and S. Fubini: *Ann. of Phys.*, **3**, 352 (1960).

is found that for this combination rescattering corrections are unimportant for the S-waves and for the P-waves with $J=\frac{1}{2}$. This is in distinction from the evaluation of the S and P wave phase shifts separately where the rescattering terms are rather important. A comparison of experimental D wave phase shifts with theory also yields good agreement when one takes into account D wave rescattering coming from the second π-$\mathcal{N}$ resonance located around 650 MeV.

In Section 2 we recall the representation derived in I for the four invariant amplitudes of π-$\mathcal{N}$ scattering. A comparison of theory with experimental S and P wave phase shifts follows in Section 3 while corrections due to rescattering are considered in Section 4, here also the results for the D waves are compared with the experimental data. An estimate of F waves is also given in this section. Finally we give a qualitative discussion to illustrate the assumptions of the theory.

2. – Representation for the invariant amplitudes.

We have shown in I that for low energies and momentum transfers the four invariant amplitudes $A^{(\pm)}$ and $B^{(\pm)}$ may be represented as follows

$$
(1)\quad \left\{
\begin{aligned}
A^{(+)}(s,\bar{s},t) &= \frac{1}{\pi}\int\limits_{(M+\mu)^2}^{\infty}\{\alpha_1^{(+)}(s')+t\alpha_2^{(+)}(s')\}\left\{\frac{1}{s'-s}+\frac{1}{s'-\bar{s}}\right\}+\frac{1}{\pi}\int\limits_{4\mu^2}^{\infty}\frac{\varrho^{(+)}(t')}{t'-t}+C_A^{(+)},\\
A^{(-)}(s,\bar{s},t) &= \frac{1}{\pi}\int\limits_{(M+\mu)^2}^{\infty}\mathrm{d}s'\{\alpha_1^{(-)}s')+t\alpha_2^{(-)}(s')\}\left\{\frac{1}{s'-s}-\frac{1}{s'-\bar{s}}\right\}+\\
&\qquad\qquad+\frac{(s-\bar{s})}{\pi}\int\limits_{4\mu^2}^{\infty}\mathrm{d}t'\,\frac{\varrho^{(+)}(t')}{t'-t},\\
B^{(+)}(s,\bar{s},t) &= g_r^2\left(\frac{1}{M^2-s}-\frac{1}{M^2-\bar{s}}\right)+\frac{1}{\pi}\int\limits_{(M+\mu)^2}^{\infty}\mathrm{d}s'\{\beta_1^{(+)}(s')+t\beta_2^{(+)}(s')\}\cdot\\
&\qquad\qquad\cdot\left\{\frac{1}{s'-s}-\frac{1}{s'-\bar{s}}\right\}+\frac{(s-\bar{s})}{\pi}\int\limits_{4\mu^2}^{\infty}\mathrm{d}t'\,\frac{\sigma^{(+)}(t')}{t'-t},\\
B^{(-)}(s,\bar{s},t) &= g_r^2\left(\frac{1}{M^2-s}+\frac{1}{M^2-\bar{s}}\right)+\frac{1}{\pi}\int\limits_{(M+\mu)^2}^{\infty}\mathrm{d}s'\{\beta_1^{(-)}(s')+t\beta_2^{(-)}(s')\}\cdot\\
&\qquad\qquad\cdot\left\{\frac{1}{s'-s}+\frac{1}{s'-\bar{s}}\right\}+\frac{1}{\pi}\int\limits_{4\mu^2}^{\infty}\mathrm{d}t'\,\frac{\sigma^{(-)}(t')}{t'-t}+C_B^{(-)}.
\end{aligned}
\right.
$$

143

The notation for the invariant amplitudes and kinematical variables is the same as in I. This representation (1) is relativistically invariant and satisfies crossing symmetry and one may further apply the unitarity condition to it as we shall see later. The weight functions α, β, ϱ, σ are all real and are given by the imaginary parts of the scattering amplitudes in the appropriate channels.

The representation gives explicit expressions not only for the pion-nucleon scattering amplitudes but also for the $\pi+\pi\to\mathcal{N}+\overline{\mathcal{N}}$ production amplitudes. To obtain the pion nucleon scattering amplitudes one multiplies the appropriate combination of invariant amplitudes by the corresponding Legendre function and integrates over $-1\leqslant\cos\theta\leqslant 1$, where θ is the scattering angle for pion-nucleon scattering. This has already been done in I. The resulting expressions for the partial wave scattering amplitudes (as functions of complex variables) have all the correct nearby singularities which agree for example with those deduced by HAMILTON and SPEARMAN [3] or FRAUTSCHI and WALECKA [4] who located the singularities directly from the Mandelstam representation.

To obtain the expression for the $\pi+\pi\to\mathcal{N}+\overline{\mathcal{N}}$ production amplitudes one must multiply the invariant functions by an appropriate combination of Legendre functions whose argument is $\cos\varphi$, the angle describing the production process, and integrate over this angle. Again one obtains partial wave production amplitudes possessing all the correct nearby singularities which are identical with those of FRAZER and FULCO [5]. The advantage of the representation presented here is that it gives a simple unified picture of the system of equations.

It is also simple to feed into this representation any experimental data or hypothesis concerning unavailable physical processes. We shall assume that for pion-nucleon scattering the (3, 3) resonance gives the only important contribution to our integrals although corrections to this assumption are discussed in Section **4**. We also suppose that the π-π scattering is dominated by a resonance in the $T=1$, $J=1$ state.

With these assumptions the spectral functions are given, with the notation of I, by

$$(2)\qquad \left\{\begin{aligned} \alpha_1^{(+)}(s') &= \frac{4\pi}{3}\left[\frac{3\,(W'+M)}{(E'+M)}+\frac{(W'-M)}{(E'-M)}\right]\frac{\sin^2\delta_{33}(q')}{q'}\,,\\ \alpha_2^{(+)}(s') &= 4\pi\left[\frac{W'+M}{E'+M}\right]\frac{1}{2q'^2}\,\frac{\sin^2\delta_{33}(q')}{q'}\,, \end{aligned}\right.$$

(3) J. HAMILTON and T. D. SPEARMAN: preprint.
(4) S. C. FRAUTSCHI and J. D. WALECKA: preprint.
(5) W. R. FRAZER ang J. R. FULCO: *Phys. Rev.*, **117**, 1603 (1960).

$$(2)\quad \begin{cases} \alpha_1^{(-)}(s') = -\frac{1}{2}\alpha_1^{(+)}(s')\,, \\ \alpha_2^{(-)}(s') = -\frac{1}{2}\alpha_2^{(+)}(s')\,, \\ \beta_1^{(+)}(s') = \dfrac{4\pi}{3}\left[\dfrac{3}{E'+M} - \dfrac{1}{E'-M}\right]\dfrac{\sin^2\delta_{33}(q')}{q'}\,, \\ \beta_2^{(+)}(s') = 4\pi\left[\dfrac{1}{E'+M}\right]\dfrac{1}{2q'^2}\,\dfrac{\sin^2\delta_{33}(q')}{q'}\,, \\ \beta_1^{(-)}(s') = -\frac{1}{2}\beta_1^{(+)}\,, \\ \beta_2^{(-)}(s') = -\frac{1}{2}\beta_2^{(+)}\,, \\ \varrho^{(-)}(t') = \dfrac{3\pi}{p'^2}\left(\dfrac{M}{\sqrt{2}}\,\mathrm{Im}\,f_-(t') - \mathrm{Im}\,f_+(t')\right), \\ \varrho^{(+)}(t') = 0\,, \\ \sigma^{(+)}(t') = 0\,, \\ \sigma^{(-)}(t') = \dfrac{12\pi}{\sqrt{2}}\,\mathrm{Im}\,f_-(t')\,. \end{cases}$$

The terms with the spectral functions represented by $\varrho^{(\pm)}$ and $\sigma^{(\pm)}$ which we call the « pion » terms represent the contribution of the pion-pion interaction. The fact that we put $\varrho^{(+)}(t') = \sigma^{(+)}(t') = 0$ means in fact that we set the pion interaction in the even J states equal to zero keeping only an interaction in the $J=1$ state. However, in this paper by restricting our discussion to the (—) states, which are affected only by a π-π interaction in the odd J states, our conclusions will be independent of any S, D, ... wave π-π scattering. Under the assumption of a narrow π-π resonance, $\varrho^{(-)}(t')$ and $\sigma^{(-)}(t')$ may be replaced by

$$(3)\quad \begin{cases} \varrho^{(-)}(t') = 6\pi^2 C_2\,\delta(t_r - t')\,, \\ \sigma^{(-)}(t') = -12\pi^2[C_1 + 2MC_2]\,\delta(t_r - t')\,, \end{cases}$$

where t_r is the square of the π-π resonance energy and C_1, C_2 are constants that were introduced in I. In I we have obtained the following values for t_r and the ratio C_2/C_1 by fitting the experimental data on the isovector part of the nucleon form factors

$$(4)\quad t_r = 22.4\mu^2\,, \qquad \frac{C_2}{C_1} = \frac{g_p - g_n}{2M} = .27\mu^{-1}\,,$$

where g_p, g_n are the gyromagnetic ratios of proton and neutron.

Assuming also a narrow width for the (3, 3) resonance we may write

$$(5)\quad \sin^2\delta_{33}(q') = \tfrac{4}{3}f^2 q_r^3\pi\,\delta(\omega_r - \omega')\,.$$

For the $\pi+\mathcal{N}\to\pi+\mathcal{N}$ channel if one makes the above assumptions and sets the π-π interaction equal to zero (and therefore, $\varrho^{(-)}=\sigma^{(-)}=0$) one obtains a set of equations for the partial wave amplitudes which reduce in the static limit to these obtained by CGLN [6].

3. – s and p waves.

S waves: $C_A^{(+)}$, $C_B^{(-)}$, and C_1 are parameters of our theory which must be determined from experiment. If we confine ourselves to the isotopic spin-flip amplitude $A^{(-)}$ and $B^{(-)}$, *i.e.* the $(T=\frac{1}{2})-(T=\frac{3}{2})$ combination of amplitudes, our results are independent of $C_A^{(+)}$. From our representation, (1) we obtain the following expressions for the s-wave isotopic spin-flip amplitude, (eq. (5.7), (5.1) and (5.14) of I),

$$f_s^{(\frac{1}{2})}-f_s^{(\frac{3}{2})}=-\frac{9}{2}\frac{M}{W}\frac{\omega}{2q^2}C_1\log\left(1+\frac{4q^2}{t_r}\right)+b\omega\,, \tag{6}$$

where b is given by

$$b=\frac{C_B^{(-)}}{4\pi}+\frac{2}{9}f^2\,. \tag{7}$$

If our representation for the s-wave scattering amplitudes is valid up to medium energies (say 400 MeV) then, by unitarity, we should expect b to be small since $q\omega$ increases rapidly with energy and

$$q(f_s^{(\frac{1}{2})}-f_s^{(\frac{3}{2})})=\frac{\sin 2\alpha_1-\sin 2\alpha_3}{2}<1\,.$$

This is borne out by fitting the experimental s-wave data as is shown in Fig. 1.

We see that in order to fit the threshold value and the high energy points, $C_1\sim-1.0$ and $b\sim.1$. To fit the points around $q=1.5$, on the other hand, both C_1 and $|b|$ must be rather large as is illustrated by the curve with $C_1=-1.54$. Such large a value of C_1 however is inconsistent with the P- and D-wave data as will be shown later.

A reasonable fit can be obtained by setting $|b|=0$ and $C_1=-1.0$. On the other hand, a value of $C_1=0$ is clearly excluded, implying that a π-π interaction in the $T=1$ state is a necessary if one wishes to explain the s-wave phase shifts.

---

(6) G. Chew, M. Goldberger, F. Low and Y. Nambu: *Phys. Rev.*, **106**, 1337 (1957).

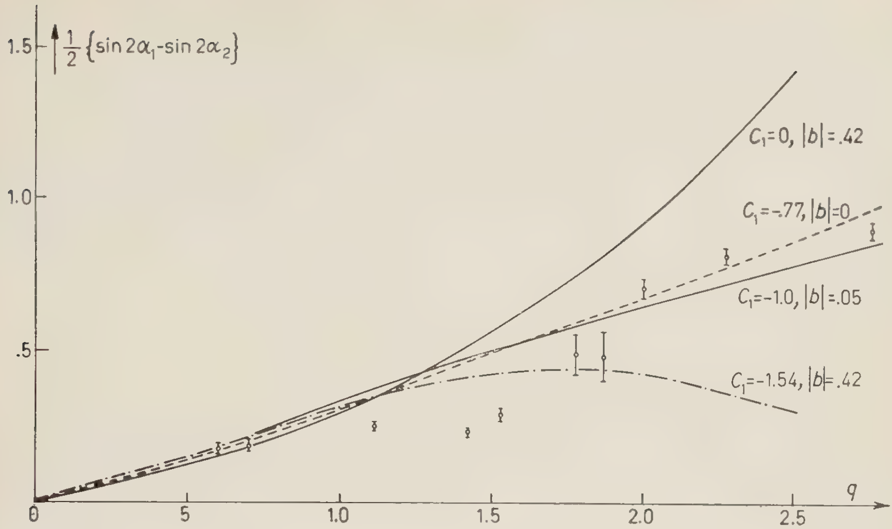

Fig. 1. – S-waves. For several values of C_1 and α we plot the theoretical curves for the isotopic spin flip S-waves. Experimental points from references ([7-9]).

P waves: If we now consider P-waves, $C_B^{(-)}$ does not contribute as was pointed out in I. Taking $C_1 = -1.0$ the contributions of the pion and nucleon terms are given in Fig. 2. A very satisfactory fit to the data is obtained

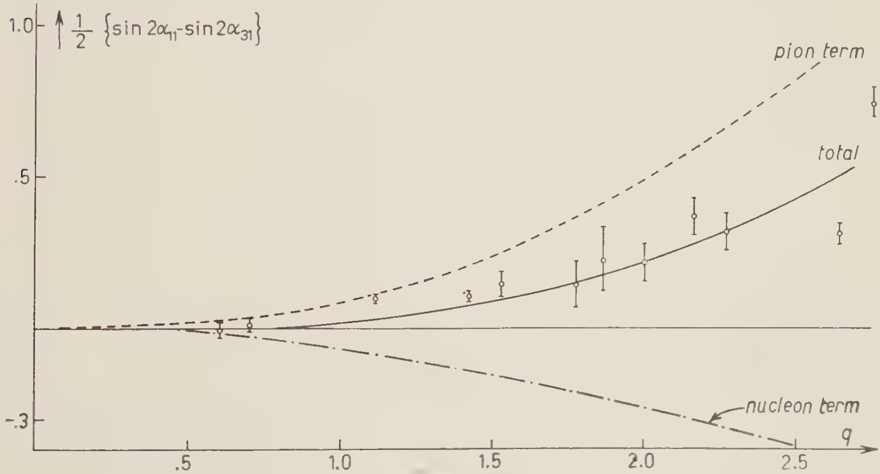

Fig. 2. – P-waves. The nucleon term is plotted together with the pion term for $C_1 = -1.0$. The total is also shown. Experimental points from references ([7-9]).

([7]) *Annual International Conference on High Energy Physics* (1958-1959).
([8]) A. Stanghellini: *Nuovo Cimento*, **10**, 398 (1958).
([9]) W. D. Walker, J. Davis and W. D. Shephard: *Phys. Rev.*, **118**, 1612 (1960).

with this value of C_1. Again we find here definite evidence for a π-π interaction since the nucleon term by itself even has the wrong sign. It can be seen moreover that a value of C_1 twice as large would lead to a poor fit.

For the $J=\frac{3}{2}$ P-wave amplitudes the pion term is considerably smaller than for the $J=\frac{1}{2}$ ones. Furthermore, the principal value integration involved in calculating the p_{33} resonance rescattering term renders comparison with experiment difficult in this case. We feel however that no essential deviation from the usual effective range approximation has to be expected.

4. – Rescattering corrections and higher waves.

Let us now consider the possible corrections to the theoretical curves given in the preceding section. In writing down expressions for the S- and P-waves we have taken the static limit both for simplicity and because of the large errors on the experimental phase shifts at higher energies. The realtivistic corrections to this limit could, however, be taken into account in a straightforward way. As calculated by HAMILTON and SPEARMAN, the relativitic corrections to the nucleon terms for S-waves are fairly small and a rough estimate of the corrections to the pion terms seems to indicate that up to energies of the order of 400 MeV, relativistic corrections will in general be less than 20%.

A more important correction, on the other hand, arises when one takes into account the absorptive parts of partial waves other than f_{33}. If one includes this rescattering but neglects crossed terms owing to the large size of the denominators one is led to integral equations for each amplitude $f_{l\pm}$ of the type

$$f_{l\pm} = f^0_{l\pm} + \frac{q^{2l}}{\pi} P\int_1^\infty \frac{\sin^2 \delta_{l\pm}(\omega')}{q'^{2l+1}(\omega'-\omega)}\, d\omega' \tag{8}$$

Here $f^0_{l\pm}$ is the sum of the nucleon and pion terms plus terms in $C_A^{(+)}$ and $C_B^{(+)}$ for S-waves. The best treatment of these equations would be to attempt to solve them as integral equations (for example by means of the N/D method). and such a programme is at present under consideration. Here we shall adopt the alternative procedure and evaluate the rescattering terms in eq. (9) using the experimental value for the phase shifts. HAMILTON and SPEARMAN have evaluated these terms for values of ω up to approximately 100 MeV. Although the rescattering corrections to the individual partial waves are large, the correction to the difference $f_s^{\frac{1}{2}} - f_s^{\frac{3}{2}}$ which is given by

$$\frac{1}{\pi} P\int_1^\infty \frac{\sin^2 \alpha_1 - \sin^2 \alpha_3}{q'(\omega'-\omega)}\, d\omega',$$

is only 10% of the total curve, owing to the near equality of the magnitudes of the two phase shifts. As this near equality persists at higher energies we expect that the rescattering correction to $f_s^{\frac12} - f_s^{\frac32}$ will remain small for values of $w > 100$ MeV.

For the $J = \frac12$ P-waves a similar situation occurs and a rough estimate again gives corrections to the isotopic spin-flip combination $f_{11} - f_{31}$ of the order of 10%.

D waves: The experimental information at present available concerning D waves is given in Table I.

TABLE I.

T_π (MeV)	q	D_{13}	D_{15}	D_{33}	D_{35}
310	2.175	—	—	2.4	-5.0
370	2.417	4.5^{+2}_{-0}	-1.6 ± 1	2.5	-3.0
430	2.645	7.1^{+2}_{-1}	-1.6 ± 1	2.5	-3.0
460	2.754	18.5 ± 2	-5.0 ± 1	$2.8\pm.7$	-3.7 ± 1
600	3.227	18.3^{+35}_{-0}	-5.6 ± 2	3.5^{+0}_{-3}	-3.3^{+2}_{-0}

If we consider $f^{(\frac12)}_{D\frac32} - f^{(\frac32)}_{D\frac32}$ we find that, as for the P waves, the nucleon term by itself gives a contribution of the wrong sign and that a π-π interaction is definitely needed to fit experiment. Because of the 600 MeV resonance in the D_{13} wave the rescattering correction is in this case sizeable and with its inclusion we are able to fit the data with the same C_1 as for the S waves *i.e.* $C_1 = -1.0$. The corresponding curves are shown in Fig. 3.

$$f^{(\frac12)}_{D\frac52} - f^{(\frac32)}_{D\frac52}$$

is almost zero experimentally and any attempt to fit the data would depend on a good evaluation of the nucleon term in this energy region, which we feel we are not able to make.

F waves: Experimentally there seems to be evidence for the resonance around 900 MeV to be in the $F^{\frac12}_{\frac52}$ wave and although there are no F wave phase shifts with which to compare our theory we might hope to be able to show that the theory gives the right conditions for a resonance to occur in that state. This is indeed so. The expressions for the F waves from the nucleon

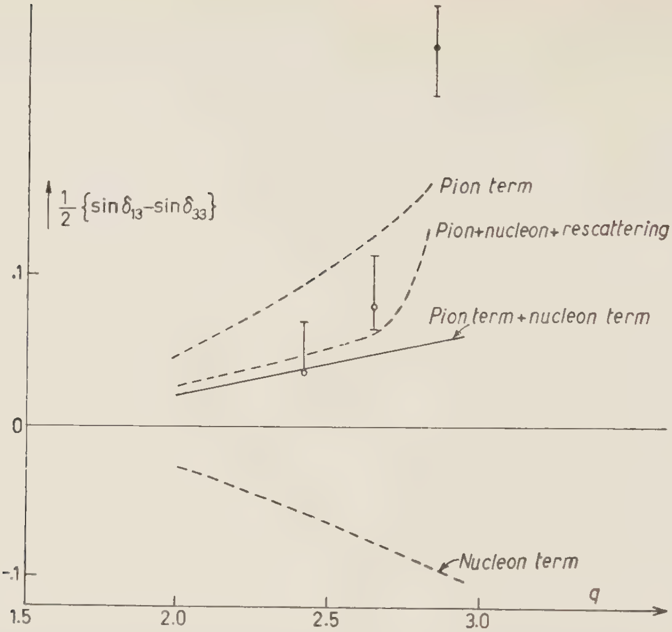

Fig. 3. – D-waves. The nucleon and pion (C_1 = – 1.0) terms are plotted together with the total and the total corrected for rescattering. Experimental points from ref. (9).

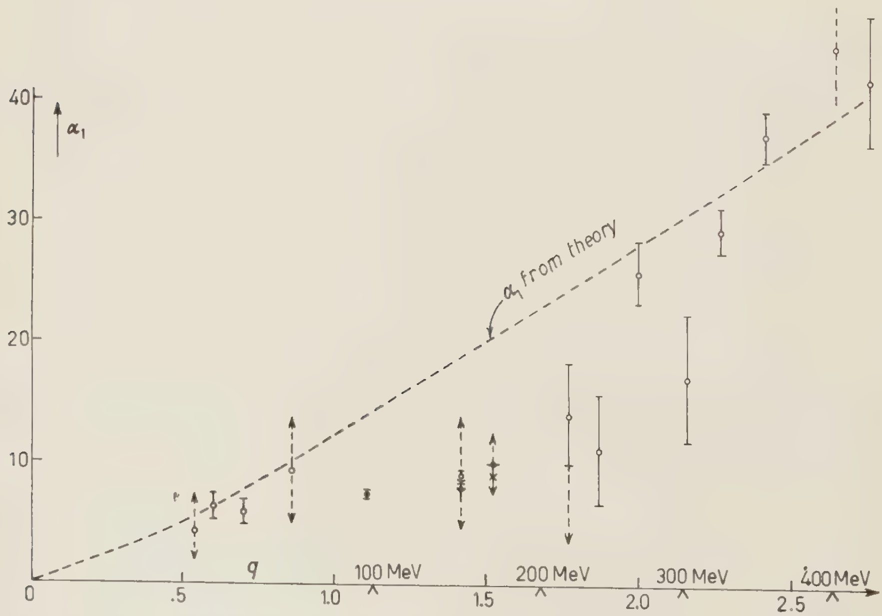

Fig. 4. – Taking ($\sin 2\alpha_1 - \sin 2\alpha_3$) from theory and α_3 from experiment α_1 is plotted. Experimental points from references (7-9).

term may be written

$$
\text{(9)} \qquad \left\{
\begin{aligned}
\delta^{\frac{1}{2}}_{F\frac{5}{2}} &= \lambda_F \left[2 + \frac{320}{9}\left(\frac{\omega}{\omega_r + \omega}\right)^3\right], \\
\delta^{\frac{3}{2}}_{F\frac{5}{2}} &= -\,\lambda_F \left[1 - \frac{80}{9}\left(\frac{\omega}{\omega_r + \omega}\right)^3\right], \\
\delta^{\frac{1}{2}}_{F\frac{7}{2}} &= -\,\lambda_F \left[12 - \frac{32}{3}\left(\frac{\omega}{\omega_r + \omega}\right)^3\right], \\
\delta^{\frac{3}{2}}_{F\frac{7}{2}} &= \lambda_F \left[6 + \frac{8}{3}\left(\frac{\omega}{\omega_r + \omega}\right)^3\right],
\end{aligned}
\right.
$$

with

$$
\text{(10)} \qquad \lambda_F = \frac{1}{105}\,\frac{f^2}{M^2}\,\frac{q^7}{\omega^3},
$$

and the pion terms

$$
\text{(11)} \qquad \left\{
\begin{aligned}
\delta^{\pi\pi}_{\frac{5}{2}}\begin{pmatrix} T=\frac{1}{2} \\ T=\frac{3}{2}\end{pmatrix} &= -\frac{3}{4}\begin{pmatrix} 2 \\ -1 \end{pmatrix}\frac{M}{W}\,\frac{q}{t_r}\left[\omega C_1(5F_3 - 3F_1) + q^2 C_2'(-5F_4 + 6F_2 - F_0)\right], \\
\delta^{\pi\pi}_{\frac{7}{2}}\begin{pmatrix} T=\frac{1}{2} \\ T=\frac{3}{2}\end{pmatrix} &= -\frac{3}{4}\begin{pmatrix} 2 \\ -1 \end{pmatrix}\frac{M}{W}\,\frac{q}{t_r}\left[\omega C_1(5F_3 - 3F_1) - \frac{3}{4}\,q^2 C_2'(-5F_4 + 6F_2 - F_0)\right].
\end{aligned}
\right.
$$

The pion-pion interaction gives its largest contribution to $f^{\frac{1}{2}}_{\frac{5}{2}}$ and this contribution is positive. The integral equation (8) for $f^{\frac{1}{2}}_{\frac{5}{2}}$ therefore has a relatively large positive inhomogeneous term. This is known to be an indication that a resonance will be formed in that state.

5. – Discussion.

We have seen in the preceding sections that experiments on pion nucleon scattering show definitely the existence of a pion-pion interaction in the $T=1$ state. Moreover we have shown that a simple resonance in the $J=1$, $T=1$ state is sufficient to give a rather good fit to the experimental data considered. The width at half maximum of this resonance (with $C_1 = -1.0$) is $.8\mu$, corresponding to a value $\gamma = .4\mu^{-1}$ in eq. (4.16) of I.

The fact that out curve does not pass through the experimental S-wave points in Fig. 1 around $q = 1.5$ might be due either to an oversimplification of the pion-pion interaction or to a deficiency of the experimental data.

Although α_3 may be well determined by doing π^+p scattering, α_1 must be determined by doing π^-p scattering where the isotopic spin states are mixed and is therefore subject to more uncertainty. Experiments with good statistics and a careful phase shift analysis in this region would be extremely useful to clear up this point.

If one also wishes to look in a similar manner for evidence of a pion-pion interaction in even J states the appropriate combination of pion-nucleon isotopic spin in the (+) state *i.e.* $(T=\frac{1}{2})+2(T=\frac{3}{2})$. Here one is immediately confronted with the problem of a reliable determination of the rescattering corrections which in this case add together instead of cancelling as for the (—) states. This is a difficult task since the corrections are principal value integrals over experimental phase shifts with appreciable errors. A more hopeful procedure is to attempt to solve the integral equations indicated in eq. (9). However, HAMILTON and SPEARMAN have estimated the rescattering corrections to S waves up to 110 MeV where the phase shifts are known rather well and their results indicate the presence of a π-π interaction in even states also.

The physical meaning of the assumption of our theory may seem clearer if one realizes that a pion-pion resonance with a narrow width may be regarded as a particle whose mass is just given by the total energy of the resonating system. Since the range of the force between scattering particles is inversely proportional to the mass of the exchanged particle we have the picture of the incoming pion interacting with the cloud of pions surrounding the nucleon and giving rise to a force whose range is longer than the force due to the interacton of the pion with the nucleon core.

One interesting feature of the pion term is that it depends strongly only on the momentum transfer t, a feature reminiscent of the inhomogeneous term in the Mandelstam representation for potential scattering. If one tries to interpret the pion-nucleon interaction in terms of a potential one finds that the nucleon terms do not correspond to a local potential but to a non-local short-range potential. Identifying the pion term with a potential gives a spin-orbit potential which is twice as deep for $T=\frac{1}{2}$ states as for $T=\frac{3}{2}$. Also those states in which the spin and orbital angular momenta are antiparallel experience the strongest attraction. This is in agreement with the P_{11} phase shift which is quite strongly positive although the nucleon terms alone predict P_{11} to be four times as strongy negative as P_{13} or P_{31}, both of which are negative. It is also in qualitative agreement with the higher π-N resonances if these are interpreted as $T=\frac{1}{2}$, $D_{\frac{3}{2}}$ and $F_{\frac{5}{2}}$.

* * *

We wish to thank Professor S. FUBINI for many fruitful discussions and for his continual encouragement during the course of this work.

We are also grateful to Dr. I. DERADO, Dr. VAN DE WALLE and Dr. PELLEGRINI for useful advice regarding experimental data.

RIASSUNTO (*)

Usando il formalismo sviluppato in un lavoro precedente abbiamo esaminato le conseguenze di una interazione pione-pione sugli spostamenti di fase pione-nucleone a bassa energia. Limitando le nostre considerazioni alle combinazioni isotopiche di spin flip delle onde possiamo isolare gli effetti dovuti ad una interazione pione-pione nello stato $T=1$. Troviamo che tale interazione è definitivamente necessaria per avere un accordo con gli esperimenti e che una risonanza semplice nello stato $J=1$, $T=1$ dà una buona concordanza con i dati.

(*) *Traduzione a cura della Redazione.*

IL NUOVO CIMENTO Vol. XIX, N. 1 1° Gennaio 1961

Field Theories with «Superconductor» Solutions.

J. Goldstone

CERN - Geneva

(ricevuto l'8 Settembre 1960)

Summary. — The conditions for the existence of non-perturbative type « superconductor » solutions of field theories are examined. A non-covariant canonical transformation method is used to find such solutions for a theory of a fermion interacting with a pseudoscalar boson. A covariant renormalisable method using Feynman integrals is then given. A « superconductor » solution is found whenever in the normal perturbative-type solution the boson mass squared is negative and the coupling constants satisfy certain inequalities. The symmetry properties of such solutions are examined with the aid of a simple model of self-interacting boson fields. The solutions have lower symmetry than the Lagrangian, and contain mass zero bosons.

1. – Introduction.

This paper reports some work on the possible existence of field theories with solutions analogous to the Bardeen model of a superconductor. This possibility has been discussed by Nambu (1) in a report which presents the general ideas of the theory which will not be repeated here. The present work merely considers models and has no direct physical applications but the nature of these theories seems worthwhile exploring.

The models considered here all have a boson field in them from the beginning. It would be more desirable to construct bosons out of fermions and this type of theory does contain that possibility (1). The theories of this paper have the dubious advantage of being renormalisable, which at least allows one to find simple conditions in finite terms for the existence of « supercon-

(1) Y. Nambu: Enrico Fermi Institute for Nuclear Studies, Chicago, Report 60-21.

ducting » solutions. It also appears that in fact many features of these solutions can be found in very simple models with only boson fields, in which the analogy to the Bardeen theory has almost disappeared. In all these theories the relation between the boson field and the actual particles is more indirect than in the usual perturbation type solutions of field theory.

2. – Non-covariant theory.

The first model has a single fermion interacting with a single pseudoscalar boson field with the Lagrangian

$$L = \overline{\psi}\left(i\gamma^\mu \frac{\partial\psi}{\partial x^\mu} - m\psi\right) + \frac{1}{2}\left(\frac{\partial\varphi}{\partial x^\mu}\frac{\partial\varphi}{\partial x_\mu} - \mu_0^2\varphi^2\right) - g_0\overline{\psi}\gamma^5\psi\varphi - \frac{1}{24}\lambda_0\varphi^4 .$$

(The last term is necessary to obtain finite results, as in perturbation theory.) The new solutions can be found by a non-covariant calculation which perhaps may show more clearly what is happening than the covariant theory which follows.

Let $\varphi(\boldsymbol{x}) = (1/\sqrt{V})\sum q_k \exp[i\boldsymbol{k}\cdot\boldsymbol{x}]$ and let p_k be the conjugate momentum to $q_{\boldsymbol{k}}$. Let $a^\dagger_{k\sigma}$, $b^\dagger_{k\sigma}$ be the creation operators for Fermi particles of momentum $\boldsymbol{k}$ spin σ and antiparticles of momentum $-\boldsymbol{k}$, spin $-\sigma$ respectively. Retain only the mode $\boldsymbol{k} = 0$ of the boson field in the Hamiltonian. (The significance of this approximation appears below.) Then

$$\begin{aligned} H &= H_F + H_B + H_I , \\ H_F &= \sum_i E_i(a_i^\dagger a_i + b_i^\dagger b_i) , \end{aligned} \tag{1}$$

(k, σ is replaced by a single symbol i)

$$\begin{aligned} H_B &= \tfrac{1}{2}(p_0^2 + \mu_0^2 q_0^2) , \\ H_I &= \frac{g_0}{\sqrt{V}}\, q_0 \sum_i (a_i^\dagger b_i^\dagger + b_i a_i) + \frac{\lambda_0}{24V}\, q_0^4 . \end{aligned}$$

When H_I is treated as a perturbation, its only finite effects are to alter the boson mass and to scatter fermion pairs of zero total momentum. These effects can be calculated exactly (when $V \to \infty$) by writing $a_i^\dagger b_i^\dagger = c_i^\dagger$ and treating $c_i^\dagger$ as a boson creation operator (2). The Hamiltonian becomes

$$H' = \sum 2E_i c_i^\dagger c_i + \frac{1}{2}(p_0^2 + \mu_0^2 q_0^2) + \frac{g_0}{\sqrt{V}}\, q_0 \sum (c_i^\dagger + c_i) .$$

---

(2) N. N. Bogoliubov: *Žurn. Èksp. Teor. Fiz.*, **34**, 73 (1958); *Sov. Phys. J.E.T.P.*, **7**, 51 (1958).

The $(1/V)q_0^4$ terms has no finite effects. Let

$$\frac{c_i^\dagger + c_i}{\sqrt{4E_i}} = q_i; \qquad i\sqrt{E}(c_i^\dagger - c_i) = p_i \,,$$

then

$$H' = \frac{1}{2}(p_0^2 + \mu_0^2 q_0^2) + \sum_i \frac{1}{2}(p_i^2 + 4E_i^2 q_i^2) + \frac{g_0}{\sqrt{V}} q_0 \sum_i \sqrt{4E_i}\, q_i - \sum_i E_i \,.$$

H' represents a set of coupled oscillators and is easily diagonalized. The frequencies of the normal modes are ω_0, ω_i, given by the roots of the equation

$$\mu_0^2 - \omega^2 = \frac{g_0^2}{V} \sum_i \frac{4E_i}{4E_i^2 - \omega^2} \,.$$

In the limit as $V \to \infty$, this becomes

$$\text{(2)} \qquad \mu_0^2 - \omega^2 = \frac{2g_0^2}{(2\pi)^3} \int \frac{4E_k}{4E_k^2 - \omega^2}\, \mathrm{d}^3\boldsymbol{k} = \frac{2g_0^2}{(2\pi)^3} \int \mathrm{d}^3\boldsymbol{k} \left\{ \frac{1}{E_k} + \frac{\omega^2}{4E_k^3} + \frac{\omega^4}{4E_k^3(4E_k^2 - \omega^2)} \right\} .$$

The first two terms in the integral diverge. This procedure corresponds exactly to the covariant procedure of calculating the poles of the boson propagator

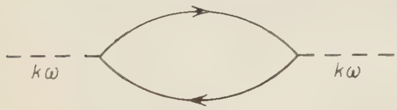

Fig. 1.

$$D(k, \omega) = \frac{1}{\omega^2 - k^2 - \mu_0^2 - \Pi(k, \omega)} \,,$$

and including in Π only the lowest polarization part shown in Fig. 1.

This comparison shows that the two divergent terms can be absorbed into the renormalized mass and coupling constant. The renormalization is carried out at the point $k_\mu = 0$ instead of as usual at the one-boson pole of D. Thus if

$$\Pi(0, \omega) = A + B\omega^2 + g_0^2 \Pi_1(\omega^2) \,,$$

then

$$D(0, \omega) = \frac{Z}{\omega^2 - \mu_1^2 - g_1^2 \Pi_1(\omega^2)} \,,$$

$$Z = \frac{1}{1 - B} \,, \qquad \frac{\mu_1^2}{Z} = \mu_0^2 - A \,, \qquad g_1^2 = \frac{g_0^2}{Z} \,.$$

Equation (2) becomes

$$\mu_1^2 - \omega^2 = \frac{2g_1^2}{(2\pi)^3}\, \omega^4 \int \frac{\mathrm{d}^3\boldsymbol{k}}{4E_k^3(4E_k^2 - \omega^2)} = F(\omega^2) \,.$$

The isolated root of this equation, ω_0^2, is found as shown in Fig. 2. When $\mu_1^2 > 0$, ω_0^2 is the square of the physical boson mass. When $\mu_1^2 \sim 4m^2$, this root disappears. This is the case when the boson can decay into a fermion pair. There is always another root for ω^2 large and negative. This corresponds to the well-known « ghost » difficulties and will be ignored here. When $\mu_1^2 < 0$ (but not too large), there is a negative root for ω^2. This is usually taken to mean simply that the theory with $\mu_1^2 < 0$ does not exist. Here it is taken to indicate that the approximation used is wrong and that the Hamiltonian (1) must be investigated further.

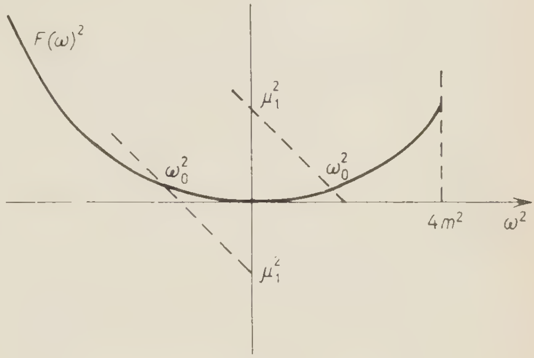

Fig. 2.

This is done by a series of canonical transformations based on the idea that in the vacuum state the expectation value of the boson field is not zero. Let

$$q_0 = q_0' + \frac{\Delta}{g_0}\sqrt{V}, \qquad p_0 = p_0',$$

Δ is a parameter to be fixed later. Also make a Bogoliubov transformation on the fermion field

$$a_i = \cos\frac{\theta_i}{2}\,\alpha_i - \sin\frac{\theta_i}{2}\,\beta_i^\dagger,$$

$$b_i = \sin\frac{\theta_i}{2}\,\alpha_i^\dagger + \cos\frac{\theta_i}{2}\,\beta_i,$$

$$\operatorname{tg}\theta_i = \frac{\Delta}{E_i}.$$

Then

$$H = H_0 + H_1 + H_2 + H_3,$$

$$H_0 = -\sum_i\left(\sqrt{E_i^2+\Delta^2} - E_i\right) + \frac{\mu_0^2}{2}\frac{\Delta^2}{g_0^2}V + \frac{\lambda_0}{24}\frac{\Delta^4}{g_0^4}V,$$

$$H_1 = q_0'\sqrt{V}\left\{\mu_0^2\frac{\Delta}{g_0} + \frac{\lambda_0}{6}\frac{\Delta^3}{g_0^3} - \frac{g_0}{V}\sum_i\frac{\Delta}{\sqrt{E_i^2+\Delta^2}}\right\},$$

$$H_2 = \frac{1}{2} p_0'^2 + \frac{1}{2} q_0'^2 \left(\mu_0^2 + \frac{\lambda_0}{2}\frac{\Delta^2}{g_0^2}\right) + \sum_i \sqrt{E_i^2 + \Delta^2}\,(\alpha_i^\dagger \alpha_i + \beta_i^\dagger \beta_i) + \\ + \frac{g_0}{\sqrt{V}} q_0' \sum_i \frac{E_i}{\sqrt{E_i^2 + \Delta^2}} (\alpha_i^\dagger \beta_i^\dagger + \beta_i \alpha_i)\,,$$

$$H_3 = \frac{\lambda_0}{24V} q_0'^4 + \frac{\lambda_0}{6}\frac{\Delta}{g_0}\frac{1}{\sqrt{V}} q_0'^3 + \frac{g_0}{\sqrt{V}} q_0' \sum_i \frac{\Delta}{\sqrt{E_i^2 + \Delta^2}} (\alpha_i^\dagger \alpha_i + \beta_i^\dagger \beta_i)\,.$$

Now choose Δ so that $H_1 = 0$. H_0 is just a constant proportional to V and H_3 has no finite effects. This leaves H_2, which can be diagonalised by the method used above for the original Hamiltonian (1).

One solution of $H_1 = 0$ is $\Delta = 0$. This gives the original approximation, which is no use when $\mu_1^2 < 0$. Other solutions are given by

$$(3) \qquad \mu_0^2 + \frac{1}{6}\lambda_0 \frac{\Delta^2}{g_0^2} = \frac{g_0^2}{V}\sum_i \frac{1}{\sqrt{E_i^2 + \Delta^2}} = \frac{2 g_0^2}{(2\pi)^3}\int \mathrm{d}^3\boldsymbol{k} \left\{\frac{1}{E_k} - \frac{\Delta^2}{2E_k^3}\right\} + g_0^2 G(\Delta^2)\,,$$

where G is a finite function. Let

$$\mu_0^2 - \frac{2g_0^2}{(2\pi)^3}\int \frac{\mathrm{d}^3\boldsymbol{k}}{E_k} = \frac{\mu_1^2}{Z}\,,$$

$$\lambda_0 + \frac{6 g_0^4}{(2\pi)^3}\int \frac{\mathrm{d}^3\boldsymbol{k}}{E_k^3} = \frac{\lambda_1}{Z^2}\,, \qquad g_0^2 = \frac{g_1^2}{Z}\,,$$

μ_1^2, λ_1, Z can be identified as the lowest order perturbation theoretic values of the renormalized boson mass, four-boson interaction constant and wave function renormalization, arising from the graphs in Fig. 1 and 3.

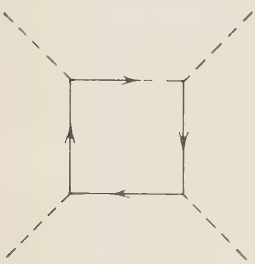

Fig. 3.

As before, the renormalizations are carried out at $k_\mu = 0$. Equation (3) becomes

$$(4) \qquad \mu_1^2 + \frac{1}{6}\lambda_1 \frac{\Delta^2}{g_1^2} = g_1^2 G(\Delta^2)\,,$$

Thus an equation for Δ^2 is obtained which is finite in terms of constants which would be the renormalized parameters of the theory in the ordinary solution. It will be shown below that when $\mu_1^2 < 0$, equation (4) has solutions for a certain range of λ_1, and that then there does exist a real boson.

3. – Covariant theory.

A first approach to a covariant theory can be made by calculating the fermion Green's function in a self-consistent field approximation. In perturbation theory the term represented by Fig. 4 vanishes by reflection invariance.

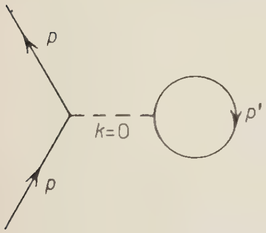

Fig. 4.

However, suppose it gives a contribution $\gamma_5 \Delta$ to the fermion self-energy. Then

$$S(p) = \frac{1}{\gamma_\mu p^\mu - m - \gamma_5 \Delta},$$

and evaluating Fig. 4 with this value of S gives

$$\Delta = -\frac{1}{\mu_0^2}\frac{g_0^2}{(2\pi)^4 i}\int \mathrm{d}^4 p \,\mathrm{Tr}\,\gamma_5 \frac{1}{\gamma_\mu p^\mu - m - \gamma_5 \Delta} = -\frac{4g_0^2}{\mu_0^2}\frac{1}{(2\pi)^4 i}\int \mathrm{d}^4 p \,\frac{\Delta}{p^2 - m^2 - \Delta^2},$$

which is the same as equation (3) without the λ term, and again has the perturbation solution $\Delta = 0$ and possibly other solutions.

A general covariant theory can be found by using the Feynman integral technique. This gives an explicit formula for the fermion Green's function

$$S(x', x) = \frac{\int S(x', x; \varphi)\exp[-iW(\varphi)]\exp[i\int L_M(\varphi)\,\mathrm{d}^4x]\,\delta\varphi}{\int \exp[-iW(\varphi)]\exp[i\int L_M(\varphi)\,\mathrm{d}^4x]\,\delta\varphi}.$$

Here $S(x'x\varphi)$ is the fermion Green's function calculated in an external boson field φ (and without interacting bosons). $\mathrm{Exp}[-iW(\varphi)]$ is the vacuum-vacuum S-matrix amplitude in an external field and $L_M(\varphi)$ is the boson part of the Lagrangian. The integration are carried out over all fields $\varphi(\boldsymbol{x}, t)$.

Let

$$\varphi(\boldsymbol{x}t) = \frac{1}{\Omega}\sum_k \varphi_k \exp[ikx],$$

where k is now a 4-vector and Ω a large space-time volume. To obtain the Bardeen-type solutions, first do all the integrations except that over φ_0 (this has $\boldsymbol{k} = \omega = 0$) and put $\varphi_0 = \Omega\chi$ (χ finite). Then

$$S(x', x) = \frac{\int S(x', x; \chi)\exp[-i\Omega F(\chi)]\,\mathrm{d}\chi}{\int \exp[-i\Omega F(\chi)]\,\mathrm{d}\chi},$$

$$F(\chi) = w(\chi) + \frac{\mu_0^2}{2}\chi^2 + \frac{\lambda_0}{24}\chi^4,$$

S is the one particle Green's function calculated in a constant external field $\varphi(x)=\chi$ and including all the interacting boson degrees of freedom except $\boldsymbol{k}=\omega=0$. Exp $[-i\Omega w]$ is the vacuum-vacuum amplitude calculated in the same way. The idea is to look for stationary points of $F(\chi)$ other than $\chi=0$. If $F'(\chi_1)=0$, then in the limit $\Omega\to\infty$, $S(x'x)=S(x'x\chi_1)$.

$-i\Omega w(\chi)$ is given by the sum of all connected vacuum diagrams. It is easy to see that

$$w(\chi)=\sum_{n=0}^{\infty}V_{2n}\frac{\chi^{2n}}{2n!},$$

where V_{2n} is the perturbation theory value of the $2n$-boson vertex with all external momenta zero. For example $V_2=\Pi(0)$. In perturbation theory, $V_{2n}=V^{(r)}_{2n}/Z^n$ where $\sqrt{Z}$ is the boson wave function renormalization, and $V^{(r)}_{2n}$ is finite provided the terms μ_0^2 and λ_0 are absorbed into V_2 and V_4. As before, the renormalizations are carried out at $k=0$. Thus if

$$\chi=\sqrt{Z}\chi^{(r)},\qquad\text{then}\qquad F(\chi^{(r)})=\sum\frac{V^{(r)}_{2n}}{2n!}\chi^{(r)2n},$$

an expression from which all the divergences have been removed. It also follows that if $F'(\chi_1^{(r)})=0$, the new values for the vertex parameters V_n are given by

$$V'_n=\frac{\partial^n}{\partial\chi_1^{(r)n}}F(\chi_1^{(r)}).$$

In particular the new boson mass is given by

$$\mu^2=F''(\chi_1^{(r)}).$$

(This is really the mass operator at $k=0$, not the mass.) Thus one condition for the existence of these abnormal solutions is that $F(\chi)$ should have a minimum at some non-zero value of χ.

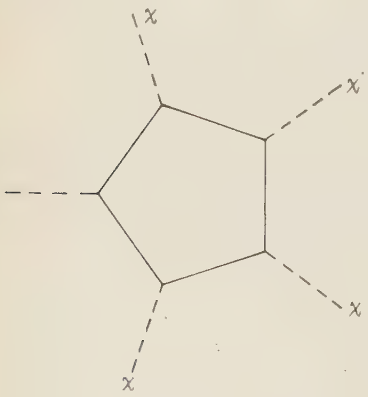

Fig. 5.

$F'(\chi)$ is in fact easier to evaluate than F. It is given by the sum of all diagrams with one external boson line. The previous approximations are recovered by putting $g_0\chi=\Delta$ and including only the diagrams in Fig. 5.

This gives

$$F'(\chi)=\mu_0^2\chi+\frac{\lambda_0}{6}\chi^3+\frac{4g_0^2}{(2\pi)^4 i}\int\frac{\chi}{p^2-m^2-g_0^2\chi^2}\,\mathrm{d}^4p.$$

Hence

$$F'(\chi^{(r)}) = \mu_1^2\chi^{(r)} + \frac{\lambda_1}{6}\,\chi^{(r)3} + \frac{4g_1^2}{(2\pi)^4 i}\int\frac{\chi^{(r)}g_1^4\chi^{(r)4}}{(p^2-m^2)^2(p^2-m^2-\Delta^2)}\,\mathrm{d}^4p\,.$$

Thus Δ is given by

$$0 = \frac{\mu_1^2}{g_1^2} + \frac{\lambda_1}{6g_1^4}\,\Delta^2 - \frac{m^2}{4\pi^2}\left\{\left(1+\frac{\Delta^2}{m^2}\right)\log\left(1+\frac{\Delta^2}{m^2}\right)-\frac{\Delta^2}{m^2}\right\}.$$

Let

$$\frac{4\pi^2\mu_1^2}{m^2g_1^2} = A\,,\qquad \frac{2\pi^2}{3}\,\frac{\lambda_1}{g_1^4} = B\,,\qquad \frac{\Delta^2}{m^2} = x\,.$$

Then

$$A + Bx = (1+x)\log(1+x) - x = h(x)\,.$$

The new boson mass is given by

$$\mu^2 = F''(\chi) = \frac{m^2g_1^2}{2\pi^2}\,x\{B - h'(x)\}\,.$$

It can be seen from Fig. 6 that there will be roots with $\mu^2 > 0$ only when $\mu_1^2 < 0$ and $B > B_{\text{crit}}$, where B_{crit} is given by $h'(x) = B$. Thus the abnormal solutions exist when

$$B > 0\,,\qquad 0 > A > -(e^B - 1 - B)\,.$$

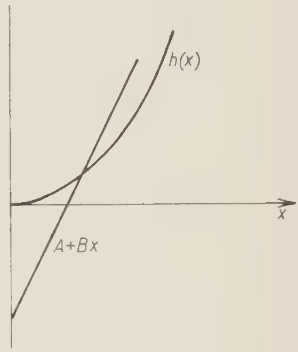

Fig. 6.

This calculation is exact in the limit $g_1 \to 0$ keeping μ_1^2/g_1^2, λ_1/g_1^4 and $g_1\chi^{(r)}$ finite. Thus in at least one case a solution of the required type can be established as plausibly as the more usual perturbation theory solutions.

4. – Symmetry properties and a simple model.

It is now necessary to discuss the principal peculiar feature of this type of solution. The original Lagrangian had a reflection symmetry. From this it follows that $F(\chi)$ must be an even function. Thus is $\chi = \chi_1$ is one solution of $F'(\chi_1) = 0$, $\chi_1 = -\chi_1$ is another. By choosing one solution, the reflection symmetry is effectively destroyed. It is possible to make a very simple model which shows this kind of behaviour, and also demonstrates that so long as there is a boson field in the theory to start with, the essential features of the abnormal solutions have very little to do with fermion pairs.

Consider the theory of a single neutral pseudoscalar boson interacting with itself,

$$L = \frac{1}{2}\left(\frac{\partial\varphi}{\partial x_\mu}\frac{\partial\varphi}{\partial x^\mu} - \mu_0^2\varphi^2\right) - \frac{\lambda_0}{24}\varphi^4 .$$

Normally this theory is quantized by letting each mode of oscillation of the classical field correspond to a quantum oscillator whose quantum number gives the number of particles. When $\mu_0^2 < 0$, this approach will not work. However, if $\lambda_0 > 0$, the function

$$\frac{\mu_0^2}{2}\varphi^2 + \frac{\lambda_0}{24}\varphi^4 ,$$

is as shown in Fig. 7.

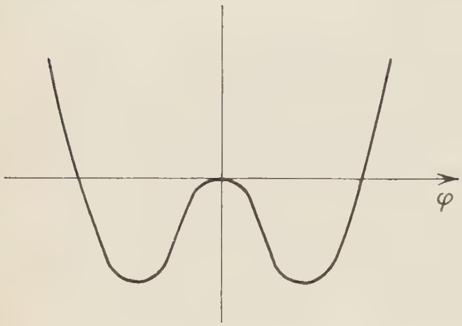

Fig. 7.

The classical equations

$$(\Box^2 + \mu_0^2)\varphi + \frac{\lambda_0}{6}\varphi^3 = 0 ,$$

now have solutions $\varphi = \pm\sqrt{-6\mu_0^2/\lambda_0}$ corresponding to the minima of this curve. Infinitesimal oscillations round one of these minima obey the equation

$$(\Box^2 - 2\mu_0^2)\,\delta\varphi = 0 .$$

These can now be quantized to represent particles of mass $\sqrt{-2\mu_0^2}$. This is simply done by making the transformation $\varphi = \varphi' + \chi$

$$\chi^2 = -\frac{6\mu_0^2}{\lambda_0} .$$

Then

$$L = \frac{1}{2}\left(\frac{\partial\varphi'}{\partial x_\mu}\frac{\partial\varphi'}{\partial x^\mu} + 2\mu_0^2\varphi'^2\right) - \frac{\lambda_0}{24}\varphi'^4 - \frac{\lambda_0\chi}{6}\varphi'^3 + \frac{3}{2}\frac{\mu_0^2}{\lambda_0} .$$

This new Lagrangian can be treated by the canonical methods.

In any state with a finite number of particles, the expectation value of φ is infinitesimally different from the vacuum expectation value. Thus the eigenstates corresponding to oscillations round $\varphi = \chi$ are all orthogonal to the usual states corresponding to oscillations round $\varphi = 0$, and also to the eigenstates round $\varphi = -\chi$. This means that the theory has two vacuum states, with a complete set of particle states built on each vacuum, but that there is a superselection rule between these two sets so that it is only necessary to

consider one of them. The symmetry $\varphi \to -\varphi$ has disappeared. Of course it can be restored by introducing linear combinations of states in the two sets but because of the superselection rule this is a highly artificial procedure.

Now consider the case when the symmetry group of the Lagrangian is continuous instead of discrete. A simple example is that of a complex boson field, $\varphi = (\varphi_1 + i\varphi_2)/\sqrt{2}$

$$L = \frac{\partial \varphi^*}{\partial x_\mu} \frac{\partial \varphi}{\partial x^\mu} - \mu_0^2 \varphi^* \varphi - \frac{\lambda_0}{6} (\varphi^* \varphi)^2 .$$

The symmetry is $\varphi \to \exp[i\alpha]\varphi$. The canonical transformation is $\varphi = \varphi' + \chi$

$$|\chi|^2 = -\frac{3\mu_0^2}{\lambda_0} .$$

The phase of χ is not determined. Fixing it destroys the symmetry. With χ real the new Lagrangian is

$$L = \frac{1}{2}\left(\frac{\partial \varphi_1'}{\partial x_\mu} \frac{\partial \varphi_1'}{\partial x^\mu} + 2\mu_0^2 \varphi_1'^2\right) + \frac{1}{2} \frac{\partial \varphi_2'}{\partial x_\mu} \frac{\partial \varphi_2'}{\partial x^\mu} - \frac{\lambda_0 \chi}{6} \varphi_1'(\varphi_1'^2 + \varphi_2'^2) - \frac{\lambda_0}{24} (\varphi_1'^2 + \varphi_2'^2)^2 .$$

The particle corresponding to the φ_2' field has zero mass. This is true even when the interaction is included, and is the new way the original symmetry expresses itself.

A simple picture can be made for this theory by thinking of the two dimensional vector φ at each point of space. In the vacuum state the vectors have magnitude χ and are all lined up (apart from the quantum fluctuations). The massive particles φ_1' correspond to oscillations in the direction of χ. The massless particles φ_2' correspond to « spin-wave » excitations in which only the direction of φ makes infinitesimal oscillations. The mass must be zero, because when all the $\varphi(x)$ rotate in phase there is no gain in energy because of the symmetry.

This time there are infinitely many vacuum states. A state can be specified by giving the phase of χ and then the numbers of particles in the two different oscillation modes. There is now a superselection rule on the phase of χ. States with a definite charge can only be constructed artificially by superposing states with different phases.

5. – Conclusion.

This result is completely general. Whenever the original Lagrangian has a continuous symmetry group, the new solutions have a reduced symmetry and contain massless bosons. One consequence is that this kind of theory

cannot be applied to a vector particle without losing Lorentz invariance. A method of losing symmetry is of course highly desirable in elementary particle theory but these theories will not do this without introducing non-existent massless bosons (unless discrete symmetry groups can be used). SKYRME (3) has hoped that one set of fields could have excitations both of the usual type and of the « spin-wave » type, thus for example obtaining the π-mesons as collective oscillations of the four K-meson fields, but this does not seem possible in this type of theory. Thus if any use is to be made of these solutions something more complicated than the simple models considered in this paper will be necessary.

(3) T. H. R. SKYRME: *Proc. Roy. Soc.*, A **252**, 236 (1959).

RIASSUNTO (*)

Si esaminano le condizioni per l'esistenza di soluzioni « superconduttrici » del tipo non perturbativo delle teorie di campo. Si usa un metodo non covariante di trasformazioni canoniche per trovare queste soluzioni per la teoria di un fermione interagente con un bosone pseudoscalare. Si espone poi un metodo covariante rinormalizzabile usando integrali di Feynman. Si trova un soluzione « superconduttrice » ogniqualvolta nella soluzione normale del tipo perturbativo la massa bosonica elevata al quadrato è negativa e le costanti di accoppiamento soddisfano ad alcune ineguaglianze. Si esaminano le proprietà di simmetria di tali soluzioni con l'aiuto di un semplice modello di campi di bosoni auto-interagenti. Le soluzioni hanno simmetria inferiore al lagrangiano, e contengono bosoni di massa zero.

(*) *Traduzione a cura della Redazione.*

IL NUOVO CIMENTO Vol. XIX, N. 1 1° Gennaio 1961

On a Gauge Theory of Elementary Interactions.

A. Salam

Imperial College - London

J. C. Ward

Carnegie Insitute of Technology - Pittsburgh

(ricevuto il 15 Settembre 1960)

Summary. — A theory of strong as well as weak interactions is proposed using the idea of having only such interactions which arise from generalized gauge transformations.

1. – Introduction.

One of the problems engaging current interest in field theory is the problem of determining which fields are « elementary » in some fundamental sense, and which are not. An equally, if not more, important, problem is that of finding a guiding principe for writing fundamental interactions of fields. The only such principle which exists at the present time seems to be the gauge-principle. Whenever a symmetry property exists, the associated gauge transformation leads in a definite manner to the postulation of an interaction through the mediation of a number of intermediate particles. There exist, at present, numerous attempts to understand all known elementary interactions in this manner. In an earlier paper (1), the authors considered a gauge-transformation in [3] « charge-space » to generate weak and electro-magnetic interactions. Recently J. J. Sakurai (2) has used similar ideas to postulate five intermediate vector mesons which may be responsible for mediating strong interactions.

All these attempts suffer from certain weaknesses. Our earlier attempt (1) to understand weak and electro-magnetic interactions produced only parity-

(1) A. Salam and J. C. Ward: *Nuovo Cimento*, **11**, 568 (1959).

(2) J. Sakurai: *Ann. of Phys.*, **11**, 1 (1960).

conserving interactions in a natural manner. Besides, the weak interactions did not obey the $\Delta I = \frac{1}{2}$ rule. Sakurai's strong Lagrangian suffers from the defect that it contains no Yukawa-like terms permitting single emission of pions or K-mesons by baryons.

In this note we wish to reconsider the problem. Our basic postulate is that it should be possible to generate strong, weak and electro-magnetic interaction terms (with all their correct symmetry properties and also with clues regarding their relative strengths), by making local gauge transformations on the kinetic-energy terms in the free Lagrangian for all particles. This is the statement of an ideal which, in this paper at least, is only very partially realized.

It may however be of interest to set down the procedure which has been followed.

2. – A simple model.

Consider the π-nucleon system. Following SCHWINGER we assume the existence of a scalar iso-scalar particle σ. Write the free Lagrangian kinetic energy terms in the form

$$N_L^+ \gamma_4 \gamma_\mu \partial_\mu N_L + N_R^+ \gamma_4 \gamma_\mu \partial_\mu N_R + \tfrac{1}{2}(\partial_\mu \boldsymbol{\pi}) \cdot (\partial_\mu \boldsymbol{\pi}) + \tfrac{1}{2}(\partial_\mu \sigma)^2 \,, \tag{1}$$

where

$$N_L = \tfrac{1}{2}(1 + \gamma_5) N \,,$$

$$N_R = \tfrac{1}{2}(1 - \gamma_5) N \,.$$

Following a suggestion made by SCHWINGER (3), GELL-MANN and LEVY (4) one may consider $\begin{pmatrix} N_L \\ N_R \end{pmatrix}$ as forming a spinor and $\begin{pmatrix} \sigma \\ \boldsymbol{\pi} \end{pmatrix}$ a 4-vector in a [4] Euclidean space. Since there are 6 rotations in such a space, the gauge-principle will give rise to six fields X, Y with the interactions

$$\begin{aligned} L_{\text{int}} = \frac{1}{2}\left(\sigma \frac{\partial \boldsymbol{\pi}}{\partial x_\mu} - \frac{\partial \sigma}{\partial x_\mu} \boldsymbol{\pi} + \boldsymbol{\pi} \wedge \frac{\partial \boldsymbol{\pi}}{\partial x_\mu} - \frac{\partial \boldsymbol{\pi}}{\partial x_\mu} \wedge \boldsymbol{\pi}\right) \cdot \boldsymbol{X}_\mu + \\ + i N_L^+ \gamma_4 \gamma_\mu \boldsymbol{\tau} \cdot \boldsymbol{X}_\mu N_L + \frac{1}{8}(\boldsymbol{X} \cdot \boldsymbol{\pi})^2 + \frac{1}{8}(\boldsymbol{\pi} \wedge \boldsymbol{X})^2 + \frac{1}{8} \boldsymbol{X}^2 \sigma^2 + \\ + \frac{1}{2}\left[\left(\sigma \frac{\partial \boldsymbol{\pi}}{\partial x_\mu} - \frac{\partial \sigma}{\partial x_\mu} \boldsymbol{\pi}\right) + \left(\frac{\partial \boldsymbol{\pi}}{\partial x_\mu} \wedge \boldsymbol{\pi} - \frac{\partial \boldsymbol{\pi}}{\partial x_\mu} \wedge \boldsymbol{\pi}\right)\right] \cdot \boldsymbol{Y}_\mu + \\ + i N_R^+ \gamma_4 \gamma_\mu \boldsymbol{\tau} \cdot \boldsymbol{Y}_\mu N_R + \frac{1}{8}(\boldsymbol{Y} \cdot \boldsymbol{\pi})^2 + \frac{1}{8}(\boldsymbol{\pi} \wedge \boldsymbol{Y})^2 + \frac{1}{8} \boldsymbol{Y}^2 \sigma^2 \,. \end{aligned} \tag{2}$$

(3) J. SCHWINGER: *Ann. of Phys.*, **2**, 407 (1957).
(4) M. GELL-MANN and M. LEVY: *Nuovo Cimento*, **14**, 705 (1960).

The « free » Lagrangians for the $\boldsymbol{X}$ field is as follows

$$\left[\left(\frac{\partial}{\partial x_\mu}\boldsymbol{X}_\nu - \boldsymbol{X}_\mu \wedge \boldsymbol{X}_\nu\right) - \left(\frac{\partial}{\partial x_\nu}\boldsymbol{X}_\mu - \boldsymbol{X}_\nu \wedge \boldsymbol{X}_\mu\right)\right]^2,$$

with a similar expression for the $\boldsymbol{Y}$ field.

One can rewrite the above interaction slightly differently, introducing fields

$$\tfrac{1}{2}(\boldsymbol{X} + \boldsymbol{Y}) = \boldsymbol{u}\,,$$

$$\tfrac{1}{2}(\boldsymbol{X} - \boldsymbol{Y}) = \boldsymbol{v}\,.$$

Thus

$$(3) \qquad L_{\text{int}} = \left[\left(\boldsymbol{\pi}\wedge\frac{\partial\boldsymbol{\pi}}{\partial x_\mu} - \frac{\partial\boldsymbol{\pi}}{\partial x_\mu}\wedge\boldsymbol{\pi}\right) + N^+\gamma_4\gamma_\mu\boldsymbol{\tau}N\right]\cdot\boldsymbol{u} + \\ + \left[\sigma\frac{\partial\boldsymbol{\pi}}{\partial x_\mu} - \frac{\partial\sigma}{\partial x_\mu}\boldsymbol{\pi} + N^+\gamma_4\gamma_\mu\gamma_5\boldsymbol{\tau}N\right]\cdot\boldsymbol{v} + \text{terms quadratic in } \boldsymbol{u} \text{ and } \boldsymbol{v}\,.$$

We wish to identify the σ-containing part of the above Lagrangian as representing strong interactions and the remaining Lagrangian as representing weak interactions. The leptons (e^+, ν, e^-) or (μ^+, ν', μ^-) form a 3-vector in the space we are considering and a gauge-transformation will only link them with the u-field. The strength of the strong coupling comes about if we assume that the vacuum expectation value of σ ($\langle\sigma\rangle_0$) does not equal zero but equals $(g_s/2M_N)(1/g_\omega)$ (*).

Thus terms in the Lagrangian with $\sigma(\partial\boldsymbol{\pi}/\partial x_\mu)\cdot\boldsymbol{v}$ and $M^+\gamma_4\gamma_\mu\gamma_5\boldsymbol{\tau}\cdot\boldsymbol{v}N$ together give the conventional pseudo-vector strong Yukawa interaction with pions emitted singly. This is not to say that we are considering σ as an alternative expression for the strong coupling constant. There is every possibility that σ-particles are emitted (and absorbed) as physical particles.

Notice that the weak interactions in this model conserve parity. This unfortunate situation seems to persist in subsequent work also (**).

3. – Extension to strange particles.

In the above model σ, $\boldsymbol{\pi}$ form a 4-vector in a [4]-Euclidean manifold while N_L and N_R form a 4-spinor. A direct extension of this to include K-mesons is possible, provided we consider σ, π and K-particles to form a vector in an [8]-space while the sixteen baryons (eight-baryons each decomposed into their left and right components) form a 16-component spinor in such a space.

(*) Notice the terms $\sigma^2(X^2+Y^2)$ in (2) could give the mass-terms for u and v particles.

(**) The theory of weak interactions recently proposed by GELL-MANN and LÉVY [4] effectively proceeds by identifying the terms containing $\boldsymbol{X}_\mu$ only in (2) with the strangeness-conserving weak Lagrangian. The gauge-transformations giving rise to $\boldsymbol{Y}_\mu$ fields are not considered.

The formalism we use was essentially developed by TIOMNO [5]. Let us first recapitulate this. Write

$$\frac{1}{\sqrt{2}}(\Lambda^0-\boldsymbol{\tau}\cdot\boldsymbol{\Sigma})=\begin{pmatrix}Z^0 & \Sigma^+\\ \Sigma^- & Y^0\end{pmatrix}=(\Sigma_2,\Sigma_1)\,,$$

$$K^+=K_1-iK_2\,,\qquad K^0=K_3-iK_4\,.$$

If all K-coupling constants are equal, the conventional p.s. (or p.v.) strong K-Lagrangian can be written as

$$L_K=(N^+\Xi^+)(i\gamma_4\gamma_5)\begin{pmatrix}K^0 & K^+\\ K^- & -\bar{K}^0\end{pmatrix}\begin{pmatrix}\Sigma_1\\ \Sigma_2\end{pmatrix}+\text{h.c.}\,. \tag{4}$$

Write $\psi=\begin{pmatrix}N\\ \Xi\\ \Sigma_1\\ \Sigma_2\end{pmatrix}$; then L_K equals

$$\sum_{\alpha=1}^{4}\psi^+ i\gamma_4\gamma_5\Gamma_\alpha K_\alpha\psi\,, \tag{5}$$

where

$$\Gamma=\begin{pmatrix} & \boldsymbol{\tau}\times 1\\ \boldsymbol{\tau}\times 1 & \end{pmatrix},\qquad \Gamma_4=\begin{pmatrix} & i\times 1\\ -i\times 1 & \end{pmatrix}. \tag{6}$$

These Γ matrices are 8×8 matrices pertaining to a (six or) seven dimensional manifold. The spinor ψ is an 8×1 column.

It is possible to write the conventional p.s. (or p.v.) π-interactions in term of ψ.

Define three additional matrices,

$$\Gamma_{5,6,7}=\begin{pmatrix}1\times\boldsymbol{\tau} & & & \\ & 1\times\boldsymbol{\tau} & & \\ & & -1\times\boldsymbol{\tau} & \\ & & & -1\times\boldsymbol{\tau}\end{pmatrix}=\tau_3\times 1\times\boldsymbol{\tau}\,. \tag{7}$$

Then the matrices $\Gamma_1, \Gamma_2, \ldots, \Gamma_7$ anti-commute. If all π-couplings are equal (and in particular if $g_{\mu\mathcal{N}}=-g_{\pi\Sigma\Sigma}$), one can write the π-Lagrangian

$$L_\pi=\sum_{\alpha=5,6,7}\psi^+ i\gamma_4\gamma_5(\Gamma_\alpha\pi_\alpha)\psi\,. \tag{8}$$

It is clear that π's and K's form a vector in a [7]-space.

So much for Tiomno's formalism. We can now follow a procedure analogous to Section 2 and obtain an expression which would contain terms like

$$\sigma\frac{\partial\boldsymbol{\pi}}{\partial x_\mu}\cdot\boldsymbol{V}_\mu\,,\qquad \sigma\frac{\partial K_\alpha}{\partial x_\mu}Z_\alpha\,,\qquad \sum_{\alpha=1}^{4}\psi^+(i\gamma_4\gamma_\mu\gamma_5)\Gamma_\alpha Z_\alpha\psi\,,$$

[5] J. TIOMNO: *Nuovo Cimento*, 6, 69 (1957).

to give an effective strong p.v. Lagrangian of the Tiomno type. Write

$$L_f = \psi_L^+ \gamma_4 \gamma_\mu \partial_\mu \psi_L + \psi_R^+ \gamma_4 \gamma_\mu \partial_\mu \psi_R + \tfrac{1}{2}[\partial_\mu \sigma + (\partial_\mu \boldsymbol{\pi})^2 + (\partial_\mu K_\alpha)^2]\,. \tag{9}$$

The sixteen-component entity $\begin{pmatrix}\psi_L\\ \psi_R\end{pmatrix}$ forms a spinor in [8]-space. One anti-commuting Dirac set for such a space is

$$\left|\begin{array}{ll} \Gamma^{(8)}_{1,2,3} & = \tau_1 \times (\tau_1 \times \boldsymbol{\tau}) \times 1\,, \\ \Gamma^{(8)}_4 & = \tau_1 \times (\tau_2 \times 1) \times 1\,, \\ \Gamma^{(8)}_{5,6,7} & = \tau_1 \times (\tau_3 \times 1) \times \boldsymbol{\tau}\,, \\ \Gamma^8_8 & = \tau_2 \times 1 \times 1 \times 1\,. \end{array}\right. \tag{10}$$

In [8] space there are 28 rotations. Seven of these rotations ($\sigma \to \sigma + \boldsymbol{\epsilon}\cdot\boldsymbol{\pi} + \varepsilon_\alpha K_\alpha$, $\boldsymbol{\pi} \to \boldsymbol{\pi} - \boldsymbol{\epsilon}\sigma$, etc.) with the corresponding spinor rotation matrices

$$\frac{1}{2i}\,(\Gamma^{(8)}_\lambda \Gamma^8_\lambda - \Gamma^{(8)}_\lambda \Gamma^{(8)}_8)\,,$$

give

$$L_{\text{int}} = \frac{1}{2}\left(\sigma \frac{\partial \boldsymbol{\pi}}{\partial x_\mu}\cdot v_\mu + \sigma \frac{\partial K_\alpha}{\partial x} Z_\alpha - \frac{\partial \sigma}{\partial x_\mu}\boldsymbol{\pi}\cdot\boldsymbol{v} - \frac{\partial \sigma}{\partial x_\mu} K_\alpha Z_\alpha\right) \tag{11}$$

i.e. Tiomno Lagrangian with $(i\gamma_4\gamma_5\boldsymbol{\tau}\cdot\boldsymbol{\pi})$ replaced by $(i\gamma_4\gamma_\mu\gamma_5\boldsymbol{\tau}\cdot\boldsymbol{v}_\mu)$ and $(i\gamma_4\gamma_5\Gamma_\alpha K_\alpha)$ replaced by $i\gamma_4\gamma_\mu\gamma_5\Gamma_\alpha Z_{\alpha,\mu}$. The fields $\boldsymbol{V}_\mu$ and Z_μ behave, so far as isotopic spin, etc., is concerned just like $\boldsymbol{\pi}$ and K mesons.

In so far as these seven rotation matrices do not form a Lie-Algebra, the interaction Lagrangian must contain 21 other fields corresponding to the remaining 21 rotations. From the point of view adopted in Section 2, these give weak interactions only. A general analysis of these terms has been given by GÜRSEY ([6]) in a recent paper which also adopts the Tiomno formalism to give an analogue of the Gell-Mann–Lévy theory of weak interactions.

It may be more profitable from our point of view to consider two fields σ and σ' in such a way that $(\sigma, \boldsymbol{\pi})$ form a 4-vector and (σ', K_α) a 5-vector. The resulting strong Lagrangian would then contain two coupling parameters $\langle\sigma\rangle_0$ and $\langle\sigma'\rangle_0$. $(\sigma, \boldsymbol{\pi})$ and (σ', K_α) spaces in a sense form two (disconnected) pieces of a [9] space. Even for the Tiomno Lagrangian it was possible to consider $\boldsymbol{\pi}$ and K-mesons as particles corresponding to disjunct pieces of the 7-dimensional space. Thus if we replace $\Gamma_\alpha \pi_\alpha$ in eq. (8) by $\Gamma'_\alpha \pi_\alpha$ where $\Gamma'_\alpha = 1 \times 1 \times \boldsymbol{\tau}$ (*i.e.* $g_{\pi\mathcal{N}} = + g_{\pi\Sigma\Sigma}$) we see that $\boldsymbol{\pi}$ and K no longer form a 7-vector. The per-

([6]) F. GÜRSEY: preprint.

mitted rotations have to be limited in such a way that π-mesons are not transformed into K-mesons.

Returning to the [9] space, if $(\sigma, \boldsymbol{\pi})$ form a [4] subspace and (σ', K) a [5] sub-space, it is clear that the total number of intermediate bosons will be $6+10=16$. Of these seven will mediate strong (p.v.) interaction, and 9 will mediate weak (v.) interactions. All these interactions conserve parity and isotopic-spin.

4. – $\Delta|I| = \frac{1}{2}$ rule.

One simple way to introduce strangeness violation consistent with the $\Delta|I| = \frac{1}{2}$ rule is to remark that the other field besides σ (or σ') which can have a non-zero expectation-value is the field corresponding to the θ^0 particle $(CP = +I)$. In the notation above $\langle K_4 \rangle \neq 0$ and would in fact be proportional to g_w even in the conventional theory. Thus all strangeness conserving terms like $\Lambda N \boldsymbol{\tau}\cdot\boldsymbol{\pi} K$ describe also the matrix-elements for (parity-conserving) weak decay of $\Lambda \to N + \pi$ consistent with $\Delta I = \frac{1}{2}$ provided we take the vacuum expectation value of the K-meson.

The non-zero expectation value of θ^0 is the perfect realization of the spurion idea of Wentzel so that it may not be necessary to introduce any additional fields to violate strangeness.

From what has been said above, it is clear that seven fields (three with transformation character of π-mesons and four with that of K-mesons) are necessary to mediate strong-interactions. The number of those necessary for weak interactions depends on the model used. However in all this work parity-violation for weak interactions remains a complete mystery.

* * *

We are deeply indebted to Professor R. G. SACHS for an invitation to the University of Wisconsin Summer Institute where part of the above work was completed.

RIASSUNTO (*)

Si propone una teoria delle interazioni sia forti che deboli nell'ipotesi di avere solo interazioni dovute a trasformazioni di gauge generalizzate.

(*) *Traduzione a cura della Redazione.*

IL NUOVO CIMENTO Vol. XIX, N. 1 1° Gennaio 1961

Parity Conservation and Baryon Mass-Differences in Strong Interactions.

N. Dallaporta and L. K. Pandit (*)
Istituto di Fisica dell'Università - Padova

(ricevuto il 21 Ottobre 1960)

Summary. — In some earlier work [1,2] a scheme of strong interactions was proposed which took account of the baryon mass-differences. It was found that P conservation follows automatically for the whole Lagrangian of this scheme once CP invariance is assumed. It is shown here that this is due to the fact that the Lagrangian can be considered as consisting of different pieces, each of which satisfies certain symmetry conditions of the type formulated by Feinberg and Gürsey [3].

In an earlier work [1] dealing with the symmetries of strong interactions of the baryons with the π- and the K-mesons, a scheme was proposed—on rather phenomenological grounds—which qualitatively took account of the baryon mass-differences with only four independent coupling constants. It was found that, even with the baryon mass-differences as introduced in this scheme, the interaction Lagrangian (which we always take of non-derivative Yukawa type) turns out to be necessarily P conserving once CP invariance is assumed. A further investigation on this point [2] led to the conclusion that P conservation follows from CP invariance even for a more general Lagrangian containing eight different coupling constants, provided that the Lagran-

(*) On a visit from Tata Institute of Fundamental Research, Bombay.

(1) N. Dallaporta and L. K. Pandit: *Nuovo Cimento*, **16**, 135 (1960), referred to as A in the following.

(2) N. Dallaporta: *Proc. of the X Annual International Conference on High Energy Physics* (Rochester, 1960), referred to as B in the following.

(3) G. Feinberg and F. Gürsey: *Phys. Rev.*, **114**, 1153 (1959), referred to as C in the following; and earlier works referred to in this paper.

gian satisfies certain general conditions which, however, were presented in a rather tentative form whose physical meaning was not obvious. An attempt is made here to formulate these conditions in a physically more precise form. This, in addition, provides us with another way of understanding the introduction of the various interaction terms in (A).

Generally speaking, for obtaining $CP \to P$, the baryons are basically treated as forming four isobaric doublets ([3]). Then the desired result follows for the π-interactions on account of charge-symmetry. The minimal conditions, called here (α) and (β), required for obtaining $CP \to P$ also for the K-interactions have been formulated by FEINBERG and GÜRSEY ([3]) (in Section **3** of C). A further condition, called (γ), is applied by these authors in order to ensure the usual charge-symmetry (when the different particles behave according to isobaric spin assigments of the Gell-Mann–Nishijima scheme). This further reduces the number of coupling constants left after imposing (α) and (β) and leads, in fact, to a highly symmetrical scheme with only one coupling constant for the K-interaction and one for the π-interaction. Of course, such a highly symmetrical scheme (*), satisfying (α), (β) and (γ), does not allow for the baryon mass-differences and, as pointed out by PAIS ([4]), leads to contradictions with experiments on reaction rates.

At first sight then, it appears strange that P conservation should follow from CP invariance for the interactions of (A) and (B) even though the high symmetries are broken there to account for the baryon mass-differences. As a clarification of this point, we show here that this result is obtained since the Lagrangians of (A) and (B) are really linear combinations of different sub-schemes, each of which satisfies conditions of the type (α), (β) and (γ). These conditions, of course, are different for each sub-scheme in certain signs, breaking thereby the high symmetry, so that we obtain $CP \to P$ on the one hand, and the mass-differences on the other.

Let us call the four baryon doublets as defined in (I)

$$N_1 = \begin{pmatrix} p \\ n \end{pmatrix}, \qquad N_2 = \begin{pmatrix} -\Sigma^+ \\ A^0 \end{pmatrix}, \qquad N_3 = \begin{pmatrix} B^0 \\ \Sigma^- \end{pmatrix}, \qquad N_4 = \begin{pmatrix} \Xi^0 \\ \Xi^- \end{pmatrix},$$

where

$$A^0 = \frac{\Sigma^0 + \eta\Lambda^0}{\sqrt{2}}, \qquad B^0 = \frac{\Sigma^0 - \eta\Lambda^0}{\sqrt{2}}. \qquad (\eta^2 = 1): \tag{1}$$

The charge independent π-interaction with these doublets is already P conserving on account of charge symmetry ([3]). To this we add the most general

(*) Such a scheme will be called a « sub-scheme » in the following for the sake of clarity of exposition.

([4]) A. PAIS: *Phys. Rev.*, **110**, 574 (1958).

K-interaction to obtain the total hermitian Lagrangian density:

$$L = L_K + L_\pi .$$

$$(2)\quad \begin{cases} L_K = \bar{N}_1(g_s + g_p\gamma_5)N_2K^0 + \bar{N}_2(g_s^* - g_p^*\gamma_5)N_1K^{0\dagger} + \\ \qquad + \bar{N}_1(g'_s + g'_p\gamma_5)N_3K^+ + \bar{N}_3(g'^*_s - g'^*_p\gamma_5)N_1K^{+\dagger} + \\ \qquad + \bar{N}_3(f_s + f_p\gamma_5)N_4K^0 + \bar{N}_4(f_s^* - f_p^*\gamma_5)N_3K^{0\dagger} + \\ \qquad + \bar{N}_2(f'_r + f'_p\gamma_5)N_4K^+ + \bar{N}_4(f'^*_s - f'^*_p\gamma_5)N_2K^{+\dagger}; \\ L_\pi = G_1(i\bar{N}_1\gamma_5\boldsymbol{\tau}N_1\cdot\boldsymbol{\pi}) + G_2\bar{N}_2O\boldsymbol{\tau}N_2\cdot\boldsymbol{\pi} + G_3\bar{N}_3O\boldsymbol{\tau}N_3\boldsymbol{\pi} + G_4\bar{N}_4O'\boldsymbol{\tau}N_4\cdot\boldsymbol{\pi} , \end{cases}$$

where G_i $(i=1,2,3,4)$ are real, and O, $O'=1$ or $i\gamma_5$ quite independently.

As against L_π, for $L_K P$ conservation does not follow from CP invariance. However, FEINBERG and GÜRSEY (Section 3 of (¹)) show that this becomes possible for the K^0-interactions if one assumes invariance under the transformation (α), and for the K^+-interactions if one assumes invariance under the transformation (β), where:

$$(3)\quad \begin{cases} (\alpha):\quad N_1 \leftrightarrow N_2 ,\quad N_3 \leftrightarrow N_4 ,\quad K^0 \leftrightarrow K^{0\dagger} ,\quad K^+ \leftrightarrow \varepsilon_+ K^+ , \\ \qquad\qquad \boldsymbol{\pi} \leftrightarrow \varepsilon_\pi \boldsymbol{\pi} ,\quad (\varepsilon_+^2 = 1,\ \varepsilon_\pi^2 = 1) ; \\ (\beta):\quad N_1 \leftrightarrow N_3 ,\quad N_2 \leftrightarrow N_4 ,\quad K^+ \leftrightarrow K^{+\dagger} ,\quad K^0 \leftrightarrow \varepsilon_0 K^0 , \\ \qquad\qquad \boldsymbol{\pi} \leftrightarrow \varepsilon'_\pi \boldsymbol{\pi} ,\quad (\varepsilon_0^2 = 1,\ \varepsilon'^2_\pi = 1) . \end{cases}$$

We include here a possible change of phase of the $\boldsymbol{\pi}$ under these transformations as a generalization of the Feinberg-Gürsey conditions. (α) and (β) are now the minimal conditions for P conservation. The Lagrangian which is invariant under CP, (α) and (β) is:

$$(4)\quad \begin{cases} L' = L'_K + L'_\pi ; \\ L'_K = g_{K^0}(\bar{N}_1O_{K^0}N_2K^0 + \text{h. c.}) + g_K(\bar{N}_1O_{K^+}N_3K^+ + \text{h. c.}) + \\ \qquad + \varepsilon_0 g_{K^0}(\bar{N}_3O_{K^0}N_4K^0 + \text{h. c.}) + \varepsilon_+ g_{K^+}(\bar{N}_2O_{K^+}N_4K^+ + \text{h. c.}) , \end{cases}$$

where

$$g_{K^0} = \begin{cases} g_s = \varepsilon_0 f_s ,\quad O_{K^0} = 1 \\ g_p = \varepsilon_0 f_p ,\quad O_{K^0} = \gamma_5 \end{cases} ;\qquad g_{K^+} = \begin{cases} g'_s = \varepsilon_+ f'_s ,\quad O_{K^+} = 1 \\ g'_p = \varepsilon_+ f'_p ,\quad O_{K^+} = \gamma_5 . \end{cases}$$

The g_{K^0} and g_{K^+} are now real constants.

$$(5)\quad L'_\pi = iG_\pi[\bar{N}_1\gamma_5\boldsymbol{\tau}N_1\cdot\boldsymbol{\pi} + \varepsilon_\pi\bar{N}_2\gamma_5\boldsymbol{\tau}N_2\cdot\boldsymbol{\pi} + \varepsilon'_\pi\bar{N}_3\gamma_5\boldsymbol{\tau}N_3\cdot\boldsymbol{\pi} + \varepsilon_\pi\varepsilon'_\pi\bar{N}_4\gamma_5\boldsymbol{\tau}N_4\cdot\boldsymbol{\pi}] ,$$

where

$$G_\pi = G_1 = G_2 = G_3 = G_4 \,. \tag{5}$$

Let us now, with FEINBERG and GÜRSEY, impose a third condition (γ) to ensure that the total interaction is invariant under the *usual* charge symmetry with the Gell-Mann–Nishijima assignements for isobaric spin:

$$\tag{6} \begin{cases} (\gamma): \quad \Sigma^+ \leftrightarrow \Sigma^-, \quad A^0 \leftrightarrow -B^0 \qquad (\Lambda^0 \leftrightarrow \Lambda^0,\ \Sigma^0 \leftrightarrow -\Sigma^0)\,, \\ \pi^+ \leftrightarrow \pi^-\,, \quad \pi^0 \leftrightarrow -\pi^0\,, \\ K^+ \leftrightarrow K^0\,, \quad p \leftrightarrow n\,, \quad \Xi^0 \leftrightarrow -\Xi^-\,. \end{cases}$$

Then we must have

$$O_{K^0} = O_{K^+} \equiv O_K\,, \qquad \varepsilon_0 = -\varepsilon_+ \equiv \varepsilon_K\,, \qquad \varepsilon_\pi = \varepsilon'_\pi\,;$$

$$g_{K^0} = -g_{K^+} \equiv \varepsilon_K G_K\,.$$

Therefore, the interaction Lagrangian density becomes:

$$\tag{7} \begin{aligned} \mathscr{L} = G_K[\{\varepsilon_K(\bar N_1 O_K N_2 K^0 - \bar N_1 O_K N_3 K^+) + (\bar N_3 O_K N_4 K^0 + \bar N_2 O_K N_4 K^+)\} + \text{h. c.}] + \\ + iG_\pi[\bar N_1 \gamma_5 \boldsymbol{\tau} N_1 \boldsymbol{\pi} + \varepsilon_\pi(\bar N_2 \gamma_5 \boldsymbol{\tau} N_2 \boldsymbol{\pi} + \bar N_3 \gamma_5 \boldsymbol{\tau} N_3 \boldsymbol{\pi}) + \bar N_4 \gamma_5 \boldsymbol{\tau} N_4 \boldsymbol{\pi}]\,, \end{aligned}$$

resulting in what we call the highly symmetrical « sub-scheme » with only one coupling constant for the K- and for the π-interaction. The parities of all the N's are the same now.

We make first the conventional choice $\varepsilon_\pi = +1$. Then we can still take $\varepsilon_K = +1$ or -1, and for each of these cases, η appearing in the definitions of A^0 and B^0 can be $+1$ or -1.

We then have the following four cases.

Case I. – $\eta = +1$, $\varepsilon_K = +1$.

$$A^0 = Y^0\,, \qquad B^0 = Z^0\,; \qquad \left(Y^0 = \frac{\Sigma^0 + \Lambda^0}{\sqrt{2}}\,, \quad Z^0 = \frac{\Sigma^0 - \Lambda^0}{\sqrt{2}}\right).$$

The interaction may then be written as

$$\mathscr{L}^I = G_K^I \sum_{L=1}^{4} \bar\Psi O_K \omega_L \Psi \Phi_L + G_\pi^I \sum_{j=1}^{3} \bar\Psi \gamma_5 T_j \Psi \Pi_j\,, \tag{8}$$

where

$$\Psi = \begin{bmatrix} p \\ n \\ \Xi^0 \\ \Xi^- \\ -\Sigma^+ \\ Y^0 \\ Z^0 \\ \Sigma^- \end{bmatrix},$$

and

$$\omega_1 = i\left[\begin{array}{cc|cc} 0 & & 0 & I \\ & & I & 0 \\ \hline 0 & -I & 0 & \\ -I & 0 & & \end{array}\right], \qquad \omega_2 = \left[\begin{array}{cc|cc} 0 & & 0 & I \\ & & -I & 0 \\ \hline 0 & -I & 0 & \\ I & 0 & & \end{array}\right],$$

$$\omega_3 = i\left[\begin{array}{cc|cc} 0 & & I & 0 \\ & & 0 & -I \\ \hline -I & 0 & 0 & \\ 0 & I & & \end{array}\right], \qquad \omega_4 = \left[\begin{array}{cc|cc} 0 & & I & 0 \\ & & 0 & I \\ \hline I & 0 & 0 & \\ 0 & I & & \end{array}\right],$$

$$\omega_5 = \omega_1\omega_2\omega_3\omega_4\,, \qquad I = \begin{pmatrix} 1 & 0 \\ 0 & 1 \end{pmatrix},$$

$$T_j = \left[\begin{array}{cc|cc} \tau_j & 0 & 0 & \\ 0 & \tau_j & & \\ \hline 0 & & \tau_j & 0 \\ & & 0 & \tau_j \end{array}\right],$$

$$K^+ = \frac{\varphi_1 - i\varphi_2}{\sqrt{2}}\,, \qquad K^- = \frac{\varphi_1 + i\varphi_2}{\sqrt{2}}\,, \qquad K^0 = -\frac{\varphi_3 - i\varphi_4}{\sqrt{2}}\,, \qquad \bar{K}_0 = \frac{\varphi_3 + i\varphi_4}{\sqrt{2}}\,.$$

Case II. – $\eta = +1$, $\varepsilon_K = -1$.

$$A^0 = Y^0\,, \qquad B^0 = Z^0\,.$$

The interaction may be written as:

$$(9)\qquad \left\{\begin{array}{l} \mathscr{L}^{II} = G_K^{II}\sum\limits_{L=1}^{4}\bar{\Psi}O_K\omega'_L\Psi\Phi_L + G_\pi^{II}\sum\limits_{j=1}^{3}\bar{\Psi}\gamma_5 T_j\Psi\Pi_j\,, \\ \text{where} \\ \omega'_1 = -i\omega_2\omega_5\,, \quad \omega'_2 = i\omega_1\omega_5\,, \quad \omega'_3 = -i\omega_4\omega_5\,, \quad \omega'_4 = i\omega_3\omega_5\,. \end{array}\right.$$

Case III. – $\eta = -1$, $\varepsilon_K = +1$.

$$A^0 = Z^0 , \qquad B^0 = Y^0 .$$

i.e., the roles of Y^0 and Z^0 have been interchanged in respect of the Case I. Then we may write the interaction as:

$$\mathscr{L}^{III} = G_K^{III} \sum_{L=1}^{4} \overline{\Psi} O_K \overline{\omega}_L \Psi \Phi_L + G_\pi^{III} \sum_{j=1}^{3} \overline{\Psi} \gamma_5 \overline{T}_j \Psi \Pi_j , \tag{10}$$

where,

$$\overline{\omega}_L = J \omega_L J , \qquad \overline{T}_j = J T_j J ;$$

$$J = \begin{bmatrix} 1 & 0 & 0 & 0 & & & & \\ 0 & 1 & 0 & 0 & & & 0 & \\ 0 & 0 & 1 & 0 & & & & \\ 0 & 0 & 0 & 1 & & & & \\ & & & & 1 & 0 & 0 & 0 \\ & & 0 & & 0 & 0 & 1 & 0 \\ & & & & 0 & 1 & 0 & 0 \\ & & & & 0 & 0 & 0 & 1 \end{bmatrix} .$$

J really interchanges Y^0 and Z^0 in the Ψ as defined above.

Case IV. – $\eta = -1$, $\varepsilon_K = -1$.

The interaction has the same form as in Case II with Y^0 and Z^0 interchanged there. Thus

$$\mathscr{L}^{IV} = G_K^{IV} \sum_{L=1}^{4} \overline{\Psi} O_K \overline{\omega}'_L \Psi \Phi_L + G_\pi^{IV} \sum_{j=1}^{3} \overline{\Psi} \gamma_5 \overline{T}_j \Psi \Pi_j , \tag{11}$$

where,

$$\overline{\omega'_L} = J \omega'_L J .$$

Interchanging the roles of Y^0 and Z^0 in the N_2 and N_3 doublets is equivalent to considering instead the hyperon doublets to be

$$N'_2 = \begin{pmatrix} -\Sigma^+ \\ Z^0 \end{pmatrix} , \qquad N'_3 = \begin{pmatrix} Y^0 \\ \Sigma^- \end{pmatrix} .$$

We may remark here that under the operations CP, C, P, etc., the phases to be attached to N_2, N_3 and N'_2, N'_3 will be the same. This is because a phase

176

is a multiplicative factor which must be the same for Λ^0 and Σ^0, in order that Y^0 and Z^0 transform both in a definite way, thus, the same phase must appear for Y^0 and Z^0. Also the $\Sigma^{\pm}$ must transform with this very phase as they form doublets with Y^0 and Z^0.

The interaction has, in each of the four cases taken separately, a 4-dimensional rotational invariance leading to hypercharge- and hypernumber-independence as discussed in (A).

We may construct a linear combination of the four preceding cases which will give us a general Lagrangian containing 6 independent constants (4 for the K-interactions and 2 for the π-interactions). The total Lagrangian considered in (A) (equations (28), (31)) may now be considered as one consisting of a special choice for these 6 constants, namely

$$(12) \qquad \begin{cases} O_{\mathrm{K}} = \gamma_5\colon \qquad G_{\mathrm{K}}^{I} = F\,, \qquad G_{\mathrm{K}}^{II} = F'\,, \qquad G_{\mathrm{K}}^{III} = bF\,, \\ \qquad\qquad G_{\mathrm{K}}^{IV} = bF'\,, \qquad G_{\pi}^{I} + G_{\pi}^{II} = g\,, \qquad G_{\pi}^{III} + G_{\pi}^{IV} = bg\,; \\ O_{\mathrm{K}} = 1\colon \qquad F \to -iF\,, \qquad F' \to -iF'\,. \end{cases}$$

We still have to say a word about the other possible choice of -1 for ε_{π}. This will only change the sign of the Λ- and Σ-interactions with the pions in all the four cases discussed above. This possibility, as may be easily seen, will only lead, by taking a linear combination of all the eight different cases, to a similar result as before for the K-interactions, but will introduce three independent constants in the π-interactions (one for $\Sigma\Sigma\pi$, one for $\Lambda\Sigma\pi$ and a third one which is the same for $\mathcal{N}\mathcal{N}\pi$ and $\Xi\Xi\pi$). We thus obtain a P conserving Lagrangian with seven independent constants. This is, therefore, similar to the general one considered in B (equation (18)) excepting for the $\mathcal{N}\mathcal{N}\pi$- and $\Xi\Xi\pi$-interactions which still have equal interaction constants. Different constants for these two terms could be introduced only by postulating a hypercharge-dependent pion interaction as done in B (equation (14)) which, however, would not be invariant under transformations (α) and (β) and therefore does not follow from the above procedure. The CP to P derivation for this term would still follow, as for the other π-interactions, from the assumption of its charge independence.

In conclusion we may say that the principle leading to the choice of interaction schemes of the type of those in A and B, may be expressed in the following way. We take a linear combination of all the sub-schemes each of which is invariant under the transformations (α), (β) and (γ) with all possible choice of the sign factors ε_{K}, ε_{π} and η. The whole combination of course, will not be invariant for any of the special choices, and this will lead to the breaking down of the high symmetry resulting in the mass-differences of the baryons, but the $CP \to P$ derivation will be preserved.

* * *

One of us, (L. K. PANDIT), wishes to espress his gratitude for the kind hospitality received by him at the Istituto di Fisica dell'Università di Padova.

RIASSUNTO

In precedenti lavori ([1,2]) è stato proposto uno schema delle interazioni forti che spiega qualitativamente le differenze di massa dei barioni. È stato inoltre trovato che per l'intero lagrangiano di tale schema la conservazione della parità risulta quale conseguenza dell'invarianza per *CP*. Si fa vedere nel presente lavoro, che tale proprietà è dovuta al fatto che il lagrangiano può venire considerato come formato da tanti pezzi, ognuno dei quali soddisfa a certe condizioni di simmetria del tipo discusso da FEINBERG e GÜRSEY ([3]).

Nature of the $K^+ + n \to K^0 + p$ Angular Distribution (*).

E. Helmy, D. J. Prowse and D. H. Stork

Physics Department, University of California - Los Angeles, Cal.

(ricevuto il 21 Luglio 1960)

The attractive nature of the p-wave interaction in the $T=0$ K^+-nucleon isotopic spin state was recently strongly suggested by Melkanoff, Prowse, Stork and Ticho (MPST) (1). The $T=1$ interaction has been investigated by Kycia Kerth and Beander (2) who show that the best fit to experimental data on K^+-p scattering is given by a predominantly s-wave interaction which is repulsive. Previous evidence of much lower statistical weight obtained in nuclear emulsions had also indicated this s-wave repulsion in the $T=1$ state (3). The analysis of MPST was based upon the optical model potential and total charge exchange fraction, but not the K^+-n charge-exchange (C.E.) angular distribution. This distribution is of course determined by the phase shift solutions of MPST which are given by:

solution A:

$$a_{00} = 0.07f,\ a_{01}^3 = -0.21f^3,\ a_{03}^3 = -0.01f^3;$$

solution B:

$$a_{00} = 0.09f,\ a_{01}^3 = 0.05f^3,\ a_{03}^3 = -0.13f^3;$$

where

$$\operatorname{tg}\delta_{00} = -a_{00}k, \quad \operatorname{tg}\delta_{01} = -a_{01}^3 k^3, \quad \operatorname{tg}\delta_{03} = -a_{03}^3 k^3.$$

These solutions result in the phase shifts given in Table I at 230 MeV.

Table I. – *MPST phase shift at* 230 MeV.

	Solution A	Solution B
δ_{00}	$-6°$	$-8°$
δ_{01}	$+39°$	$-11°$
δ_{03}	$+2°$	$+27°$
δ_{10} (*)	$-34°$	$-34°$

(*) From Kerth *et al.* (2).

In principle the angular distributions of K^+-n scattering may be used to confirm these phase shifts. The angular distributions are given by

$$I(\theta) = A + B\cos\theta + C\cos^2\theta,$$

(*) Partially supported by the U. S. Atomic Energy Commission.

(1) M. A. Melkanoff, D. J. Prowse, D. H. Stork and H. K. Ticho: *Phys. Rev. Lett.*, **5**, 108 (1960).

(2) T. F. Kycia, L. T. Kerth and R. G. Baender: *Phys. Rev.*, **118**, 553 (1960).

(3) *E.g.*, M. F. Kaplan: 1958 *Annual International Conference on High Energy Physics at CERN*, edited by B. Ferretti (Geneva, 1958).

where

$$A = (|a|^2 + |c|^2)/4 ,$$
$$B = \pm \tfrac{1}{2} \operatorname{Re}(a^* b) ,$$
$$C = (|b|^2 - |c|^2)/4 ,$$

and

$$a = \exp[i\delta_{10}] \sin \delta_{10} \pm \exp[i\delta_{00}] \sin \delta_{00} ,$$
$$b = 2 \exp[i\delta_{03}] \sin \delta_{03} + \exp[i\delta_{01}] \sin \delta_{01} ,$$
$$c = \exp[i\delta_{03}] \sin \delta_{03} - \exp[i\delta_{01}] \sin \delta_{01} .$$

The $+$ signs are to be taken for the elastic scattering and the $-$ signs for the C.E. scattering. Whether or not the distribution is forward or backward peaked depends entirely on the sign of B. δ_{00} is always small and δ_{10} is strongly repulsive. The attractive nature of the p-wave interaction thus requires the C.E. distribution to be peaked forward and the elastic distribution to be peaked backwards.

An attempt has been made by CEOLIN *et al.* ([4]) to measure the C.E. distribution by a momentum balance analysis of C.E. events in nuclear emulsion. They concluded that it was peaked backwards and they used this information to rule out the suggestion originally made by PAIS ([5]) that the K^+ and K^0-mesons might not have the same parity. It may be noted that if these particles do not form an isotopic doublet, all phase-shift analyses of K^+-meson scattering which have been made are invalid. If however, their conclusion is correct, it would also be in disagreement with the phase shift analysis of MPST.

We have therefore examined our nuclear emulsion experimental data at 260 MeV in an attempt to re-determine the gross features of the C.E. angular distribution. The K^+-p cross-section is isotropic and by comparing the distribution in energy and angle of the protons emerging from C.E. events with those emerging from non-C.E. events it is possible to obtain information on the elementary C.E. angular distribution. Fig. 1 shows such a comparison of the proton energy spectra and angular distributions for these two classifications. Only those protons having an energy greater than 10% of the incident K^+-meson energy are plotted as there is an excess of slow protons coming both from secondary neutron scatters and from evaporation processes, the latter being isotropically distributed in angle. A very noticeable difference between the two distributions is the many more fast protons in the forward direction from the non-C.E. events. The contour lines drawn are approximate lines of constant $\cos\alpha$ where α is the most probable angle of scatter of the K-meson in the c.m. of the K-nucleon system. Individual events cannot be identified with this angle, α, because of the smearing effect of the internal momentum distribution of the struck nucleons. It should be noted that the potentials of the nucleon and K-meson significantly affect the shape and position of the constant $\cos\alpha$ curves.

Fig. 2 shows the distribution in $\cos\alpha$ for both classes of events. These distributions should not be the same as the elementary angular distributions because of the effect of double collisions. However, this effect does not modify a direct comparison. On the other hand a contamination of knock on protons from ordinary K-n scattering may be expected in the non-C.E. distribution. These knock on protons will be more isotropic in the laboratory system and have lower energy than the primary proton secondaries. They may thus make a comparison of the distributions for positive $\cos\alpha$ difficult. We therefore limit our attention to $\cos\alpha$ near -1.0. In Fig. 2 the ratio of C.E. to non-C.E. events is seen to decrease in the backward hemi-

([4]) C. CEOLIN, N. DALLAPORTA, L. GUERRIERO, I. LABORAGINE, G. A. SALANDIN and L. TAFFARA: *Nuovo Cimento*, **13**, 818 (1959).

([5]) A. PAIS: *Phys. Rev.*, **110**, 574 (1958).

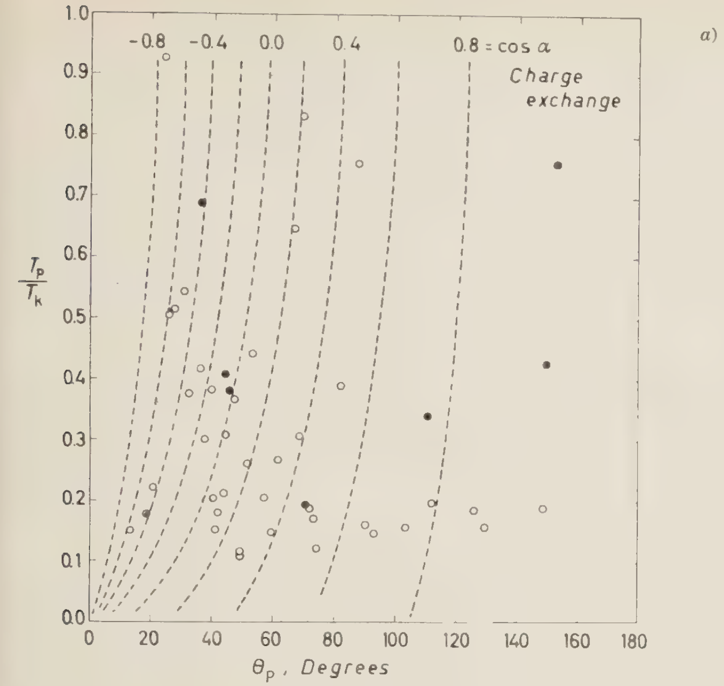

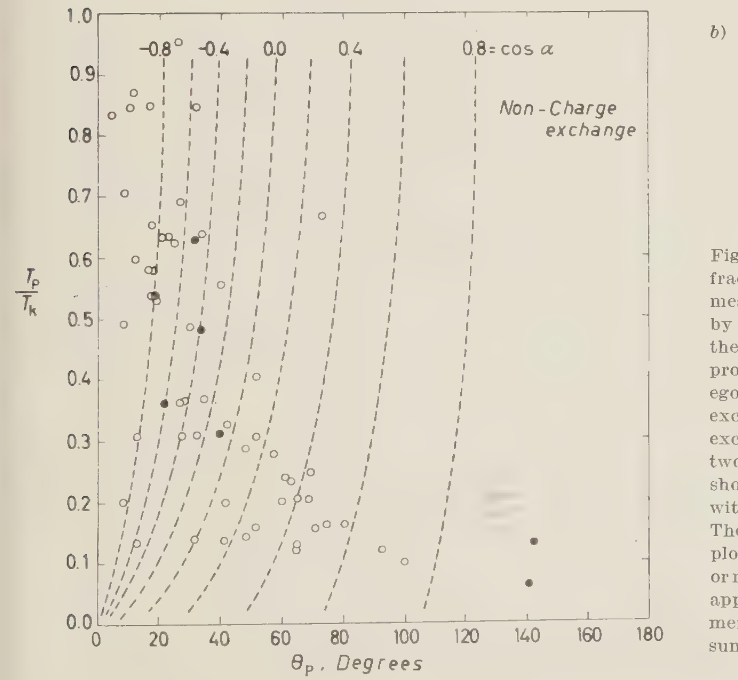

Fig. 1. – Plot of T_p/T_K, the fraction of the incident K-meson energy carried away by the fast proton, against the angle of emission of the proton, θ_p, for the two categories of events (*a*) charge exchange and (*b*) non-charge exchange. Events which have two or more fast protons are shown as black circles, those with only one as open circles. The values of T_p/T_K and θ_p plotted for events with two or more fast protons are those applicable to a proton of momentum equal to the vector sum of the fast protons observed.

sphere. Since the K+-p scattering is isotropic, the decreasing ratio for more

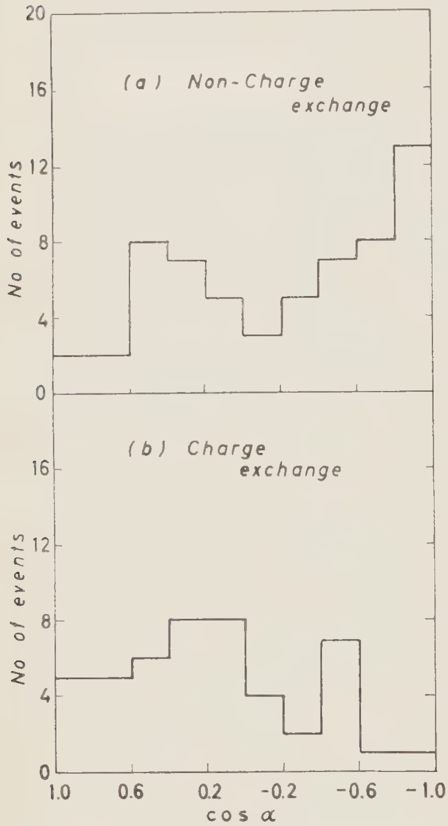

Fig. 2. – Histogram of cos α, the cosine of the most probable angle of scatter of the K-meson in the c.m. system for the two categories of events.

negative cos α indicates a backward dip in the C.E. cross section. From the ratio expected from isotropy ([6]) we may furthermore infer that there is corresponding forward peaking. Although these results are only semiquantitative, they are in good agreement with the forward-backward C.E. ratio predicted by MPST, who obtain 1.7 for solution A and 1.4 for solution B. These results are inconsistent with a backward peaking and support the conclusion of an attractive p-wave contribution in the p-wave state.

This result is not in agreement with the momentum balance analysis of CEOLIN *et al.* We believe this is because the momentum of evaporation prongs was included by these authors with the result of introducing pseudo-forward K-scattering events in the non-C.E. distribution. An analysis of our data along the lines indicated by CEOLIN *et al.* but omitting all evaporation prongs (which are isotropically distributed in angle) gives results in substantial agreement with these presented above.

* * *

We would like to express our appreciation to Dr. E. J. LOFGREN and the Bevatron crew who made the emulsion exposures possible and to our scanners, Miss Janet SCHLAN, Mrs. Claire SWAN and Mr. Dalton CANTEY for much of the microscope work. Prof. H. K. TICHO is thanked for numerous discussions and constant encouragement.

([6]) The phase-shifts of MPST suggest a charge exchange cross-section of 7 mb at 230 MeV. KYCIA *et al.* a K+-p cross section of about 15 mb. The ratio expected for isotropy is hence about 0.46.

Internal Conversion from Resonance Absorption (*).

H. Frauenfelder (**), D. R. F. Cochran, D. E. Nagle and R. D. Taylor
University of California, Los Alamos Scientific Laboratory - Los Alamos, New Mex.

(ricevuto il 28 Ottobre 1960)

The classical investigations on optical resonance fluorescence and on nuclear resonance fluorescence (1) were performed as scattering experiments. In contrast, nearly all the recent experiments on recoilless emission and absorption of nuclear γ-rays (Mössbauer effect) were done in a transmission geometry (2), partly because of the higher intensities obtainable. The effect of internal conversion further reduces the intensity in scattering experiments: the Mössbauer effect is most pronounced in γ-decays of low-lying states with long lifetimes occurring in nuclei of high atomic number. These are just the conditions where internal conversion, characterized by the conversion coefficient α, competes effectively with γ-ray emission. Thus when γ-rays are resonantly absorbed, only a fraction $1/(1+\alpha)$ of the excited states will decay again by γ-emission while a fraction $\alpha/(1+\alpha)$ will emit conversion electrons. The competition by internal conversion impedes the observation of the recoil-free scattered γ-rays.

We have observed the Mössbauer re-emission spectrum in ^{57}Fe, taking advantage of the large internal conversion. The basic idea is not to look for the re-emitted 14.4 keV γ-rays, but to observe the K X-rays (6.3 keV) following internal conversion. The cross sections in iron for the 14.4 keV γ-ray and for the iron K X-ray are such that the experiment is easy to perform: the cross section for resonance absorption of the 14.4 keV γ-ray, $\sigma_0 = 1.5 \cdot 10^{-18}$ cm^2 is much larger than the photoelectric absorption of either the 14.4 keV γ-ray ($\sigma_p = 6 \cdot 10^{-21}$ cm^2) or the 6.3 keV X-ray ($\sigma_p = 7 \cdot 10^{-21}$ cm^2). The scattering foil (4.6 mg/cm^2 ^{57}Fe, 75% enriched) chosen for the present experiment is evidently many mean-free paths thick for resonant γ-rays, but is thin for X-rays.

The experimental arrangement is sketched in Fig. 1. The source, approximately 10 mC of ^{57}Co plated onto Armco iron sheet and annealed in vacuum for 1 h at 900 °C, is mounted on an 8-in high-compliance speaker. A stable audio

(*) Work done under the auspices of the U. S. Atomic Energy Commission.

(**) Permanent address: Department of Physics, University of Illinois, Urbana, Illinois.

(1) See *e.g.*, K. G. Malmfors in: *Beta and Gamma Ray Spectroscopy*, edited by K. Siegbahn (Amsterdam, 1955).

(2) The scattering experiment performed by C. Tzara and R. Barloutaud: *Phys. Rev. Lett.*, **4**, 405 (1960), does not involve nuclear resonance fluorescence directly; the sharp γ-rays from Mössbauer emission are used to investigate Rayleigh scattering.

oscillator and amplifier provide a sine-wave velocity drive at a frequency of 11 s^{-1}. The absorber-scatterer is attached

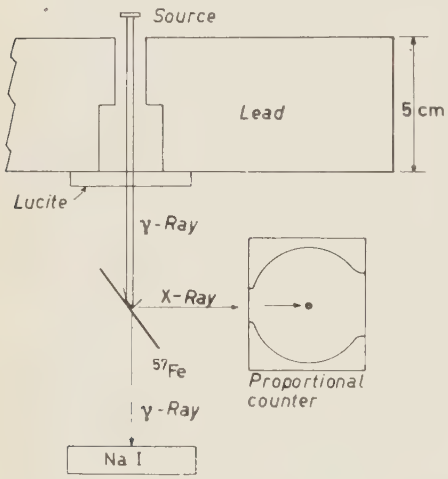

Fig. 1. – Experimental arrangement. The source is mounted on a loud speaker which is driven by an 11 s^{-1} sine wave. A NaI crystal and photomultiplier detects the transmitted 14.4 keV γ-rays. The proportional counter detects the 6.3 keV X-rays associated with the internal conversion.

to a thin sheet of polystyrene held rigidly at approximately 45° to the beam. The transmitted beam is detected by means of a NaI scintillation crystal and photomultiplier tube. These photomultiplier pulses are amplified and the 14.4 keV γ-ray selected using a single-channel analyzer. Pulses of constant amplitude from the single-channel analyzer are modulated with a sawtooth voltage locked in with the speaker drive. The modulated pulses are displayed on a 400-channel analyzer giving directly the ^{57}Fe hyperfine overlap spectrum (see Fig. 2). This transmission experiment serves to calibrate the velocity drive using the results of HANNA *et al.* (3).

(3) S. S. HANNA, J. HEBERLE, C. LITTLEJOHN, G. J. PERLOW, R. S. PRESTON and D. H. VINCENT: *Phys. Rev. Lett.*, **4**, 177 (1960).

The second counter, as shown in Fig. 1, is a proportional counter designed to respond to 6.3 keV radiation with an internal efficiency of about 95%. A 6 mm sheet of Lucite in front of the source filters out the iron X-rays in the primary beam so that the gas counter detects mostly those soft X-rays created by the absorption of the 14.4 keV γ-ray in the absorber. Lead shielding helps to reduce the background count. As before, the output of the proportional counter is gated, modulated, and then displayed on the 400 channel analyzer as a Mössbauer absorption-emission spectrum.

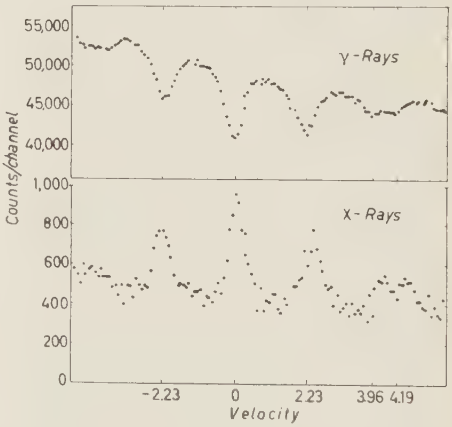

Fig. 2. – Recoilless resonance absorption in ^{57}Fe. The upper curve shows the transmission spectrum of the 14.4 keV γ-ray. The lower curve shows the resonance peaks as detected by the proportional (X-ray) counter.

Fig. 2 shows the spectra obtained with the two counters. The lower curve is the data taken with the proportional counter and scattering geometry, corresponding to the re-emission and the observation of the X-rays; it shows the resonances as maxima in the counting rate. The upper curve displays the pattern taken under the same conditions of velocity drive, but in the transmission geometry with the γ-ray counter. The resonances appear at the same velocities

as before, but as minima. The velocity scale is taken from the transmission experiment of HANNA *et al.* [3]. The two curves are direct tracings from an electronic plotter, and the velocity scale is identical for both plots without any realignment. There does not appear to be any shift in the velocity scale between the two curves. A slight dilation of the velocity scale in the lower curve may be the result of a very small drift in amplifier gain.

Comparison of the two curves demonstrates that the minor peaks at 3.96 and 4.19 mm/s, which are difficult to resolve in transmission [3], appear clearly in the X-ray curve, which exhibits the low background (and low intensity) characteristic of scattering.

That the resonances in the scattering geometry are the result of K X-ray re-emission was verified by examining the pulse height spectrum of the scattered resonant radiation. It was concluded that at least 99% of the scattered resonant radiation detected in our experiment was the 6.3 keV K X-rays. The resonant contribution at the 14.4 keV channel was $(1.2 \pm 0.9)\%$.

The method should be useful for investigating the Mössbauer spectra of highly converted γ-rays, and in some cases it should be possible to determine conversion coefficients.

* * *

The authors wish to thank R. HANFT for his assistance.

Remark Concerning the Gravitational Interaction of Matter and Anti-Matter.

F. WINTERBERG
Case Institute of Technology - Cleveland, Ohio

(ricevuto l'11 Novembre 1960)

A number of speculations have been made recently about the question whether the gravitational interaction of matter and anti-matter is different from that of matter with matter. More specifically it is argued that the gravitational interaction of matter and anti-matter may have the same magnitude as for matter with matter but being of opposite sign.

One can easily show that under the existence of a red-shift of light-rays in a gravitational field such an assumption leads to a violation of the law of energy-conservation.

The proof of this statement can be given by considering a simple cycling process. A sufficient amount of energy say E_0 may produce at a place in the gravitational field with the potential Φ_0 a particle-anti-particle pair. If the anti-particle shows an « anti-gravity » rather than an ordinary gravitational attraction the pair is weightless. It is therefore possible to lift the pair without work to another place in the gravitational field possessing the potential Φ_1. Both particles shall be destructed at this place creating a photon. The photon is sent back to the place on the field where the potential is Φ_0. It gains energy equal to $\Delta E = [(\Phi_1 - \Phi_0)/c^2]E_0$: The energy at the end of this cycling process is therefore

$$E_0 + \Delta E = E_0 \left(1 + \frac{\Delta\Phi}{c^2}\right) > E_0 ,$$

a result which is in contradiction with the energy-conservation-law. This consideration is not confined to light-rays. An analogical situation is given if instead of light rays, π-mesons are produced as a result of the pair annihilation.

* * *

The author is indebted to Professor L. FOLDY for discussions on this subject.

IL NUOVO CIMENTO Vol. XIX, N. 1 1° Gennaio 1961

The Photofission of Bi, Th and U between 300 and 1000 MeV (*).

H. G. de Carvalho (**), A. Celano, G. Cortini and R. Rinzivillo
Istituto di Fisica Superiore dell'Università - Napoli
Istituto Nazionale di Fisica Nucleare - Sottosezione di Napoli

G. Ghigo
Laboratori Nazionali del C.N.R.N. - Frascati

(ricevuto il 18 Novembre 1960)

The fission process produced by high energy γ-rays in heavy nuclei was investigated up to an energy of 500 MeV by Jungerman and Steiner (1), who examined the following nuclei: ^{238}U, ^{235}U, ^{232}Th, ^{209}Bi and ^{197}Au, by means of the University of California and of the Cal. Tech. syncrotrons. The present letter gives our preliminary results on photofission obtained by means of the Frascati syncrotron, between 300 and 1000 MeV, with an improved nuclear emulsion technique, on ^{238}U, ^{232}Th and ^{209}Bi. The work is still in progress, but it seems useful to give a preliminary account of it as some U, and Th results are different from those by Jungerman and Steiner (1).

The photoemulsion technique is that described by de Carvalho *et al.* (2,3), which makes it possible to get only very clear fission tracks, on a background of up to 10^9 α decays per square centimeter, under heavy γ-irradiations (up to $1000r$). Bismuth loaded KO pellicles were kindly supplied by Ilford Ltd.; U and Th loaded pellicles were prepared from KO gel emulsion in this laboratory. Technical details about the loading, the precise ($\sim 1\%$) measurement of the weight of the included elements, and the difficulties met with the processing of the loaded emulsions will be described elsewhere.

Emulsions were exposed perpendicularly to the collimated γ-ray beam. The collimator diameter was very small, so that it was possible to make a complete scanning of the small (8 mm diameter) emulsion area hit by the γ-rays. Between 1000 and 6000 fission tracks

(*) Communication presented at the 46th Conference of the S.I.F., Naples, Sept. 29-Oct. 5 1960.

(**) On leave of absence from the Centro Brasileiro de Pesquisas Fisicas and Comissão Nacional de Energia Nuclear (Brasil).

(1) J. A. Jungerman and H. M. Steiner: *Phys. Rev.*, **106**, 585 (1957).

(2) H. G. de Carvalho and A. G. da Silva: to be published in *Nuovo Cimento.*

(3) H. G. de Carvalho, A. Celano and R. Rinzivillo: communication at the S.I.F. Conference, Naples (October 1960).

were counted in any scanned plate. The intercalibration of different scanners, with and without a track mapping, was carefully performed and gave a $\sim 95\%$ scanning efficiency. Dose and energy measurements were obtained by means of the standard Frascati facilities.

Our results are shown in Fig. 1, in comparison with those by JUNGERMAN and STEINER [1]. The Bismuth results are in good agreement, but on the contrary the U and Th results are rather different: JUNGERMAN and STEINER got rather dispersed points and reached the conclusion that any increase in the yield curve at high energy was masked by the big background coming out from fissions produced by the bremsstrahlung spectrum in the giant resonance region ($\sim$15 MeV). We found, instead, that when the maximum bremsstrahlung energy E is increased from 300 to 1000 MeV a marked increase of the cross section σ_Q^F, per quantum equivalent is observed; our five experimental points (Fig. 1 *a*, *b*) are aligned along a straight line. Probably some difference of calibration between the two machines used by the previous authors is mainly responsible for this discrepancy. *If the straight-line approximation is accepted,* as a consequence the cross-section per photon $\sigma_K^F = \mathrm{d}\sigma_Q^F/\mathrm{d}\ln E$ results to be constant and the least-square calculations give (see graphs in Fig. 1), in units of 10^{-27} cm²:

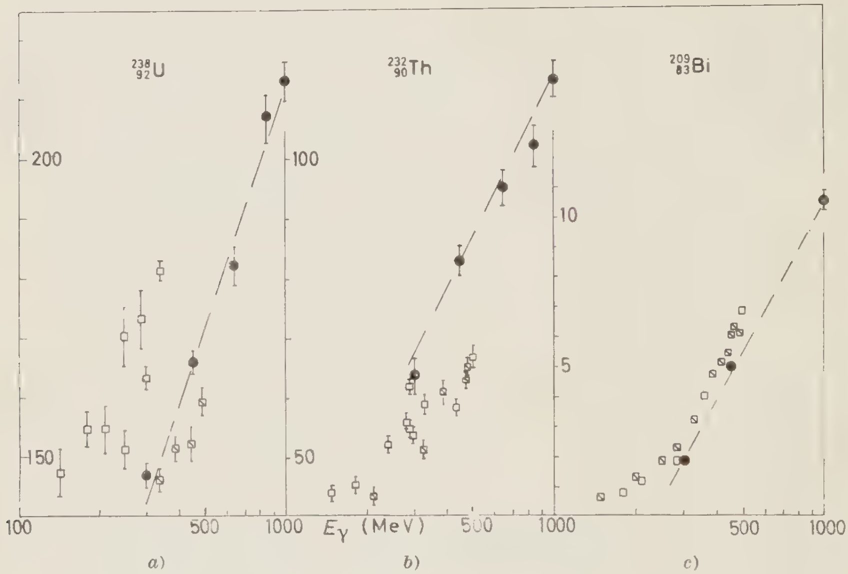

Fig. 1.

$$\sigma_K^F(\mathrm{U}) = 60\,; \tag{1}$$

$$\sigma_K^F(\mathrm{Th}) = 36\,; \tag{2}$$

$$\sigma_K^F(\mathrm{Bi}) = 6.5\,. \tag{3}$$

The overall experimental errors are evaluated to be of the order of 10%. The above results can be compared with those obtained by several authors [4,5] about the photoproduction of stars in the elements of the photoemulsions.

---

(4) R. D. MILLER: *Phys. Rev.*, **82**, 260 (1951); S. KIKUCHI: *Phys Rev.*, **86**, 41 (1952); E. P. GEORGE: *Proc. Phys. Soc. (London)*, A **69**, 110 (1956); V. Z. PETERSON and C. E. ROOS: *Phys. Rev.*, **105**, 1620 (1957); V. Z. PETERSON: private communication.

(5) C. CASTAGNOLI, M. MUCHNICK, G. GHIGO and R. RINZIVILLO: *Nuovo Cimento*, **16**, 683 (1960).

Inside the experimental errors, these results are consistent among them and with the assumption of a cross-section approximately constant between 300 and 1000 MeV.

Now, according to the accepted theoretical scheme (6) the stars are produced by high energy photons via the photoproduction of mesons which are reabsorbed in the nucleus. On the other hand, the experimental photostar cross-section is so high that one must assume that a star is produced any time a photomeson is produced, that is that the reabsorption probability is nearly unity. This conclusion is reached by taking into account any type of multiple meson production, with the appropriate statistical weight (5).

Therefore, it is possible to get a reasonable guess about the photostar production cross-section, in any nucleus, by simply taking account of its number of nucleons (disregarding the rather small difference between the inelastic cross sections of γ-rays against the two kinds of nucleons) (7).

By means of this procedure, starting from the slope of the straight line giving the σ_Q^S of photostars in photoemulsions plotted against $\ln E$, we get the following cross-sections for photostar production (in mb)

$$(1') \qquad \sigma_K^S(\mathrm{U}) = 73\,;$$

$$(2') \qquad \sigma_K^S(\mathrm{Th}) = 71\,;$$

$$(3') \qquad \sigma_K^S(\mathrm{Bi}) = 64\,;$$

with errors of $\sim 20\%$ (5).

For the «fissionability» defined as $x=\sigma_K^F/\sigma_K^S$ we obtain

$$(4) \qquad \left\{\begin{aligned} x(\mathrm{U}) &= 0.85\,; \\ x(\mathrm{Th}) &= 0.52\,; \\ x(\mathrm{Bi}) &= 0.10\,. \end{aligned}\right.$$

All these values of x appear to be approximately constant, at least between 500 and 1000 MeV. They are consistent with the fissionabilities obtained by STEINER and JUNGERMAN (8) with protons between 100 and 340 MeV.

Of course much work is still necessary in order to confirm eqs. (4) and give them a clearer significance. These points will be discussed in a next paper, when more experimental data will be available. For the moment we want to note two points. The first one is that x depends very strongly on the considered nucleus, but is quite insensitive to the excitation energy. A possible explanation of this behaviour cannot be derived from the fact that the U and Th nuclei (having a low threshold) can undergo fission even when a produced meson is not reabsorbed. In fact the fission probability in an excited nucleus, at low energy, is only $\sim 10\%$. Besides, this argument is not at all able to explain the quoted results with high energy protons (8).

The second point is that some enhancement effect due to a coherent production of π^0-mesons and of $\pi^+\pi^-$ pairs (9) could contribute to the star production and be partly responsible for the unexpectedly high observed cross sections.

* * *

Our deepest thanks are due to Mr. GREENBERG of Ilford Ltd. for his very kind co-operation in preparing bismuth loaded pellicles, to the Frascati Syncrothron crew and to the Naples mycroscope scanners, and to Dr. M. NAGASAKI for many useful discussions.

(6) G. BERNARDINI, R. REITZ and E. SEGRÈ *Phys. Rev.*, **90**, 573 (1953).

(7) C. NEUGEBAUER, W. D. WALES and R. L. WALKER: *Phys. Rev*, **119**, 1726 (1960).

(8) H. M. STEINER and J. A. JUNGERMAN: *Phys. Rev.*, **101**, 807 (1956).

(9) G. DE SAUSSURE and L. S. OSBORNE: *Phys. Rev.*, **99**, 843 (1955).

IL NUOVO CIMENTO Vol. XIX, N. 1 1° Gennaio 1961

Some Tests for Compound Models of Elementary Particles.

G. Bhamathi (*), S. Indumathi (**), A. P. Balachandran (***)

University of Madras - Madras

and

N. G. Deshpande

(ricevuto il 30 Novembre 1960)

Compound models of elementary particles have been suggested by many authors. We wish to suggest in this note some possible experimental means of testing the validity of such models.

a) In a composite particle model for a hyperon, it is possible to predict the asymmetry parameter for its decay products if the decay characteristics of its constituent particles are known. Such calculations have already been carried out for the Σ-particle as the bound state of a Λ and a π (1) and for the Ξ-particle as the bound state of a Λ and a K (2,3) and in the former case, the asymmetry parameters are seen to agree with experimental results. Such analyses can also be carried out for other compound models and can provide a valuable check as to the correctness of the basic assumptions of such models. For instance, the Goldhaber-Györyi model (4) is not capable of explaining the decay features of the composite particle since the basic weak interaction is the decay of $\overline{\mathrm{K}}$ into pions.

b) In the effective range theory, there is a relation between the binding energy of the compound particle and the scattering length, effective range as well as the *S*-wave scattering phase shift of its constituent particles. This fact may be used to test the validity of a compound particle model. Thus for instance if $\Lambda=(1/\sqrt{2})(pK^- - nK^0)$ and $P(N\overline{K}\Lambda)$ is even so that the bound state is an *S*-state (4), the $T=0$ *S*-wave K⁻-p scattering parameters may be related to the binding energy E_g of the Λ where $E_g = -318.7$ MeV. The K⁻-p elastic

(*) Council of Scientific and Industrial Research, Junior Research Fellow.

(**) University Grants Commission, Junior Research Fellow.

(***) Atomic Energy Commission, Senior Research Fellow.

(1) S. Barshay and M. Schwartz: *Phys. Rev. Lett.*, **4**, 618 (1960).

(2) N. Dallaporta: *Nuovo Cimento*, **7**, 200 (1959); P. Budini, N. Dallaporta and L. Fonda: *Nuovo Cimento*, **9**, 316 (1958).

(3) A. P. Balachandran and N. R. Ranganathan: *Nuovo Cimento* (to be published).

(4) S. Goldhaber: *Phys. Rev.*, **101**, 433 (1956); G. Györgyi: *Žurn. Èksper. Teor. Fiz.*, **32**, 152 (1957).

scattering is almost entirely through S-waves at laboratory energies up to 100 MeV [5,6] and takes place through the two isotopic spin channels $T=0$ and $T=1$. If δ_T denotes the S-wave phase-shift in the isotopic spin channel T and A_T and R_T are the corresponding scattering length and effective range respectively, we have the usual formula

$$k \operatorname{ctg} \delta_T = \frac{1}{A_T} + \frac{1}{2} R_T k^2 + \dots , \tag{1}$$

where δ_T, and A_T and R_T are complex because of the presence of absorption channels with production of hyperons. Following JACKSON, RAVENHALL and WYLD [6], we may neglect all but the first term in the expansion (1) below laboratory energies of about 100 MeV so that we may write

$$k \operatorname{ctg} \delta_T = \frac{1}{a_T + i b_T} , \tag{2}$$

where $A_T = a_T + i b_T$. The bindingenergy E_g may be related to the real part of the $T=0$, S-wave scattering phase shift δ_0 through the formula

$$k \operatorname{ctg} [\operatorname{Re} \delta_0] = k_g ,$$

where

$$k_g = \sqrt{\frac{-2\mu E_g}{\hbar^2}} = \tag{3}$$
$$= 2.324 \cdot 10^{-13}\ \text{cm}^{-1} ,$$

and μ is the reduced mass of the K^--p system. Thus we have, to a good approximation

$$a_0 = \frac{1}{k_g} = 0.43 \text{ fermis} . \tag{4}$$

DALITZ and TUAN [5] obtain the value $a_0 = 0.20$ fermis for their (a_+) solutions and $a_0 = 1.88$ fermis for their (b_+) solutions. The agreement between (4) and the Dalitz-Tuan solutions is not good.

A similar analysis for Σ considered as a $\overline{K}$ and an N [4] bound in an S-state (*i.e.* we assume $P(N\overline{K}\Sigma)$ is even) gives $a_1 \simeq 0.50$ fermis which is to be compared with the Dalitz-Tuan (a_+) and (b_+) solutions of 1.62 fermis and 0.40 fermis respectively [5]. For the Barshay model of Σ as the bound S-state of a Λ and π (*i.e.* $P(\Lambda\pi\Sigma)$ is even) [1] we obtain $a_1 \simeq 1.55$ fermis while for the model of Ξ as the bound S-state of a Λ and a $\overline{K}$ (*i.e.* $P(\Lambda\overline{K}\Xi)$ is even) [2], $a_1 \simeq 0.44$ fermis. In the low energy region, there is no absorption channel in the last two cases and the scattering phase shifts are real. Thus the elastic scattering cross-sections are given by

$$\sigma = \frac{4\pi}{k^2 + k_g^2} .$$

c) By requiring that charge conjugation C and parity P be good operators, it is possible to derive selection rules for K^+K^- or $K^0\overline{K}^0$ annihilation into pions by standard methods [7]. Similarly the application of P, C and charge symmetry operations will give selection rules for $K^+\overline{K}^0$ and K^-K^0 annihilations into pions. The results are summarized in the following tables.

These selection rules may prove useful in testing some of the compound models. Thus for instance if information can be obtained on the K^+ or K^0 capture by Λ's and it is found that in the low energy region uncharged 3π states or states with one charged pion are absent in the final state, the result may be taken as an indication of the validity

(5) R. H. DALITZ and S. F. TUAN: *Ann. Phys.*, **8**, 100 (1959).

(6) J. D. JACKSON, D. G. RAVENHALL and H. W. WYLD jr.: *Nuovo Cimento*, **9**, 834 (1958).

(7) C. N. YANG: *Phys. Rev.*, **77**, 242 (1950); L. WOLFENSTEIN and D. G. RAVENHALL: *Phys. Rev.*, **88**, 279 (1953); L. MICHEL: *Nuovo Cimento*, **10**, 319 (1953).

TABLE I.

K^+-K^- or K^0-$\overline{K}^0$	$\pi^0\,\pi^0$	$\pi^+\,\pi^-$	$\pi^0\,\pi^0\,\pi^0$	$\pi^+\,\pi^-\,\pi^0$
S_0	S_0	S_0	—	—
P_1	—	P_1	—	Pp_1, Ff_1, Hh_1, ...
D_2	D_2	D_2	Dp_2, Df_2, Gf_2, Gh_2, ...	Dp_2, Df_2, Gf_2, ...

of the Goldhaber-Györgyi model. Here we assume that the mechanism of the reaction is the capture of K by the $\overline{K}$

K^+-$\overline{K}^0$ or K^--K^0	$\pi^\pm$-π^0	3π
S_0	—	—
P_1	P_1	—
D_2	—	Pp_2, Dp_2, ...
F_3	F_3	—

in Λ. Analogous results for the Ξ-particle may indicate that the Ξ may be considered as the bound state of a Λ and a $\overline{K}$ if similar assumptions can be made. The angular distribution of the pions in the final state in such interactions may also serve as a test for such models. Similar arguments can also be applied to the annihilation of antibaryons with baryons, with pions or K-mesons in the final state to provide a test for some of the compound models of the baryons.

* * *

We wish to thank Professor ALLADI RAMAKRISHNAN, Mr. N. R. RANGANATHAN and Mr. K. VENKATESAN for instructive discussions. One of us (G.B.) would like to thank the Council of Scientific and Industrial Research, Government of India, another (S.I.) the University Grants Commission, Government of India and the third (A.P.B.) the Atomic Energy Commission, Government of India, for the award of fellowships which enabled this work to be carried out.

IL NUOVO CIMENTO Vol. XIX, N. 1 1° Gennaio 1961

On Pion Production in Coulomb Field.

B. Ferretti

Istituto di Fisica dell'Università - Bologna

(ricevuto il 29 Dicembre 1960)

It has been suggested independently by the Author in a meeting held at CERN during the spring of 1959, and by O. Piccioni during the 1959 High Energy Conference in Kiew that it might be interesting to investigate the production of pions by a pion in a Coulomb field, in order to clarify the pion-pion interaction.

It is the purpose of this letter to give some information on the state of this problem.

First it should be pointed out that Piccioni's and Author's suggestions although quite similar are not identical. Piccioni indeed has suggested to investigate the production of one meson, and the Author the production of two mesons. The difference is less trivial than it might appear. The advantage of Piccioni's suggestion is that his effect can be investigated at a lower energy. On the other hand, the other process seems to be connected, from a theoretical point of view, in a simpler and more fundamental way to the problem of the pion-pion interaction. In fact, due to symmetry laws, no vertex part with three pion lines can give contributions different from zero, and consequently for Piccioni's effect one « fourfold vertex » with three pions and one electromagnetic line is essential.

In second place, the results of some calculations on the production of two pions in a Coulomb field will be given.

These calculations have been performed using a model in which one supposes that the interaction between pions is mainly due to a resonating state. A perhaps interesting result of these calculations is that apparently the cross section for the effect is strongly dependent on the nature of the intermediate resonating state. In fact, not surprisingly, the cross section seems to increase with energy much more rapidly in the case in which the resonating state is supposed to have angular momentum equal to one, than in the case in which the angular momentum is supposed to be equal zero (angular momenta greater than one have not been investigated).

In the case of a primary energy of about twenty GeV and for instance in lead, the cross section for the production of two pions in the Coulomb field (supposing a resonating state with angular momentum equal to one and a resonating mass not higher than three-four pion masses) is of the order of a few hundredths

of the pion-pion scattering cross section at the resonance. In the case of angular momentum equal to zero and at the same energy the cross section is about ten times smaller.

Information on the position and width of the resonance can be derived from the energy dependence of the cross section for production of two pions in Coulomb field. For all these reasons the results of the calculations seems to confirm the guess that the study of the production of two pions in a Coulomb field by an incoming pion might be quite illuminating in clarifying the pion-pion interaction.

In third place one should add a last remark. It is essential from an experimental point of view that the cross section for the production of two pions in Coulomb field should be roughly proportional to Z^2 (this should be true at least asymptotically at a very high energy; at an energy not very high the effect of the finite size of the nucleus will modify the Z^2 law). Now it has been suggested that an effect proportional to $Z^2(A^2)$ might be due to a coherent production of two pions by the nucleons of the nucleus. One should however remark that an A^2 dependence should be expected for coherent production only in the case in which for *all channels* the predominant process ought to imply one nucleon only. Now such a situation seems for general reasons quite improbable in the case investigated; anyhow one should expect then very probably a similar A^2 effect for instance even for the diffraction scattering of one pion, and this effect might be easily investigated in the relevant energy region. Should one take seriously this doubt, it appears therefore possible to check experimentally, studying for instance the diffraction scattering of the pion, whether there are A^2 effects not depending from the Coulomb field.

LIBRI RICEVUTI E RECENSIONI

G. RIBAUD – *Conduction de la chaleur en régime variable.* Gauthier Villard Editeur, Paris, 1960.

Questo volumetto in ottavo, novanta pagine, trentaquattro figure, edito nel 1960, è il 65° della serie dei *Memorial des Sciences Physiques* curata da H. VILLAT e da G. RIBAUD.

Lo scopo del presente fascicolo è di dare a fisici, chimici ed ingegneri che si trovino alle prese con i problemi della conduzione termica, un panorama abbastanza completo, ma, per quanto possibile, semplice, dell'argomento.

Siccome i problemi di conduzione del calore in regime variabile od in condizioni di pre-regime sono in genere quelli che richiedono strumenti matematici più complessi che non quelli relativi agli stati stazionari, è ai problemi del primo tipo che è dedicata la maggior parte del volume.

Nel primo capitolo si richiamano le leggi generali della trasmissione del calore e si trattano i principali casi che si presentano in regime stazionario. Nel secondo capitolo si comincia lo studio della conduzione termica in regime variabile stabilendone i principi generali. Il terzo capitolo è dedicato alla ricerca di soluzioni particolari dell'equazione di Fourier del tipo $\varphi(t) f[x\psi(t)]$; le varie soluzioni sono illustrate con problemi concreti riferentisi a condizioni reali o realizzabili in pratica. Il quarto capitolo è dedicato allo studio dei casi in cui una o più di una delle superfici limite di un conduttore termico vengono portate a temperature che variano nel tempo secondo una legge periodica sinusoidale. Il quinto capitolo tratta di soluzioni dell'equazione di Fourier del tipo $\varphi(t) \cdot \psi(x)$. Anche qui esempi concreti illustrano la trattazione matematica. Il sesto capitolo studia il procedere verso l'interno di un corpo di una brusca variazione di temperatura, subita dalla sua superficie esterna, e ciò nel caso in cui la forma del corpo sia geometricamente semplice (sfera, cilindro, cubo e qualche altro). I capitoli settimo e ottavo sono dedicati rispettivamente alla trasmissione del calore complicata dalla presenza di sorgenti di calore nella massa che è sede del fenomeno di conduzione termica, ed ad un'introduzione all'uso della trasformazione di Laplace. Il capitolo nono spiega alcuni sistemi di soluzione grafica o numerica di problemi di trasmissione termica che il calcolo non riesce a risolvere.

L'impressione che il lettore prova a libro ultimato è che la trattazione si è mantenuta sufficientemente semplice e che, sia pure in poco spazio, è stato detto tutto l'essenziale sull'argomento tenendosi sempre in stretto contatto con la realtà dei problemi che si incontrano nei laboratori e nell'industria.

Il fisico interessato alla ricerca fondamentale ci resta un poco a bocca asciutta perchè nessun cenno vien fatto nell'opera all'interpretazione della tra-

smissione del calore in termini della struttura dei corpi; ma questo non è un appunto agli Autori del volumetto che non si propongono affatto di affrontare l'argomento; è semmai un avviso agli eventuali lettori di non chiedere al libro cose che esso non si propone di dare.

F. Gaeta

Applied Gamma-Ray Spectrometry; edito da C. E. Crouthamel; Pergamon Press, Oxford, 1960; pp. xii-443; 50 s.

Questo trattato ha lo scopo dichiarato di mettere a disposizione degli sperimentatori che si avvalgono della spettrometria gamma quelle notizie, dati e considerazioni specifiche che possano riuscire di guida per una interpretazione qualitativa ed una effettiva valutazione quantitativa dei risultati spettrometrici. L'opera, edita e redatta da C. E. Crouthamel colla collaborazione di alcuni suoi colleghi dello « Argonne National Laboratory », ha prevalentemente carattere sperimentale e pratico ma non trascura elementi di teoria che permettano al lettore di interpretare correttamente i fatti osservati.

Il volume è suddiviso in quattro Capitoli e quattro Appendici. Il primo capitolo riguarda le variabili intrinseche che influenzano i risultati spettrometrici, quali gli schemi di decadimento e i processi di interazione della radiazione con la materia. Il secondo è dedicato essenzialmente agli elementi costitutivi dello spettrometro a scintillazione, procedendo da un'impostazione statistica delle variabili esterne, sulla linea di Breitenberger: questo capitolo è indubbiamente assai utile allo sperimentatore, pur richiedendo al lettore un'adeguata preparazione specializzata. Il terzo capitolo tratta dei metodi di calcolo e della determinazione sperimentale della efficienza dei rivelatori; conclude la parte descrittiva dell'opera, un capitolo dedicato alle applicazioni specifiche della spettrometria gamma, con particolare riguardo alla misura dell'attivazione indotta da neutroni.

Nelle Appendici sono esposti, con abbondanza di dati sperimental e di valori calcolati, numerose tabelle intese a favorire una rapida interpretazione qualitativa degli spettri gamma. Di particolare interesse, nell'Appendice II, un compilazione degli spettri gamma di oltre un centinaio di nuclidi, ottenuti mediante un cristallo cilindrico di ioduro di sodio attivato al tallio, di 4 pollici di diametro e altrettanti di spessore.

La trattazione è caratterizzata da una equilibrata fusione tra le considerazioni teoriche e i dati sperimentali: se può apparire a prima vista un po' arida e scarsamente organica, l'opera contiene in realtà una documentazione ampia ed accurata, e può essere degnamente considerata un prezioso ausiliario del ricercatore scientifico.

C. Manduchi

Direttore responsabile: G. POLVANI — Tipografia Compositori - Bologna

Questo fascicolo è stato licenziato dai torchi il 16-I-1961.